Genetic dissection of regulatory domains and signalling interactions of PRL1 WD-protein in *Arabidopsis*

**Inaugural-Dissertation
zur
Erlangung des Doktorgrades
der Mathematisch-Naturwissenschaftlichen Fakultät
der Universität zu Köln**

vorgelegt von

Dóra Szakonyi
aus Kecskemét

KÖLN 2006

CONTENTS

FIGURES

TABLES

I ABBREVIATIONS AND SYMBOLES

A   adenine
ABA   abscisic acid
Ac   acetate
ADP   adenosine 5'-diphosphate
AMP   adenosine 5'-monophosphate
APC   Anaphase Promoting Complex/Cyclosome E3 ligase
A. thaliana   *Arabidopsis thaliana*
ATP   adenosine 5'-triphosphate
ATPase   adenosine 5'-triphosphatase

bp   base pair
BSA   bovine serum albumin

C   cytosine
°C   grad Celsius
CaMV   Cauliflower Mosaic Virus
cDNA   complementary DNA
CSM   *A. thaliana* Cell Suspension culture Medium
CS   *A. thaliana* Cell Suspension culture
C-terminal   carboxyterminal
C-terminus   carboxyl terminus
CTAB   cetyltrimethylammonium bromide

2,4-D   2,4-Dichlorophenoxy acetic acid
DAPI   4,6-diamine-2-phenylindole dihydrochloride
DMSO   dimethyl sulfoxide
DNA   Deoxyribonucleic acid
dNTP   deoxyribonucleotide triphosphate
DTT   dithiotreitol

E. coli   *Escherichia coli*
EDTA   ethylenediaminetetraacetic acid
EtBr   ethidium bromide
EtOH   ethanol

G   guanine
GA   gibberellin
g   gram
g   relative centrifugal field unit
GST   glutathione-S-transferase
GTC   guanidium thiocyanate

h   hour
HIS3   imidazole-glycerol-phosphate-dehydratase gene

IAA   indole-3-acetic acid
IGEPAL   (octylphenoxy)polyethoxyethanol
IgG   immunoglobuline G
IP   immunoprecipitation

kb   kilobase
kDa   kilo Dalton (1,000 Da)

l   liter
lacZ   *E. coli* β-galactosidase gene

M	Molar
µg	microgram
µl	microliter
µM	micromolar
mA	milliampere
mg	milligram
min.	minute
ml	milliliter
mM	millimolar
mRNA	messenger RNA
nt	nucleotide
N-terminal	amino terminal
N-terminus	amino terminus
OD	optical density
O/N	overnight
PAGE	polyacrylamide gel electrophoresis
POD	peroxidase
PCR	polymerase chain reaction
PEG	polyethylene glycol
pH	negative logarithm of the proton concentration
PMSF	phenylmethylsulfonyl fluoride
PRL1	*PLEIOTROPIC REGULATORY LOCUS 1*
PVDF	polyvinylidene difluoride
RNA	ribonucleic acid
RNase	ribonuclease
rpm	revolution per minute
RT	room temperature
S. cerevisiae	*Saccharomyces cerevisiae*
SDS	sodium dodecylsulfate
sec.	second
T	thymine
T	Total
TAE	Tris-acetate (40 mM); EDTA (1mM)
TCA	trichloroacetic acid
TE	Tris.HCl (10mM); EDTA (1mM)
TEMED	N,N,N',N' tetramethylenethylendiamine
Tris	Tris(hydroxymethyl) aminomethane
U	unit
Ub	ubiquitin
UTR	untranslated region
UV	ultraviolet light
V	Volt
vol.	volume
X-Gal	5-bromo-4-chloro-3-indolyl-β-D-galactopyranoside
X-Gluc	5-bromo-4-chloro-3-indolyl-β-D-glucuronic acid
wt	wild type

Aminoacids

A	Ala	Alanine
C	Cys	Cysteine
D	Asp	Aspartic acid
E	Glu	Glutamic acid
F	Phe	Phenylalanine
G	Gly	Glycine
H	His	Histidine
I	Ile	Isoleucine
K	Lys	Lysine
L	Leu	Leucine
M	Met	Methionine
N	Asn	Asparagine
P	Pro	Proline
Q	Gln	Glutamine
R	Arg	Arginine
S	Ser	Serine
T	Thr	Threonine
V	Val	Valine
W	Trp	Trptophan
Y	Tyr	Tyrosine
X		any amino acid

II SUMMARY - ZUSAMMENFASSUNG

Der *Arabidopsis PLEITROPIC LOCUS (PRL1)* kodiert für ein nukleares WD40-Protein. Pflanzen, die eine *PRL1*-Insertionsmutation tragen, sind kleiner als der Wildtyp, haben kürzere Wurzeln, Blätter mit gesägten Blatträndern und kürzere Petiolen. In photosynthetisch aktiven Geweben der *prl1*-Mutante lassen sich erhöhte Mengen an Glukose, Saccharose, Fruktose, Stärke, Anthozyanin und Chlorophyll nachweisen. Der Verlust der *PRL1*-Funktion führt zur Hypersensitivität gegenüber Glukose, Saccharose und Pflanzenhormonen, einschliesslich Cytokinin, Ethylen, Abscisinsäure und Auxin.

Für die Analyse der regulatorischen Funktion von *PRL1* entwickelten wir zunächst molekulare Werkzeuge um die *PRL1*-Genexpression zu charakterisieren. Ein Volllängen- (4.2 kb) *PRL1*-Promotor, der die Expression des *β-Glukuronidase* (*GUS*)-Reportergens als Fusion mit den ersten 69 Aminosäuren der kodierenden Sequenz des PRL1-Proteins steuert, liess sich in den meisten Geweben als exprimiert beobachten. Zur Identifizierung der regulatorischen Bereiche des *PRL1*-Gens wurde eine Anzahl von Promotordeletionen erzeugt und sowohl in Gewebekultur als auch *in planta* propagiert. Unsere Ergebnisse zeigten, dass intergenische Regionen entscheidend für eine korrekte Genexpression sind, da *PRL1*-Konstrukte, denen das zweite Intron fehlt, nur eine geringe Aktivität aufweisen. Ein kurzer Promotor, der eine alternative TATA-Box, 5′-UTR und einen 0.5 kb grossen kodierenden Bereich einschliesslich der ersten beiden Introns von *PRL1* enthält, zeigt eine GUS-Aktivität ähnlich der des zuvor charakterisierten Volllängenpromotors. Während stromaufwärts gelegene regulatorische Sequenzen (~ 3.5 kb) allein nicht für eine korrekte mRNA-Expression ausreichend sind, konnten Konstrukte die das zweite Intron tragen, in genetischen Komplementationsversuchen vor dem *prl1*-Mutantenhintergrund als funktional nachgewiesen werden. Die Sequenzanalyse legte die Bedeutung einer TC-reichen Region im zweiten Intron nahe. Die Deletion dieser Region führte jedoch nicht zu einer dramatischen Veränderung der Genexpression. Als PRL1 mit dem grünen fluoreszierenden Protein (GFP) markiert wurde, ließ es sich in den meisten Zelltypen als exprimiert und hauptsächlich als im Nukleus lokalisiert nachweisen. Zur Unterscheidung der Rolle des PRL1-Proteins in der Organentwicklung, wurden ein genomisches *PRL1*-Fragment und die cDNA hinter den heterologen Promotoren der *AtKNAT1*; *AtSTM*; *AtUFO*; *AtAS1*; *AtSUC2* und *TobRB7* Gene exprimiert. Während die genomischen Konstrukte in allen Fällen den *prl1*-Phänotyp komplementierten, konnten nur cDNA-Konstrukte, die von den *AtAS*- und *AtSUC2*-Promotoren angetrieben werden, den Blattphänotyp der *prl1*-Mutante komplementieren.

Aufgrund unseres Befundes, dass das Protein instabil ist, wurde eine posttranslationale Regulation für PRL1 postuliert. Der reversible Proteasominhibitor MG132 stabilisiert PRL1 und so liegt die Vermutung nahe, dass PRL1 in einer Proteasom-abhängigen Weise abgebaut wird. Im N-terminalen Bereich von PRL1 konnte ein Zerstörungs- (destruction, D-) Boxmotiv identifiziert werden, welches ein mögliches *Degron* für den „Anaphase Promoting Complex / Cyclosome E3 Ligase (APC) Komplex" darstellt. Entsprechende Punktmutationen wurden eingeführt um die D-Box-Konsensussequenz zu unterbrechen, mit der Zielsetzung so das PRL1-Protein zu stabilisieren. In

Zellsuspension konnte ein höheres Niveau von GFP-markiertem PRL1-Protein als mögliches Ergebnis der stabilisierenden Mutationen nachgewiesen werden, aber in drei Wochen alten Keimlingen war dies nicht der Fall. Aus diesem Grund sind weitere Untersuchungen für ein volles Verständnis der Kontrolle des PRL1-Abbaus erforderlich.

Biochemische Studien belegten die Anwesenheit von PRL1 in einem grossen nuklearen Proteinkomplex assoziiert mit dem Spliceosomkomponenten AtCDC5 Protein. Unsere Daten zeigen, dass AtCDC5 mit verschiedenen Komponenten des Proteindegradationssystems interagiert, wie z.B. mit den 20S Kern- und den 19S Deckelpartikeln des Proteasoms, der CSN5 Untereinheit des COP9-Signalosoms und der SCF E3-Ubiquitinligaseuntereinheit Cullin1. Ausserdem lassen sich ubiquitinylierte Proteine in „pull-down" Versuchen mit AtCDC5 nachweisen, was vermuten lässt, dass Substrate, die für das Proteasom bestimmt sind, möglicherweise mit diesem Komplex assoziiert sind.

Diese Ergebnisse deuten aufgrund seiner Interaktion mit AtCDC5 auf mögliche Rollen für PRL1 beim mRNA-Spleissen und beim Proteasom-abhängigen Proteinabbau hin. Fortlaufende Projekte mit der Zielsetzung eines erweiterten Verständnisses der *PRL1*-Funktion bedienen sich genetischer Ansätze und ortspezifischer Mutagenese.

The *Arabidopsis PLEIOTROPIC REGULATORY LOCUS 1 (PRL1)* encodes a nuclear WD40 protein. Plants carrying a *prl1* insertion mutation are smaller than wild type, have shorter roots, leaves with serrated leaf margins and shorter petioles. In photosynthetic tissues of the *prl1* mutant elevated glucose, sucrose, fructose, starch, anthocyanin and chlorophyll levels are detected. Loss of the *PRL1* function results in hypersensitivity to glucose, sucrose and plant hormones, including cytokinin, ethylene, abscisic acid and auxin.

***

To study the regulatory function of *PRL1*, we first developed molecular tools for characterization of *PRL1* gene expression. A full length (4.2 kb) *PRL1* promoter driving the expression of *β-glucuronidase* (*GUS*) reporter gene in fusion with coding sequences for the first 69 amino acids of PRL1 protein was found to be expressed in most tissues. To identify regulatory regions in the *PRL1* gene, a set of promoter deletions was generated and propagated in cell suspension and *in planta*. Our results demonstrated that intragenic sequences are crucial for correct gene expression as *PRL1* constructs lacking the second intron showed only low activity. A short promoter containing an alternative TATA-box, 5'-UTR and 0.5 kb coding region with the first two introns of *PRL1* showed GUS activity similar to the previously characterized full-length promoter. Whereas upstream regulatory sequences (~3.5 kb) alone were not sufficient for correct mRNA expression, constructs containing the second intron proved to be fully functional in genetic complementation assays in the *prl1* mutant background. Sequence analysis suggested the importance of a TC-rich region in the second intron. However, deletion of this sequence did not affect gene expression dramatically. When PRL1 was tagged with green fluorescent protein (GFP), it was found to be expressed in most cell types and localized mainly in the nucleus. To differentiate the role of PRL1 protein in organ development, a

PRL1 genomic fragment and cDNA were misexpressed using the heterologous promoters of *AtKNAT1; AtSTM; AtUFO; AtAS1; AtSUC2, At4CL1* and *TobRB7* genes. Whereas genomic constructs complemented the *prl1* phenotype in all cases, only cDNA construct driven by the *AtAS1* and *AtSUC2* promoters were able to complement the *prl1* mutant leaf phenotype.

Posttranslational regulation for PRL1 was suggested by our result indicating that the protein is unstable. The reversible proteasome inhibitor MG132 stabilized PRL1 suggesting that PRL1 is degraded in a proteasome-dependent manner. In the N-terminal region of PRL1, a destruction box (D box) motif was identified, which represents a putative degron for the Anaphase Promoting Complex/Cyclosome (APC) E3 ligase complex. Point mutations were introduced to disrupt the D box consensus sequence, in order to stabilize PRL1 protein. In cell suspension higher level of GFP-tagged PRL1 protein could be detected as potential result of stabilizing mutations, but this was not the case in three-week-old seedlings. Therefore, full understanding the control of PRL1 degradation requires further investigations.

Biochemical studies revealed that PRL1 is present in a large nuclear protein complex associated with the spliceosome component AtCDC5 protein. Our data indicate that AtCDC5 interacts with various elements of the protein degradation system, such as the 20S core and 19S lid particles of the proteasome, the CSN5 subunit of the COP9 signalosome and the SCF E3 ubiqutin ligase subunit CULLIN 1. In addition, ubiquitinated proteins were detected in pull-down assays with AtCDC5 suggesting that substrates targeted to the proteasome are potentially also associated to this complex. These results indicate potential roles for PRL1 through its interaction with AtCDC5 in mRNA splicing and proteasome-dependent protein degradation. Ongoing projects aim at further understanding of the *PRL1* function using genetic and site-specific mutagenesis approaches.

.

1. INTRODUCTION

1.1. <u>Sugar signalling in plants</u>

In plant research, a vastly growing interest focuses on the understanding of potential regulatory roles of sugar molecules. Sugars derived from glucose play well-defined roles in various metabolic reactions. For example, oxidation of sugars provides energy for all the life functions and sugar-derived metabolites are used as building blocks in amino acid and fatty acid synthesis and in biosynthetic pathways of secondary metabolites (Lea and Leagold, 1993). The excess of sugars is turned into storage compounds, such as starch, to build reserves in seeds or for starvation conditions. Plants possess a distinctive feature that after a short heterotrophic period can synthesize sugars through photosynthetic pathways. Mature leaf mesophyll cells function as source of photosynthesis-derived sugar compounds and carbohydrates are transported through the vascular system to sink organs, including roots, developing leaves, flowers and seeds that require energy import (Lemoine, 2000).

In plants, carbohydrates play also a pivotal role in development (for review see: Paul and Pellny, 2003; Gibson, 2005). High concentrations of externally provided glucose and sucrose are thus known to delay seed germination; but the germination rate remains apparently unaffected by internal increase of sugar concentrations (Dekkers et al., 2004). A contradictory role of carbohydrates was shown in combination with abscisic acid (ABA) as exogenously provided sugars alleviate the inhibitory effect of ABA on seed germination (Finkelstein and Lynch, 2000). During seedling development, 6% glucose in combination with continuous light conditions inhibits greening and expansion of cotyledons, rosette leaf initiation, root and hypocotyl elongation (Jang et al., 1997). Higher sugar levels stimulate leaf expansion. The timing of developmental changes is also affected by carbohydrates. Several reports suggest that sugar treatment induces flowering (Corbesier et al., 1998; Roldan et al., 1999). However, in other studies both high and low concentrations of exogenous sucrose inhibited the transition to flowering (Ohto et al., 2001). The intrinsic sugar content of plants also appears to control the regulation of onset of senescence as exogenous sugars can induce leaf senescence (Quirinho et al., 2000).

Physiological studies unravelled that carbohydrates act as important signalling molecules that modulate gene expression in connection with sugar metabolism, developmental processes and hormonal pathways (for review see: Smeekens, 2000; Rolland et al., 2002). Sugar signal perception is primarily connected to the functions of cell wall invertases catalyzing the cleavage of sucrose into glucose and fructose that are exported into the cell by specific hexose transporters (see Figure 1). Invertases are also located in the cytoplasm and vacuolar membranes. Sucrose transporters are responsible for sucrose translocation into the cytoplasm. The transported sucrose is subsequently converted into fructose and UDP-glucose by sucrose synthases (for review see: Koch, 2004; Roitsch and Gonzalez, 2004). The prominent sugar signalling cascade is connected to a hexokinase (HXK2), which was proposed to be a major sugar sensor in plants (Jang et al., 1997). Hexokinase substrates, such as glucose, mannose and 2-deoxyglucose inhibit the expression of photosynthetic genes

suggesting a feasible effect of hexokinase signalling on gene expression (Jang and Sheen, 1994). A disaccharide, trehalose was reported to affect plant development and biochemical pathways (for review see Eastmond et al., 2003). Trehalose-6-phosphate is synthesized in *Arabidopsis* by trehalose-6-phosphate synthase and is thought to be an inhibitor of hexokinase transcription (Avonce et al., 2004). The downstream signalling pathways connected to hexokinases are still largely unknown. Analysis of mutations causing sugar insensitivity and oversensitivity revealed that many of them are allelic to mutations previously isolated in ABA and ethylene signalling pathways. These results indicate a close cross-talk between sugar and hormone signalling (for review see: Gazzarrini and McCourt, 2001; Leon and Sheen, 2003). The glucose signalling pathway(s) likely involve also AMP-activated protein kinases that mediate the sensing of the cells' energy status, modulate the activity and stability of metabolic enzymes, regulate gene expression and control the activity and stability of transcription factors (Hardie et al., 1998).
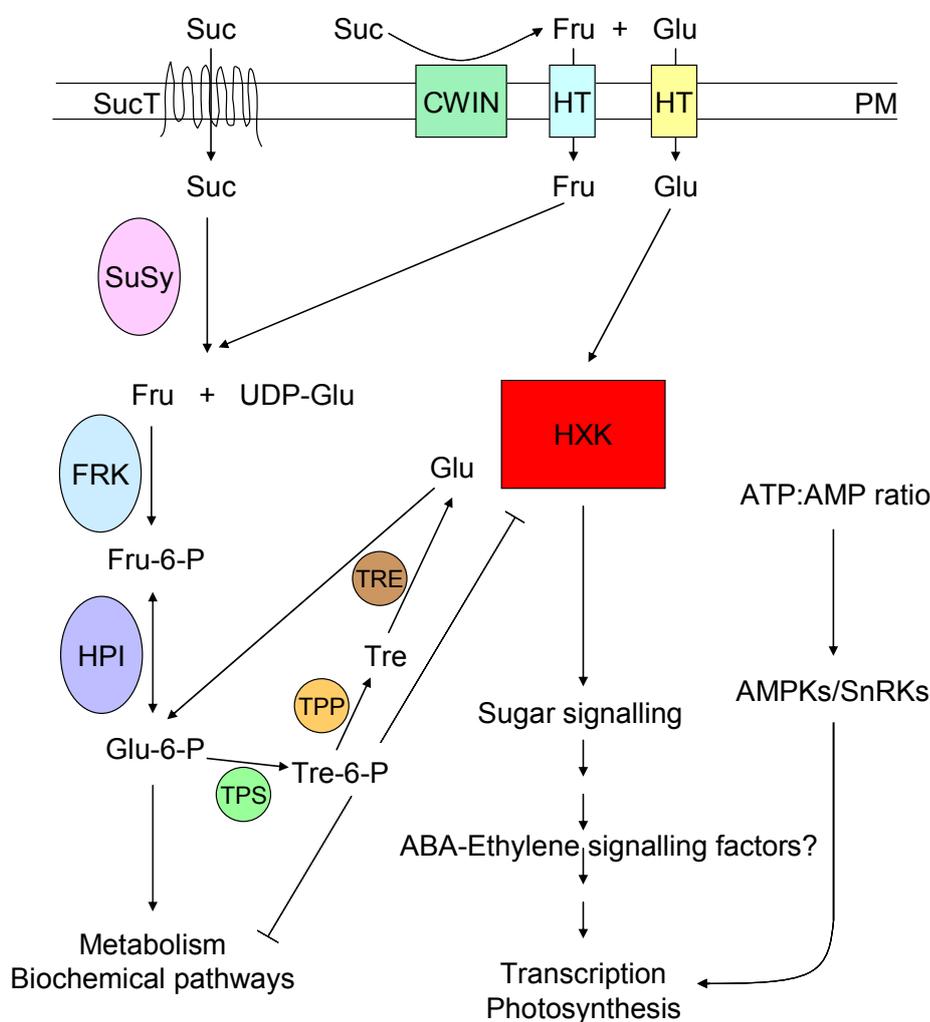
Figure 1.   Simplified model of glucose signalling
Extracellular sucrose (Suc) is either directly transported into the cell by sucrose transporters (SucT) or hydrolyzed into fructose (Fru) and glucose (Glu) by cell wall invertases (CWIN). These monosaccharides are exported directly into the cell by hexose transporters (HT). Sucrose synthases (SuSy) catalyze the sucrose→fructose + UDP-glucose reaction. Subsequently, fructose is phosphorylated by fructokinases (FRK). Fructose-6-phosphate (Fru-6-P) can be turned into glucose-6-phosphate (Glu-6-Pho) by hexose phosphate isomerases and in this form can enter into glycolysis, and further to fatty acid and amino acid biosynthesis.

Hexokinase (HXK2) phosphorylates glucose and is postulated to be a sugar sensor in plant cells. Downstream components of the sugar signalling pathway are not well known. It is suggested that ABA and ethylene signalling factors are also involved. Trehalose-6-phosphate (Tre-6-P), a negative regulator of hexokinase transcription, is synthesized from glucose-6-phosphate by trehalose phosphate synthases (TPSs). Trehalose-6-phosphate is subsequently converted to trehalose (Tre) by trehalose-6-phosphate phosphatases (TPP) and trehalose is hydrolyzed into glucose molecules by trehalase (TRE). AMP activated protein kinases (AMPKs) represent sensors of cellular energy status and also involved in glucose signalling.

1.2. Identification and characterization of the *prl1* mutant

Classical genetic approaches provide powerful tools for identification of genes involved in biochemical or developmental pathways of interest (Koornneef, 1991). Moreover, mutant isolation allows further characterization of potential genetic interactions (e.g., suppressor screens, epistasis analysis etc.). In order to identify novel factors in the sugar signalling pathway, a T-DNA tagged population of *Arabidopsis thaliana* Col-0 wild type plants was germinated on MSAR plates supplemented with either glucose or sucrose (0.1, 0.5, 2, 4, 6, 8 and 10%). 1200 segregating M2 mutant families were screened to identify mutants showing germination defect and/or growth retardation in response to high sugar content (Nemeth et al., 1998). The life cycle of a candidate mutant was arrested on medium containing 6% sucrose or 5% glucose, and mutant plants died subsequently under these conditions (Figure 2 A).
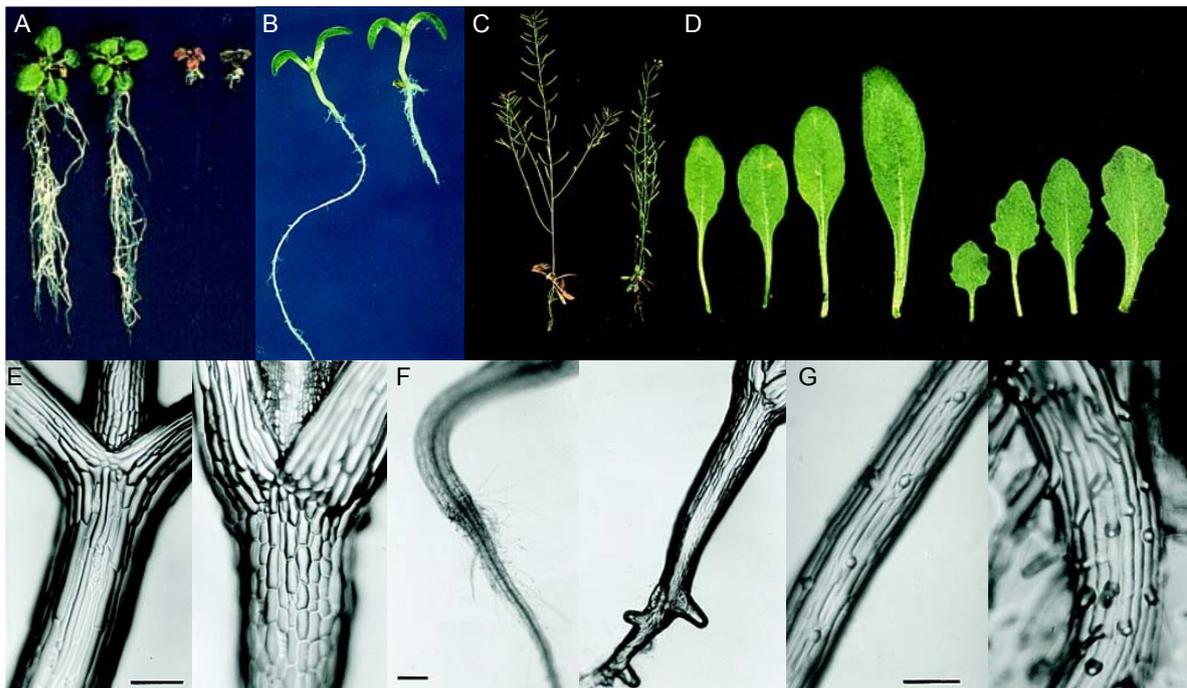
Figure 2. **Phenotype of the *prl1* mutant.**
The effects of a T-DNA insertion in the *PRL1* locus were analyzed in comparison to wild-type Col-0 plants (placed left on the pictures). The figure was adapted and modified from Nemeth et al. (1998). (A) Seedlings were grown on 6% sucrose. (B) Seedlings on MSAR plates containing 0.5% sucrose at light conditions. (C) Soil-grown plants. (D) Phenotype of rosette leaves. (E) Hypocotyls. (F) Roots five days after germination. (G) Root hair formation.

The identified T-DNA insertion event in the *PLEIOTROPIC REGULATORY LOCUS 1* (*PRL1*) resulted in a recessive mutation. Soil-grown mutant plants were smaller then wild type plants, the

leaves were smaller with shorter petioles and had serrated margins (Figure 2 C and D). Chlorophyll and anthocyanin accumulated in the mutant; hence these plants were darker than the wild type. Glucose, fructose, sucrose and starch content of the leaves showed two- to five-fold increase in comparison to the wild type. The most characteristic phenotypic trait for the *prl1* mutation was that the root elongation was reduced two- to three-fold both in light and dark conditions (Figure 2 B). Analysis of the root structure revealed that *prl1* mutant seedlings developed early on side roots and showed ectopic root hair formation (Figure 2 F and G). In addition, elongation of the epidermal cells was inhibited and their number was duplicated in the hypocotyls (Figure 2 E). Hormone responses of the *prl1* mutant were tested on MSAR plates containing auxins (2,4-dichlorophenoxyacetic acid- 2,4-D or 1-naphtaleneacetic acid-NAA), cytokinins (N6-(isopentenyl)adenosine riboside or N6-benzyladenine), abscisic acid, salicylic acid, methyl jasmonate, brassinosteroids, gibberellins and ethephone (i.e. ethylene generating agent). In response to auxin treatment roots of the *prl1* plants were converted into proliferating callus, while wild type roots developed numerous lateral roots densely covered by root hairs. In response to ABA treatment the *prl1* mutant displayed hypersensitive seed germination and bleaching of seedlings at higher ABA concentrations. Combined cytokinin and sucrose treatment of wild type seedlings grown in the light was observed to phenocopy developmental defects of the *prl1* mutation. Etiolated plants treated with ethylene exhibited about 20 to 30% reduction of hypocotyl elongation. In addition, the *prl1* mutant showed growth reduction at 14°C.

1.3. The *Arabidopsis PRL1* gene and PRL1 orthologs

Molecular characterization of the *prl1* mutation revealed that the T-DNA insertion was located in the fourth chromosome disrupting sequences of the gene At4g15900 between exons 15 and 17 (Nemeth et al., 1998). The transcribed region of the *PRL1* gene is approximately 3.5 kb, covering a 38 bp 5' UTR, 17 exons and a 3' UTR of 222 bp. The *PRL1* cDNA of 1461 bp encodes a protein of 54 kDa carrying seven WD40 repeats in its C-terminal region. The *PRL* gene family is small; only one homolog of *PRL1* was identified in the *Arabidopsis* genome. PRL2 (At3g16650) shows 83% amino acid identity with PRL1. The N-terminal region of PRL2 differs considerably from PRL1 (65% identity) as compared to homology between the C-terminal domains of these proteins (89% identity).

A potential ortholog of PRL1, Prp5, was identified in a mutant screen for pre-mRNA splicing defects in fission yeast (*Schizosaccharomyces pombe*, Potashkin et al., 1998). The temperature sensitive *prp5-1* (*precursor mRNA processing 5-1*) mutant was shown to accumulate unspliced U6 snRNA precursor. The phenotype of *prp5-1* yeast cells was analyzed under restrictive conditions. The mutant displays conventional cell division cycle (cdc) phenotype: the yeast cells are elongated and the chromatin is condensed into thin U-shaped structures. Flow-cytometry analysis revealed that the cells were arrested with 2C DNA content. This result indicated that the life cycle of *prp5-1* mutant proceeds through the S phase of cell cycle and stops in G2. Prp46p, another ortholog of PRL1 in *Saccharomyces cerevisiae*, was identified in an extensive two-hybrid screen designed for isolation of mutations in new splicing factors that show interaction with the Prp22p DEAH-box RNA helicase

(Albers et al., 2003). Subsequently, Prp46p was found to interact with Prp45p, a direct binding partner of Prp22p. Deletion of the *PRP46* gene results in non-viable haploid spores. Construction of a conditional mutant strain demonstrated that *PRP46* is essential in budding yeast.

PRL1-related proteins are highly conserved also in other eukaryotes. Fission yeast Prp5p shares 69% identity with *Arabidopsis* PRL1, whereas budding yeast Prp46p shares 63% amino acid identity with PRL1. Analogously, sequence identity is 62% with a *C. elegans* PRL1 homologue and 59% with the human homologue PLRG1 (Nemeth et al., 1998).

1.4. **Conserved WD-repeat proteins**

The family of WD-repeat (also known as Trp-Asp, WD40 or β-transducin motif) proteins contains factors with diverse cellular functions, biochemical activity and subcellular localization. A unique feature of these proteins is that they share short, about 40 amino acid long tandem repeats starting with Gly-His and terminating mainly in Trp-Asp dipeptide motives (van der Voorn and Ploegh, 1992). Notably, sequence identity is low among the members of the WD-repeat family. Rather, they share a common three dimensional structure, which was first described in the case of the Gβ subunit of a heterotrimeric GTPase (Lambright et al., 1996). The β propeller structure of WD-40 proteins consists of seven blades formed by four antiparallel β sheets of WD-repeats (Figure 3). It was reported that one blade is not produced by a single repeat but the C-terminus of the first repeat interlocks with the N-terminus of the next repeat, which might stabilize the three dimensional structure of these proteins (Jawad and Paoli, 2002). The overall structure is a hollow truncated cone, where the small hollow is completely occupied by water molecules (Madrona and Wilson, 2004). This arrangement is known to provide a solid platform for interacting proteins to bind.
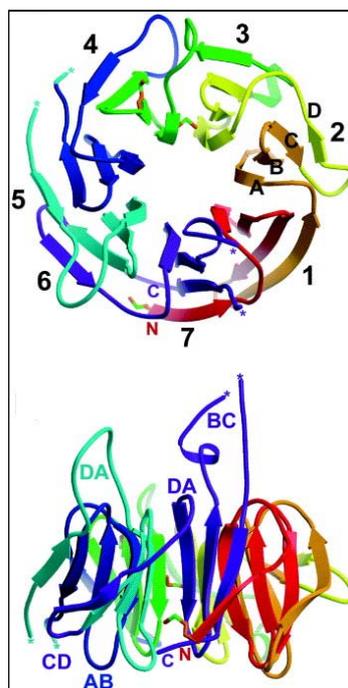
Figure 3.   **Three dimensional structure of WD40 proteins**
The structure of ScBub3p was chosen as a representative of WD-repeat proteins (Larsen and Harrison, 2004). WD40 repeats form four antiparallel β sheets organized into a seven-bladed β propeller structure.

Comparative analysis of WD-40 proteins in the *Arabidopsis* genome was performed by van Nocker and Ludwig (2003). This investigation revealed that 269 *Arabidopsis* proteins contain at least a single WD40-motif, but the majority of the proteins (237) carry four or more tandem repeats. CONSTITUTIVE PHOTOMORPHOGENIC 1 (COP1) is one of the well-characterized members of this family. COP1 carries three distinct domains: a RING-finger motif followed by a coiled coil domain and the WD40 domain (for review see: Yi and Deng, 2005). COP1 was identified as negative regulator of light-dependent photomorphogenic development, since *cop1* mutants show constitutive photomorphogenic phenotype in the darkness (Deng et al., 1991). COP1 functions as E3 ubiquitin ligase that controls the degradation of transcription factors HY5, HYH, LAF1 and HFR1 by the 26S proteasome complex (Saijo et al., 2003; Jang et al., 2005).

1.5. PRL1 family members are subunits of conserved splicing-associated complexes

Biochemical studies revealed that PRL1 orthologs are subunits of evolutionary conserved spliceosome-associated protein complexes. Mass spectrometric analyses have identified components of such complexes in *Schizosaccharomyces pombe* (McDonald et al., 1999; Ohi et al., 2002), *Saccharomyces cerevisiae* (Tsai et al., 1999; Ohi et al., 2002; Hazbun et al., 2003) and human cell cultures (Ajuh et al., 2000). Some of these experiments used the budding yeast SpCdc5p, fission yeast ScCef1p and human HsCDC5L proteins as baits and therefore the associated factors were termed as Cwfs or Cwcs (complexed with Cef1p/Cdc5p) or CCAPs (CDC5L complex associated proteins). Sequence analysis of spliceosome-associated proteins isolated by immunopurification of CDC5 complexes exposed that the Cwf/CCAP complexes (Tarn et al., 1994, Chen et al., 2001, 2002) share common components with the exhaustively studied Prp19p-associated complex (Ntcstands for Prp n̲ine̲teen c̲omplex; Tsai et al., 1999, Ohi and Gould, 2002). The Ntc complex contains at least 11 proteins, whereas 27 distinct factors were identified in the Cwf/Cwc complexes. The common core of Prp and Cwf/Cwc complexes is composed of the Prp19p, Syf1p (Ntc90p), Cef1p (Ntc85p), Clf1p (Ntc77p), Prp46p (Ntc50p), Cwc2p (Ntc40p), Syf2p (Ntc31p), Isy1p (Ntc30p), Snt309p (Ntc25p) and Ntc20p protein subunits. Elements of Prp and Cwf/Cwc complexes are not yet characterized in *Arabidopsis thaliana* (Table 1).

1.5.1. Prp19

Budding yeast Prp19 was identified in a screen searching for temperature sensitive mutants with impaired pre-mRNA splicing (Vijayraghavan et al., 1989). Prp19 was found to carry three canonical domains: a U-box, a coiled coil and a WD40 domain. Members of the U-box protein family were recently identified to function as novel E3 ubiquitin ligases. Comparative sequence analyses and protein modelling studies suggest that the U-box is a derivative of the RING-domain. However, the zinc chelating cysteine residues are not conserved in the U-box proteins (Aravind and Koonin, 2000). The structure of Prp19p was defined using NMR spectroscopy (Ohi et al., 2003) and x-ray crystallography with multi-wavelength anomalous diffraction experiments (Vander Kooi et al., 2006).

The Prp19p U-box domain folds into a similar tertiary structure like RING-fingers; a central α-helix is surrounded by four β-strands and a hydrophobic core. Instead of Zn^{2+} ions, hydrogen bonds and salt bridges stabilize the U-box structure (Ohi et al., 2003). Prp19p forms homotetramers *in vitro* through its coiled coil domain (Figure 4). The U-box domains are located at close proximity of the central coiled coil bundle, whereas the WD40-repeats are flexibly attached (Ohi et al., 2005, Vander Kooi et al., 2006). It is suggested that the U-box is responsible for binding of an E2 ubiquitin conjugating enzyme and that the WD40-repeats can bind the target proteins. Point mutations in the coiled coil region inhibiting tetramerization of Prp19p cannot complement the lethal phenotype of budding yeast *prp19* mutant suggesting that the tetramer formation is essential for proper function of the Ntc complex *in vivo* (Ohi et al., 2005). The Prp19 U-box protein displays ubiquitin ligase activity *in vitro* (Hatakeyama and Nakayama, 2003, Ohi et al., 2003). Surprisingly, the *prp19-1* splicing mutant suffered a V14I substitution in the U-box domain resulting in splicing deficiency. This mutation disrupted the three dimensional structure of the central hydrophobic core region, which might be responsible for interaction with an E2 ubiquitin conjugating enzyme (Ohi et al., 2003). Point mutations disrupting the predicted E2 interface cannot complement the *prp19-1* mutant phenotype; however, the protein folding is not affected (Ohi et al., 2003). Human HsPrp19 interacts directly with the β7 subunit of the 20S proteasome (Loscher et al., 2005). There are only two U-box genes, *UFD2* and *PRP19* in budding yeast, and six genes *UFD2a*, *UFD2b*, *CHIP*, *UIP5*, *CYC4* and *PRP19* in mammals. In *Arabidopsis*, 37 genes are predicted to encode U-box-like factors, two of them represent homologues of Prp19p (At1g04510 and At2g33340; for review see Azevedo et al., 2001).

S. cerevisiae	*A.thaliana*	*Conserved domains*	*Reference*
Prp19p	AtPrp19a At1g04510	U-box, coiled coil, WD40	Ohi et al., 2002; Chen et al., 2002
	AtPrp19b At2g33340		
Syf1p (Ntc90p)	AtSyf1 At5g28740	Tetratricopeptide repeats	Chen et al., 2002
Cef1p (Ntc85p)	AtCDC5 At1g09770	Myb repeats	McDonald et al., 1999; Ohi et al., 2002
Clf1p (Ntc77p)	AtCRN1a At5g45990	Tetratricopeptide repeats	Chung et al., 1999; Chen et al., 2002
	AtCRN1b At3g13210		
	AtCRN1c At5g41770		
	AtCRN2 At3g51110		
Prp46p (Ntc50p)	AtPRL1 At4g15900	WD40	Ajuh et al., 2001; Ohi et al., 2002
	AtPRL2 At3g16650		
Cwc2p (Ntc40p)	AtECM2-1a At1g07360	RNA recognotion motif	Ohi et al., 2002
	AtECM2-1b At2g29580		
	AtECM2-2 At5g07060		
Syf2p (Ntc31p)	AtSyf2 At2g16680	not identified	Chen et al., 2002
Isy1p (Ntc30p)	AtIsy1 At3g18790	Isy1-like splicing family	Chen et al., 2001
Snt309p (Ntc25p)	not found	not identified	Chen et al., 1998; 1999
Ntc20p	not found	not identified	Chen et al., 2001

Table 1. Components of the yeast Prp19-associated protein complexes and their potential orthologs in *Arabidopsis*
The table was adapted and modified from Wang and Brendel (2004).
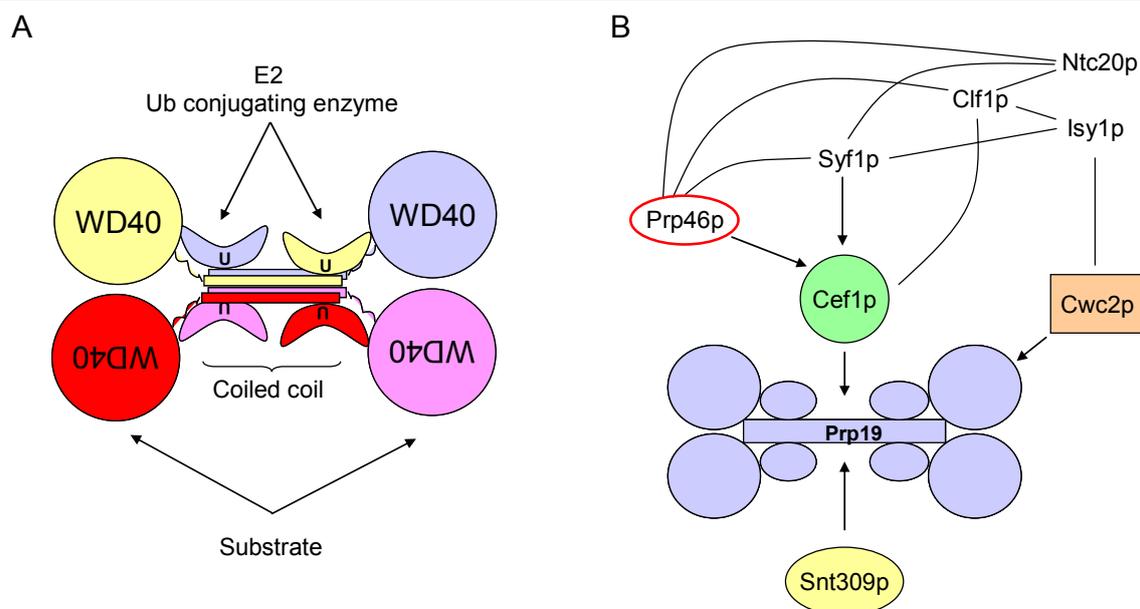
Figure 4.   The Prp19-associated complex
(A) Prp19 forms a homotetrameric complex through its coiled coil domains. The U-box domains (U) probably interact with E2 ubiquitin conjugating enzymes, whereas the WD40-repeats are likely involved in substrate binding. (B) Identified protein interactions in the Prp19- Ntc- complex. The figure was adapted from Ohi et al. (2005).

A weak thermo-conditional mutant allele of *prp19* was isolated in a mutant screen searching for photoactivated psoralen-sensitive yeast mutants (*pso* mutants, for review see: Brendel et al., 2003). These chemicals are successfully used in treatment of skin disorders; however, the risk of skin cancer among the patients increased significantly due to induced DNA lesions. Mutations in the *PSO4* gene were found to cause pleiotropic defects, including increased sensitivity to DNA damaging agents (chemicals and irradiation), low frequency of spontaneous and induced recombination (i.e., gene conversion, crossing over and intrachromosomal recombination). The *pso4* mutation, which entirely blocks pre-meiotic DNA synthesis and sporulation, proved to be allelic with the *prp19* mutation indicating involvement of PRP19 in error-prone DNA repair (Grey et al., 1996). The core Ntc complex (Prp19, Cdc5, Prlg1 and Spf27) is associated with the WRN protein, a RecQ-type DNA helicase and involved in inter-strand cross-link repair (Zhang et al., 2005). In other studies, Prp19 was shown to interact with the terminal deoxynucleotidyl transferase and to play an important role in double-strand DNA repair (Mahajan and Mitchell, 2003). Prp19 was also found in a survey for differentially expressed genes in senescent human cells (SNEV= Senescence Evasion Factor; Grillari et al., 2000). *SNEV* transcription is repressed in senescent human cells, whereas higher SNEV mRNA level is detected in tumour cell lines (Voglauer et al., 2006). Overexpression of SNEV results in an extended life span of endothelial cell lines *in vitro*. This phenomenon is not connected to increased telomerase activity, but the cells show elevated resistance to genotoxic and oxidative stress factors causing double-stranded DNA breaks. The natural occurrence of DNA damage was also significantly lower in the SNEV overexpression lines. SNEV mRNA is upregulated in malignant breast cancer cells.

However, patients expressing enhanced level of SNEV had better survival rate and the formation of lymph node metastases was significantly decreased.

Proteome analysis of nuclear matrix proteins with increased capability of reassembling resulted in the isolation of human nuclear matrix protein 200 (hNMP 200), which was later shown to be identical to Prp19 (Gotzmann et al., 2000). Study of subcellular localization of GFP-tagged hNMP 200 indicated that this protein is mainly located in the nucleus, but not in the nucleolus. At the nuclear periphery, speckle formation was detected. In prophase, hNMP 200 is uniformly distributed and not associated with the chromosomes. In metaphase, an enhanced hNMP 200 signal is detected around the aligning chromosomes. During anaphase, hNMP 200 is localized to the mitotic spindles throughout chromosome segregation.

1.5.2. CDC5

Cdc5p is highly conserved both structurally and evolutionally through various model organisms (Ohi et al., 1998; Hirayama and Shinozaki, 1996). Initially, cdc5$^+$ was identified as a cell division cycle mutant in *S. pombe*. The *cdc5-120* mutation arrests cells in the G2 phase of cell cycle before mitosis (Ohi et al., 1994). The N-terminal region of Cdc5 carries three helix-turn-helix DNA-binding Myb domains referred to as R1, R2 and R3. However, the third repeat is imperfect as it possesses a Val-Leu substitution at a critical position (Carr et al., 1996; Ogata et al., 1996). In the *Arabidopsis* genome, three groups of Myb proteins are encoded: Myb1R factors with one, R2R3-type Myb factors with two, and Myb3R proteins with three Myb repeats (for review see Jin and Martin, 1999; Stracke et al., 2001). Two well-characterized members of the MybR1 family are the circadian clock-related transcription factors CCA1 (Circadian Clock Associated 1) and LHY1 (Late elongated Hypocotyl 1). The majority of plant Myb-like regulators carries two repeats and is involved in diverse regulatory processes (e.g., Transparent testa 2-TT2, Production of anthocyanin pigment 1-PAP1, Glabrous 1-GL1, Assymetric leaves 1-AS1, Werewolf-WER). The Myb3R factors are involved in cell cycle regulation.

Arabidopsis CDC5 binds double-stranded DNA in a sequence specific manner. CDC5 recognizes the CTCAGCG (complementary CGCTGAG) consensus sequence (Hirayama and Shinozaki, 1996). Human HsCdc5 binds a consensus sequence of 12 bp (GATTTAACATAA). The core ANCA motif is a typical target for Myb-like helix-turn-helix transcription factors. The flanking symmetrical TTA/TAA sequence increases the binding affinity of Cdc5 (Lei et al., 2000). A CDC5 ortholog in the basidiomycete mushroom *Lentinula edodes* specifically binds to the sequence GCAATGT (Miyazaki et al., 2004). However, budding yeast ScCef1p, which can complement the fission yeast *cdc5-120* mutation, was not observed to have any DNA binding activity (Ohi et al., 1998).

Cdc5 is phosphorylated by a cAMP-dependent protein kinase in Lentinula (Miyazaki et al., 2004). PCDC5RP immunopurified from COS-7 cells is also phosphorylated (Bernstein and Coughlin, 1997), whereas rat Cdc5 is suggested to be a substrate for protein kinase CK2 (Engemann et al., 2002).

Human CDC5L is known as a mitotic phosphoprotein; it is phosphorylated *in vitro* by cyclinB-cdc2 and cyclin E-cdc2 (Stukenberg et al., 1997; Boudrez et al., 2000). CDC5 was found to interact with a DAP-like serine/threonine-specific protein kinase in the yeast two-hybrid system and this result was verified by *in vitro* binding experiments (Engemann et al., 2002). Co-localization studies further support direct interaction between these proteins, since the DAP-kinase and CDC5 are both localized to nuclear speckles. However, Cdc5 is not phosphorylated by the DAP-like kinase *in vitro*. Cdc5 is also a binding partner of NIPP1, a member of PP1 serine/threonine protein phosphatase regulator factors that shows co-purification and co-localization with PP1C and CDC5L (Boudrez et al., 2000). This interaction depends on the phosphorylation state of CDC5L, only phosphorylated CDC5L is able to bind to NIPP1.

In *Arabidopsis* a single gene encodes a CDC5 ortholog. *Arabidopsis* AtCDC5 (At1g09770) can complement the *S. pombe cdc5-120* mutation suggesting functional similarity of CDC5 orthologs between different organisms (Hirayama and Shinozaki, 1996). Expression of the *AtCDC5* gene was analyzed by *in situ* hybridization and Northern blot experiments. The AtCDC5 mRNA shows a strong localization to shoot and root apical meristems and leaf primordia. AtCDC5 is expressed in most tissues studied; the highest transcript levels are detected in roots.

1.5.3.   Crooked neck (CRN) proteins

The *Crooked neck (crn)* locus was originally identified in a genetic screen for *Drosophila* embryo lethal mutations and mapped into the X chromosome. *Crn* mutant embryos display serious disorders during the development of nervous system, midgut and muscles (Perrimon et al., 1984). Yeast *crn* knockout mutant shows a cell cycle phenotype, the dividing cells are arrested between the G2 and M phase (Russell et al., 2000; Zhu et al., 2002) The CRN protein belongs to the tetratricopeptide repeat (TPR) family. The TPR motif is involved in mediation of protein-protein interactions (for review see Blatch and Lassle, 1999). Orthologs of CRN (Clf1p/Syf3p/Ntc77p) protein were characterized in connection with the spliceosome complex in yeast (Chung et al., 1999; Wang et al., 2003), in *Drosophila* (Raisin-Tani and Leopold, 2002) and in humans (Chung et al., 2002). In yeast, however, Clf1p (Crooked neck-like factor 1) is considered as one of the moonlighting proteins with a novel role in DNA replication (Jeffery, 2003). Temperature sensitive *clf1* mutants show cell cycle arrest between the G2/M transition (Zhu et al., 2002). However, when cells are blocked in G1 with α-factor, they display a delay in DNA accumulation and fail to enter the S phase. Physical interaction between Clf1p and the replication origin binding ORC complex was detected by yeast two-hybrid analysis and co-immunoprecipitation. A possible link between Clf1 and vesicular transport proteins is also suggested (Vincent et al., 2003). The *Arabidopsis* genome encodes four Crn orthologs: AtCRN1a (At5g45990), AtCRN1b (At3g13210), AtCRN1c (At5g41770) and AtCRN2 (At3g51110), but these genes are yet not characterized.

1.6.   <u>Function of the Prp19-associated complex in splicing</u>

Transcription of eukaryotic genes that carry protein coding exons and non-coding intervening sequences, called introns, results in the synthesis of precursor RNA molecules. The intron sequences are excised from the pre-mRNAs in the nucleus and the messenger RNAs are transported to the cytoplasm for protein translation. Pre-mRNAs carry short consensus sequence elements at the 5' (GU) and 3' (AG) ends of intron boundaries flanking an internal branch site (UACUAAC).These sequences are recognized by the splicing machinery. The splicing reaction occurs by two trans-esterification reactions, in which covalent bonds are transferred from one location to another. This reaction does not require ATP hydrolysis. A free 2'-hydroxyl group of the branch site attacks the phosphate at 5'-end, and the reaction yields a looped lariat intermediate with the intron sequence and a cut mRNA. In the second step, the 3'-hydroxyl group of 5'-exon attacks the 3' splice site resulting in a spliced and ligated mRNA molecule and a lariat form of intron sequence.

The large holoenzyme complex catalyzing the intron excision is named spliceosome that carries small nuclear ribonucleoprotein particles (snRNPs; U1, U2, U4, U5 and U6). The assembly of spliceosome and the splicing reaction are highly organized sequential process (for reviews see: Staley and Guthrie, 1998; Murray and Jarrell, 1999; Lorkovic et al., 2000) (Figure 5). The first step is the formation of the E (early presplicing) complex, in which the U1 snRNP binds to the 5' splice junction in a sequence specific manner aided by complementary snRNA of this ribonucleoprotein complex. Subsequently, U2 binds to the branch site and the A complex of spliceosome, which is also called a pre-spliceosome, is assembled. The B complex is formed in two steps. First, the U5/U4/U6 tri-snRNPs bind to the precursor RNA-splicing complex, which undergoes a structural rearrangement by releasing the U1 and U4 particles. This step is followed by formation of base pair interactions between U6 and U2, and between U6 and the 5' splice site. During these stages, an enzymatically active spliceosome C complex is assembled that can catalyze intron excision and exon ligation by two trans-esterification reactions.

With the discovery of AT-AC type introns, which represent a minor class of intron regions defined by evolutionarily conserved but distinct consensus sequences at the 5' and 3' splicing junctions, the existence of an alternative spliceosome became evident (for reviews see Kreivi and Lamond, 1996; Tarn and Steitz, 1997; Lorkovic et al., 2000). This alternative splicing complex shares only the U5 snRNP component with the canonical spliceosomal complex and contains unconventional U11, U12, U4atac and U6atac particles.

The Prp19/Cdc5 related complex is associated with the U2/U5/U6 tri-snRNP complex (Tarn et al. 1994; Ohi et al., 2002). The assembly of spliceosome and formation of intermediates can be analyzed using different ATP concentrations *in vitro*. At low ATP concentration inactive pre-splicing forms of spliceosome (Complex A and B) accumulate, while increasing the ATP concentration induces the assembly and rearrangement of spliceosome as these steps requires ATP hydrolysis. The analysis of distinct snRNP complexes revealed that the Ntc complex is associated to the spliceosome after the release of the U4 particle (Chan et al., 2003). After dissociation of U4 snRNP, the splicing

complex is reorganized and the spliceosome becomes activated. Three complementary binding sites were identified for the U6 snRNP at the 5'-splice junction by cross-linking experiments (Chan et al., 2003). One was predominantly found in inactive spliceosome complexes, whereas the two others were identified during the splicing reaction suggesting that a switch in binding happens during spliceosome activation. The Ntc-depleted U6 snRNP is exclusively found in inactive binding regions (Chan and Cheng, 2005). Similarly, the U5 snRNP occupies only two inactive binding sites in Ntc-depleted splicing reactions. These data suggest that the Ntc complex is required for the stable association of U5/U6 snRNPs to the mRNA complementary sequences, and that the Ntc helps to lock the spliceosome at the active position.
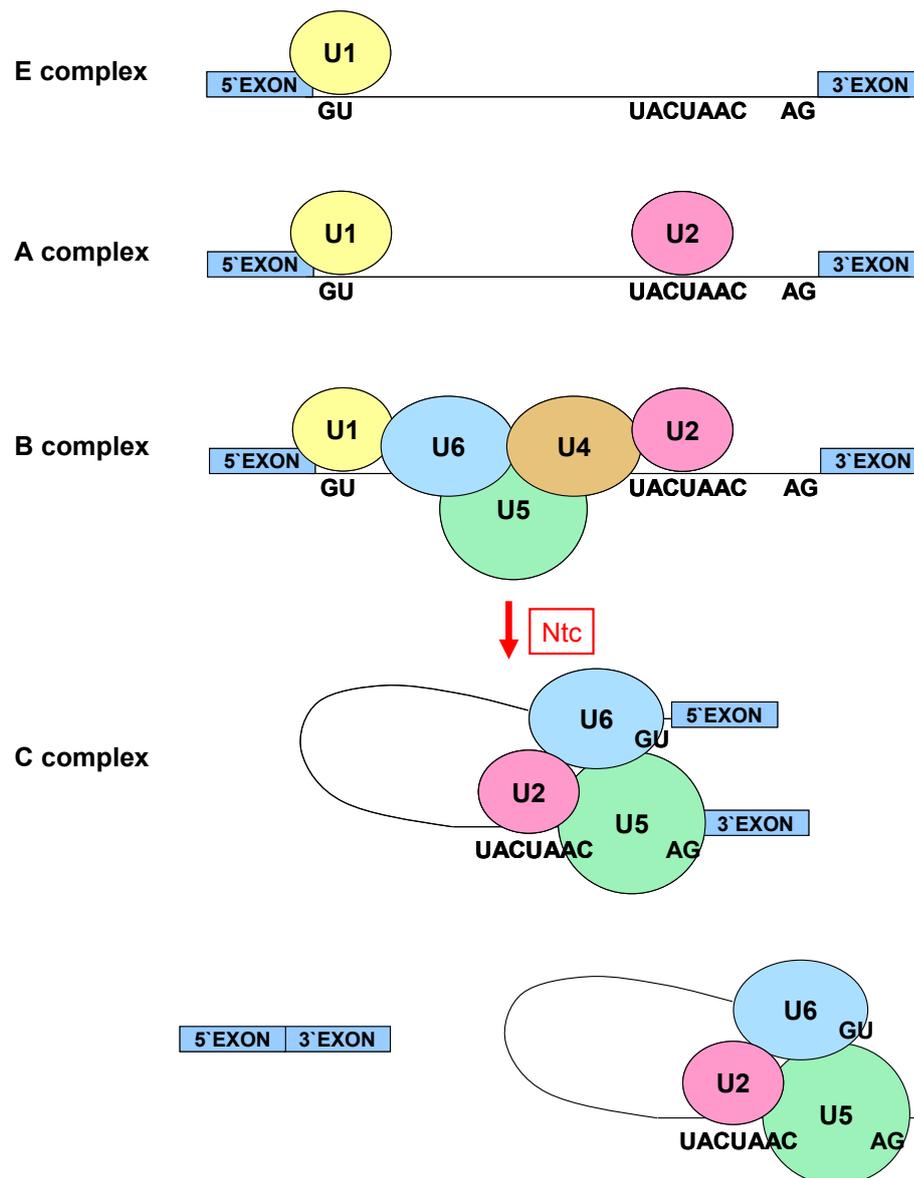
Figure 5.   Role of Ntc Prp19-complex in splicing
Intron excision and exon ligation are highly organized sequential processes. Splicing starts with the recognition of 5'-splice site by the U1 snRNP (E complex). Subsequently, the U2 particle binds to the branch site of the intron (A complex). The B complex, carrying all five snRNPs on the precursor RNA, is still inactive. After the releasing of U1 and U4 snRNPs the spliceosome becomes activated by the Ntc complex (C complex). The active spliceosome catalyzes two trans-esterification reactions that result in the removal of intervening intron and ligation of adjacent exons.

1.7. PRL1 interacts with SNF1 related protein kinases of AMP-activated (AMPK) kinase family

Since mutation of the *PRL1* gene causes severe sugar and hormone-related phenotypic defects, it was assumed that signalling through PRL1 could be connected to overall regulation of these pathways by AMP-activated protein kinases (AMPKs). These kinases play a central role in the maintenance of a constant high ratio of ATP:ADP to store adequate energy source for normal cellular functions. Under stress, when ATP is limiting, the adenylate kinase catalyses the reaction of 2ADP→ATP + AMP, and accumulation of the AMP signal is an indicator of cell starvation (for reviews see: Hardie et al., 1998; Hardie, 2004). AMPKs play in role in the regulation of stress responses (e.g., oxidative stress and hypoxia) that lead to sudden decrease of intracellular ATP level. AMPK core complexes consist of three distinct subunits, the catalytic α, substrate targeting β and activating γ subunits. AMPK α subunits (e.g., Snf1 in yeast) carry a conserved serine/threonine protein kinase domain at their N-termini and a C-terminal regulatory domain targeted by interactioning proteins. The substrate targeting β subunits (e.g., Sip1, Sip2 and Gal83 in yeast) carry a KIS (kinase interaction sequence) domain, which is known to bind glycogen in mammalian cells, and an interaction domain called ASC (association with SNF1 complex). Downstream of the highly variable N-terminal sequences, the AMPK γ-subunits (e.g., Snf4 in yeast) contain four tandem CBS (cystathionine β-synthase) domains, which are important for AMP and ATP binding. Snf1, the prototype of AMPK family in yeast, plays a key role in glucose repression through inhibiting the Mig1p transcriptional repressor of glucose regulated genes and activation of Sip4 and Cat8 positive regulators, which activate gene expression in response to glucose starvation (for review see: Carlson, 1999).

Using *Arabidopsis* PRL1 in fusion with the Gal4 activation domain, possible PRL1 interactions with budding yeast Snf1p (sucrose non-fermenting 1) and Snf4p AMPK subunits were tested in two hybrid experiments by Bhalerao et al. (1999). The activation of *HIS3* and *LacZ* reporter genes was observed in the yeast strain expressing *SNF1-GBD* and *PRL1-GAD*. Three orthologs of Snf1p were identified in *Arabidopsis* referred to as SNF-related protein kinase 1α (SnRK1α) or AKIN10, AKIN11 and AKIN12. Two of them, AKIN10 and AKIN11, were demonstrated to interact with PRL1 in the yeast two-hybrid system. The positions of the interaction domains in PRL1 and the SnRK1α kinase subunits AKIN10 and AKIN11 were mapped using a set of deletion constructs. These data indicated that an N-terminal region of PRL1 residing between amino acid residues 35 and 195 is required for interaction with AKIN10 and AKIN11. The C-terminal WD40-repeat domain of PRL1 appeared to inhibit binding of these kinases as the strength of interaction observed with the full-length PRL1 protein was weaker as compared to the N-terminal domain. The PRL1-binding region was mapped to the C-terminal SNF4-binding region of AKIN10 kinase subunit. The interaction between PRL1 and AKIN10/11 kinases was induced in yeast by low glucose (0.05%) treatment (i.e. glucose starvation). The interaction between PRL1 and AKIN10/11 kinases was confirmed in protein binding assay *in vitro*. PRL1 was observed to inhibit in a concentration dependent fashion the phosphorylation activity of both AKIN10 and AKIN11 kinases towards the specific TRX-KD substrate *in vitro*.

1.8.   *Arabidopsis* SnRK1α kinases are found in association with the proteasome

Recent studies highlighted the essential role of protein degradation in the control of basic cellular functions in plants. Surprisingly, approximately 5% of the *Arabidopsis* proteome represents factors involved in protein degradation (for review see Smalle and Vierstra, 2004; Moon et al., 2004). From the various proteolysis pathways, the ubiquitin/proteasome pathway is the best characterized and thought to be the most important in the plant system. In this pathway, proteins targeted for degradation are marked with ubiqutin (Ub) chain formation on lysine residues. The ubiquitination cascade is ATP dependent and requires three catalytic steps. An ubiquitin activating enzyme (E1) forms a thioester bond with the Ub and transfers Ub to the ubiquitin conjugating enzyme (E2). Ubiquitin ligases (E3s) play crucial roles in the recognition of substrates and in subsequent formation of Ub-chains on their substrate targets. The 26S proteasome degrades the ubiquitinated proteins. This multisubunit enzyme complex consists of a cylindrical 20S core particle and two 19S lid subunits at the ends.
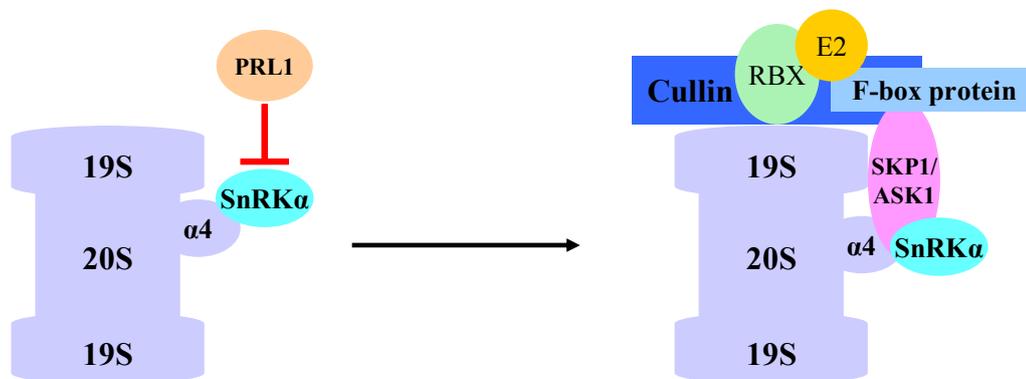
Figure 6.   **Proteasomal complexes of SnRK1α AMPK kinases**
PRL1 is a negative regulator of SnRK1α kinases (AKIN10/11) and competes for a common binding site shared with the SKP1/ASK1 SCF E3 ubiquitin ligase subunit. The model proposes that SnRK1α kinase and the SCF E3 ligase subunits CULLIN 1 and SKP1/ASK1 are assembled in a common SCF-proteasome complex when PRL1 is depleted (e.g., degraded). This figure is adapted from Farras et al. (2001).

The SnRK1α subunits, AKIN10 and AKIN11 were used as baits in yeast-two-hybrid assay, in order to find specific interacting partners. Some well-known elements of the proteasomal degradation system were uncovered by this screen. SKP1/ASK1 (S phase kinase-associated protein 1/*Arabidopsis* Skp1-like 1) and the α4/PAD1 subunit of the 20S proteasome were found to bind specifically to the C-terminal domains of AKIN10 and AKIN11 kinases (Farras et al., 2001). These data were also confirmed by *in vitro* binding assay. The ASK1-binding domain of SnRK1α kinases were identified using a series of deletion constructs and mapped to the region of C-terminal regulatory domain of AKIN11, which interacts with the β and γ SnRK1 subunit and PRL1. Competitive binding experiments showed that PRL1 inhibits interaction of SKP1/ASK1 with the SnRK1α kinase subunits. The SnRK1α subunits co-purified with the 26S proteasome isolated from *Arabidopsis* cell suspension. Co-immunoprecipitation experiments with total protein extract and purified proteasome from CaMV35S::ASK1-HA expressing cell suspension revealed that an SnRK1α kinase subunit, either AKIN10 or AKIN11 occurs in common proteasomal complexes with the SKP1/ASK1 and CULLIN 1

subunits of SCF E3 ubiqutin ligase complexes. These data suggested that when PRL1 binds to the SnRK1α kinases the SKP1/ASK1 subunit of SCF E3 ubiquitin ligases is competed out (Figure 6). Hence, PRL1 and SKP1/ASK1 are predicted to occur in distinct proteasomal complexes. Consequently; when the SnRK1α kinase is no longer inhibited by PRL1, interaction of the kinase with SKP1/ASK1 can target SCF E3 ubiquitin ligase complexes and their specific substrates to the proteasome.

1.9. <u>Aims of the present work</u>

Carbohydrates play a central role in plant metabolic and developmental processes. Nonetheless, the mechanisms governing sugar signalling are still not understood in detail. With the isolation of the *prl1* insertion mutant, a potential novel regulator in the sugar signalling cascade was identified (Nemeth et al., 1998). The *prl1* mutant displayed hypersensitivity to sucrose, glucose and plant hormones, such as ethylene, ABA, auxin and cytokinin. Moreover, several sugar, ethylene and ABA regulated gene was found to be upregulated by the *prl1* mutation. Several PRL1 interacting partners, including the SnRK1α subunits of *Arabidopsis* AMP-activated kinase orthologs, were identified in yeast-two-hybrid screens and confirmed by *in vitro* pull-down assays (Bhalerao et al., 1999). Further studies suggested that PRL1 inhibits the activities of SnRK1α kinases and competes with binding of the SKP1/ASK1 subunits of SCF E3 ubiquitin ligase subunit to proteasome-associated SnRK1α proteins (Farras et al., 2001). This data connected PRL1 function to SCF and proteasome-dependent protein degradation pathways.

The major goal of the Ph.D. project was to characterize some of the regulatory roles played by PRL1 in sugar, hormone and developmental pathways. The studies described in this thesis were designed

⇨ To characterize temporal and spatial regulation of *PRL1* promoter activity using *β-Glucuronidase* reporter gene fusions with *PRL1* transcription regulatory sequences,

⇨ To characterize regulatory elements of the *PRL1* promoter using a set of promoter deletions,

⇨ To search for transcription factors that bind to regulatory elements of the *PRL1* promoter in yeast one-hybrid assays,

⇨ The study cellular and subcellular localization of the PRL1 protein using HA-epitope labelled and GFP-tagged PRL1 constructs in combination with indirect immunofluorescence confocal laser scanning microscopy,

⇨ To analyse the effects of PRL1 misexpression using genomic and cDNA constructs expressed by cell type and tissue specific promoters in a *prl1* genetic complementation system,

⇨ To study the stability of PRL1 protein *in planta* using a chemically-inducible gene expression system,

⇨ To test possible involvement of proteasome-dependent degradation in the regulation of PRL1 protein stability in cell suspensions and *in planta* using proteasome inhibitors,

⇨ To identify possible destruction signals (degrons) and analyse their effects on the stability of PRL1 protein by site-specific mutagenesis and expression studies in cell suspension and *in planta*.

⇨ To perform basic biochemical characterization of the PRL1 protein complex using epitope labelling and immunoprecipitation approaches,

⇨ To test potential interaction of PRL1 with the evolutionary conserved spliceosome-associated AtCDC5 protein in yeast two-hybrid and immunoprecipitation assays,

⇨ To investigate potential proteasomal interaction of PRL1 and AtCDC5 proteins using immunoprecipitation and western blotting with specific antibodies.

⇨ To identify new *prl1* mutant alleles and search for mutations in the *PRL2* gene that codes for a PRL1 homologue,

⇨ To initiate the construction of *prl1* double mutants with mutations in genes coding for PRL1 interacting proteins, and

⇨ To perform site-directed alanine scanning mutagenesis of PRL1 for further mapping of regulatory and protein interaction domains.

2. MATERIALS AND METHODS

2.1. <u>Materials</u>

2.1.1. Chemicals, enzymes and laboratory supplies

<u>Company</u>	<u>Product</u>
Affiniti Research Products Ltd., Mamhead, UK:	Antibodies
Amersham Biosciences GmbH, Freiburg, Germany:	ECL^{TM} Enhanced Chemiluminescence Kit Gradient mixer Hybond^{TM}-N nylon membrane Hyperfilm^{TM} Peristaltic pump
Beckman Instruments Inc., Palo Alto, USA:	Centrifuge tubes
Bethyl Laboratories Inc., Montgomery, USA:	Anti-Ubiquitin antibody
BIOMOL GmbH, Hamburg, Germany:	X-Gal(5-Bromo-4-Chloro-3-Indolyl-1-ß-D-galactopyranoside) X-Gluc(5-Bromo-4-Chloro-3-Indolyl-1-ß-D-glucuronide CHA-salt) MG132
Bio-Rad, München, Germany:	Bradford Reagent Pre-stained Protein Standard Goat anti-Rabbit-HRP IgG (H+L)
Boehringer Mannheim, Germany:	RNase A
Calbiochem Corp., Darmstadt, Germany:	Ethidium bromide Miracloth
Clontech, Palo Alto; USA:	Salmon sperm carrier-DNA TransfromerTM site-directed mutagenesis kit
Corning Inc., Corning, USA:	Costar® Disposable Serological Pipettes
Difco Laboratories, Detroit, USA:	Bacto-agar Bacto-peptone Bacto-tryptone Yeast Extract Yeast Nitrogen Base without amino acids
Duchefa, Haarlem, the Netherlands:	ATP Carbenicillin Disodium Salt Cefotaxime sodium Phytoagar Ticarcillin/Clavulanic Acid
Eppendorf AG, Hamburg, Germany:	Safe-lock tubes (0.5, 1.5 and 2.0 ml) Single use pipette tips
Eastman Kodak Co., Rochester, USA:	Kodak X-Omat AR-5 Film
Cambrex Bio Science Inc., Rockland, USA:	Seakem® LE Agarose

Invitrogen GmbH, Karlsruhe, Germany:	1kb molecular mass marker Gateway® LR Clonase™ enzyme mix Platinum® *Pfx* DNA polymerase Restriction endonucleases *Taq* DNA Polymerase, recombinant
Greiner bio-one GmbH, Kermsmünster, Austria:	Petri dishes Falcon tubes (15 and 50 ml) Cellstar® Suspension culture plates
Heirler Cenovis GmbH, Radolfcell, Germany:	Milk Powder
Merck, Darmstadt, Germany:	2-propanol Chloroform Ethanol D-Glucose Glycine Nystatine N,N-dimethylformamide General chemicals
Metabion International AG, Martinsried, Germany	Oligonucleotides
Millipore, Bedford, USA:	Filter 0.025μm white VSWP Immobilon™-P (PVDF membrane) Sterivex™ 0.22μM filter units
New England Biolabs, Frankfurt am Main, Germany:	Antarctic Phosphatase Restriction Endonucleases T4 DNA ligase T4 Polymerase
Qiagen GmbH, Hilden, Germany:	QIAprep® Spin Miniprep kit QIAquick® Gel extraction kit QIAquick® PCR purification kit
Peqlab Biotechnologie GmbH, Erlangen, Germany:	E.Z.N.A.® Plasmid miniprep kit I.
Pierce Biotechnology Inc., Rockford, USA:	Goat anti-Chicken IgG, (H+L), HRP Goat anti-Rabbit IgG, (H+L), HRP Rabbit anti-Chicken IgG, (H+L), HRP Restore™ Western Blot Stripping Buffer
Riedel de Haen, Seelze, Germany:	Ca-hypochlorite
Roche Diagnostics GmbH, Mannheim, Germany:	Alkaline phosphatase from calf intestine anti-GFP anti-HA anti-c-Myc Hygromycin
Carl Roth GmbH, Karlsruhe, Germany:	dNTP solutions Filter units 0.22μm Phenol Rotiphorese® 40 (29:1)
Santa Cruz Biotechnology Inc., Santa Cruz, USA:	Protein A/G PLUS-Agarose

HA probe (F-7)

Sartorius AG, Göttingen, Germany: Minisart 0.22µm and 0.45µm filter units

Serva Electrophoresis GmbH, Heidelberg, Germany: Bromphenol Blue-Na-salt
Ponceau S solution
Sarcosyl
SDS

Sigma-Aldrich Co., St. Louis, USA: Amino acids
Ammoniumpersulfate
Antibiotics
BSA
c-Myc peptide
Cyclohexymide
CTAB (Cetyl-trimethylammonium bromide)
DTT (Dithiothreitol)
Goat anti-Rat IgG, (H+L), HRP
HA-peptide
Igepal
Lithium acetate
Lyticase
MS-Basal salt mixture
MS-Basal salt with minimal organics/ MSMO
PEG (Polyethylene glycol) MW 3350
PMSF (Phenylmethylsulphonyl fluoride)
PVP-40 (Polyvinyl pyrrolydone-40)
β-mercaptoethanol
Sodium deoxycholate
Sucrose
TEMED
TritonX-100
Tween-20
General chemicals

Upstate Co., Lake Placid, USA: Anti-Histone 2A antibody

Takara Bio Inc., Otsu, Shiga, Japan: TaKaRa LA Taq^{TM} DNA Polymerase

Whatman, Maidstone, USA: 3MM paper
Whatman circles

2.1.2. Bacterial Strains

2.1.2.1. *E. coli strains*

BMH 71-18 mutS   *thi sup*EΔ(*lac-pro*AB) [*mutS*::Tn10][F' *pro*AB, *lac*I^q ZΔM15]

DB3.1   F$^-$ *gyr*A462 *end*A1 (*sr*1-*rec* A) *mcr* B *mrr hsd* S20(rB$^-$,mB$^-$) *sup* E44 *ara*14 *gal*K2 *lac*Y1 *pro*A2 *rps*L20(Sm^R) *xyl* 5 .*leu mtl*1

HB101 (DH10B)   Δ(*mrr-hsd* RMS-*mcr*BC) *mcr*A *rec*A1

2.1.2.2.   *Agrobacterium tumefaciens strains*

GV3101 (pMP90)   C58C1, rif, pMP90 (pTiC58ΔT-DNA), Gm^r (Koncz and Schell, 1986)

GV3101 (pMP90RK)   C58C1, rif, pMP90RK (pTiC58ΔT-DNA), Gm^{r,} Km^r (Koncz and Schell, 1986)

2.1.2.3.   *Yeast strains*

Y190   MAT**a**, ura3-52, his3-Δ200, lys2-801, ade2-101, trp1-901, leu2-3, 112, gal4Δ, gal80Δ, URA3::GAL1$_{UAS}$-GAL1$_{TATA}$-lacZ, cyh^{r}2, LYS::GAL1$_{UAS}$-HIS3$_{TATA}$-HIS3 (Flick and Johnson, 1990; Harper et al., 1993)

Y187   MATα, ura3-52, his3-200, ade2-101, trp1-901, leu2-3, 112, met, gal4Δ, gal80Δ, URA3::GAL1$_{UAS}$-GAL1$_{TATA}$-lacZ (Harper et al., 1993)

YM4271   MATa, ura3-52, his3-200, ade2-101, lys2-801, leu2-3, 112, trp1-901, tyr1-501, gal4-Δ512, gal80-Δ538, ade5::hisG (Liu et al., 1993; Wilson et al., 1991).

2.1.3.   Plant material

2.1.3.1.1.   <u>Arabidopsis thaliana</u>

<u>Genotype</u>	<u>Ecotype</u>	<u>Obtained from</u>
Wild type	Col-0	Rédei, 1992
prl1	Col-0	Nemeth et al., 1998
prl1 SALK_008466	Col-8	Alonso et al., 2003
prl1 SALK_039427	Col-8	Alonso et al., 2003
prl1 SALK_096289	Col-8	Alonso et al., 2003
prl1 SAIL_1276G04	Col	Sessions et al., 2002
prl2 GABI_228D02	Col-0	Rosso et al., 2003
prl2 KONCZ16136	Col-0	Rios et al., 2002
pip-a GABI_197C07	Col-0	Rosso et al., 2003
pip-c SALK_010773	Col-8	Alonso et al., 2003
pip-c SALK_039094	Col-8	Alonso et al., 2003
pip-d SAIL 586 H06	Col	Sessions et al., 2002
pip-d KONCZ38225	Col-0	Rios et al., 2002
cpb20 KONCZ372	Col-0	Papp et al., 2004
pip-e SAIL_613D12	Col	Sessions et al., 2002
pip-f SALK_014647	Col-8	Alonso et al., 2003
pip-h KONCZ65425	Col-0	Rios et al., 2002
pip-i SALK_000718	Col-8	Alonso et al., 2003
pip-i SALK_011213	Col-8	Alonso et al., 2003
pip-i GABI_160C01	Col-0	Rosso et al., 2003
pip-i Wisc446659	Col-0	Sussman et al., 2000
pip-k SAIL_1284G09	Col	Sessions et al., 2002
pip-k KONCZ77621	Col-0	Rios et al., 2002
pip-l SALK_037227	Col-8	Alonso et al., 2003
CS85391	Col er 105	NASC
CS86061	Col er 105	NASC

CS86130	Col er 105	NASC
CS87948	Col er 105	NASC
CS91910	Col er 105	NASC
CS92359	Col er 105	NASC
CS93156	Col er 105	NASC
CycB1.1::GUS	C24	Ferreira et al., 1994, Himanen et al., 2002

2.1.3.1.2.   <u>Arabidopsis *cell suspensions*</u>

Experiments were performed using *Arabidopsis thaliana* (Col-0) photosynthetic light-grown and root-derived dark-grown cell suspensions.

2.1.4.   Plasmids vectors and constructs

2.1.4.1.   Plasmid vectors

pACT2	Clontech, Durfee et al., 1993
pAS2	Clontech, Durfee et al., 1993
pBluescript II SK -	Stratagene, La Jolla, USA
pDONR207	Invitrogen
pER8-XVE(Hygr)	Zuo et al., 2000
pER8-XVE(Km)	Ph.D. thesis M. Lafos, 2006
pGreen-MSC	gift of I. Searle
pHISi-1	Clontech
pLacZi	Clontech
pODB8	Loevet et al., 1997
pPAMnptII	gift of B. Ülker
pPAMpat	gift of B. Ülker
pPCV002	Koncz et al., 1994
pPCV812	Koncz et al., 1994
pPily	Ferrando et al., 2000

2.1.4.2.   Plasmid constructs

pACT2-PRL1	Nemeth et al.,. 1998
pAS2-PRL1	Nemeth et al.,1998
pAS2-PRL2	Ph.D. thesis F.Breuer, 2000
pAS2-PRL1-Cterm	Bhalerao et al., 1999
pAS2-PRL1-Nterm	Bhalerao et al., 1999
pBS-PRL1	K. Nemeth, unpublished
pBS-PRL1-cDNA	K. Nemeth, unpublished
pBS-PRL1-Sma	gift of I. Kovács
pER8(Hygr)-AKIN11-HA	Ph.D. thesis K. Berendzen, 2005
pER8(Hygr)-PAM1	A. Obershall, unpublished
pPCV002-35S::PRL1-HiA	J. Jásik unpublished
pDONR207-AS1prom	H. An, unpublished
pDONR207-4CL1prom	H. An, unpublished
pDONR207-KNAT1prom	An et al., 2004
pDONR207-STMprom	An et al., 2004
pDONR207-SUC2prom	An et al., 2004
pDONR207-TobRB7prom	An et al., 2004
pDONR207-UFOprom	An et al., 2004
pER8-iGUS	gift of I. Kovács
pPCV812-UFD1-HiA	I. Kovács, unpublished
pACT-CDC5	This work

pBS-PRL1-cDNA-GFP	This work
pBS-PRL1-cDNA-HA	This work
pBS-PRL1-2introns-cDNA-GFP	This work
pBS-PRL1-2introns-cDNA-HA	This work
pBS-PRL1-2introns-cDNA-SMA1	This work
pBS-PRL1gen-HA-ATG	This work
pBS-PRL1-HA	This work
pBS-PRL1-HA-G77E	This work
pBS-PRL1-PROM-UTR	This work
pBS-PRL1-STAB-2introns-GFP	This work
pBS-STAB-PRL1 -cDNA-GFP	This work
pER8(Km)-PRL1cDNA-HA	This work
pER8(Km)-PRL1gen-HA	This work
pGreen-AS1::PRL1cDNA-HA	This work
pGreen-AS1::PRL1gen-HA	This work
pGreen-4CL1::PRL1cDNA-HA	This work
pGreen-4CL1::PRL1gen-HA	This work
pGreen-KNAT1::PRL1cDNA-HA	This work
pGreen-KNAT1::PRL1gen-HA	This work
pGreen-PRL1-cDNA-HA	This work
pGreen-PRL1gen-HA-ATG	This work
pGreen-STM::PRL1cDNA-HA	This work
pGreen-STM::PRL1gen-HA	This work
pGreen-SUC2::PRL1cDNA-HA	This work
pGreen-SUC2::PRL1gen-HA	This work
pGreen-TobRB7::PRL1cDNA-HA	This work
pGreen-TobRB7::PRL1gen-HA	This work
pGreen-UFO::PRL1cDNA-HA	This work
pGreen-UFO::PRL1gen-HA	This work
pHISi-1-PRL1-PROM	This work
pLacZi-PRL1-PROM	This work
pPAMnptII-PRL1-cDNA-GFP	This work
pPAMnptII-STAB-PRL1-cDNA-GFP	This work
pPAMpat-CDC5-HA	This work
pPCV002-ODB	This work
pPCV002-PRL1-GFP	This work
pPCV002-PRL1-HA	This work
pPCV002-PRL1-HA-G77E	This work
pPCV002-PRL1-HA-XhoI	This work
pPCV002-PRL1-cDNA-HA	This work
pPCV002-PRL1-2introns-cDNA-HA	This work
pPCV002-PRL1-PROM-UTR	This work
pPCV002-PRL1-STAB-GFP	This work
pPCV812-PRL1-PROM	This work
pPCV812-PRL1-PROM-ATG	This work
pPCV812-PRL1-PROM-POLIT	This work
pPCV812-PRL1-PROM-TTTShort	This work
pPCV812-PRL1-PROM-UTR	This work
pPCV812-PRL1-PROM-XhoI-BmgBI	This work
pBS-PRL1-HA-MUT1	This work
pBS-PRL1-HA-MUT2	This work
pBS-PRL1-HA-MUT3	This work
pBS-PRL1-HA-MUT4	This work
pBS-PRL1-HA-MUT5	This work
pBS-PRL1-HA-MUT6	This work
pBS-PRL1-HA-MUT7	This work
pBS-PRL1-HA-MUT8	This work

pBS-PRL1-HA-MUT9	This work
pBS-PRL1-HA-MUT10	This work
pBS-PRL1-HA-MUT11	This work
pBS-PRL1-HA-MUT12	This work
pBS-PRL1-HA-MUT13	This work
pBS-PRL1-HA-MUT14	This work
pBS-PRL1-HA-MUT15	This work
pBS-PRL1-HA-MUT16	This work
pBS-PRL1-HA-MUT17	This work
pBS-PRL1-HA-MUT18	This work
pBS-PRL1-HA-MUT19	This work
pBS-PRL1-HA-MUT20	This work
pBS-PRL1-HA-MUT21	This work
pBS-PRL1-HA-MUT22	This work
pBS-PRL1-HA-MUT23	This work
pBS-PRL1-HA-MUT24	This work
pBS-PRL1-HA-MUT25	This work
pBS-PRL1-HA-MUT27	This work
pBS-PRL1-HA-MUT28	This work
pBS-PRL1-HA-MUT30	This work
pPCV002-PRL1-HA-MUT1	This work
pPCV002-PRL1-HA-MUT2	This work
pPCV002-PRL1-HA-MUT3	This work
pPCV002-PRL1-HA-MUT4	This work
pPCV002-PRL1-HA-MUT5	This work
pPCV002-PRL1-HA-MUT6	This work
pPCV002-PRL1-HA-MUT7	This work
pPCV002-PRL1-HA-MUT8	This work
pPCV002-PRL1-HA-MUT9	This work
pPCV002-PRL1-HA-MUT10	This work
pPCV002-PRL1-HA-MUT11	This work
pPCV002-PRL1-HA-MUT12	This work
pPCV002-PRL1-HA-MUT13	This work
pPCV002-PRL1-HA-MUT14	This work
pPCV002-PRL1-HA-MUT15	This work
pPCV002-PRL1-HA-MUT16	This work
pPCV002-PRL1-HA-MUT17	This work
pPCV002-PRL1-HA-MUT18	This work
pPCV002-PRL1-HA-MUT19	This work
pPCV002-PRL1-HA-MUT20	This work
pPCV002-PRL1-HA-MUT21	This work
pPCV002-PRL1-HA-MUT22	This work
pPCV002-PRL1-HA-MUT23	This work
pPCV002-PRL1-HA-MUT24	This work
pPCV002-PRL1-HA-MUT25	This work
pPCV002-PRL1-HA-MUT27	This work
pPCV002-PRL1-HA-MUT28	This work
pPCV002-PRL1-HA-MUT30	This work

2.1.5. Arabidopsis yeast two hybrid cDNA library

A cDNA library was prepared from *A. thaliana* (Col-0) cell suspension (K. Salchert, 1997; Nemeth et al., 1998). The cDNA products were cloned in fusion with the Gal4-DNA activation domain (GAD), using *EcoRI*-(5') and *XhoI*-(3') adaptors in plasmid pACT2.

2.1.6. Oligonucleotides

2.1.6.1. Oligonucleotides for DNA sequencing

3GAD	5'-GTTTTTCAGTATCTACGATTC-3'
5GAD	5'-CAAACCCAAAAAAAGAGATC-3'
CDC5-seq	5'-GCTCAGAGACAGGATGCTCCAG-3'
END-SEQ	5'-CTATGATTGAGCTCTAGGGAAACC-3'
Frev	5'-AGCGGATAACAATTTCACACAGGA-3'
GR-seq	5'-CTCCTTACCTACTGCTTCCAGAC-3'
GUS-UP	5'-ACAGGCCGTCGAGTTTTTTGATTTCAC 5'-
HA-seq	5'-AGCATAATCTGGAACCTGCACATC-3'
Junction down	5'-CATGCGAGGCTGATAAGACGA-3'
Junction up	5'-CCATGGACGGGAGAGAGAAGAG-3'
P1	5'-CTATACAGGTTCCTCAGGGAAG-3'
P2	5'-GGTCATTGCTCGGACAGATTTC-3'
SeqG77E	5'-CTCTGTTGTGTATGTTACTG -3'
T3 primer	5'-ATTAACCCTCACTAAAG-3'
T7 primer	5'-AATACGACTCACTATAG-3'

2.1.6.2. Oligonucleotides for cloning

CDC5-F	5'-GGAATTCGCATGAGGATTATGATTAAGGGAGG-3'
CDC5-R	5'-CCCTCGAGTTATGCAGAAGCTTCCATGGCTATG-3'
GFP-F	5'-GCTCTAGAATGGGTAAAGGAGAAGAAC-3'
GFP-R	5'-TCCCCGCGGTTATTTGTATAGTTCATCC-3'
GR-HA	5'-GCTCTAGATATCCATACGATGTTCCAGATTATGCTGAAG CTCGAAAAACAAAGAAAA-3'
GR-R	5'-TCCCCGCGGTCATTTTTGATGAAACAGAAGC-3'
GUS-F	5'-GCTCTAGAATGTTACGTCCTGTAGAAACCCCAACC-3'
GUS-R	5'-TCCCCGCGGTCATTGTTTGCCTCCCTGC-3'
HASpe	5'-CACTAGTTTAAGCATAATCTGGAACATCGTATGGATAGA AGCGCCTAATCTCCT-3'
MycSpe	5'-CACTAGTTTAAAGATCCTCCTCAGAAATCAACTTTTGCTC GAAGCGCCTAATCTCCTT-3'
POLI	5'-TCCCCCCGGGGGCTGAGACGAATCTGCTTGC-3'
PR-F	5'-GGAATTCGCCATAAGGTAAAACATTGAGTCTC-3'
PR-R	5'-GCTCATTGATGCGGTCAGGTTGA-3'
Prl1ndef	5'-GGAATTCCATATGCCGGCTCCGACGACG-3'
SexAI	5'-GCATAAGACACTAAAACCTGG-3'
UTR	5'-TCCCCGGGCGTTCTTCTTTTAGGGTTTAGAGAG -3'
XhoIF	5'-CCGCTCGAGATGCCGGCTCCGACGACGG-3'

2.1.6.3. Oligonucleotides for site-directed mutagenesis

G77E	5'-GTTGCGTTTGAAGGTGTAGAACCTG-3'
Mut1	5'-CCGGCTCCGACGACGGCTATCGCACCCATCGCAGCACAGT CACTG-3'
Mut2	5'-AAAGAACGATGGCTGCTGCTACGACGGAGATCGAAGCTAT CGAAGCACAG-3'
Mut3	5'-GAAGCACAGTCACTGGCAGCTCTCAGTCTCAAATCC-3'
Mut4	5'-AAGCTCAGTCTCGCATCCCTCGCACGATCACTTGAA-3'
Mut5	5'-CTGAAAAAGCTCGCTCTCAAAGCTCTCAAACGATCA-3'
Mut6	5'-AAATCCCTCAAAGCAGCACTTGAACTCTTC-3'
Mut7	5'-CGATCACTTGCACTCTTCGCTCCCGTCCATGTC-3'
Mut8	5'-GAACTCTTCTCTGCTGTCCATGGCCAA-3'
Mut9	5'-TTCTCTCCCGTCGCTGGCGCATTCCCTCCTCCT-3'

Mut10	5'-TTCCCTCCTCCTGCTCCGGCAGCGTTAGTCTTC-3'
Mut11	5'-GCAGCAAGCAGATTGCTCTCGCTCATAAGGTAAAA-3'
Mut12	5'-CAGATTCGTCTCAGCGCTGCTGTAAAACATTGAGTC-3'
Mut13	5'-TTTGTACAGATGGCAGTTGCGGCTGGAGGTGTAGAA-3'
Mut14	5'-TTTGGAGGTGTAGCACCTGTTGTGGCTCAACCTCCACGT-3'
Mut15	5'-AGTCAACCTCCAGCTGCACCTGACCGCATC-3'
Mut16	5'-CCTCCACGTCAACCTGCTGCTATCAATGAGCAGCCA-3'
Mut17	5'-CCTGACCGCATCAATGCTGCTCCAGGACCTTCA-3'
Mut18	5'-CAGCCAGGACCTGCAAATGCTCTTGCTCTCGCAGGTGTT-3'
Mut19	5'-GCAGCTCCTGCAGGGGCTAAGAGTACGCAA-3'
Mut20	5'-CTCCTGAAGGGTCTGCTGCTACGCAAAAGGGTGCG-3'
Mut21	5'-GGGTCTAAGAGTACGGCAGCTGGTGCGACAGAGAGT-3'
Mut22	5'-AGGGTGCGACAGCTGCTGCTATTGTTGTTGG-3'
Mut23	5'-AACTATACAGGTGCTGCAGGGAAGAGCACC-3'
Mut24	5'-ACAGGTTCCTCAGGGGCTGCTACCACCATTATACCTGCA-3'
Mut25	5'-CCTGCAAATGTAGCTGCATATCAAAGGTTT-3'
Mut26	5'-AAGATGTGGAAAGCAGCTGCTAATGCAACTCCA-3'
Mut27	5'-AATGCAACTCCAGCAACTGCTCCTATCAATTTC-3'
Mut28	5'-CCTATCAATTTCGCTCCACCAAAGGAGATT-3'
Mut29	5'-TTCTTCAAACCACCAGCTGCTATTAGGCGCTTCTAT-3'
Mut30	5'-CCAAAGGAGATTGCTGCCTTCTATCCATACGAT-3'
NotI	5'-ACCGCGGTGACTGCCGCTCTAGAA-3'
Nsi	5'-GTTCTACAAAAACGCATCCCGAGAGC-3'
Sca	5'-CTGTGACTGGTGACCACTCAACCAAGTC-3'
STABmut	5'-GTTGGTCCAACTTTACTGGGTCCAATAGTGCCTAAAGGCT TGAACTATAC-3'
TTT	5'-GTAAAGATGGTTGATTTACTTAGATTTTTTTTTTTTTTTGT TGTGTATGTTACTGATTTTAGAAG -3'

2.1.6.4.   *Oligonucleotides to screen for T-DNA insertion mutants in* **Arabidopsis**

FISH1	5'-CTGGGAATGGCGAAATCAAGGCATC-3'
FISH2	5'-CAGTCATAGCCGAATAGCCTCTCCA-3'
LB1-sail	5'-GCCTTTTCAGAAATGGATAAATAGCCTTGCTTCC-3'
LB3-sail	5'-TAGCATCTGAATTTCATAACCAATCTCGATACAC-3'
PRL1 3'	5'-AACCTGTATTATCATAACACGCTGC-3'
PRL1 5'	5'-ACTTGAACTCTTCTCTCCCGTCCAT-3'
PRL1 ups	5'-GATGCGTTTCAGATCTTGGCGTG-3'
PRL1-5'rev	5'-ATGGACGGGAGAGAAGAGTTCAAGT-3'
PRL2 5'	5'-GAACAGGGAGGTCGAAACTCAGTCAC-3'
PRL2 3'	5'-TTCACTCTCCAGCGAACCTAACCAT-3'
SAIL DAP RB2	5'-GTATGTTGTGTGGAATTGTGAGCGGATAAC-3'
SALK LB	5'-TTTGGGTGATGGTTCACGTAGTGGG-3'

2.2.   General buffers, stock solutions and growth media

2.2.1.1.   *Solutions*

Phenol/Chloroform/Iso-amylalcohol:	mix to a ratio of 25:24:1
TE:	10 mM Tris.HCl, 1 mM EDTA, pH 8.0
X-gal	20 mg/ml in N,N-dimethyl formamide
X-gluc	20 mg/ml in N,N-dimethyl formamide
Cycloheximide	100 mM in ethanol

| β-estradiol | 10 mM in DMSO |
| MG132 | 50mM in DMSO |

2.2.2. Antibiotics

Antibiotics	Stock solution	Working concentration
Ampicillin	50 mg/ml in water	50 mg/l
Basta	200 mg/ml	250 mg/l
Carbenicillin	50 mg/ml in water	50 mg/l
Cefotaxime/Claforan	200 mg/ml in water	200-400 mg/l
DL-Phosphinotricine	10 mg/ml in water	10 mg/l
Hygromycin	15 mg/ml in water	15 mg/l
Kanamycin	50 mg/ml in water	50mg/l for bacteria; 100mg/l for plants
Nystatine	50 mg/ml in DMSO	25-50 mg/l
Rifampicin	25 mg/ml in methanol	100 mg/l
Spectinomycin	50 mg/ml in water	100 mg/l
Sulfadiazine	7.5 mg/ml in water	15 mg/l
Tetracyclin	10 mg/ml in water	12.5 mg/l
Ticarcillin/Clavulanic acid	150 mg/ml in water	150 mg/l

All antibiotics were filter sterilized and stored at -20°C.

2.2.3. Plant hormones

Abscisic acid (ABA)	1 mg/ml in methanol
6-Benzylaminopurine (BAP)	1 mg/ml 1N NaOH
2,4-dichlorophenoxyacetic acid (2,4-D)	1 mg/ml ethanol
Gibberellin (GA3)	1 mg/ml in ethanol
Indole 3-acetic acid (IAA)	1 mg/ml in 1N KOH
Kinetin	1 mg/ml 1N NaOH
Methyl jasmonate	10 mg/ml in ethanol
1-naphtylacetic acid (NAA)	1 mg/ml 1N KOH
Salicylic acid (SA)	0.5 M in ethanol

All hormone solutions were filter sterilized and stored at -20°C.

2.2.4. Culture media

2.2.4.1. Bacterial media

2.2.4.1.1. LB medium:

Bacto-Tryptone	10g/l
Bacto-Yeast Extract	5g/l
NaCl	10g/l

Adjust pH to 7.5 with NaOH. For solid media add 20g/l Bacto-Agar. Autoclave for 20 min at 120°C.

2.2.4.1.2. YEB medium:

Beef Extrect	5g/l
Bacto yeast extract	1g/l
Bactopeptone	1g/l

Sucrose	5g/l

Adjust pH to 7.4 with NaOH. For solid medium add 15g/l Bacto-agar. Autoclave for 20min at 120°C and after sterilization 20ml/l of 0.1M $MgCl_2$ was added.

2.2.4.2. Yeast media

2.2.4.2.1. YPD yeast medium

Difco-peptone	20g/l
Yeast extract	10g/l
Glucose	20g/l

For solid media add 20g/l Bacto-agar. Autoclave for 15 min at 120°C.

2.2.4.2.2. Synthetic Minimal medium

Yeast Nitrogen Base w/o amino acids	6.7g/l
Glucose	20g/l

Dissolve in 900 ml of water. Adjust pH to 5.8 with NaOH. For solid media add 20g/l Bacto-agar. Autoclave 15 min at 120°C.

10X Drop-out solution:

L-Isoleucine	300mg/l
L-Valine	1500mg/l
L-Adenine hemisulfate salt	200mg/l
L-Arginine-HCl	200mg/l
L-Histidine-HCl	200mg/l
L-Leucine monohydrate	1000mg/l
L-Lysine-HCl	300mg/l
L-Methionine	200mg/l
L-Phenylalanine	500mg/l
L-Threonine	2000mg/l
L-Tryptophan	200mg/l
L-Tyrosine	300mg/l
L-Uracil	200mg/l

2.2.4.3. Plant media

2.2.4.3.1. Arabidopsis cell suspension culture medium

Root derived cell suspension:	MS Basal Mix	4.3 g/l
	B5 vitamin (100X)	10 ml
	Sucrose	3%

Adjust pH to 5.8 with KOH, autoclave at 120°C for 15 min and before use add 2,4-D to final concentration of 1mg/l.

B5 Vitamin (100X)	Nicotinic Acid	1mg/ml
	Pyridoxin-HCl	1g/ml

	myo-Inositol	100mg/ml
	Thiamine-HCl	10mg/ml

Photosynthetic cell suspension:	MSMO Salts	4.4 g/l
	Sucrose	3%

Adjust pH to 5.8 with KOH, autoclave at 120°C for 15 min and before use add 0.5mg/l NAA and 0.1mg/l kinetin pH adjusted to 5.8 with KOH

2.2.4.3.2. *Plant culture medium*

MSAR medium (Koncz et al., 1994)

	Macroelements	25.0 ml/l
	Microelements	1.0 ml/l
	Fe-EDTA	5.0 ml/l
	$CaCl_2 \cdot 2H2O$	5.8 ml/l
	KI	2.2 ml/l
	B5 vitamin	2.0 ml/l
	Sucrose	5g/l

pH was adjusted to 5.8 with KOH and 0.6 g/l phytoagar was added.

Macroelements:	20 g/l NH_4NO_3, 40 g/l KNO_3, 7.4 g/l $MgSO_4 \cdot 7\ H_2O$, 3.4 g/l KH_2PO_4, 2 g/l $Ca(H_2PO_4)_2 \cdot\ H_2O$
Microelements:	6.2 g/l H_3BO_3, 16.9 g/l $MnSO_4 \cdot 4H_2O$, 8.6 g/l $ZnSO_4 \cdot 7H_2O$, 0.25 g/l $Na_2MoO_4 \cdot 2\ H_2O$, 0.025 mg/l $CuSO_4 \cdot 5H_2O$, 0.025 mg/l $CoCl_2.6H_2O$
Fe-Na_2-EDTA:	5.56 g/l $FeSO_4 \cdot 7H_2O$, 7.46 g/l Na_2-EDTA$\cdot 2\ H_2O$
KI:	375 g/l KI
$CaCl_2$:	75g/l $CaCl_2 \cdot 2H_2O$

2.2.5. Antibodies

2.2.5.1. *Primary antibodies*

Anti-Amidase: Rabbit polyclonal antibody raised against *Arabidopsis* amidase (ATAM1 At5g07360) peptide. Dilution: 1:2,000.

Anti-c-Myc: Mouse monoclonal antibody raised against a peptide from human c-Myc protein. Dilution: 1:1,000.

Anti-CULLIN 1: Rabbit polyclonal antibody raised against *Arabidopsis* CULLIN 1 protein (Gray et al., 1999)   Dilution: 1:6,000.

Anti-HA: Rat monoclonal antibody (clone 3F10) to a peptide derived from the hemagglutinin protein of the human influenza virus (Roche) Dilution: 1:1,000.

Anti-Histone H2A: Rabbit antiserum recognizing a synthetic peptide corresponding to amino acids 88-97 of human Histone 2A (Upstate Co) Dilution: 1:1,000

Anti-PRL1:   Rabbit polyclonal antibody raised against a PRL1 specific peptide (Nemeth *et al.,* 1998) Dilution: 1:1,000.

Anti-19S Proteasome: Rabbit polyclonal antibody to 19S regulator non-ATPase subunit Rpn6 (S9) (Affiniti Research). Dilution: 1:2,000.

Anti-20S Proteasome: Mouse monoclonal antibody raised against the human 20S proteasome particle subunits α1, 2, 3, 5, 6 and 7 (Affiniti Research). Dilution: 1: 1,000.

Anti-SKP1:   Rabbit polyclonal antibody recognizing the C-terminal peptide of SKP1 protein.

Anti-SnRK1α: Rabbit polyclonal antibody raised against the tobacco NPK5 protein (Muranaka et al., 1994). Dilution: 1: 5,000 or 1:10,000.

Anti-tubulin: Mouse monoclonal antibody to α-tubulin (clone DM 1A), purified chick brain tubulin was used as immunogen (Sigma). Dilution: 1:1,000 or 1:2,000.

Anti-ubiquitin: Rabbit antibody recognizing a peptide corresponding to amino acids 1-50 of soybean ubiquitin (Bethyl Laboratories Inc). Dilution: 1:1,000.

2.2.5.2.   *Secondary antibodies*

Goat anti-Rabbit IgG, (H+L), HRP   Dilution: 1:10,000

Goat anti-Rat IgG, (H+L), HRP   Dilution: 1:10,000

Rabbit anti-Chicken IgG, (H+L), HRP   Dilution: 1:10,000

2.2.6.   Bioinformatic Resources

2.2.6.1.   *Softwares*

- Adobe Acrobat 6.0 Professional
- Adobe Photoshop CS and Adobe Photoshop Elements 2.0
- Bioedit Sequence Alignement Editor version 4.8.10
- Clone Manager 7 version 7.01
- CLUSTAL W Multiple Sequence Alignment Program version 1.83 (Feb 2003)
- Diskus version 4.30.102
- DNASTAR (GeneQuest, Editseq, MapDraw, Megalign, Primer Select, Protean, SeqMan)
- Kodak 1D Image Analysis Software version 3.6.5 K2
- Leica Confocal Software LCS Lite version 2.61
- Microsoft Office 2003

2.2.6.2.   *Databases*

- *Arabidopsis* Information Resource (TAIR) http://www.arabidopsis.org/
- The Institute for Genomic Research (TIGR) http://www.tigr.org/
- The European Bioinformatics Institute (EBI) http://www.ebi.ac.uk/

- National Center for Biotechnology Information (NCBI) http://www.ncbi.nih.nlm.gov/
- European Molecular Biology Laboratory (EMBL) http://www.embl-heidelberg.de/
- Salk Institute Genomic Analysis Laboratory *Arabidopsis* sequence indexed T-DNA insertion http://signal.salk.edu/
- Arabidopsis thaliana microarray database and analysis toolbox (http://www.genevestigator.ethz.ch; Zimmermann et al., 2004)
- Database of plant cis-acting regulatory DNA elements (http://www.dna.affrc.go.jp/PLACE; Higo et al., 1999)

2.3.   METHODS

2.3.1.   General molecular biology methods

2.3.1.1.   *Preparation of plasmid DNA by alkaline lysis (modified from Birnboim and Doly, 1979)*

A single *E. coli* colony was inoculated in 2-5ml of LB medium supplemented with appropriate antibiotics. Bacterial cultures were grown overnight at 37°C with vigorous shaking (250 rpm). Cultures were transferred into 2ml eppendorf tubes and pelleted at maximum speed for 1 min in a tabletop centrifuge. Then, the supernatant was removed and the cell pellets were dried for 1 min in inverted position. (Alternatively the pellet was frozen and kept on -20°C for later use.) Cells were resuspended by vortexing in 280 µl of ice-cold solution I. Bacterial cells were lysed by adding 360 µl of freshly prepared solution II, and the tubes were gently inverted few times in order to mix solutions. After 5 min incubation, 540 µl of ice-cold solution III was added to neutralize the lysate and the mixture was kept at 4°C for 10 min. The cell debris was removed by centrifugation at 13,000 rpm for 10 min. 1ml of the supernatant was transformed into new eppendorf tube and nucleic acids were precipitated with 0.5 ml of isopropanol at -20°C for at least 10 min. Nucleic acids were pelleted by centrifugation at 13,000 rpm for 10 min and the supernatant was removed. Dried nucleic acids were resuspended in 0.5 ml of 25 µg/µl RNase A solution and incubated at 37°C for 1 h. Subsequently, DNA was precipitated with 0.6 ml of solution IV and dissolved in 50 µl of water or TE buffer.

Solution I: 50 mM Tris.HCl (pH 8.0), 50 mM glucose, 10mM EDTA
Solution II: 200 mM NaOH, 1% SDS (freshly prepared)
Solution III: 3 M NaOAc (pH 4.8) or 3 M KAc (pH 6.0)
Solution IV: 88% isopropanol, 0.2 M KAc

For sequencing, DNA was prepared using QIAprep® plasmid isolation kit (Qiagen) or E.Z.N.A.® Plasmid miniprep kit I. (Peqlab) to obtain high quality and purity.

2.3.1.2. DNA sequencing

Plasmids and DNA fragments were sequenced in collaboration with the Automatic DNA Isolation and Sequencing (ADIS) service of MPIZ. For sequencing, an Applied Biosystems 3730XL Genetic Analyser was used.

2.3.1.3. Phenol/Chloroform extraction

To remove contaminating proteins, DNA samples were supplemented with 1/10 volume of 3 M sodium acetate solution (pH 5.2) and then mixed by vortexing with equal volume of phenol/chloroform solution (1:1, v/v) and centrifuged at 13,000 rpm for 5 min. The aqueous upper phase was collected in a new eppendorf tube and the extraction step with phenol/chloroform was repeated until there was no more precipitated protein ring between the water and organic solvent phases. Then, to remove phenol traces from the solution, equal amount of chloroform:iso-amylalcohol (24:1) mixture was added and vortexed. Phases were separated by centrifugation and DNA was precipitated by 2 volumes of ethanol.

2.3.1.4. DNA precipitation

DNA was precipitated using ethanol or isopropanol. In the case of ethanol precipitation, 1/10 volume of 3 M sodium acetate (pH 5.2) and 2 volumes of absolute ethanol were added to DNA samples, mixed and incubated at -20°C for at least 10 min. DNA was pelleted by centrifugation at top speed for 10 min. The DNA pellet was washed with 70% ethanol and centrifuged again. For isopropanol precipitation 0.7 volumes of isopropanol was added to the samples and incubated on ice for at least 20 min. Then, DNA was pelleted by high speed centrifugation (13,000 rpm for 10 min). DNA pellets were dissolved in water or TE buffer.

2.3.1.5. Agarose gel electrophoresis

Plasmids, DNA fragments and PCR products were separated by agarose gel electrophoresis. The agarose concentration of the gel depends on the size of the DNA fragments being analyzed. Generally, 0.8-1% (w/v) agarose concentration was used. For large fragments (>5kb) 0.5% (w/v), whereas for small fragments (<0.5 kb) 3% (w/v) agarose gels were prepared. Agarose was dissolved in 1 X TAE buffer supplemented with 25 µl/l ethidium bromide and heated in a microwave oven until boiling. The solution was allowed to cool down to approximately 65°C and then poured into a plastic tray sealed at the edges with tape and casted with appropriate combs and allowed the gel to set completely. Then, the gel was transferred into a gel tank. DNA samples were mixed with loading dye and loaded into the gel slots. For size estimation, 1kb DNA ladder (Invitrogen) or *Pst*I or *Hind*III digested λ phage DNA marker was used. Electrophoresis was performed in 1X TAE buffer at between 50 to 150 V. DNA was visualized using an UV light transilluminator. Gel images were captured by a Kodak DC-120 ZOOM digital camera and processed with the Kodak Digital Science 1D V.3.0.2 software.

TAE buffer:	1X	50X
	40 mM Tris	242 g Tris
	40 mM Acetic acid	57.1 ml glacial acetic acid
	1 mM EDTA	100 ml 0.5 M EDTA (pH 8.0)

<u>6 X Loading dye:</u>   40% sucrose, 0.25% bromphenol blue

2.3.1.6.   *Purification of DNA fragments from agarose gels*

After gel electrophoresis, DNA fragments were excised from the agarose gel placed on an UV light transilluminator. DNA was extracted and purified using QIAquick® Gel Extraction Kit (Qiagen) following the manufacturer's instructions.

2.3.1.7.   *Measurement of nucleic acid concentration*

DNA concentration was determined by spectrophotometry. OD_{260} value of 1 corresponds to 50 µg/ml of double stranded DNA concentration and 40 µg/ml RNA concentration. In pure preparations OD_{260}/OD_{280} ratio should be between 1.8/2.0 (Sambrook et al., 1989).

2.3.1.8.   *Digestion with restriction endonucleases*

Digestions of DNA samples were performed with restriction endonucleases according to the manufacturers' instructions. Typically, reactions were carried out in 1.5 ml Eppendorf tubes in a final volume of 20 or 50 µl using 1-5 U enzyme/µg DNA. The duration of the digestion varied from 2 h to overnight.

2.3.1.9.   *Generating blunt ends of digested DNA fragments*

Overhanging DNA ends were blunted with T4 DNA polymerase (NEB). This enzyme catalyzes DNA synthesis in 5'-3' direction and has 3'-5' exonuclease activity (Ausubel et al., 1999). Hence, T4 polymerase can used for 3' overhang removal and 3' recessed end fill-in. Digested vector DNA was dissolved in 1X restriction enzyme reaction NEBuffer supplemented with 100 µM dNTPs. 1 unit enzyme/µg DNA was added to the reaction and incubated 15 min at 12°C. T4 DNA polymerase was inactivated by adding EDTA to the mixture (10 mM final concentration) followed by heating to 75°C for 20 min.

2.3.1.10.   *Dephosphorylation of DNA ends*

In order to prevent self-ligation of linearized vectors, digested plasmids were treated with phosphatases. These enzymes catalyze the removal of 5' phosphate groups from DNA and RNA molecules that are essential for ligation (Chaconas and van de Sande, 1980).

2.3.1.10.1. <u>Calf-intestine alkaline phosphatase (CIAP) treatment</u>

2 units of CIAP was added to 1 µg linearised DNA and incubated at 37°C for 30 min. The enzyme was removed by gel electrophoresis or phenol/chloroform extraction.

2.3.1.10.2. <u>Antarctic phosphatase treatment</u>

Preferably antartic phosphatase (NEB) was used for dephosphorylation of DNA. This enzyme can be heat inactivated and therefore no further purification is necessary. Linearized vectors were purified after gel electrophoresis and 1/10 volume of antartic phosphatase reaction buffer was added to the sample. Reaction mixture was supplemented with 5 U of antartic phosphatase and incubated for 1 h at 37°C. Enzyme was inactivated at 65°C for 5-10 min.

2.3.1.11. **DNA ligation**

Ligation of linearized vectors and DNA fragments was performed using T4 DNA ligase (NEB). 20 µl of reaction mixture contained T4 DNA Ligase Reaction buffer, vector and insert fragment in a molar ratio of 1:3, 1 µl of T4 DNA ligase and supplementing amount of water. Recirculization of cloning vectors was controlled by ligation containing exclusively the vector. Generally, ligations were performed overnight at 12°C.

2.3.1.12. **Gateway® LR cloning reaction**

Gateway® technology is based on the site-specific recombination of λ phage. LR Clonase™ enzyme mix promotes recombination between entry clone and destination vector. Following components were mixed in 1.5 ml eppendorf tube:

Entry clone (100-300 ng)	1-10 µl
Destination vector (~300 ng)	2 µl
5X LR Clonase™ Reaction Buffer	4 µl
LR Clonase™ enzyme mix	1 µl
TE buffer, pH 8.0	up to 20 µl

Reactions were incubated at 25°C 1-2 h then enzyme mix was inactivated by adding 2 µl of Proteinase K solution and the samples were incubated at 37°C for 10 min.

2.3.1.13. **PCR amplification**

2.3.1.13.1. <u>Recombinant Taq *DNA polymerase*</u>

For amplification of DNA fragments, recombinant *Taq* DNA polymerase (Invitrogen) was used. A master mix was prepared for multiple reactions from the following components on ice:

10X PCR buffer (-MgCl$_2$)	10 µl
10 mM dNTP mixture	2 µl

50 mM MgCl$_2$	3 µl
Primer mix (10 µM each)	5 µl
Template DNA	1 µl
Taq DNA polymerase (5 U/ µl)	1 µl
Autoclaved distilled water to	100 µl

For PCR amplification a Byozym Multicycler PTC 240 Tetrad^{TM} 2 machine was used. The reactions were performed in 20 µl final volume using the following program:

1. Denaturation:	95°C for 5 min
2. Denaturation:	95°C for 30 sec
3. Annealing:	58°C for 30 sec
4. Extension:	72°C for 30 sec-3 min depending on fragment length
5. Terminal step:	72°C for 5 min.

Normally 25-30 cycles were performed. Samples can be stored at 4°C before further analysis.

2.3.1.13.2. *Platinum® Pfx DNA polymerase*

For cloning purposes *Pfx* DNA polymerase were used. This enzyme possesses proofreading 3'-5' exonuclease activity and provides high fidelity. Following components were mixed in 200 µl PCR tubes:

10X *Pfx* Amplification buffer	5 µl
10 mM dNTP mixture	1.5 µl
50 mM MgSO$_4$	1 µl
Primer mix (10 µM each)	1.5 µl
Template DNA	1 µl
Platinum *Pfx* DNA Polymerase	1 µl
Autoclaved distilled water	to 50 µl.

After denaturation step (94°C for 2 min) three-step cycling program was used:

Denaturation:	94°C for 15 sec
Annealing:	55°C for 30 sec
Extension:	68°C for 1 min/kb.

25-30 cycles were performed followed by a longer extension step (68°C for 5 min). Reaction temperature was maintained at 4°C.

2.3.1.14. *Site-directed mutagenesis of plasmids*

Site-directed mutagenesis was performed using the Transformer^{TM} Site-Directed Mutagenesis Kit (Clontech). The mutagenesis strategy is based on that two mutations are introduced at the same time using simultaneous annealing of specific primers to single-stranded circular DNA. In addition to the desired nucleotide changes, another primer is used containing mutations in a unique restriction site.

This facilitates the elimination of non-mutated plasmid DNA by selective restriction digestion. For site specific mutagenesis 5' end phosphorylated primers were used. The annealing reaction was prepared as follows:

10X Annealing Buffer	2 µl
Plasmid DNA	2 µl
Selection primer	2 µl
Mutagenic primer	2 µl
Water	12 µl

The template plasmid DNA was denatured in a boiling water bath (100 °C) for 3 min, and then the samples were chilled on ice for 5 min. For DNA synthesis, the annealing reaction mix was supplemented with

10X Synthesis buffer	3 µl
T4 DNA polymerase	1 µl
T4 DNA ligase	1 µl
Water	5 µl.

The reaction mixes were incubated for 30 min at 37°C. The enzymes were inactivated by heating at 70°C for 5 min. 3 µl of synthesis reaction was digested with a preselected restriction enzyme in order to linearize the parental plasmid DNA. After restriction digestion, 0.5 µl of reaction mix was transformed into electro-competent *E. coli mut*S (repair deficient) cells in order to amplify the mutagenized strand. After 1 h recovery, transformed bacteria were inoculated into 4 ml of liquid LB containing antibiotics for selection and incubated overnight with vigorous shaking. Next day, from the *E. coli* culture the plasmid DNA was purified, and 2 µl DNA (~50 ng) was digested with the selective endonuclease to eliminate once again the non-mutated plasmid molecules. 0.5 µl of digested plasmid DNA was transformed into *E. coli* HB101 cells, which were then plated on selective LB medium. 12-24 independent colonies were tested for their restriction digestion pattern and 3-6 positive clones were sequenced in order to verify the presence of desired point mutations.

2.3.1.15. *Isolation of plasmid DNA from Agrobacterium tumefaciens*

Agrobacterium culture (5 ml) was grown for 2 days with constant shaking at 28°C. Bacterial cells were pelleted and then resuspended in 150 µl of solution I. Subsequently 300 µl of solution II was added to the cells and lysis was performed at 55°C for 10 min. Then, 225 µl of solution III was added and mixture was incubated on ice for 10 min. Cell debris was removed by centrifugation at 13,000 rpm for 10 min. Subsequently, DNA was precipitated with 2 volumes of 100% ethanol and centrifuged at 13,000 rpm for 10 min. Pellet was washed with 70% ethanol, centrifuged and dried. DNA was dissolved in 50 µl of water or TE buffer. Plasmids were either analyzed by PCR amplification or they were transformed to *E. coli* for further analysis after preparation of plasmid DNA. Solutions I, II and III are described under 2.2.1.1.

2.3.1.16. *Transformation of bacterial cells*

2.3.1.16.1. <u>*Preparation of electrocompetent* E. coli *cells (Dower et al., 1998)*</u>

A single colony from 1-5 day-old plate was inoculated in 10 ml of liquid LB and the bacterial culture was grown overnight at 37°C with constant shaking (200 rpm). The next evening, 1 ml of this culture was inoculated into 300 ml of liquid LB and incubated overnight at 37°C with shaking. In the morning, the bacterial culture was diluted to OD_{600} 0.1-0.2 and cells were incubated at 16-20°C with shaking until the OD_{600} reached 0.5-0.6. From this step on the bacteria were kept on ice. All centrifugation steps were performed at 4°C in plastic tubes pre-chilled at -20°C. For washing, ice cold distilled water was used. Bacteria were pelleted by centrifugation in GSA tubes at 5,000 rpm for 20 min and resuspended in 200 ml of cold water. This washing step was repeated 3 times to remove salts, and then cells were resuspended in 50 ml of water and transferred into a 50 ml falcon tube. Competent bacteria were spun down for 10 min at 5,000 rpm. Supernatant was removed completely and the cells were resuspended in 800 µl of 7% DMSO solution and divided into 50 µl aliquots in eppendorf tubes. Competent cells were frozen immediately in liquid nitrogen and kept at -70°C.

2.3.1.16.2. <u>*Preparation of electrocompetent* A. tumefaciens *cells*</u>

Competent *Agrobacterium tumefaciens* was prepared using a similar protocol as in case of *E. coli* cells. Agrobacteria were incubated in liquid YEB medium at 28°C. After final washing step, cells were resuspended in sterile 10% glycerol solution.

2.3.1.17. *Transformation of E.coli cells by the heat-shock method*

1-5 µl of plasmid DNA was added to 50 µl competent bacterial cells. Cells were incubated on ice for 30 min and then heat-shocked at 42°C for 0.5-1.5 min. Recovery was done at 37°C for 1 h upon adding 1 ml of LB medium. The transformation mixture was plated onto selective LB plates.

2.3.1.18. *Electroporation of bacterial cells*

An aliquot of competent *E. coli* or *A. tumefaciens* cells was thawed on ice. Cells were mixed with 0.5-3 µl of either plasmid DNA or pre-dialysed ligation mixture and transferred into prechilled 0.2 cm electroporation cuvettes. Transformation was performed in a Bio-Rad Gene Pulser set to 2.5 kV voltage, 25 µF capacitance and 200 Ω resistance. After electroporation, bacteria were suspended in 1 ml of liqiud LB medium, transferred into a centrifuge tube and incubated for 1 h at 37°C. After recovery phase, cells were spread on solid LB media supplemented with antibiotics. In the case of *A. tumefaciens*, cells were incubated at 28°C and plated on selective YEB medium.

2.3.2. **Protein biochemical methods**

2.3.2.1. *Preparation of protein extracts from plant material*

Frozen plant material was ground in liquid nitrogen in a mortar with pestle. Fine tissue powder was transferred into a centrifuge tube and extraction buffer supplemented with 25 µl/ml plant protease inhibitor cocktail was added. The extract was thawed on ice for 30 min and the protein sample was vortexed several times. Cellular debris was removed by centrifugation at 13,000 rpm in a benchtop centrifuge for 10-20 min at 4°C. The supernatant was transferred into new tube and 5X SDS protein loading buffer was added to the crude extract. Proteins were denatured for 5 min at 95°C.

Extraction buffer:	50 mM Tris.HCl (pH 7.5), 10% glycerol, 1 mM EDTA, 150 mM NaCl, 0.2% Igepal
Protease inhibitor cocktail:	1 mM benzamide, 2µg/ml pepstatin, 5µg/ml of aprotinin, leupeptine
5X SDS protein loading buffer:	2% SDS, 10% glycerol, 50 mM Tris-HCl (pH 6.8), 5% β-mercaptoethanol, 0.1% Bromphenol blue

2.3.2.2. *Determination of protein concentration*

To determine the protein concentration of samples, the Bradford assay was used (Bradford, 1976). After extraction, 1 or 2 µl of protein sample was mixed with 1 ml BioRad Protein Assay Concentrated Dye Reagent, which was previously diluted 5 times in water. After 5 min incubation at RT, OD_{595} value was measured with a spectrophotometer. The protein amount was determined by the help of a standard curve obtained previously using a series of dilutions of bovine serum albumin (BSA).

2.3.2.3. *Electrophoretic separation of proteins*

SDS-polyacrylamide gel electrophoresis (SDS-PAGE, Laemmli, 1970) was used to separate proteins according to their size. Protein gels were poured between 10 cm x 8 cm glass plates (Protean mini gel system) using 1 mm spacers. Generally, 4.5 ml of 12% separating gel was poured first and overlayed with butanol. After polymerization, the butanol was removed and the surface of gel was rinsed with water. On the top of the separating gel, a stacking gel layer was poured and casted with a 10 or 15-well comb. The gel was placed into an electrophoresis buffer tank and protein samples were loaded using a Hamilton syringe and run in SDS-PAGE running buffer at 30 mA. The size of separated proteins was estimated using prestained protein markers (Bio-Rad).

Components for two 12% gels

Separation gel (12%):	5.4 ml ddH$_2$O
	3.0 ml 29:1 acrylamide to bisacrylamide (40%)
	2.5 ml 1.5 M Tris.HCl [pH 8.8]
	0.1 ml 10% SDS
	50 µl 10% APS
	5 µl TEMED

Stacking gel (4 %):	2.4 ml ddH2O
	1 ml 1 M Tris.HCl [pH 6.8]
	0.5 ml 29:1 acrylamide to bisacrylamide (40%)
	40 µl 10% SDS
	30 µl 10% APS
	5 µl TEMED

SDS-running buffer:	25 mM Tris
	192 mM glycine
	0.1% SDS

2.3.2.4. Western blotting

2.3.2.4.1. *Transfer of proteins from SDS-PAGE gels onto membranes*

In order to detect proteins with specific antibodies, proteins separated by SDS-PAGE were transferred and immobilized onto PVDF membranes (Towbin et al., 1979). The membrane was rinsed in 100% methanol for 30 sec and then incubated in Transfer buffer. The stacking gel was removed from the separating SDS-PAGE gel and the gel was equilibrated in 1X transfer buffer for 5 min. Then, a transfer "sandwich" was assembled from the following components: sponge layer, 3x 3MM Whatman paper, SDS-PAGE gel, PVDF membrane, 3x 3MM Whatman and sponge layer. This sandwich was placed in a wet blotter transfer apparatus such that the membrane faced the anode and the gel sandwich was fully submerged in Transfer buffer. Protein transfer was performed either for 2-3 h at 25 V or overnight at 10 V.

| Transfer buffer | 50mM Tris, 50mM Boric acid [pH 8.0] |

2.3.2.4.2. *Staining of PVDF membranes*

To monitor successful protein transfer and/or determine equal protein loading, membranes were stained in Ponceau staining solution for 1 min and the unspecific stain was washed out with water or 1X TBS solution (Hughes et al., 1988).

| Ponceau staining solution: | 0.2% Ponceau S in 3% trichloroacetic acid |

2.3.2.4.3. *Antibody Probing*

After protein transfer, the PVDF membranes were blocked in blocking solution for 1 h at room temperature or at 4°C overnight. Then, the primary antibody diluted in blocking solution was poured on the membrane and incubated for 2 h followed by washing the membrane 3 times for 10 min with washing buffer. Subsequently, the filters were incubated for 1.5 h with a horseradish peroxidase conjugated secondary antibody diluted in blocking solution. The membranes were then washed 3 times for 10 min with washing buffer.

TBS:	137 mM NaCl, 2.7 mM KCl, 20 mM Tris.HCl [pH7.4]
Blocking solution:	5% milk powder in 1X TBS with 0.05% Tween-20
Washing buffer**:**	1X TBS with 0.2% Tween-20

2.3.2.4.4. *Detection of chemiluminescent signal*

To visualize the position of proteins using horseradish peroxidase conjugated second antibodies, an enhanced chemiluminescence (ECL) detection kit was used. Freshly prepared 1:1 mixture of the two ECL reagents was applied onto the PVDF membranes. Light emission was captured on Hyperfilm^{TM} by autoradiography and the films were developed in Optimax X-ray Film Processor.

2.3.2.4.5. *Stripping of PVDF membranes*

The same membrane could be probed with another antibody after removing the IgGs of the first reaction. Stripping was performed either using Ponceau solution since it contains TCA that can denature proteins, or using Restore^{TM} Western blot stripping buffer. In the latter case, the membrane was incubated in the buffer for 5-15 min at room temperature on a shaker. Subsequently, the membrane was washed 2-3 times with 1X TBS.

2.3.2.5. *Size separation of protein complexes on linear glycerol gradient*

Plant protein complexes were separated according to their sizes on glycerol density gradient. 10 ml of 10-40% gradient was prepared by using a gradient mixer and 1 ml nuclear or total cell protein extract was loaded on the top. Separation was done in an ultracentrifuge by centrifugation at 25,000 g for min. 16 h at 4°C. 300 µl fractions were collected and were analyzed by western blotting.

Glycerol gradients:	10% or 40% glycerol, 50 mM HEPES [pH 7.5], 50 mM KCl, 5 mM MgCl2,
	10 µM ZnS04, 1 mM PMSF, 2 mM ATP, 10µl/ml plant protease inhibitor mix

2.3.2.6. *Immunoprecipitation of protein complexes*

To prepare crude protein extracts, plant material was ground to fine powder, proteins were extracted in extraction buffer (as in 2.3.2.1) and total protein amount was measured using Bradford assay. To 1 mg input protein 10 µl (2 µg) of mouse monoclonal α-HA antibody was added. The reaction mixture was incubated overnight in the cold room on a rolling platform. Next morning, 20 µl of protein A/G agarose resin was added to each 1 mg of total input protein. The protein sample was incubated for 1-4 h in the cold room on a rolling platform. The protein A/G resin carrying the immunoprecipitated proteins was collected by centrifugation at 1,000 g for 5 min at 4°C and the supernatant was removed. The beads were washed 3 times with extraction buffer in eppendorf tubes. A final washing step was then performed using extraction buffer lacking any detergent. After centrifugation, the supernatant was removed and proteins were eluted from the protein A/G resin with 1 mg/ml HA peptide, using the same volume as protein A/G for the elution volume. The elution was performed at room temperature

for 15 min with gentle shaking. After peptide elution, the beads were boiled with 1X SDS loading buffer in order to remove all proteins from protein A/G agarose. The immunoprecipitated proteins were analyzed by western blotting.

2.3.3.   Yeast molecular biology methods

2.3.3.1.   Small scale transformation of yeast cells using the lithium acetate method

S. cerevisiae cells were inoculated from a 3-5-day-old plate in 20 ml of YPD medium and were grown overnight with vigorous shaking at 28°C. From the overnight culture an aliquot was transferred into fresh YPD to prepare a starter culture of OD_{600}~0.2, which was incubated at 28°C with shaking for ~3-4 h. Cells were collected by centrifugation for 5 min at 3500 rpm and resuspended in 50 ml of water. This washing step was repeated 3 times. After centrifugation, cells were resuspented in 10 ml of 100 mM LiAc solution and incubated for 5 min at 28°C. Then, the cell suspension was divided into 1.5 ml centrifuge tubes according to the number of transformations. Cells were centrifuged and the supernatant was removed. Following components were added on top of the pellet in this order:

> 240 µl 50 % PEG
>
> 36 µl 1 M LiAc
>
> 25 µl 2 mg/ml SS-DNA
>
> 5 µl plasmid DNA
>
> 45 µl ddH$_2$O

The transformation mixture was resuspended and incubated for 30 min at 28°C and then 30 µl of DMSO was added. Subsequently, heat shock was done at 42°C for 20 min with occasional shaking by vortexing. Then, the cells were chilled on ice for 2 min and pelleted. After removal of the supernatant, cells were resuspended in water or 1X TE buffer and plated on selective SD medium.

2.3.3.2.   Plasmid isolation from yeast

A yeast colony was inoculated from a fresh plate in 10 ml of appropriate SD liquid medium and incubated O/N at 28°C with shaking (200-220 rpm). Cells were centrifuged at 13,000 rpm for 5 min. The supernatant was carefully removed and cells were resuspended in the residual liquid. 10 µl of lyticase solution was added and then cells were vortexed and incubated for 30-60 min at 37°C with shaking at 200-250 rpm. Then, 10 µl of 20% SDS was added, the samples were mixed and subjected to a freeze/thaw cycle at -20°C. The sample volume was adjusted to 200 µl with 1X TE buffer (pH 7) and then 200 µl of phenol:chloroform:isoamyl alcohol (25:24:1) was added. The samples were vortexed and centrifuged at 13,000 rpm for 10 min. The upper aqueous phase was transferred into a new centrifuge tube and mixed with 8 µl of 10 M ammonium acetate and 500 µl of 100% ethanol. The tubes were incubated at -70°C for 1 h and then the precipitated DNA was collected by centrifugation at 14,000rpm for 10 min. The DNA pellet was dried and resuspended in 20 µl of water.

<u>Lyticase solution</u>**:**   5 units/µl in TE buffer

2.3.3.3.   *β-galactosidase filter lift assay*

Yeast colonies were grown for 2-3 days at 30°C on Immobilon^{TM}-Nylon membranes. A Whatman paper was presoaked in Z-Buffer/X-Gal solution in a 100-mm Petri dish. The membrane with the colonies was placed in liquid nitrogen until it was completely frozen (about 4 sec), and then thawed at room temperature, and this procedure was repeated 3 times. Then, the filter was placed with its colony side up on the presoaked Whatman paper. The filters were incubated at 30°C and checked periodically for appearance of blue color.

Z-Buffer: 16.1 g/l $Na_2HPO_4 \cdot 7H_2O$, 5.50 g/l $NaH_2PO_4 \cdot H_2O$,
                                         0.75 g/l KCl, 0.246 g/l $MgSO_4 \cdot 7H_2O$, [pH 7.0]

Z-Buffer/X-gal solution: 100 ml Z-Buffer, 0.27 ml β-mercaptoethanol,
                                         1.67 ml X-gal (20mg/ml)

2.3.3.4.   *Yeast one-hybrid assay*

To screen for cDNA clones of transcription factors that can bind to *cis*-regulatory promoter elements of interest, a yeast one-hybrid assay was used. At first, the target promoter constructs were integrated into the genome of the YM4271 strain. Lines carrying the target-pHISi-1 construct were tested on SD/-His plates with different 3-AT concentrations (0, 15, 30, 45 and 60 mM 3-AT) in order to determine a suitable 3-AT concentration to suppress background activity of the *HIS3* reporter gene prior initiating the library screening. Colonies with target-pLacZi constructs were tested for background *lacZ* expression using a colony lift assay. Library scale transformation was done using an AD-cDNA library obtained from *A. thaliana* green cell suspension and the resultant transformation mixture was plated on SD/-His/-Leu/+25 mM 3-AT. Colonies resulting from *HIS3* activation were isolated. DNA-binding activity was confirmed by transforming target-pLacZi reporter strain with the candidate pACT clones and colony lift assay was performed to monitor *lacZ* activity.

2.3.4.   Plant tissue culture and transformation

2.3.4.1.   *Plant growth conditions in the greenhouse*

Arabidopsis thaliana plants were grown in 7 x 7 cm plastic pots at 22°C day and 18°C night temperature, 70% humidity in trays under either short day (8h light/16h dark) or long day conditions (16 h light/8 h dark) under 200 to 400 μEinstein $m^{-2}s^{-1}$ irradiance.

2.3.4.2.   *In vitro cultivation of A. thaliana seedlings*

Sterilized *Arabidopsis* seeds were germinated and grown in MSAR seed medium containing 0.5% sucrose, half concentration of macro-elements and no vitamins, under short day conditions at 20°C using 200 to 400 μEinstein $m^{-2} s^{-1}$ irradiance.

2.3.4.3.   *Maintenance of Arabidopsis cell suspensions*

Each week, 10-15 ml from 50 ml one-week-old *Arabidopsis thaliana* (ecotype Col-0) cell suspension was subcultured in 35-40 ml cell suspension medium for culture maintenance (Mathur and Koncz, 1998). The cells were grown under constant agitation of 120–150 rpm at 18-22°C. Photosynthetic cells suspensions were maintained using 200 to 400 μEinstein m^{-2} s^{-1} white light.

2.3.4.4.   *Sterilization of A. thaliana seeds*

Seeds were placed in an Eppendorf tube and immersed in 70% Ethanol for 1-2 min followed by treatment with Ca-hypochlorite solution for 15 min on a rolling platform. Seeds were then rinsed 3 times with sterile water and either plated directly on appropriate growth medium or allowed to dry in a sterile hood overnight.

Ca-hypochlorite solution: 5% $CaOCl_2$ containing 0.1% Trition X-100 in water

2.3.4.5.   *Agrobacterium-mediated transformation of A. thaliana plants by the floral dip method*

For transformation (Clough and Bent, 1998), bolting plants cultivated in 10 cm pots (10-12 plants/pot) were used. 300-500 ml overnight culture of *Agrobacterium* cells was pelleted at 5000 rpm for 10 min. Agrobacteria were resuspended in 300 ml of transformation medium and plant inflorescences were submerged in this solution for 5 min. Plants were then covered with a plastic bag, which was removed 2 days later. Seeds were collected in paper bags and selected on MSAR plates containing antibiotics.

Transformation medium: ½ MS salts
                                   1X B5 vitamins
                                   5% sucrose
                                   pH 5.7
                                   0.044 μM BAP
                                   0.005% Silwet L-77

2.3.4.6.   *Agrobacterium-mediated transformation of A. thaliana cell suspensions*

Two- to-three-day-old cell suspension was transformed with *Agrobacterium*. Bacterial overnight culture was centrifuged at 5,000 rpm for 10 min and the cells were resuspended in cell suspension medium at OD_{600} 1.0. From this bacterium inoculum, 2-4 ml was added to the *Arabidopsis* cell culture. After 1-2 h of standing, the cell suspension was cultivated as usual. After 2-3 days, antibacterial antibiotics (ticarcillin, cefotaxime) were added to the culture. The cell suspension was subcultured following the original weekly cycle with addition of antibiotics to select for the T-DNA encoded resistance marker. (Ferrando et al., 2000).

2.3.4.7. Selecting for transformed plants

2.3.4.7.1. Selection under sterile conditions

Seeds were sterilized in 15 ml tubes and sawn on MSAR medium containing appropriate antibiotic supplemented with cefotaxime to kill *Agrobacterium*. Antibiotic resistant transformants were transferred first onto non-selective media, then later into soil. Plants were cultivated in the greenhouse and seeds were collected for further analysis.

2.3.4.7.2. Selection in the greenhouse

T1 seeds were sawn on soil in 14 cm x 20 cm containers and after germination 4-5-day-old plantlets were sprayed with 250 mg/ml BASTA solution supplemented with 0.1% Tween-20. Spraying was repeated every second day until sensitive plants died. Transformed plants carrying the BASTA resistance selectable marker were transferred to single pots, cultivated in the greenhouse and seeds were collected.

2.3.4.8. Crosses of Arabidopsis plants

To perform crosses of *Arabidopsis* plants following bolting, mature flowers and siliques were removed from stems. Two to three flowers were emasculated with a pair of forceps by removing petals, sepals and immature anthers. Pollen from a mature male plant was used to dust the stigma. Seed maturation was monitored regularly and fully grown siliques were collected.

2.3.4.9. Measurement of flowering time

To assess flowering time phenotype of *Arabidopsis* mutants, the number of rosette leaves was counted when flower buds appeared at the apical meristem. Flowering time was determined at short day (8 h light/16 h dark) and long day (16 h light/8 h dark) conditions.

2.3.4.10. DNA extraction from plant material

For isolation of DNA from plants, the cetyl-methyl-ammonium bromide (CTAB) method adapted from Rogers and Bendich (1985) was used. Plant material was collected into centrifuge tubes and frozen in liquid nitrogen. Tissue was ground using a plastic rod fitted into a drilling machine. 0.5 ml of preheated (65°C) CTAB 2X was added to the grind the tissue. The crude extract was vortexed and incubated at 65°C for 5-30 min, and then placed on ice. 0.4 ml of chloroform was added and the extract was vortexed and centrifuged for 5 min at 13,000 rpm. 700 µl from the upper water phase was withdrawn and added to 1/10 volume (70 µl) of preheated (65°C) CTAB 10X. Subsequently, 400 µl of chloroform was added, the sample was mixed well and centrifuged for 5 min at 13,000 rpm. Then, 0.6 ml of DNA extract from the upper phase was added to 0.6 ml of CTAB Precipitation Buffer, and then mixed and centrifuged for 10 min at 13,000 rpm. The supernatant was completely removed and the pellet was air-dried for few minutes. The pellet was dissolved in 0.3 ml of High Salt TE buffer, and

thereafter 0.6 ml of 100% ethanol was added. DNA was precipitated at -20°C for 15 min, and then collected by centrifugation for 15 min. Finally the DNA sample was washed with 70% ethanol and after brief drying dissolved in 50 µl of 0.1 x TE.

CTAB 2X:	2% (w/v) CTAB, 100 mM Tris.HCl [8.0], 20 mM EDTA [8.0]
	1.4 M NaCl, 1% (w/v) polyvinylpyrrolidone
CTAB 10X:	10% (w/v) CTAB, 0.7 M NaCl
CTAB Precipitation Buffer:	1% (w/v) CTAB, 50 mM Tris-HCl [8.0], 10 mM EDTA [8.0]
High Salt TE:	10 mM Tris-HCl [8.0], 1 mM EDTA [8.0], 1 M NaCl

2.3.4.11. *Histochemical assay of β-glucuronidase (uidA) reporter enzyme activity in planta*

Freshly harvested seedlings or cell suspension cultures were immersed in X-Gluc solution and vacuum treated for 3 min in an exicator, and then incubated overnight at 37°C. The plant material was stored in 70% ethanol at room temperature after several washing/destaining steps using 70% ethanol (Jefferson et al., 1987).

X-Gluc solution (1L):	1 g X-Gluc dissolved in 2 ml DMSO
	0.1 % Triton X-100
	0.1 M Na phosphate buffer [pH 7.0]
	0.5 mM $K_3Fe(CN)_6$ and 0.5 mM $K_4Fe(CN)_6$

2.3.4.12. *Isolation of plant cell nuclei*

20 g of frozen plant material was ground in liquid nitrogen. The powder was mixed with 40 ml of nuclear grinding buffer and the sample was incubated in the cold room on ice until extraction buffer was melted. The extract was filtered through two layers of Miracloth and one layer of 50 µm nylon mesh and centrifuged at 3,500 rpm for 10 min at 4°C. After removal of supernatant, the crude nuclear pellet was washed three times with nuclear wash buffer followed each time by centrifugation at 3,500 rpm for 5 min at 4°C. The nuclear pellet was dried for few minutes. Extraction of nuclear proteins was performed in nuclear lysis buffer using a dounce homogenisator.

Nuclear grinding buffer:	1 M hexylene glycol
	50 mM Tris-HCl pH 7.5
	10 mM $MgCl_2$
	2 mM ATP
	0.2% Triton X-100
	1 mM DTT
	0.8 mM PMSF
	10 µl/ml PIC
Nuclear wash buffer:	0.5 M hexylene glycol
	50 mM Tris-HCl pH 7.5
	10 mM $MgCl_2$
	2 mM ATP

	0.2% Triton X-100
	1 mM DTT
	0.8 mM PMSF
	10 µl/ml PIC

Nuclear lysis buffer**:**	50 mM HEPES pH 7.5
	50 mM KCl
	5 mM MgCl$_2$
	10 µM ZnSO4
	1% Triton X-100
	0.5% Sarcosyl
	0.1% Na-deoxycholate
	0.1% Igepal
	1 mM PMSF
	10 µl/ml PIC

2.3.5. Cell biological methods

2.3.5.1. *Light microscopy*

Light microscopy was performed with Leica MZFLIII microscope and images were captured and processed with Diskus version 4.30.102 program.

2.3.5.2. *Indirect immunofluorescence microscopy*

The indirect immunofluorescence microscopy studies were performed in collaboration with Dr. Jan Jásik. Seedlings collected 7 days after germination were fixed, embedded, sectioned and probed with epitope specific antibodies as described previously by Ferrando et al. (2000). Fluorescence images were examined using Leica Aristoplan and DMRB microscopes using fluorescein-5-isothiocyanate (FITC) and rhodamine (Cy^{TM}3) filters, and recorded with a Hitachi HV-20 camera controlled by a Diskus computer program.

2.3.5.3. *Confocal laser scanning microscopy*

The localization of GFP-tagged proteins in fresh tissue samples was with the Leica SP2 AOBS (Leica, Bensheim, Germany) system. GFP was excited with the Argon laser at 488 nm and the emitted fluorescence was detected between 505 and 535 nm, the autofluorescence of chlorophyll was detected at 620-720. Simultaneous brightfield images were recorded by a transmission detector. Merging of images and calculations of 3D projections were performed with the Leica LCS software. Selected images were processed with Adobe Photoshop.

3. RESULTS

3.1. Analysis of *PRL1* gene expression pattern and identification of essential transcription regulatory regions

3.1.1. Overexpression of *PRL1* cDNA

To facilitate the isolation and biochemical analysis of PRL1-associated protein complexes, various cDNA contructs were previously generated to overexpress the PRL1 protein in fusion with short hemagglutinin (HA) or c-Myc peptide epitopes in transgenic plants and cell suspensions. The *PRL1* cDNA was thus fused to an intron-containing HiA epitope coding sequence and cloned into a gene expression cassette downstream of the CaMV35S promoter by J. Jásik (Ferrando et al., 2000). At the start of this thesis work, this construct was introduced into wild type Col-0 and *prl1* mutant plants and thereafter lines carrying the CaMV35S::*PRL1-HiA* in homozygous form were isolated. Subsequently, a genetic complementation assay was performed to test whether the overexpression construct could restore the complex pleiotropic *prl1* mutant phenotype to wild type and thereby prove that this construct was functional. The majority of *prl1* plants (over 70%) carrying the CaMV35S:*PRL1-HiA* construct showed wild type leaf and rosette phenotype when grown in soil in the greenhouse (data not shown). To determine whether the root elongation defect of the *prl1* mutant was also complemented by this construct, the root length of an isolated homozygous line was investigated (Figure 7 A).
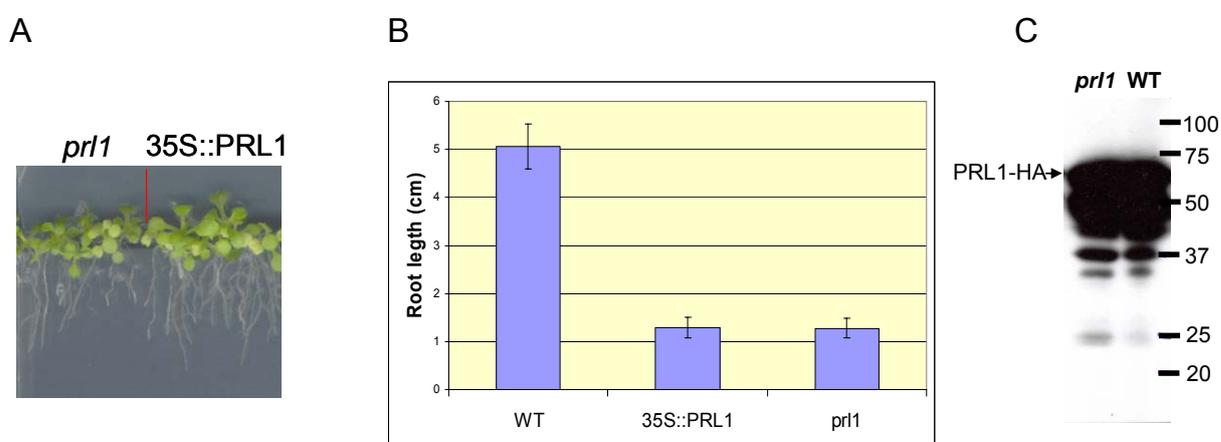
Figure 7.   Genetic complementation assay with the CaMV35S:PRL1-HiA construct
(A) Root length of a *prl1* mutant carrying the CaMV35S:*PRL1-HiA* construct was compared to that of *prl1* mutant plants on vertical plates. (B) Root length of *prl1* and wild type plants homozygous for the CaMV35S:PRL1-HiA construct were measured 15 days after germination. (C) Immunodetection of HA-tagged PRL1-HiA protein using an anti-HA antibody. Wild type and *prl1* plants homozygous for CaMV35S:PRL1-HiA were grown on MSAR medium containing 0.5 % sucrose. Total protein samples were extracted from 2-week-old seedlings and resolved on 12% SDS-PAGE gel.

Seedlings were grown on vertically oriented MSAR plates for 15 days then the root length of ten individuals from each line was measured. As control, wild type and *prl1* plants grown on the same plate were scored. Surprisingly, the data indicated that the CaMV35S:*PRL1-HiA* construct did not complement the *prl1* short root phenotype. The root length of plants homozygous for both CaMV35S-PRL1-HiA and *prl1* mutation was comparable to that of the *prl1* mutant, which has approximately 3-

fold shorter roots than wild type seedlings (Figure 7 B). Overexpression of the *PRL1-HiA* cDNA did not result in any phenotypical change in the wild type background. The synthesis of PRL1-HiA protein in these lines was verified by immunodetection using an anti-HA antibody (Figure 7 C). Total protein extracts were prepared from two-week-old seedlings carrying the CaMV35S:*PRL1-HiA* construct in homozygous state in either *prl1* or wild type background. Significantly high levels of PRL1-HiA signals were detected in both cases corresponding to the full length protein but several smaller bands were also observed suggesting possible degradation of PRL1.

3.1.2. Genetic complementation assay using an estradiol-inducible *PRL1* genomic construct

The failure to obtain genetic complementation of *prl1* root elongation defect by overexpression of *PRL1* cDNA supported the observations of Nemeth et al. (1998), who could obtain genetic complementation only with the wild type *PRL1* genomic clone. Therefore, to perform a conditional genetic complementation assay, we have labelled the *PRL1* gene with HA epitope coding sequences and cloned it in the estradiol-inducible pER8 (XVE) binary plant expression vector (Zou et al., 2000). First, the *PRL1* genomic fragment was fused to HA-tag in a pBS vector. The last 200 bp of *PRL1* coding region was amplified using HASpe and Prl1ndef primers (2.1.6.2) and the C-terminal coding region was exchanged in the pBS-PRL1 genomic clone with this PCR amplified fragment using *Nde*I-*Spe*I digestion. The pER8 binary vector, which was modified by exchanging its hygromycin resistance plant selectable marker gene for a kanamycin resistance gene (Ph.D. thesis Lafos, 2006), carries only two unique cloning sites downstream of its estradiol-inducible promoter: a 5' *Xho*I and a 3' *Spe*I site. Upon investigation of the pBS-PRL1-HA genomic construct, both sites appeared to be suitable for subcloning. As a unique *Xho*I site was present just upstream of the start codon of the *PRL1* gene, this site and an *Spe*I site downstream of the *PRL1* stop codon were used to construct the expression vector pER8(Km)-PRL1genomic-HA. This construct was transformed into *prl1* mutant plants and T1 transgenic seedlings were selected in the presence of kanamycin. All kanamycin resistant T1 plants showed wild type leaf and rosette phenotype. T2 progeny of ten T1 plants was further investigated in order to check their root elongation phenotype by growing of seedlings on MSAR plates placed vertically. All kanamycin resistant T2 progeny segregated at 3:1 or higher ratio the wild type and *prl1* root phenotype, indicating that even in the absence of estradiol induction the pER8(Km)-PRL1genomic-HA construct also complemented the root elongation defect caused by the *prl1* mutation (Figure 8 A).

To further investigate this unexpected behaviour of pER8(Km)-PRL1genomic-HA construct, an estradiol induction experiment was performed with eight T2 lines. Seeds were sterilized and plated on MSAR plates containing kanamycin. Resistant seedlings were transformed into liquid MS medium containing 0.5% sucrose and 1/2 MS salts two weeks after germination. Half of the plant material was treated with 2 μM estradiol dissolved in DMSO, while the other half was incubated with equivalent amount of DMSO. The samples were induced for 24 h and then frozen in liquid nitrogen. Crude protein extract was prepared and PRL1-HA expression was monitored by western blotting using an

anti-HA antibody. High levels of PRL1-HA protein were detected even if the seedlings had not been induced with estradiol and only a slight induction was observed as a consequence of estradiol treatment (Figure 8 B).
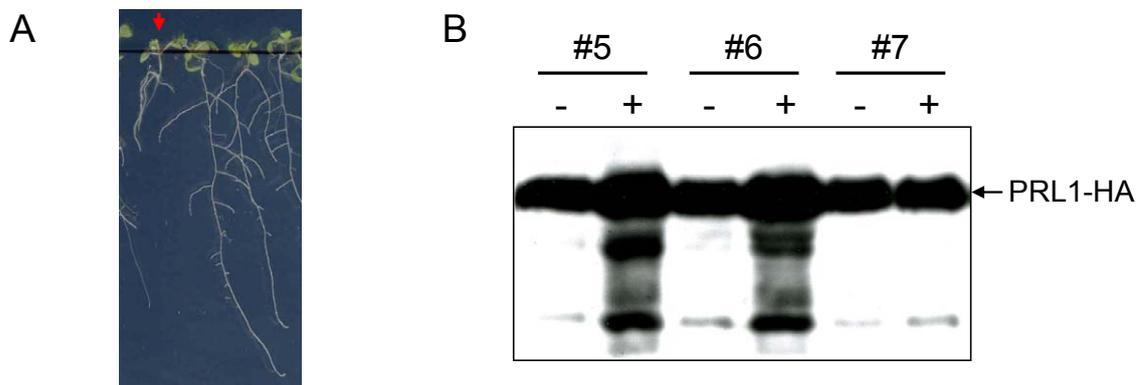
Figure 8. **Analysis of estradiol inducible PRL1-HA synthesis in transgenic plants carrying the pER8(Km)-PRL1genomic-HA construct**
(A) Root length of T2 progeny of plants carrying the estradiol-inducible pER8(Km)-PRL1genomic-HA construct was measured on vertical MSAR plates containing 0.5% sucrose. T2 families of all examined T1 lines segregated wild type-like and *prl1* mutant (marked with red arrow) at 3:1 or higher ratios. (B) Estradiol induction was performed with seedlings selected on kanamycin plates. Plants were transformed into liquid MS medium and incubated for 24h with either DMSO (-) or 2 µM estradiol dissolved in DMSO (+). Protein extracts prepared from these seedlings were separated by 12% SDS-PAGE gel and the PRL1-HA protein was detected by western blotting with anti-HA antibody.

3.1.3. Testing the stringency of estradiol induction of pER8 vector using a *GUS* reporter gene

The pER8 vector constructed by *Zuo et al.* (2000) carries a gene driven by a constitutive active G10-90 promoter that encodes a chimera protein composed of the LexA DNA-binding domain (residues 1-87), the acidic transcription activation domain of VP16 (residues 403-479) and the regulatory region of the human estrogen receptor hER (residues 282-595). As second component, pER8 carries an inducible gene expression cassette providing a multiple cloning site downstream of eight copies of LexA operator sequence and an upstream CaMV35S minimal promoter. The chimeric LexA-VP16-hER protein is constitutively expressed but can only activate transcription of the target gene by CaMV35S-LexA promoter upon estradiol treatment. The presence of estradiol induces changes in the protein conformation, allowing the LexA DNA-binding domain to recognize the LexA operator of CaMV35S-LexA promoter. In addition, pER8 carries a hygromycin resistance gene as plant selectable marker.

To determine whether genetic complementation of the *prl1* mutation by the pER8(Km)-PRL1genomic-HA construct in the absence of estradiol induction resulted from high basic level activity of the LexA-CaMV35S minimal promoter of pER8, we performed a control experiment. To monitor the stringency of estradiol-dependent gene expression from pER8, an intron containing *GUS* (*uidA*) reporter gene was inserted downstream of the inducible CaMV35A-LexA promoter in the pER8-iGUS control plasmid by I. Kovács. This plasmid was transformed into *A. tumefaciens* GV3101 (pMP90) and wild type plants were subsequently transformed. T1 seeds were germinated on hygromycin selection plates and transgenic plants were isolated. Seeds from ten T2 families were

germinated on selection plates and after two weeks plantlets were transferred into liquid MS media containing either 2 μM estradiol dissolved in DMSO or only equivalent amount of DMSO. GUS reporter enzyme activity was monitored by histochemical staining after 24 h induction. Plants that were treated only with DMSO did not show GUS staining, whereas as a result of estradiol induction high GUS activity was observed in all tissues of seedlings, although some differences in expression levels were observed between different T2 lines (Figure 9). This control experiment demonstrated that the pER8 expression system is tightly regulated by estradiol. Therefore, the results also suggested that the genomic *Xho*I-*Spe*I PRL1 fragment contains important transcription regulatory elements, which are likely sufficient to drive specific *PRL1* expression conferring genetic complementation of the *prl1* mutation.
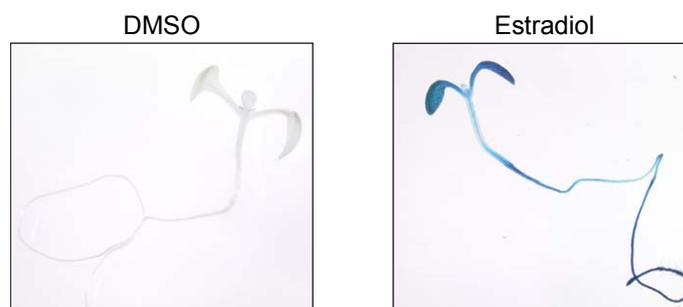
Figure 9. **Histochemical assay of GUS reporter enzyme activity of pER8-iGUS seedlings in the absence and presence of estradiol**
Seedlings were grown on selective MSAR plates for two weeks and then resistant plants were transferred into liquid MS medium supplemented with either DMSO or 2 μM estradiol dissolved in DMSO for 24 h. After induction, the seedlings were stained with X-Gluc solution overnight at 37°C.

3.1.4.   Characterization of an estradiol-inducible *PRL1* cDNA construct

To strengthen the hypothesis that transcription regulatory elements within the *PRL1* gene were responsible for estradiol-independent expression and genetic complementation conferred by the pER8(Km)-PRL1genomic-HA construct, we had to perform an additional control experiment. This experiment addressed the question whether the *PRL1* cDNA expressed by the pER8 vector would complement the *prl1* mutation. The *PRL1* cDNA was PCR amplified using the XhoIF and HASpe primers (2.1.6.2) and the obtained DNA fragment was digested with *Xho*I-*Spe*I and inserted into *Xho*I-*Spe*I cleaved pER8. The accuracy of PCR was controlled by DNA sequencing. This pER8(Km)-PRL1-cDNA-HA construct was transformed into *Agrobacterium* and then into *prl1* mutant plants to select T1 transformants on MSAR plates supplemented with kanamycin. The plants carrying the resistance marker showed *prl1* mutant phenotype both in MS medium and upon later transfer into soil. The phenotype of these transgenic plants was further characterized in the T2 generation by measuring the root lengths of seedlings germinated on vertically oriented MS plates (Figure 10 A). This control experiment clearly demonstrated that the pER8(Km)-PRL1-cDNA-HA construct failed to complement the root elongation defect of the *prl1* mutant when plantlets were growing without estradiol. Our prediction that the *Xho*I-*Spe*I *PRL1* genomic fragment that carried only 62 bp upstream of the ATG

codon carried transcription regulatory sequences required for wild type *PRL1* expression and complementation of the *prl1* mutation thus appeared to be correct.
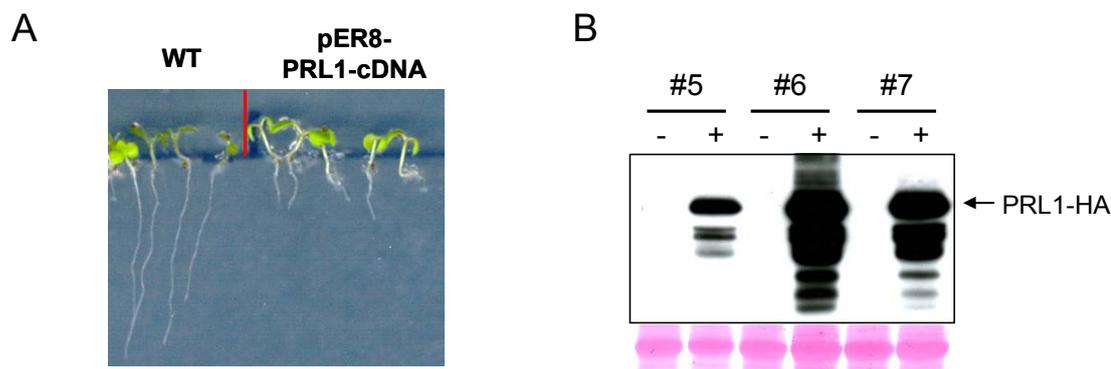
Figure 10. **Analysis of plants carrying the estradiol-inducible pER8(Km)-PRL1-cDNA-HA construct**
(A) T2 progeny of pER8(Km)-PRL1-cDNA-HA transformed plants were germinated on vertical MSAR plates and the root length was monitored after 2 weeks. (B) Immunodetection of HA epitope tagged PRL1-HA protein by western blotting using anti-HA antibody. Seedlings were selected on kanamycin containing MSAR plates for two weeks and then transferred into liquid MS medium supplemented with either DMSO (-) or 2 μM estradiol in DMSO (+). Samples containing 20 μg of total protein were resolved by 12% SDS-PAGE gel. Ponceau staining of the corresponding membrane used for western blotting is shown as a control for equal loading.

To test estradiol-inducibility of the pER8(Km)-PRL1-cDNA-HA construct in the *prl1* mutant, seedlings from eight T2 independent families were grown on kanamycin containing plates for two weeks and then transferred into liquid MS medium containing 2 μM estradiol or equivalent amount of DMSO. The plant material was snap-frozen in liquid nitrogen after 24 h incubation. Total protein samples were extracted and separated on a 12% SDS-PAGE gel and subjected to western blotting with anti-HA antibody to detect the HA-epitope-tagged PRL1-HA protein. (Figure 10 B). Despite considerable variation between the transformed lines, PRL1-HA protein was only detected in the estradiol-induced seedlings. This confirmed that the pER8 expression system was tightly regulated.

To investigate genetic complementation ability of the pER8(Km)-PRL1-cDNA-HA construct, ten lines from the T2 progeny of transformed plants were germinated on kanamycin-free vertical MSAR plates supplemented with 4 μM estradiol. Root length of seedlings was measured at the age of 7 days and 17 days (Figure 11). Five lines showed *prl1* root phenotype after 7 days and five lines (#1, #2, #5, #7 and #9) had long roots similar to wild type plants. The segregating *prl1* mutant seedlings were removed from the T2 populations and the root phenotype was assessed again at day 17 after germination for two lines (#2, #5) which showed wild type phenotype. The other lines (#1, #7 and #9), which showed complementation of the *prl1* root elongation defect after 7 days, discontinued normal root development and their root length was between those of *prl1* and wild type at day 17.

In seedlings collected from the different T2 families at day 17 after germination, the expression levels of PRL1-HA protein were compared by western blotting with anti-HA antibody (Figure 12). Crude protein samples were also extracted from lines that showed wild type root length only after 7 days. In each case, 20 μg of protein sample was resolved by 12% SDS-PAGE and equal loading was controlled by Ponceau staining and western blotting of the same membrane with an anti-tubulin antibody. Lines #2 and #5, showing wild type root elongation phenotype at both days 7 and 17
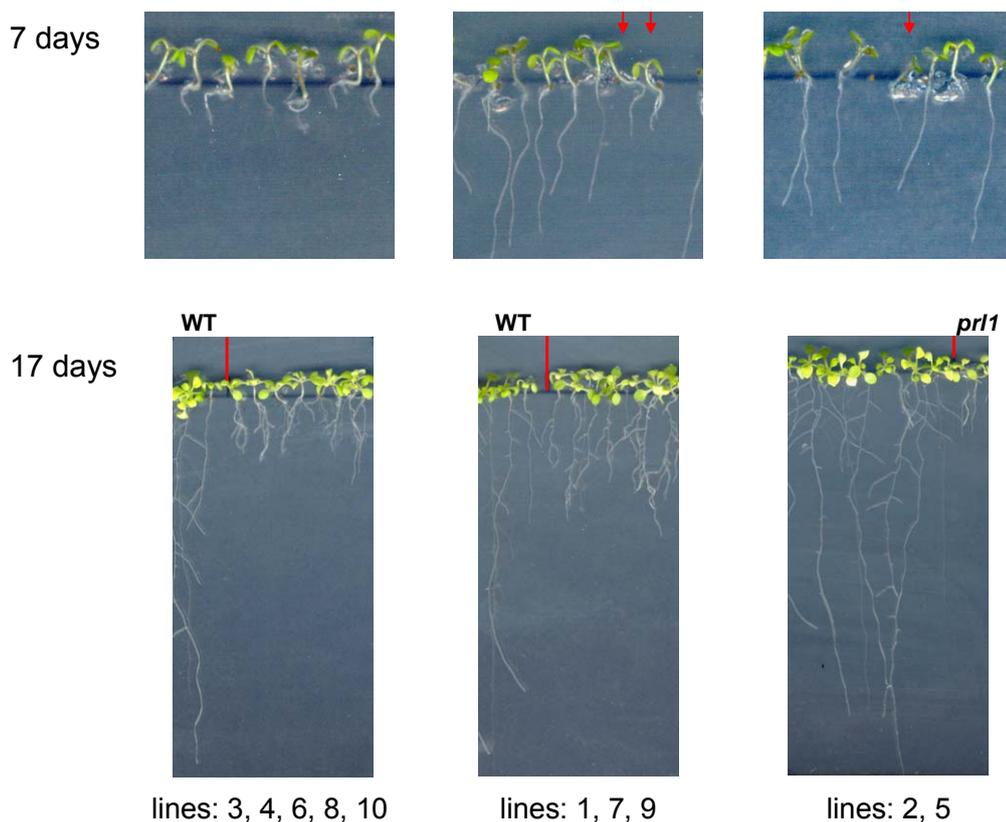
Figure 11. **Genetic complementation analysis with the estradiol-inducible pER8(Km)-PRL1-cDNA-HA construct.**

Root length of ten T2 lines was monitored on kanamycin-free vertical MSAR plates containing 4 μM estradiol at days 7 and 17 after germination. Three phenotypic classes could be distinguished: i) lines that showed *prl1* phenotype at both of the time points of root measurement (#3, #4, #6, #8 and #10), ii) lines that displayed wild type root length at day 7 but had shorter than wild type roots at day 17 (#1,#7 and #9) and iii) lines that showed wild type root phenotype both at days 7 and 17 after germination (#2 and #5). Segregating *prl1* mutant plants are marked with red arrows. Wild type (WT) and *prl1* mutant plants were germinated on each plate as controls for direct comparison (not shown for each plate).
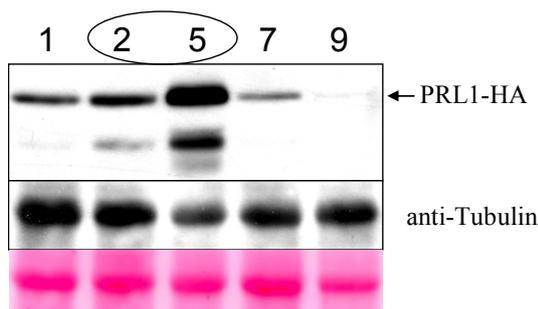
Figure 12. **Immunodetection of PRL1-HA protein in seedlings displaying full or partial complememtation of *prl1* root elongation defect by the eastradiol-inducible pER8(Km)-PRL1-cDNA-HA construct in the presence of estradiol.**

Protein extracts were prepared from lines 1, 2, 5, 7 and 9 at day 17 after germination. Each sample, containing 20 μg of protein, was resolved by 12% SDS-PAGE gel and analyzed by western blotting. The membrane was stained with Ponceau-S and subjected to immunodetection first with anti-HA IgG and then after stripping with anti-tubulin antibody.

after germination, expressed the highest level of PRL-HA protein, whereas in all other lines lower levels of PRL1-HA protein was detected. These results indicated that complementation of the *prl1* root elongation defect correlated with high level overexpression of *PRL1* cDNA. Thus, the failure of

genetic complementation with the first tested 35S::PRL1cDNA-HiA construct probably reflected the fact that a certain threshold of wild type PRL1 protein synthesis is necessary for full genetic complementation of the *prl1* root elongation defect.

3.1.5. Characterization of the *prl1-5* (SAIL_1276G04) mutant allele

We have screened the publicly available insertion mutant collections for new *prl1* alleles. In the SAIL collection, we identified a T-DNA insertion in the *PRL1* promoter region. PCR amplification of DNA fragments carrying the boundaries of the T-DNA insertion was performed using combinations of *PRL1* gene specific PRL1 ups and PRL1 5'rev primers with the right border (RB) specific DAP RB2 and left border (LB) specific SAIL LB3 T-DNA primers (2.1.6.4). PCR analysis of 19 plants from the segregating M3 population has identified homozygous lines, which did not carry the wild type DNA fragment of 1.8 kb amplified by the gene specific primers (Figure 13 A and B, lines 1, 4, 7, 10 and 15). Combinations of the T-DNA left border primer with both PRL1 ups and PRL1 5'rev gene specific primers yielded PCR products indicating that the SAIL_1276G04 mutant line carried an inverted tandem (LB-RB/RB-LB) T-DNA repeat in the *PRL1* promoter region.
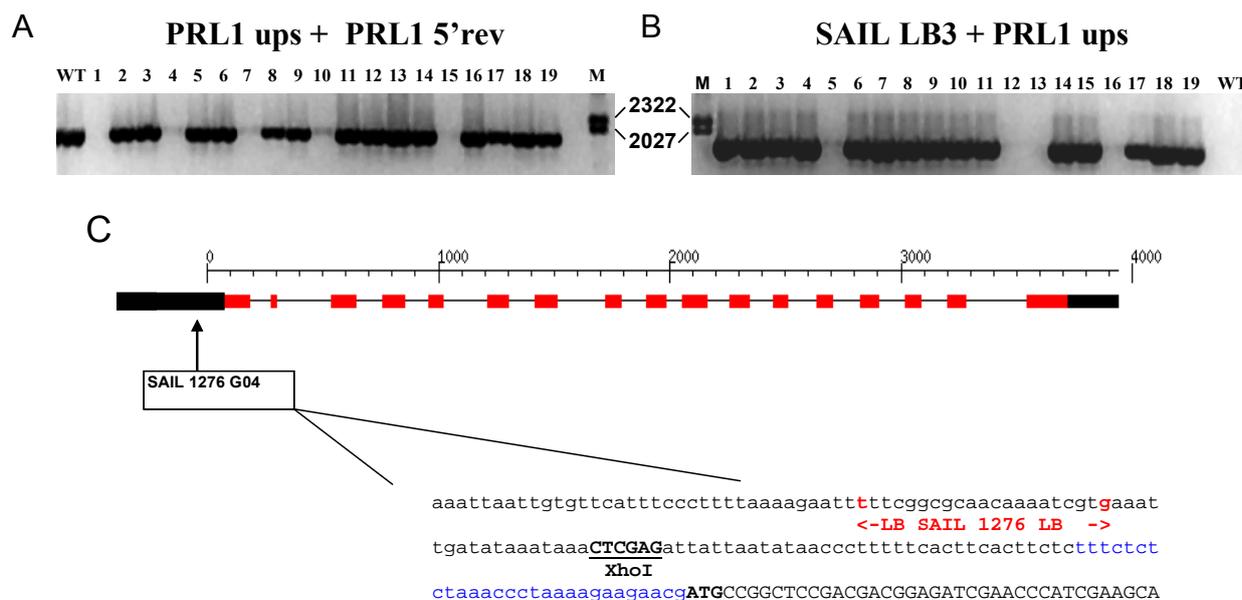
Figure 13.   **Localization of the T-DNA insertion in the *prl1-5* (SAIL_1276 G04) mutant**
(A) PCR analysis M3 seedlings using the PRL1 ups and PRL1 5'rev gene specific primers. (B) PCR amplification of the T-DNA left border junction using the SAIL LB3 and PRL1 ups primers. (C) Schematic illustration of the insertion site and sequence of the T-DNA LB junction facing the 5'-end of the *PRL1* gene in the SAIL_1276G04 mutant. The 5' UTR is marked with blue colour.

Sequencing of the PCR amplified T-DNA left border junctions revealed that the inverted T-DNA repeat was integrated 85 bp upstream of the ATG codon of the *PRL1* gene. The position of the SAIL_1276G04 T-DNA insertion (designated later as the *prl1-5* allele) was located 17 bp upstream of the *Xho*I site that represented the 5'-end of the *PRL1* gene fragment, which we used in the pER8(Km)-PRL1genomic-HA construct characterized in section 3.2.1. Sequences downstream of the T-DNA insertion and the XhoI site carried only the TATA-box and 5' non-translated UTR sequences of the

PRL1 gene (Figure 13 C). To characterize the segregation and phenotype caused by the SAIL_1276G04 T-DNA insertion, seeds from the M2 and derived M3 families were germinated on selective MSAR plates containing DL-phosphinothricin (PPT) and on non-selective MSAR plates. Plants homozygous for *prl1-5* (SAIL_1276 G04) mutation showed wild type phenotype (data not shown). This observation suggested that either the mannopine synthase 2' promoter (MAS 2') located upstream of the left border of the SAIL-1276 G04 T-DNA insert resulted in the transcription of the *PRL1* or – as suggested by our previous results – *PRL1* sequences located downstream of the *Xho*I site (at position -62 upstream of ATG) carried all regulatory elements necessary for proper transcription of the *PRL1* gene.

3.1.6. Search for putative regulatory elements in the *PRL1* promoter sequence

Our results obtained with the *prl1-5* (SAIL_1276G04) T-DNA insertion mutant and genetic complementation studies with the pER8(Km)-PRL1genomic-HA construct strongly suggested that transcription of the *PRL1* gene is controlled by an unusual promoter region, which overlaps with 5'-sequences of the coding region. The *Xho*I site used for construction of the pER8(Km)-PRL1genomic-HA vector was located only 62 bp upstream of the ATG codon in the vicinity of a putative TATA-box (TATAAAT) at position -78 bp (Figure 14).

```
                                                                UTR
 -87   TGAAATTGATATAAATAAACTCGAGATTATTAATATAACCCTTTTTCACTT
                               XhoI
 -36   CACTTCTCTTTCTCTCTAAACCCTAAAAGAAGAACGATGCCGGCTCCGA

  14   CGACGGAGATCGAACCCATCGAAGCACAGTCACTGAAAAAGCTCAGTC

  62   TCAAATCCCTCAAACGATCACTTGAACTCTTCTCTCCCGTCCATGGCCA

 111    ATTCCCTCCTCCTGACCCGGAAGCGTTAGTCTTCTTCGATCCCCAATTT

 160   TCGATTCGAATCTTCATTTTCTTCACTAAGTTTTTATGATTTCTTCGTTTT

 211   TTTTTTTTTTTTTTGCAGCAAGCAGATTCGTCTCAGCCATAAGGTAAAAC

 261   ATTGAGTCTCTCTTACCAGTCTTTAGAAATTTATTTCAGTTATTCGCTTTT

 312   AATGTCTATTGATTGGATTTTGGTTTAAAGCTTCGAACTTTAGGTTTATTC

 363   AGGTTTTTCCATAATTGTTCTAAATCTTCAGGTTTTGTTACCAATAATAGT

 414    AAAGATGGTTGATTTACTTAGACTCTCTCTCTCTCTCTGTTGTGTATGTT

 464    ACTGATTTTAGAAGTTTTCTTTGTACAGATGAAAGTTGCGTTTGGAGGTG

 514   TAGAACCTGTTGTGAGTCAACCTCCACGTCAACCTGACCGCATCAATGA
                                          BmgBI
 563   GCAGCCAGGACCTTCAAATGCTCTTTCCCTCGCAGGTGTTTTTCATATCA

 613   CTATGTCTTGGTGAAAGATAAAAACTTGTTTCTTGTTTGCTATTTGCATTC
```

Figure 14.   Putative transcription regulatory sequences in the *PRL1* promoter sequence
The *PRL1* promoter sequence was analyzed to predict the localization of putative transcription regulatory regions. TC-rich elements were present in the 5' UTR and the second intron. A polyT stretch was found in the first intron. These regions are underlined and marked with bold letters. Exons are marked with lilac letters and underlined. The 5'-UTR sequence is blue coloured. Intron and 5'-upstream promoter sequences are indicated with black letters. Putative TATA-box sequences are labelled with orange colour and underlined. Restriction enzyme recognition sites are denoted with red letters and underlined.

We have also identified an alternative TATA-box (TATTAAT) at position -60 bp, just upstream of the putative transcription initiation site CACTTCACTT sequence. This site is embedded into a TC-rich region of the 5' UTR (TCACTTCACTTCTCTTTCTCTCT) that resembles to postulated binding sites of plant GAGA-binding factors that may function as transcriptional activators (Santi et al., 2003). Within the coding region, the first intron contains an 18-nucleotide long polypyrimidine tract followed by an unusually short second exon of 24 bp. This sequence arrangement was reported to be crucial in proper splicing (Simpson et al., 2004). In the second intron, we have identified another TC-repeat (CTCTCTCTCTCTCTCT) with possible relevance in regulation of transcription.

3.1.7.   Construction of a *PRL1* promoter-driven *GUS* reporter gene

To characterize the temporal and spatial regulation of the unusual promoter region of the *PRL1* gene, a *PRL1::GUS* reporter gene construct was generated. As source construct, we used a plasmid generated by Nemeth *et al*. (1998) for genetic complementation of the *prl1* mutation using the wild type *PRL1* gene. A 7.9 kb *Xba*I-*Spe*I fragment was isolated from the pgcPRL16 genomic clone of Nemeth et al., (1998) and inserted into the binary vector pPCV002 for transformation of *prl1* plants. This genomic DNA fragment carried a 5' promoter region of 3.5 kb upstream of the coding region. In control experiments performed by J. Jásik in our laboratory this 3.5 kb promoter region, extending to the *Xho*I site upstream of the ATG, proved to be transcriptionally inactive. This, together with our previous results, also suggested that intragenic sequences might be important for proper transcription of the *PRL1* gene. Therefore, in construction of the *PRL1::GUS* reporter gene we combined the 3.5 kb upstream promoter region with sequences of the 5'-UTR and coding region extending to the start of the third exon of the *PRL1* gene. From the pBS-PRL1 plasmid, carrying the genomic region of *PRL1*, an *Xba*I-*BmgB*I DNA fragment was cloned into the promoter testing vector pPCV812 digested with *Xba*I-*Sma*I restriction enzymes. Thus, the *GUS* reporter gene was fused in frame with the third exon of the *PRL1* gene. This binary vector pPCV812-PRL1-PROM was transferred into *Agrobacterium* GV3101 (pMP90RK) and then used for transformation of dark- and light-grown cell suspensions and wild type plants. The expression of the GUS reporter enzyme was confirmed in the transformed cell suspensions by histochemical assays. To study the expression of *PRL1-GUS* reporter gene in plants, transformed T1 seedlings were selected on hygromycin plates. From 65 T1 lines isolated, T2 progeny of ten independent lines were used in subsequent study of expression pattern of the PRL1-GUS reporter construct.

3.1.8.   Characterization of *PRL1* promoter activity *in planta*

Spatial expression pattern of the *PRL1-GUS* reporter gene was characterized by monitoring the GUS enzyme activity with histochemical staining. Plant material after a short vacuum treatment was incubated in X-Gluc solution overnight at 37°C. On the following day, plants were fixed and destained in 75% ethanol. The T2 lines were tested at the age of one and two weeks in order to monitor possible

developmental changes in *PRL1* promoter activity. Comparative evaluation of the data showed that *PRL1* promoter is active in most tissues (Figure 15).
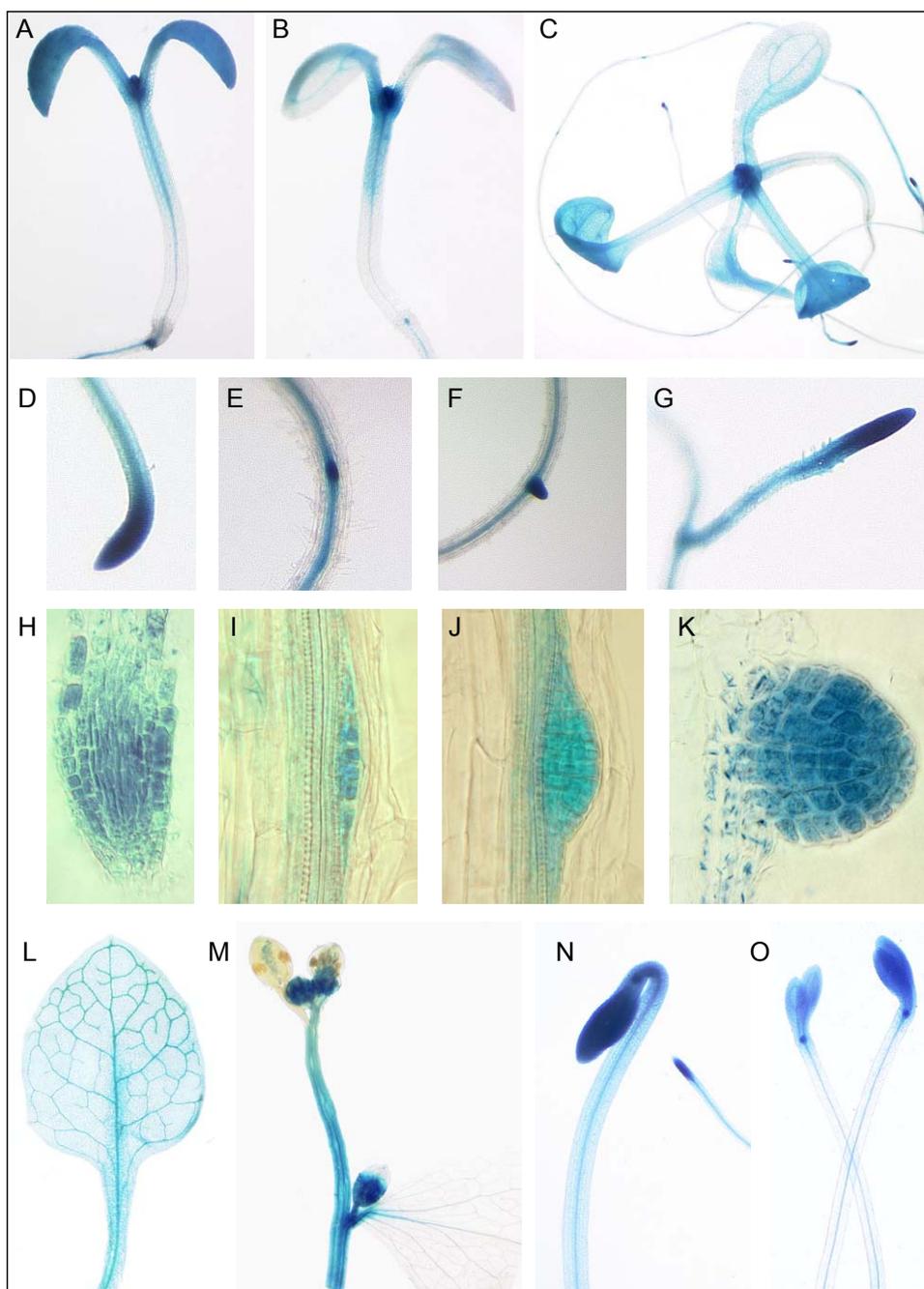
Figure 15. **Histochemical analysis of PRL1::GUS expression pattern**
(A), (B) One week-old seedlings. (C) Two weeks-old seedling. (D), (H) Root apical meristems. (E-G), (I-K) Lateral root formation. (L) Rosette leaf. (M) Stem with flowers (N), (O) Etiolated seedlings at the age of 5 and 12 days.

GUS staining was detected in roots, cotyledons, hypocotyls, leaves and petioles. Apparently, the GUS activity was the highest in apical meristems. In roots, the *PRL1::GUS* construct showed expression in the root apices, the central cylinder and meristems of emerging lateral roots. In shoots, the *PRL1* promoter showed high activity in the apical meristem and leaf primordia. During later development, GUS activity was notably restricted to vascular tissues of mature leaves. In various organs collected from fully developed plants growing in the greenhouse, GUS activity was also detected in flowers and

siliques. In shoots, the lateral meristems displayed high GUS activity. The *PRL1* promoter was also active in dark-grown seedlings showing strong expression in their apical meristems.

3.1.9. Construction of GUS reporter lines with *PRL1* promoter deletions

To identify sequence elements that play a role in regulation of *PRL1* transcription, a set of promoter deletion constructs was made. To clone a short 0.6 kb version of the *PRL1* promoter into pPCV812, the genomic clone pBS-PRL1 was digested with *Xho*I-*BmgB*I, the overhanging ends of the isolated DNA fragment were filled with T4 DNA polymerase and this fragment was inserted into *Sma*I digested and dephoshorylated pPCV812 vector. The orientation of the promoter segment and its junction sequence in the resulting pPCV812-PRL1-PROM-XhoI-BmgBI construct was checked by DNA sequencing. Downstream of the *Xho*I site (position -62 upstream of ATG), this construct contained a putative TATA-box, a transcription initiation site in the 5' UTR, and the first two exons and introns. The *GUS* reporter gene was placed in frame with the third exon of *PRL1*.

The second construct was designed to carry an extended promoter region 5'-upstream of the start codon. The pBS-PRL1 genomic clone was digested with *BstB*I and *Xma*I enzymes. The 3'end of the promoter region ending precisely upstream of the ATG codon was PCR amplified using SexAI and UTR primers (2.1.6.2). The accuracy of the PCR amplification was verified by DNA sequencing. This PCR amplified DNA fragment was digested with *BstB*I-*Xma*I and was inserted into the pBS-PRL1 genomic clone, which was digested with *BstB*I and *Xma*I enzymes to yield the construct pBS-PRL1-PROM-UTR construct. From this plasmid, a 3.5 kb promoter region extending to the position of the ATG was excised and inserted into *Xba*I-*Sma*I sites of the pPCV812 promoter testing vector as *Xba*I-*Xma*I fragment. Subsequently, the junctions of the *PRL1* promoter segment in the obtained pPCV812-PRL1-PROM-UTR plasmid were confirmed by sequencing.

The third promoter construct, pPCV812-PRL1-PROM-POLIT was designed to use the short (0.3 kb) version of the *PRL1* promoter in combination with a deletion of the second intron. The short promoter region, starting from the *Xho*I site and extending downstream to the end of second exon, was amplified by PCR using SexAI and POLI primers (2.1.6.2). The sequence of PCR amplified DNA fragment was verified by sequencing. This 0.3 kb fragment was digested with *Xho*I, its ends were filled-in with T4 DNA polymerase, cut with *Xma*I and then ligated into *Xho*I-*Sma*I sites of pPCV812. In pPCV812-PRL1-PROM-POLIT, the *GUS* gene was thus cloned in frame with the second exon of the *PRL1* gene. The plasmids carrying the described *PRL1* promoter constructs were transferred into *Agrobacterium* GV3101(pMP90RK) and transformed into wild type plants, as well as into light- and dark-grown cell suspensions for monitoring GUS reporter enzyme activities.

3.1.10. Comparison of activity of *PRL1* promoter-GUS constructs

The activity of different *PRL1* promoter constructs was first compared in stably transformed cell suspensions using GUS histochemical assay. One week-old cells were transferred into centrifuge tubes and pelleted at 1,000 rpm for 2 min. The supernatant cell suspension medium was removed and cells

were mixed with X-Gluc staining solution and incubated at 37°C overnight. Next day, the X-Gluc solution was removed, the cells were washed and kept in 75% ethanol. GUS reporter activities of the *PRL1* promoter deletion constructs were compared to that of previously characterized (3.1.7) full length *PRL1* promoter construct pPCV812-PRL1-PROM. The line carrying the pPCV812-PRL1-PROM-BmgBI-XhoI construct with a short promoter region extending from position -62 to the start of the third exon 3'-downstream, showed high GUS activity, which was only slightly lower than the activity of pPCV812-PRL1-PROM full-length promoter construct. By contrast, construct pPCV812-PRL1-PROM-UTR (i.e. carrying a deletion of exon-intron sequences downstream of the ATG) and pPCV812-PRL1-PROM-POLIT lines (i.e., containing the short promoter in combination with deletion of intron 2) showed barely detectable GUS reporter enzyme activities in both dark-grown and light-grown photosynthetic cell suspension lines (Figure 16).
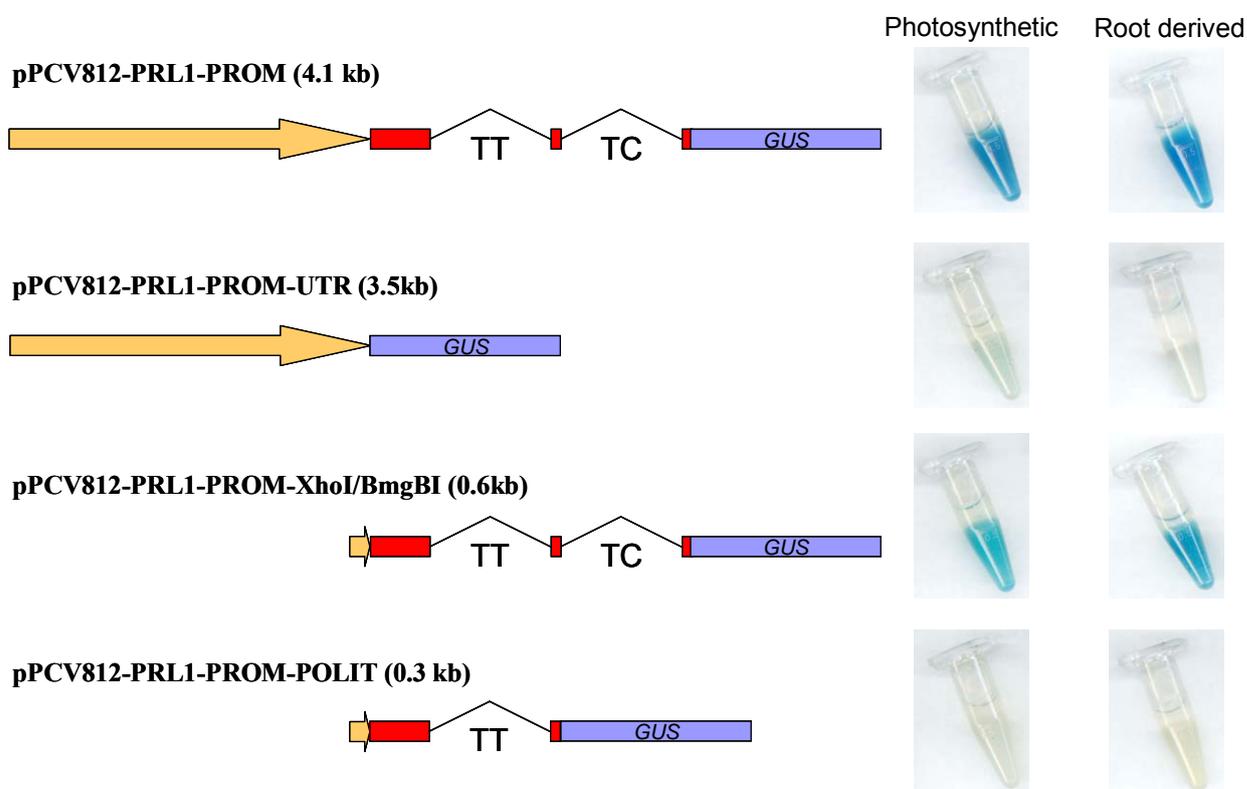
Figure 16. **GUS histochemical assay of activities of *PRL1* promoter deletion constructs in cell suspensions**

PRL1 promoter constructs were introduced into light-grown photosynthetic and dark-grown root-derived *Arabidopsis* cell suspension. Cells from stably transformed suspensions one week after medium change were incubated with X-Gluc solution overnight, destained and washed with 75% ethanol.

These data suggested that promoter sequences located 5'-upstream of the *Xho*I site (position -62 upstream of ATG) play only a minor role in the regulation of *PRL1* expression. This data is also supported by our observation that construct pER8(Km)-PRL1genomic-HA, which carried *PRL1* gene driven by the same short promoter, could fully complement the root elongation defect of the *prl1* mutant (see: section 3.1.2). On the other hand, deletion of the second intron resulted in nearly full inactivation of the short *PRL1* promoter indicating that this region of the *PRL1* gene contains essential

transcription regulatory sequences. This result indicated that the active core of the *PRL1* promoter region extends as far as the third exon into the coding region.

Spatial expression patterns of the *PRL1* promoter deletion constructs were compared by histochemical assay of GUS activities in wild type *Arabidospsis* Col-0 background. Transformed seedlings carrying the different constructs were selected on hygromycin containing MSAR plates. Seedlings representing T2 progeny of five independent T1 lines were stained with X-gluc solution overnight at 37°C two weeks after germination. As in cell suspensions, GUS activity was detected only with the pPCV812-PRL1-PROM and pPCV812-PRL1-PROM-XhoI-BmgBI constructs that both carry *PRL1* gene sequences between position -62 and start of the third exon. Deletion of sequences downstream of the ATG and deletion of the second intron resulted in inactivation of the *PRL1* promoter in all tissues (data not shown).
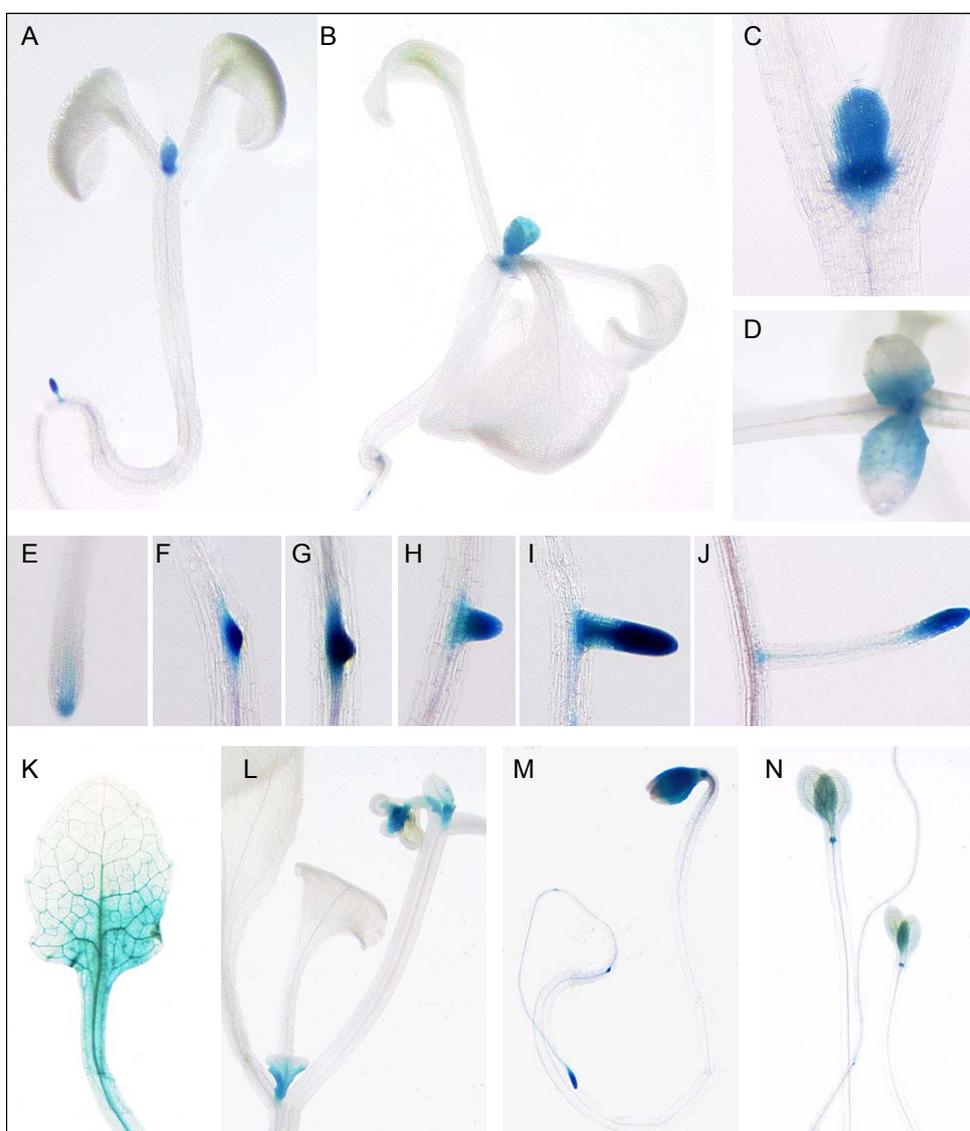
Figure 17. **Histochemical staining of GUS reporter enzyme activity controlled by the short *PRL1* promoter construct pPCV812-PRL1-PROM-XhoI-BmgBI**
Dark and light grown seedlings and various plant organs were stained with X-gluc solution as in Figure 15. (A) One week-old seedling. (B) Two weeks-old seedling. (C), (D) Developing leaves. (E-J) Root apical meristem and lateral root formation. (K) Rosette leaf. (L) Stem with flowers. (M), (N) Etiolated seedlings at the age of 5 and 12 days.

Comparison of spatial and temporal expression patterns of the short promoter pPCV812-PRL1-PROM-XhoI-BmgBI (Figure 17) and full-length promoter pPCV812-PRL1-PROM (Figure 15) lines however indicated significant quantitative differences. The activity of the short promoter appeared to be restricted to meristematic tissues (e.g., vascular cylinder, apical and root meristems, developing side-roots and cotyledons of etiolated seedlings) it showed a similar pattern as the full-length *PRL1* promoter. This data suggested that sequences located upstream of position -62 do play a role in quantitative regulation of the *PRL1* promoter. However, inactivation of the promoter by deletion of intron 2 indicated that the second intron carries essential regulatory sequences that also specify organ and tissue specificity of *PRL1* gene expression.

3.1.11. Elimination of candidate regulatory regions from the second intron

Bioinformatic analysis of potential regulatory sequences within the short *PRL1* promoter (section 3.1.6) indicated that the 5' UTR and second intron contain similar TC-rich elements. To determine whether any of these TC-rich elements play a role in the regulation of activity of the *PRL1* promoter, two additional promoter deletions were generated. To delete the TC-rich sequence, TATA-box and 5'-UTR sequences located between the *Xho*I site (position -62) and the ATG codon, the plasmid pBS-PRL1genomic-HA-ATG was first digested with *Xho*I, then filled in with T4 DNA polymerase, and cut with *BmgB*I. The obtained fragment was inserted into a dephosphorylated *Sma*I site of pPCV812 to produce pPCV812-PRL1-PROM-ATG. To remove the TC-repeat from second intron, the repeat was mutagenized into a polyT stretch using a Transformer[TM] site-directed mutagenesis kit. Plasmid pBS-PRL1-HA was used for site specific mutagenesis using the TTT and NotI primers (2.1.6.3).
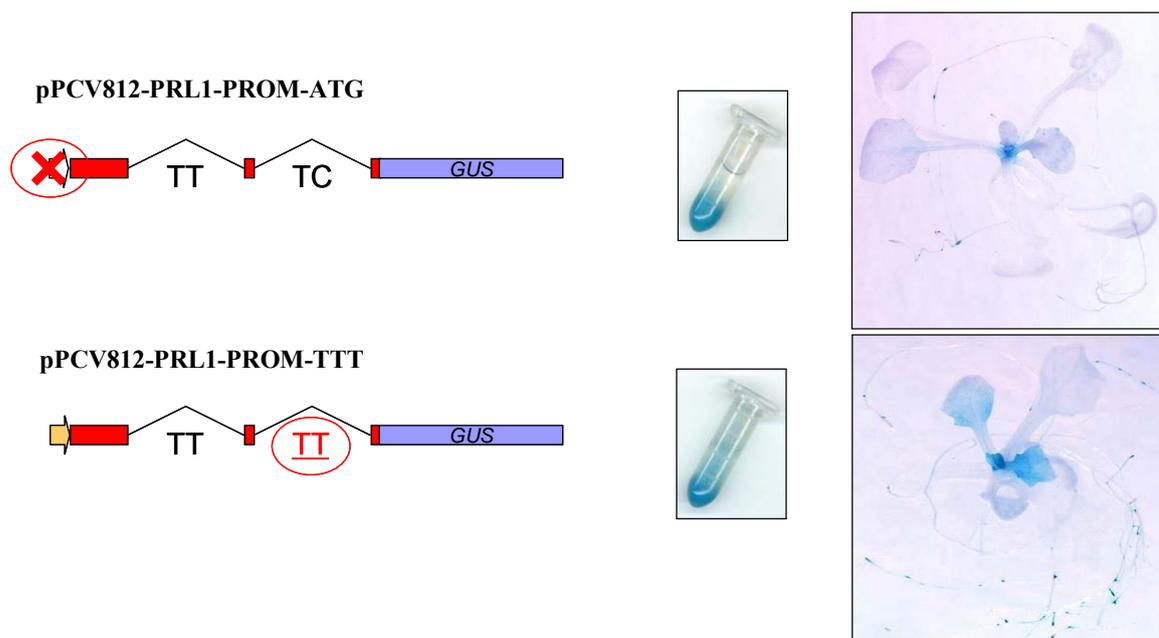
Figure 18.   Histochemical assay of promoter-GUS constructs carrying deletions of TC-rich repeat sequences.
Two constructs were created in order to remove TC-repeats from the 5'-UTR region and second intron of the *PRL1* promoter. Histochemical GUS staining was performed with transformed light-grown cell suspension and two weeks old transgenic Col-0 plants.

The presence of the mutation was confirmed by sequencing and a positive clone was used for subsequent DNA manipulation. The mutated genomic fragment was digested with *Xho*I-*Bmg*BI, the overhanging end was filled in with T4 DNA polymerase, and this fragment was ligated into pPCV812 cut with the *Sma*I restriction enzyme. This obtained pPCV812-PRL1-PROM-TTT construct was also sequenced. These vectors were transformed into wild type *Arabidopsis* plants, as well as to dark- and light-grown cell suspensions.

Histochemical GUS assays were performed with cells of stably transformed light- and dark-grown cell suspensions and the results were compared to those obtained by the control pPCV812-PRL1-PROM-BmgBI-XhoI construct that carried the wild type short *PRL1* promoter (Figure 16). Deletion of the TC-repeat from either the 5'-UTR region or the second intron did not reduce the activity of the short *PRL1* promoter in transformed cells. Similar results were obtained also by inspecting the intensity and pattern of GUS activities monitored by histochemical staining in seedlings transformed with the pPCV812-PRL1-PROM-ATG and pPCV812-PRL1-PROM-TTT constructs (Figure 18). This data indicated that the TC-rich repeat regions do not play a major role in the regulation of *PRL1* promoter activity.

3.1.12. Confirmation of importance of intragenic *PRL1* regulatory sequences by genetic complementation assays

To confirm that intragenic sequences are indeed essential for proper control of the *PRL1* gene expression, genetic complementation assays were performed with the *prl1* mutant. For these experiments a binary vector was constructed, which did not contain any promoter region upstream of the multiple cloning site. First, a variant of pPCV002 vector was created by introduction of an *Xma*I /*Sma*I cleavage site. Vectors pPCV002 and pODB8 (Louvet et al., 1997) were digested with *Xba*I and *BamH*I and a 2.5 kb fragment of pODB8 was inserted into pPCV002. This pPCV002-ODB vector was used for further DNA manipulations. A construct was designed based on the results of Nemeth *et al.* (1998), except there was an HA-epitope introduced to the C-terminal end of *PRL1*. Plasmids pBS-PRL1-HA and pPCV002-ODB were digested with *Xba*I-*Xma*I and ligated. The obtained clone pPCV002-PRL1-HA contained the 3.5 kb full length promoter and the full-length 3.7 kb *PRL1* coding region. The *PRL1-HA* gene in pPCV002-PRL1-HA is identical with the gene construct present in the complementation construct pER8(Km)-PRL1genomic-HA described in 3.1.2, but does not contain a short segment of the CaMV35S promoter upstream of the *PRL1* gene, which could have influenced the gene expression in case of pER8(Km)-PRL1genomic-HA.

To clone a full-length *PRL1* gene with short promoter (i.e., starting with the *Xho*I site at position -62), pPCV002-ODB was digested with *Xba*I, blunted with T4 polymerase and cleaved with *Xma*I. The *PRL1* gene segment was isolated from pBS-PRL1-HA by *Xho*I digestion, T4 DNA polymerase fill-in the end and subsequent *Xma*I cleavage. This fragment was ligated into filled-in *Xho*I-*Xma*I sites of pPCV002-OBD to yield the constructs pPCV002-PRL1-HA-XhoI.

To create a third construct, in which the full-length 3.5 kb *PRL1* promoter drives the expression of the *PRL1* cDNA, first, the *PRL*1 promoter was cloned into the pPCV002 vector. Plasmids pPCV002-ODB and pBSK-PRL1-PROM-UTR were both digested with *Xba*I-*Xma*I and ligated. The obtained pPCV002-PRL1-PROM-UTR plasmid was digested with *Sma*I to insert the *PRL1-HA* cDNA, which was isolated from pBS-PRL1-cDNA-HA as *Xho*I-*Spe*I fragment and treated with T4 DNA polymerase. The obtained clone was named pPCV002-PRL1-cDNA-HA.

In order to link a functional *PRL1* short promoter extending from position -62 to the third exon to the *PRL1-HA* cDNA, the promoter fragment was isolated by *Msc*I-*BmgB*I the plasmid pBS-PRL1 and cloned upstream of *PRL1-HA* cDNA by *Msc*I-*BmgB*I in pBS-PRL1-cDNA-HA to yield the pBS-PRL1-2introns-cDNA-HA. To reconstruct the full-length promoter upstream of the *PRL1-HA* cDNA coding region, the short promoter-*PRL1-HA* cDNA fragment was isolated as *Xho*I-*Spe*I fragment from pBS-PRL1-2introns-cDNA-HA, treated with T4 DNA polymerase and inserted into a dephyosphorylated *Sma*I site of pPCV002-PRL1-PROM-UTR to produce pPCV002-PRL1-2introns-cDNA-HA. All constructs were checked by restriction digestion analyses and sequencing, and then were transferred to *Agrobacterium* and transformed into *prl1* mutant plants.

Transgenic plants carrying the pPCV002-PRL1-HA, pPCV002-PRL1-HA-XhoI, pPCV002-PRL1-cDNA-HA and pPCV002-PRL1-2introns-cDNA-HA constructs were analyzed for complementation of leaf, rosette and root elongation phenotype of the *prl1* mutant. Seeds were germinated on selective MSAR plates containing kanamycin for all constructs. 63 pPCV002-PRL1-HA, 53 pPCV002-PRL1-HA-XhoI and 56 pPCV002-PRL1-2introns-cDNA-HA independent T1 lines, which were assayed for genetic complementation and all showed wild type leaf and rosette phenotype (Figure 19 A). By contrast, the progeny of all 32 kanamycin resistant T1 seedlings carrying the pPCV002-PRL1-cDNA-HA displayed *prl1* mutant phenotype.

Root length as a quantitative marker of *prl1* mutation was measured to confirm alternatively the complementation activity of different constructs. Root length of a homozygous pPCV002-PRL1-HA transformed T3 line was compared to those of five segregating T2 families of pPCV002-PRL1-HA-XhoI and pPCV002-PRL-2introns-cDNA-HA transformants. The non-complementing pPCV002-PRL1-cDNA-HA lines were excluded from this assay, since the transformants could not be distinguished from the *prl1* mutant as their root elongation was similarly blocked. Seeds were germinated on MSAR plates in vertical position and root length was measured two weeks later. As a control wild type and *prl1* mutant seeds were placed on each plate and quantified thereby also allowing comparison between plates, if desired. All transformed lines carrying the pPCV002-PRL1-HA, pPCV002-PRL1-HA-XhoI and pPCV002-PRL-2introns-cDNA-HA constructs showed wild type root length (Figure 19 B). This result demonstrated that all constructs which carried *PRL1* sequences between position -62 and the third intron (i.e., promoter *Xho*I-*Spe*I fragment) in combination with 3'-downstream sequences of the *PRL1* gene or cDNA were fully functional and complemeted the *prl1* mutation. These data also showed that the upstream promoter region is not sufficient for proper gene

expression, but the full-length promoter together with the first two introns provides adequate information for mRNA transcription.
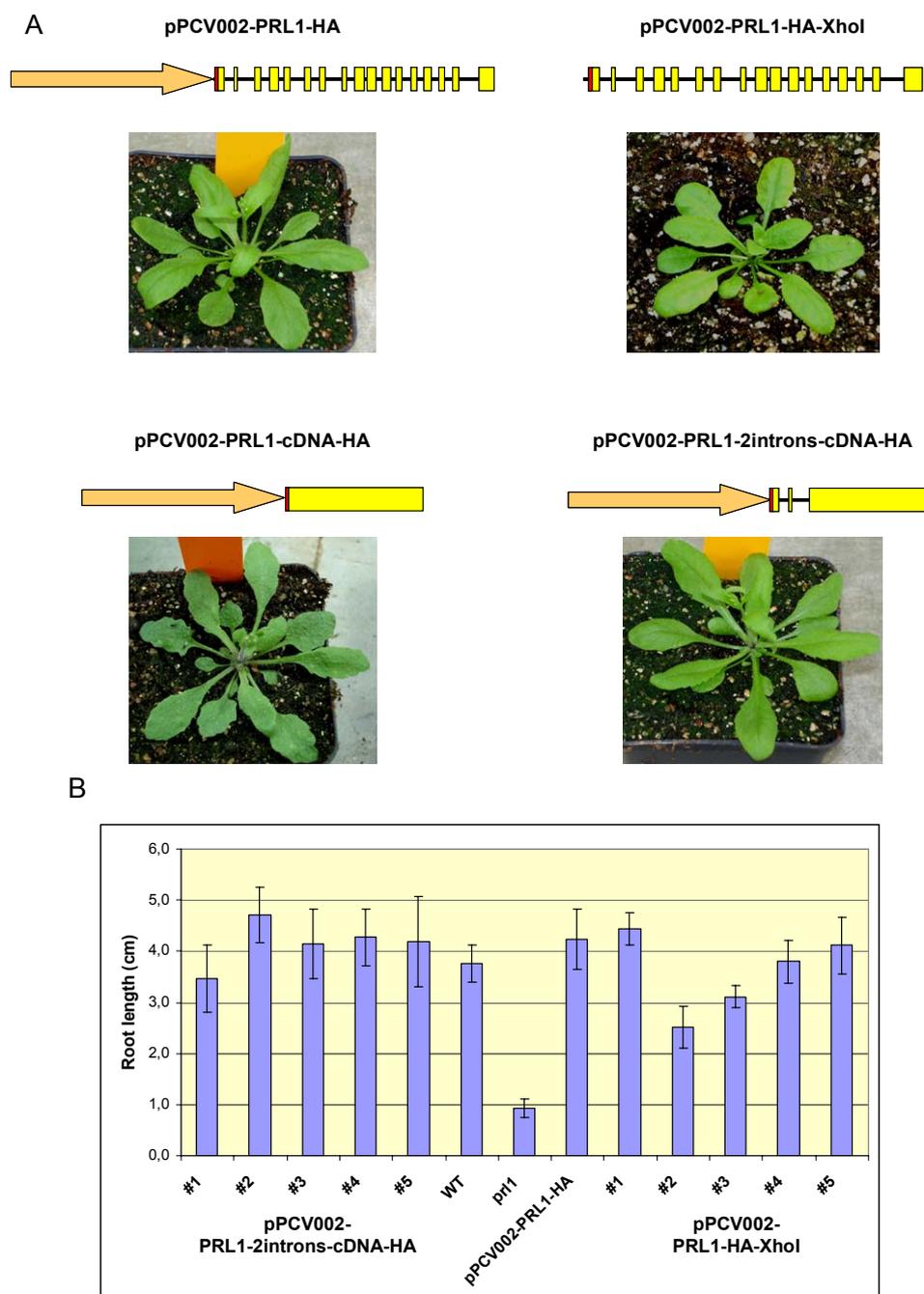
Figure 19. **Phenotypic analysis of *PRL1* complementation constructs**
(A) Phenotype of soil-grown pPCV002-PRL1-HA, pPCV002-PRL1-HA-XhoI, pPCV002-PRL1-cDNA-HA and pPCV002-PRL1-2introns-cDNA-HA transformed T1 plants. (B) Root length of a homozygous pPCV002-PRL1-HA line and five of each T2 lines carrying either pPCV002 PRL1-2introns-cDNA-HA or pPCV002-PRL1-HA-XhoI was measured two weeks after germination. Wild type and *prl1* mutant plants were used as controls.

3.1.13. Western blot analysis of *PRL1* complementation constructs

To correlate the genetic complementation data with PRL1 protein expression levels, western blot analysis of HA epitope labelled PRL1 protein was performed in five independent T2 families of

pPCV002-PRL1-HA-XhoI, pPCV002-PRL1-cDNA-HA and pPCV002-PRL1-2introns-cDNA-HA transformed *prl1* mutant plants and compared to those detected in a homozygous pPCV002-PRL1-HA *prl1* transformant as control. Seeds were germinated on selective kanamycin plates, three-week-old plants were frozen in liquid nitrogen, and total protein samples were extracted. Equal amounts (25 μg) of protein samples were size separated by 8% SDS-PAGE gels and analyzed by western blotting using an anti-HA antibody. There were minor differences observed between lines, but all *prl1* complementing lines carrying the pPCV002-PRL1-HA, pPCV002-PRL1-HA-XhoI and pPCV002-PRL1-2introns-cDNA-HA constructs expressed comparable high amount of PRL1-HA protein. By contrast, the PRL1-HA protein was only detected in few pPCV002-PRL1-cDNA-HA transformed lines after a long exposure time (1 h or O/N). In conclusion, the protein expression data excellently correlated with the observed complementation phenotype. The minimal PRL1 promoter and the full length upstream region together with the first two exons and introns were as active as the full-length *PRL1* gene. Genetic complementation of the *prl1* mutation was thus unequivocally demonstrated to critically depend on the expression level of wild type *PRL1* protein.
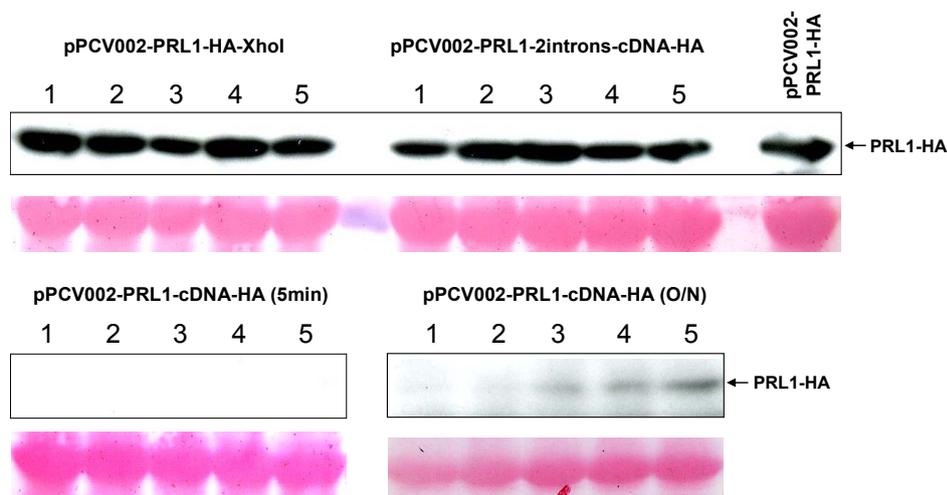
Figure 20.   **Immunodetection of PRL1-HA protein in *prl1* lines complemented with different *PRL1* gene constructs**
Seeds from T2 families of complemented lines were germinated on selective plates and plant material was harvested after three weeks. Total protein was extracted and 25 μg of protein samples were separated by 8% SDS-PAGE gels. Western blotting was performed with anti-HA antibody. Chemiluminescence was captured for 5 min for all short exposures. pPCV002-PRL1-cDNA-HA western blots were also exposed overnight. Equal loading of protein extract was verified by Ponceau staining.

3.1.14. PRL1-HA expression in different tissues of complemented lines

Initial experiments demonstrated that mature leaf material from soil-grown T1 lines tested in western blotting analysis contained less PRL1 protein in the pPCV002-PRL1-HA-XhoI transgenic lines than in pPCV002-PRL1-2introns-cDNA-HA transformed plants (data not shown). T2 plants were investigated to confirm this data. Three weeks-old seedlings were collected from selective plates and rosette leaves, stems, cauline leaves, flowers and siliques were harvested from five weeks-old soil-grown plants. Plant material was ground in liquid nitrogen and total protein samples were extracted. Proteins were resolved by 8% SDS-PAGE, on which 25 μg protein samples were loaded in each slots. PRL1-HA

expression was monitored by western blotting using anti-HA antibody. This experiment showed that there was no significant difference in PRL1-HA protein levels between the two constructs. Plants carrying the pPCV002-PRL1-HA-XhoI and pPCV002-PRL1-2introns-cDNA-HA constructs showed comparable levels of PRL1-HA protein in various tissues. The strongest PRL1-HA expression was observed in seedlings and flowers, but considerable amount of protein was also present in stems. The lowest PRL1-HA-signal was detected in rosette and cauline leaves.
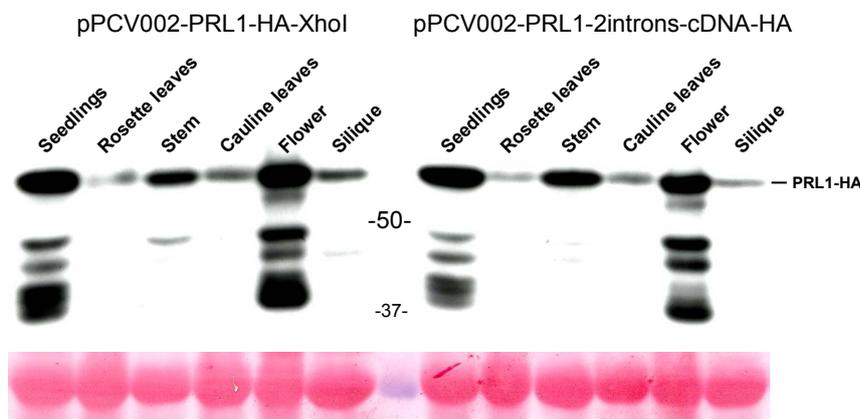
Figure 21.   Immunodetection of PRL1-HA protein in various organs of complemented lines
Plant material was collected from selective plates and five-week-old soil-grown plants. From each sample, 25μg of protein was resolved by 8% SDS-PAGE gel for western blotting with anti-HA antibody.

3.1.15.   Complementation studies using heterologous promoters

Analysis of the *PRL1* expression pattern revealed that *PRL1* was expressed in a wide variety of tissues, including meristems, leaves, cotyledons and roots. To identify precisely in which tissue *PRL1* plays a critical role for proper plant development, a misexpression approach was developed. Since *PRL1* is predominantly expressed in apical and lateral meristems, the aim was to determine, in which domain of the shoot apical meristem (SAM), if any, *PRL1* expression is critical for normal development. To undertake this study, seven heterologous promoters were chosen, from which four are shoot apical meristem specific and three promoters are active in other plant organs. The latter promoters served as internal controls. The promoters of *AtKNAT1* (*KNOTTED-LIKE 1,* At4g08150) and *AtSTM* (*SHOOT MERISTEMLESS*, At1g62360) genes are active in the entire meristem, but are not activated in leaf primordia (Lincoln et al., 1994; Long et al., 1996). The *AtUFO* (*UNUSUAL FLORAL ORGANS*, At1g30950) gene is expressed in a subset of STM expressing shoot apical meristem (SAM) cells (Ingram et al., 1995), whereas *AtAS1* (*ASYMMETRIC LEAVES 1*, At2g37630) is exclusively active in developing leaf primordia (Byrne et al., 2000). The promoter of *AtSUC2* (*SUCROSE TRANSPORTER 2*, At1g22710) is active in companion cells of the phloem (Stadler and Sauer 1996), whereas *At4CL1* (*4-COUMARATE:COA LIGASE 1*, At1g51680) promoter is xylem specific (Hauffe et al., 1993). Finally, a root-specific promoter *TobRB7* is active in the central cylinder of roots (Yamamoto et al., 1991). In the misexpression experiments, the cDNA and a *PRL1* genomic fragment starting from the ATG codon (see below) were linked to these heterologous promoters. All constructs carried coding sequences of an HA epitope immediately upstream of their stop codons. In

the cloning procedure, the pBS-PRL1-cDNA-HA and pBS-PRL1genomic-HA-ATG constructs were digested with *Xho*I-*Spe*I and the *PRL1* gene and cDNA fragments were cloned into *Xho*I-*Spe*I sites of the pGreen-MCS-GW vector (An et al., 2004). Promoters were introduced 5'-upstream from the *PRL1* coding regions using the Gateway technology. The completed constructs were sequenced and subsequently transformed into *prl1* mutant plants. Transformants were selected in the greenhouse applying BASTA selection and resistant plants were transferred into single pots and analyzed for complementation.

3.1.16. Phenotypic analysis of *PRL1* misexpressing plants

The phenotype of four weeks old T1 plants was investigated in the greenhouse. All plants transformed with the *PRL1* genomic fragment fused to different heterologous promoters showed wild type phenotype (data not shown). In combination with different upstream promoter elements, the *PRL1* regulatory sequences defined between the ATG codon and third intron in our previous experiments appeared to be sufficient to confer suitable high level of *PRL1* expression for genetic complementation.

Phenotypic analysis of lines expressing the *PRL1* cDNA from different promoters revealed that constructs with the *AtSUC2* and the *AtAS1* promoter were able to complement the serrated *prl1* leaf phenotype (Figure 22 A). The lines expressing *PRL1-cDNA-HA* sequences under the control of *At4CL1, AtUFO, AtKNAT1, AtSTM,* and *TobRB7* promoters maintained the *prl1* leaf and rosette phenotype. T2 generations of the *cDNA* constructs were investigated further. The root phenotype of lines transformed with the various cDNA expression constructs was inspected in five independent T2 families in each case by growing seedlings on vertical MSAR plates. All examined lines showed short, *prl1*-type root structure, including the *AtSUC2*, *AtAS1*, and root specific *TobRB7* promoter driven cDNA constructs (Figure 22 B). These data suggested that the developmental alteration leading to serrated leaf phenotype in the *prl1* mutant can be corrected in *PRL1* is specifically expressed in the differentiating vascular meristem or in the entire area of leaf primordia, but not by expression of *PRL1* in different layers of SAM. The analysis of the root and other cell type specific *PRL1* misexpression lines also showed that the PRL1 signal is not transmittable.

To compare expression levels of the PRL1-HA protein in the *PRL1* misexpressing lines, western blot analyses were performed with protein extracts prepared from three weeks old seedlings grown on selective MSAR plates (Figure 22 C). Equal amounts of protein samples (25 μg) were separated by SDS-PAGE and the PRL1-HA signal was detected with anti-HA antibody. Plants transformed with *AtKNAT1*, *AtAS1* and *AtTobRb7* promoter driven *PRL1-cDNA-HA* constructs expressed high levels of PRL1-HA, whereas lines carrying the *AtSUC2* and *At4CL1* cDNA constructs showed lower PRL1-HA levels. However, in lines transformed with the *STM::PRL1-cDNA-HA* and *AtUFO::PRL1-cDNA-HA* genes no signal was detected when 25 μg of total protein was analyzed. The experiments were repeated with these lines by using 40 μg of protein samples, which provided faint HA-signals after overnight exposure on the western blots. Unlike in our experiments with *PRL1*

promoter deletions, the overall level of PRL1-HA expression detected in the transformed lines showed no correlation with the results of genetic complementation assays. Evidently, confined expression of *PRL1* to specific cell types and developmental phases is only sufficient for rescuing some aspects of the complex developmental defect caused by the *prl1* mutation, as seen in case of leaf phenotype.
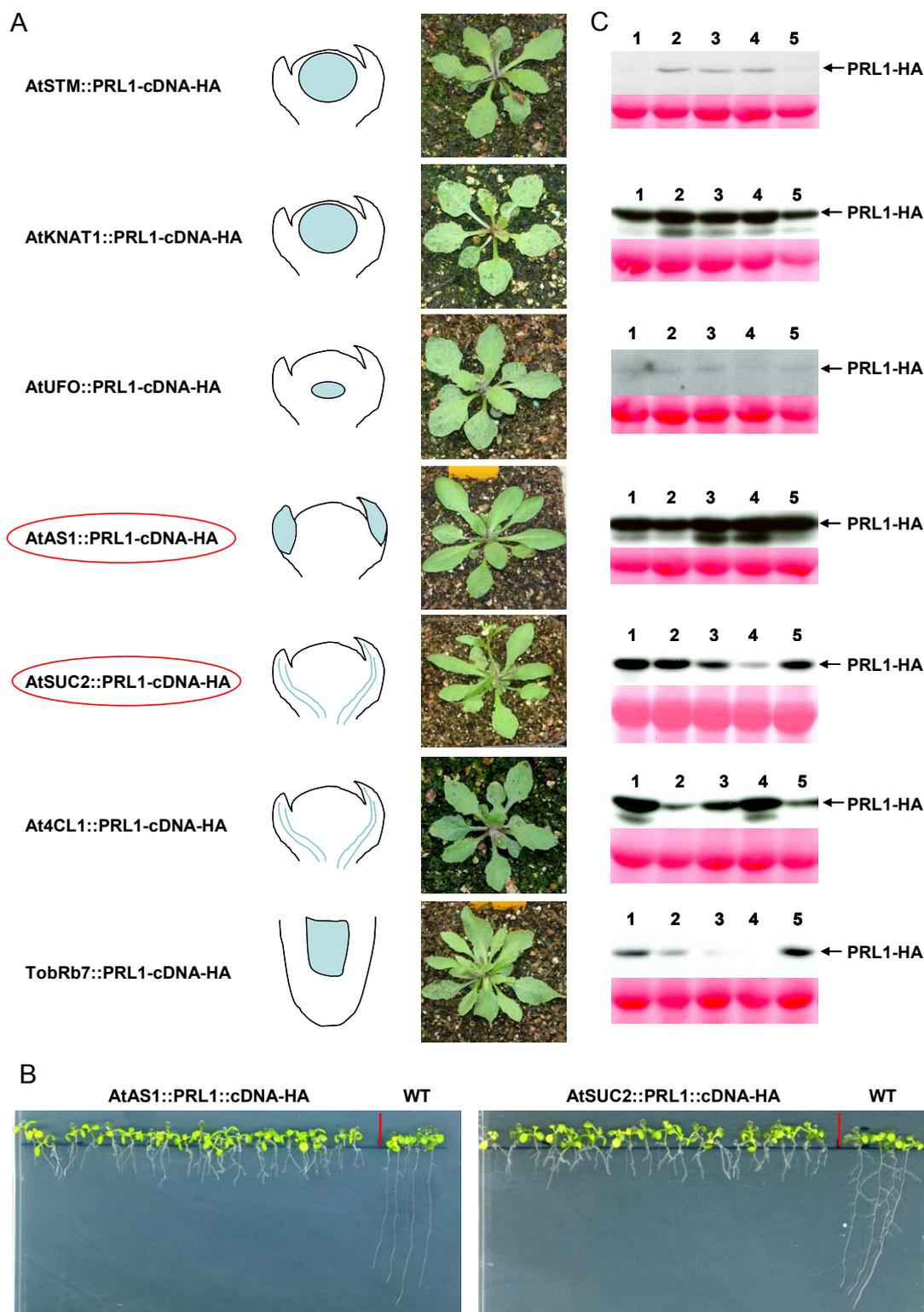
Figure 22.   Genetic complementation assays using misexpression of the PRL1 cDNA from different heterologous promoters

The *PRL1* cDNA was expressed by different heterologous promoters (described in the text) in the *prl1* mutant. (A) Phenotype of soil-grown plants. (B) Root phenotype of *AtAS1::PRL1-cDNA-HA* and *ATSUC2::PRL1-cDNA-HA* plants (all others are not shown). (C) Immunodetection of PRL1-HA with anti-HA antibody in protein samples prepared from 3 weeks old T2 seedlings. 25 μg of protein samples were resolved by 8% SDS-PAGE.

3.2. Yeast-one-hybrid screening for transcription factors binding to intragenic *PRL1* promoter sequences

3.2.1. Construction of promoter testing vectors and selection of test strains for yeast-one-hybrid assay

Analysis of the *PRL1* promoter-GUS fusion constructs showed that sequences in the second intron of the *PRL1* gene play an important role a role in regulation of *PRL1* gene expression. To search for transcription factors that recognize sequences within the second intron of *PRL1* gene, a yeast-one-hybrid experiment was performed. Two test constructs were generated. One was placed into the pHISi-1 vector for the library screen and the same promoter fragment was inserted into pLacZi for an independent control of the candidate clones. Sequences of the second intron were PCR amplified using PR-F and PR-R primers (2.1.6.2). This DNA fragment was digested with *Xba*I-*BmgB*I and ligated into *EcoR*I-*Sma*I sites of the yeast one-hybrid vectors pHISi-1 and pLacZi (2.3.3.4). Subsequently, the pHISi-1 clone was used for the library screen, whereas the same promoter fragment inserted in pLacZi served as an independent control to identify the candidate clones.

The first step of one-hybrid assay requires that the target constructs are integrated into the genome of the yeast YM4271 strain. To achieve this, the pHISi-1-PRL1-PROM construct was linearized by *Xho*I digestion and the pLacZi-PRL1-PROM plasmid was digested with *Nco*I restriction enzyme. Subsequently, the vector DNAs were transformed separately into yeast cells by the lithium acetate method (2.3.3.1). Transformants were selected on SD/-His plates incubated for 3-5 days at 28°C and large positive colonies were investigated further. The pHISi-1 vector was reported to be leaky therefore, unspecific *HIS* expression must be suppressed by adding a competitive inhibitor 3-AT (3-aminotriazol) to the medium. Six pHISi-1-PRL1-PROM yeast transformants were plated on SD/-His plates containing various (0, 15, 30, 45 and 60 mM) concentrations of 3-AT in order to identify a transformant displaying low background of *HIS* expression and to determine simultaneously the correct 3-AT concentration for eliminating the residual HIS activity during the screen. One out of six transformants failed to grow in the presence of 15 mM 3-AT and was therefore selected as host for the one-hybrid screen (Figure 23). In the library screen the 3-AT selection level was set to 25 mM. Background *lacZ* activity was checked by colony-lift assay and none of the 16 transformed yeast colonies tested showed *lacZ* expression (data not shown).

| SD/-His
0 mM 3-AT | SD/-His
15 mM 3-AT | SD/-His
30 mM 3-AT | SD/-His
45 mM 3-AT | SD/-His
60 mM 3-AT |
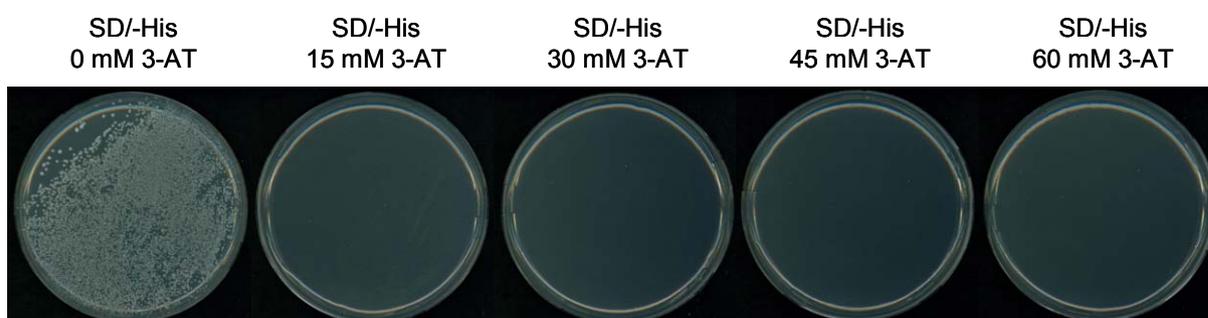
Figure 23.   Selection of pHISi-1 reporter strain
Intron 2 sequences of the *PRL1* promoter inserted pHISi-1 constructs were integrated into the genome of yeast strain YM4271. Six independent transformants were analyzed on SD/-His medium supplemented with 0, 15, 30, 45 and 60 mM 3-AT. Line #2 showed the lowest HIS background expression since colonies failed to grow in the presence of 15 mM 3-AT.

3.2.2. Isolation of a cDNA encoding a *PRL1* intron 2 binding factor

To search for transcription factors recognizing intron 2 sequences of intragenic PRL1 promoter region, the yeast host strain carrying chromosomally integrated pHISi-1-PRL1-PROM was transformed with a pACT2 cDNA library constructed from mRNA isolated from an *Arabidopsis thaliana* cell suspension. Large-scale Li-acetate transformation was performed and cells were plated on SD/-His/25mM 3-AT plates. The screen yielded approximately $6x10^7$ transformants. Seven candidates were isolated that were able to grow on medium lacking histidine in the presence of 25 mM 3-AT (Figure 24). The activation of *HIS* gene was confirmed on 25 and 50 mM 3-AT containing plates, while an empty pACT2 vector transformed line was used as negative control. DNA was isolated from the HIS+ colonies and used for transformation of the indicator pLacZi-PRL1-PROM containing test strain. Colony LacZ filter lift assays indicated the activation of PRL1 intron 2 containing pLacZi-PRL1-PROM reporter gene. Sequencing these candidate pACT2 constructs revealed that the cDNA inserts of all seven clones encoded a plant specific transcription factor *AtNAM* (No apical meristem, At1g52880). The *AtNAM* coding sequence was in frame with the *GAL4* activation domain in all plasmids.
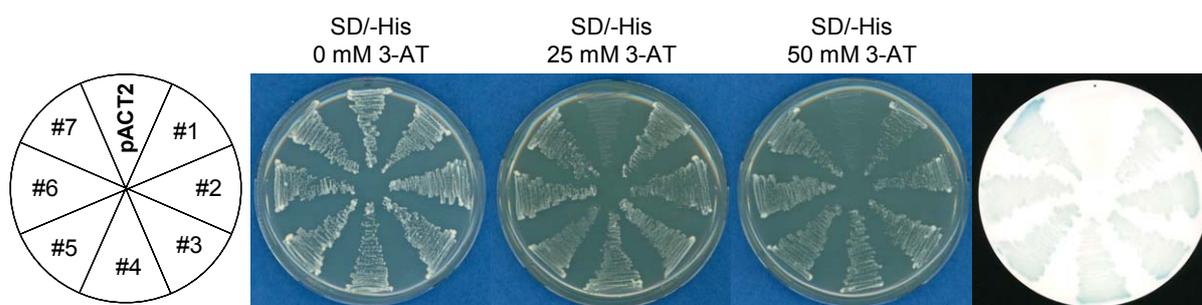
Figure 24. **Yeast one-hybrid assay**
The library screen resulted in seven transformants, which grew on SD/-His medium supplemented with 25 mM 3-AT. These transformants were tested on selective medium containing 0, 25 and 50 mM 3-AT. The host strain carrying the pHISi-1-PRL1-PROM target construct was also transformed with empty pACT2 vector and this transformant was used as control. Plasmid DNAs isolated from the HIS+ clones growing in the presence of 50 3-AT were introduced by transformation into the pLacZi-PRL1-PROM test strain to confirm the activation capability of pACT-cDNA clones.

AtNAM belongs to the plant specific NAC (NAM, ATAF1/2, CUC2) family of transcription factors that contains over hundred genes in *Arabidopsis*. The longest cDNA in the pACT clones carried a full-length coding region for the AtNAM protein of approximately 30kDa. AtNAM carries a highly conserved DNA-binding NAC domain and histidine repeats in its N-terminal domain, whereas the C-terminal domain is responsible for trans-activation (Figure 25 A). A putative NAC binding site was previously identified in the CaMV35S promoter by DNaseI foot-printing by Duval et al. (2002). Although *PRL1* intron 2 sequences lack putative NAC-binding sites, the target sequences inserted in the yeast reporter constructs pHISi-1-PRL1-PROM and pLacZi-PRL1-PROM also carried a short segment of exon 3, which contained two potential NAC recognition sites (Figure 25 B). It is likely that these NAC binding sites were responsible for activation of the expression of *HIS* and *LacZ* reporter genes in the one-hybrid assay.

Analysis of publicly available Genevestigator expression database indicated that *AtNAM* is transcribed in siliques, senescent leaves and sepals but its expression is barely detectable in radicles, ovary, pollen and shoot apex (Figure 25 C). In comparison, *PRL1* mRNA is detected also by microarray analysis in most tissues in a relatively constant distribution, showing the highest levels in callus and shoot apex, and the lowest expression in pollen. During different developmental stages *PRL1* was expressed evenly and strongly, whereas *AtNAM* appears to be silent during germination and bolting. Therefore, if at all, AtNAM may only represent a potential regulator of *PRL1* in specific tissues and developmental phases, the confirmation of which requires further studies.

A
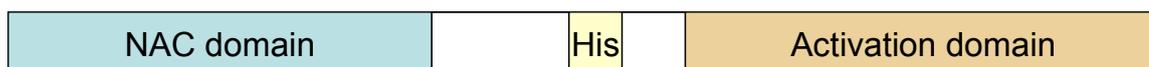
B

aGGGAnGa=tCnTCCCT

GCCATAAGGTAAAACATTGAGTCTCTCTTACCAGTCTTTAGAAATT
TATTTCAGTTATTCGCTTTTAATGTCTATTGATTGGATTTTGGTTTA
AAGCTTCGAACTTTAGGTTTATTCAGGTTTTTCCATAATTGTTCTAA
ATCTTCAGGTTTTGTTACCAATAATAGTAAAGATGGTTGATTTACTT
AGACTCTCTCTCTCTCTGTTGTGTATGTTACTGATTTTAGAAGTT
TTCTTTGTACAGATGAAAGTTGCGTTT**GGAGGTG**TAGAACCTGTTG
TGAGTC**AACCTCC**AC

C
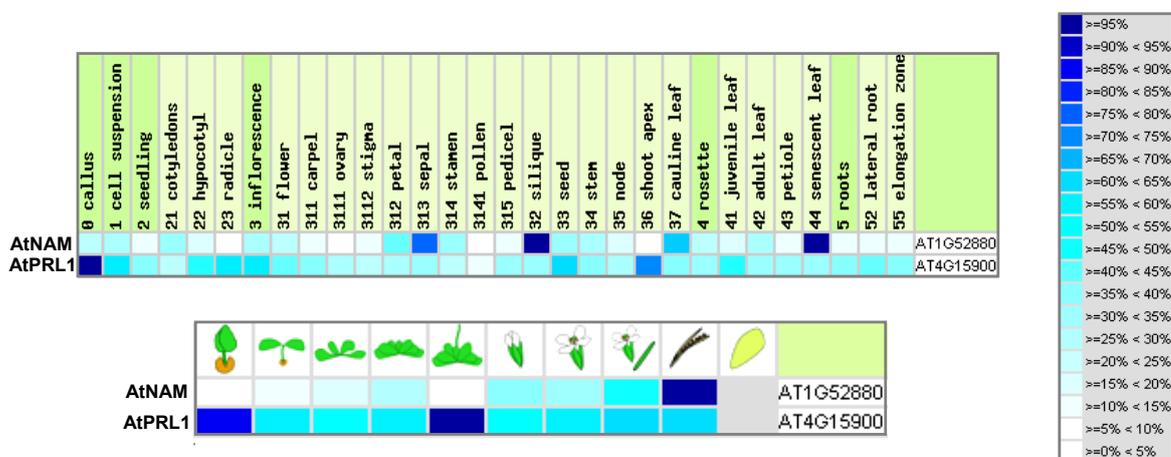
Figure 25.   Domain structure, binding site and regulation of expression of AtNAM
(A) Domain structure of *AtNAM*. A conserved DNA-binding NAC-domain is located in the N-terminus and the activation domain is present at the C-terminal region. A histidine repeat is found downstream of the NAC domain. (B) Putative recognition sequence of *AtNAM* (sense and antisense sequence) and analysis of potential NAC-binding sites in the *PRL1* promoter sequence used in the one-hybrid bate. The sequence of *PRL1* intron 2 is printed in black, whereas sequences derived from exon 3 are marked with blue colour. Potential NAC-binding sites in exon 3 sequences are highlighted with red and underlined. (C) Transcription of *AtNAM* and *PRL1* genes in different organs and developmental stages as displayed in the Genevestigator database.

3.3. <u>Analysis of expression pattern and cellular localization of PRL1 protein</u>

3.3.1. Construction of a vector for expression of a PRL1-GFP fusion protein

To characterize the expression pattern of PRL1 protein in diverse plant tissues, the green fluorescent protein (GFP) was fused to the C-terminus of the PRL1 protein. In the construction of PRL1-GFP expression vector, we relied on our previous observation showing that that the 3.5 kb *PRL1* promoter and the first two introns are sufficient for the proper regulation of *PRL1* gene expression. To eliminate the stop codon of the *PRL1* gene, the pBS-PRL1-2introns-cDNA-HA plasmid was digested with *Spe*I, the ends were filled in with T4 DNA polymerase, and after *Bgl*II digestion the DNA was ligated with a *Sma*I-*Bgl*II fragment isolated from pBS-PRL1-SMA to reconstruct the 3'-end of the *PRL1* gene in pBS-PRL1-2introns-cDNA-Sma. This plasmid was digested with *Xba*I and *Sac*II to clone the GFP coding region, which was PCR amplified using the primers GFP-F and GFP-R (2.1.6.2), and then digested with *Xba*I-*Sac*II. The obtained plasmid pBS-PRL1-2introns-cDNA-GFP was digested with *Xho*I-*Sac*II, the ends were filled in with T4 DNA polymerase and the isolated PRL1-GFP expression cassette was inserted into *Sma*I digested pPCV002-PRL1-PROM-UTR. This pPCV002-PRL1-GFP construct was introduced into light-grown cell suspension, as well as wild type and *prl1* mutant plants.

3.3.2. Localization of PRL1-GFP fusion protein *in planta*

Subcellular localization of the PRL1-GFP fusion protein was first assayed in photosynthetic cell suspension one week after subculturing, then the analysis was extended to seven days old seedlings expressing the *PRL1* promoter driven PRL1-GFP reporter protein in the *prl1* mutant. The confocal laser scanning microscopy was performed in collaboration with Dr. E. Schmeltzer. The PRL1-GFP fusion protein was detected in all investigated plant organs and cell types (Figure 26). The PRL1 protein was predominantly present in the nucleus, although in cell suspension low level of GFP signal was also observed in the cytoplasm. The highest level of PRL1-GFP was detected in meristematic cells of the root apex and in the early leaf primordia. However, GFP signal was also captured in considerably lower intensity in fully developed cells of leaves and roots.

3.3.3. Subcellular immunolocalization of PRL1-HA protein

To examine the subcellular localization of the PRL1 protein in more detail, *prl1* mutant plants were transformed with the pPCV002-PRL1-HA construct (3.1.12). Seven days old T2 seedlings, showing genetic complementation of the *prl1* mutation, were fixed, embedded, sectioned and probed with HA epitope specific antibodies as described previously by Ferrando et al. (2000) and Farras et al. (2001). Indirect immunoflourescence localization studies performed in collaboration with Dr. Ján Jásik confirmed that the PRL1-HA protein was localized nearly exclusively in nuclei of all cells in shoots and roots showing particularly high levels in the apical meristems (Figure 27).
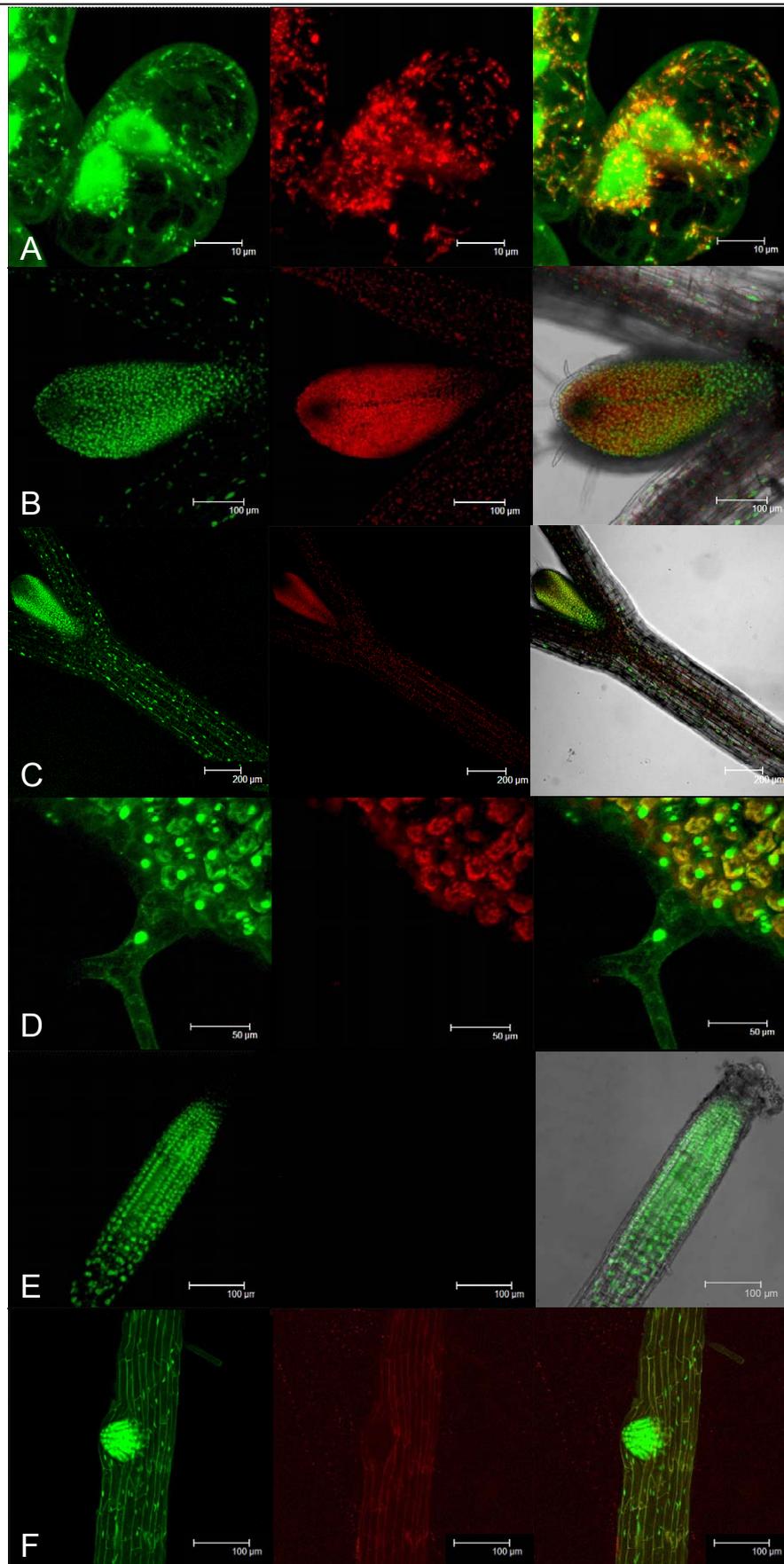
Figure 26. **Analysis of PRL1-GFP expression pattern *in planta* by confocal laser scanning microscopy**
Cellular localization of PRL1-GFP fusion protein in (A) cell suspension, (B) leaf primordia, (C) hypocotyl with leaf primordia, (D) leaf trichome, (E) root apical meristem and (F) lateral roots. The first row represents the GFP fluorescence, the second is the chloroplast autofluorescence and the third row is the merge of the two independent images (in the case of B, C and E the light microscopic picture is also merged).
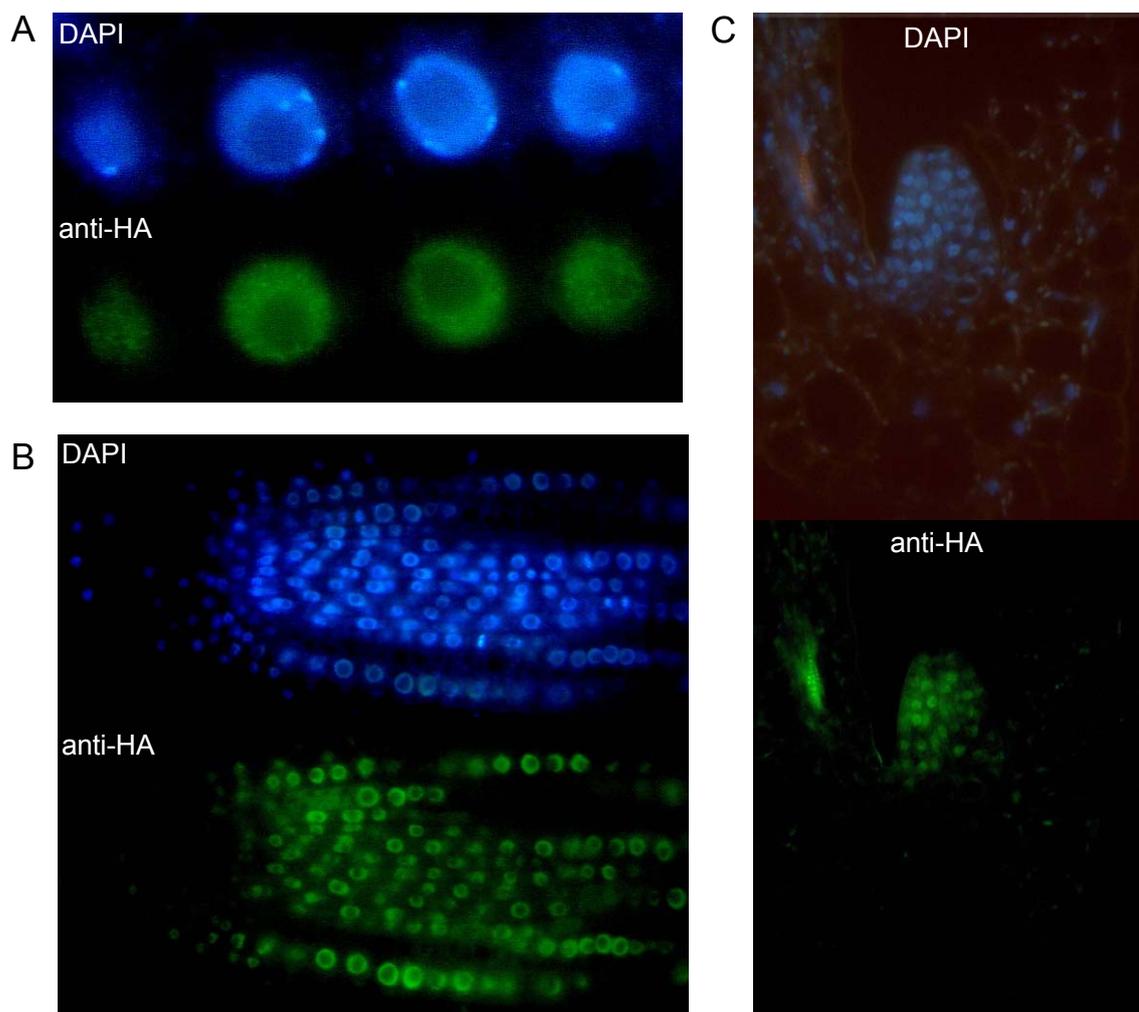
Figure 27. **Cellular localization of PRL1-HA in a complemented *prl1* mutant**
Transgenic *prl1* mutant plants carrying the pPCV002-PRL1-HA were used for immunolocalization.
Sections were stained with the fluorescent DNA dye DAPI and with mouse monoclonal anti-HA
antibody. (A) Subcellular localization of PRL1-HA protein in root cells. (B) Longitudinal root section.
(C) Shoot apical meristem.

3.3.4. Effects of plant hormone treatments on PRL1 protein level

To investigate potential effects of various hormones on PRL1 protein expression levels, homozygous
transgenic *prl1* mutant plants transformed with the *PRL1* promoter driven PRL1 genomic construct
pPCV002-PRL1-HA were subjected to various hormone treatments. Four homozygous lines were
analyzed simultaneously. Seeds were germinated on MSAR medium containing 0.5% sucrose on
nylon mesh. Seedlings were transferred into liquid MS media supplemented with plant hormones after
two weeks and each hormone treatment was performed for 24 h. The control seedlings were incubated
in liquid MS medium containing 0.5% sucrose. Crude protein samples were extracted and resolved by
8% SDS-PAGE. Western blotting was performed with anti-HA antibody to detect PRL1-HA protein
and equal loading was confirmed with an anti-tubulin antibody. The results showed that hormone
treatments caused no dramatic changes in PRL1-HA protein levels. The highest level of PRL1-HA
protein was detected in plants treated with 6% sucrose, whereas PRL1-HA level was slightly
decreased in response to ABA treatment (Figure 28).
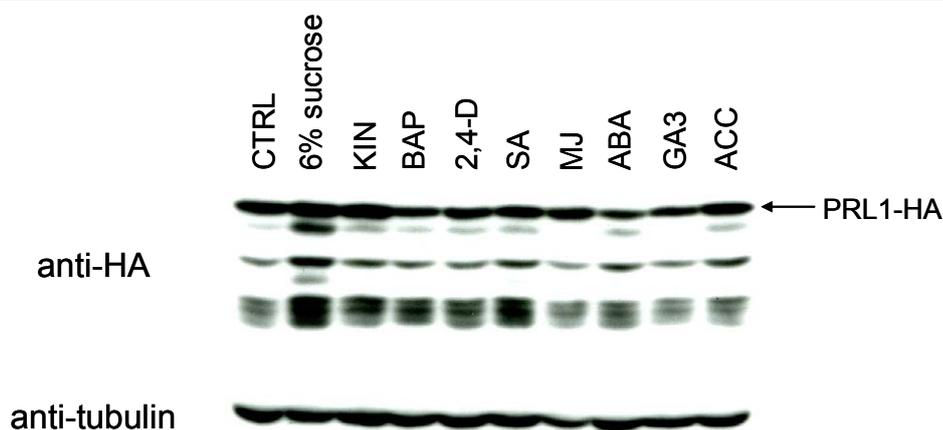
Figure 28.   Effects of hormone treatments on PRL1 protein levels
Two weeks old *prl1* plants carrying the complementing pPCV002-PRL1-HA construct were incubated with various plant hormones for 24 h. 25 µg of protein samples were resolved by 8% SDS-PAGE, and western blotting was performed with anti-HA antibody to detect HA-tagged PRL1 protein. The same membrane was probed with an anti-tubulin antibody to verify equal loading. CTRL: control, plants were kept for 24 h in liquid MS medium containing 0.5% sucrose. In other cases, the liquid MS medium was supplemented with: 6% sucrose, 0.2 mg/l kinetin (KIN), 0.2 mg/l 6-Benzylaminopurine (BAP), 0.5 mg/l 2,4-dichlorophenoxyacetic acid (2,4-D), 0.05 µM salicylic acid (SA), 10 µM methyl-jasmonate (MJ), 0.1 mg/l abscisic acid (ABA), 0.1 mg/l gibberellin GA3 (GA3) and 10 µM 1-aminocyclopropane-1-carboxylic acid (ACC, ethylene precursor).

In a second experiment, homozygous PRL1::PRL1-HA plants in *prl1* mutant background were grown for 3 weeks on MSAR plates on nylon mesh. Subsequently, the seedlings were transferred to liquid MS medium supplemented with various hormone solutions and treated for 5 h and 24 h before isolation of protein samples that were analyzed by immunoblotting with anti-HA antibody. As a result of 50 mM salicylic acid treatment, the seedlings died after 24 h, which was not noted with any other hormone. Samples collected after 5 h SA-treatment showed a significant reduction of PRL1-HA level whereas PRL1-HA remained constant in case of other hormone treatments. This result suggested induction of cell death by SA overdose possibly stimulates destruction of the PRL1 protein.
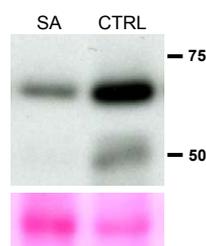
Figure 29.   Immunodetection of PRL1 protein in seedlings treated with 50mM salicylic acid
Seedlings were treated for 5 h in MS medium in the absence (CTRL) or presence of 50mM salicylic acid (SA). Protein extracts were immunoblotted with anti-HA antibody. As loading control, the membrane was stained with Ponceau-S.

3.3.5.   Regulation of PRL1 mRNA levels by hormones

The Genevestigator microarray database (Zimmermann et al., 2004) was searched to examine thus far observed effects of various plant hormones on *PRL1* gene expression. The search was restricted to experiments performed on wild type Col-0 plants. Microarray data from the following hormone

treatments were analyzed: 10 μM ABA for 1h an 3h, 10 μM ACC for 1h and 3 h, 10 nM brassinolide
(BL) for 1h and 3h, 5ppm ethylene for 3h, 1 μM GA3 for 1h and 3h, 1 μM IAA for 1h and 3h or 5 μM
for 1h and 2h, 10 μM methyl-jasmonate for 1h and 3 h, 10 μM salicylic acid for 3h and 1 μM zeatin
for 1h and 3h (Figure 30).

Treatment	# of Chips	Mean	Std-Err	245358_at IAT4G15900 Linear 2000 1000 0	Ratio	245358_at IAT4G15900 Linear 0 1000 2000	Std-Err	Mean	# of Chips	Control
Chemical: 6-benzyl adenine (+)	2	1469	106		1.07		249	1368	2	Chemical: 6-benzyl adenine (-)
Hormone: ABA (+)	4	1132	94		0.86		24	1315	4	Hormone: ABA (-)
Hormone: ACC (+)	4	1357	55		1.03		24	1315	4	Hormone: ACC (-)
Hormone: BL (+)	4	1243	78		0.95		24	1315	4	Hormone: BL (-)
Hormone: ethylene (+)	3	1112	68		0.95		60	1169	3	Hormone: ethylene (-)
Hormone: GA3 (+)	4	1261	49		0.96		24	1315	4	Hormone: GA3 (-)
Hormone: IAA (+)	11	1354	35		0.99		40	1363	7	Hormone: IAA (-)
Hormone: MJ (+)	4	1321	77		1		24	1315	4	Hormone: MJ (-)
Hormone: salicylic acid (+)	2	1395	55		1.1		134	1263	2	Hormone: salicylic acid (-)
Hormone: zeatin (+)	4	1461	25		1.11		24	1315	4	Hormone: zeatin (-)
Nutrient: glucose/sucrose (+)	4	1764	139		1.17		196	1508	5	Nutrient: glucose/sucrose (-)

**Figure 30.   Genevestigator microarray data on changes of *PRL1* transcript levels in response hormone
treatments**
Plant microarray data was taken from the Genevestigator database and sorted according to changes in *PRL1*
mRNA levels in response to various hormone treatments.

Experimental setups for 6-benzyl-adenine and sugar treatments were not found in the database.
Comparative analysis of the data indicated that the PRL1 mRNA level was reasonably constant in all
conditions examined, although a slight decrease in mRNA expression was detected in ABA treated
samples and an increase of PRL1 transcript levels was observed in sugar treated plant samples.

3.4.   Posttranscriptional regulation of PRL1

3.4.1.   Comparison of PRL1 transcript and protein levels in different plant organs

Preliminary comparison of PRL1 transcript and protein levels in different plant organs suggested
possible posttranscriptional regulation of PRL1 expression. K. Németh from our laboratory previously
performed a series of northern hybridization experiments using wild type plants and analyzed *PRL1*
mRNA levels in cell suspension, roots, shoots and shoot apex. The results showed that *PRL1*
expression levels were largely comparable in all the tissues (Nemeth, 1994). Comparison of *PRL1*
mRNA levels based on data obtained from the Genevestigator microarray database is shown in Figure
31 A. The *PRL1* gene is evenly expressed in all plant organs. *PRL1* mRNA levels are somewhat
higher in cell suspension, radicles, carpel, shoot apex, juvenile leaves and lateral roots, but lower in
cotyledons, stamens and pollen. In order to examine the PRL1 protein levels in plant organs, plants
carrying the 35S::PRL1cDNA-HiA and native PRL1::PRL1genomic-HA (pPCV002-PRL1-HA)
construct in *prl1* mutant background were analyzed (Figure 31B). Protein extracts were isolated from
seedlings grown for 2 weeks on MSAR medium, as well as from soil-grown plants, resolved by 12%
SDS-PAGE gels and subjected to western blotting with anti-HA antibody. In both 35S::PRL1cDNA-
HiA and pPCV002-PRL1-HA transformed plants high levels of PRL1-HA protein were detected in

roots and flowers, whereas surprisingly no PRL1-HA protein was detectable in rosette and cauline leaves. As *PRL1* mRNA levels did not show dramatic differences in the examined organs, the data suggested that in leaves the PRL1 protein levels are down-regulated probably as a result of PRL1 proteolysis. Plans expressing *PRL1* both from the CaMV35S and native *PRL1* promoters showed similar decrease in PRL1 protein level in leaves indicating a posttranscriptional regulatory effect.
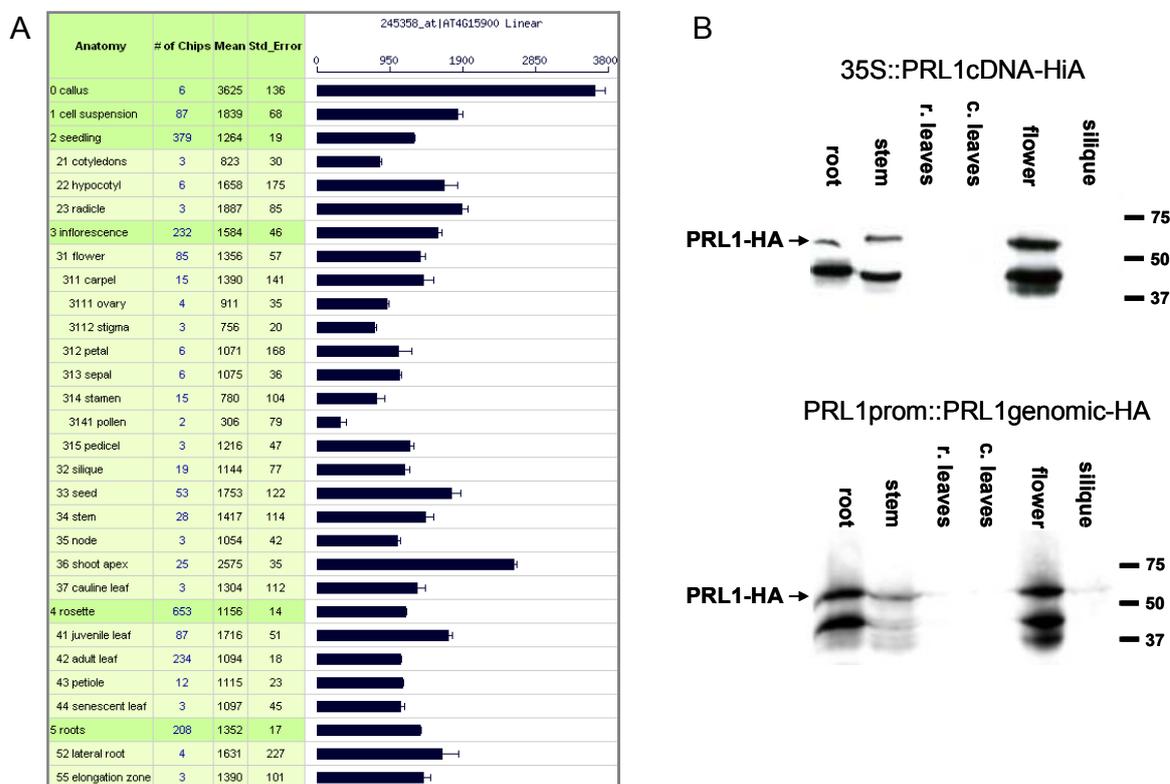
Figure 31.   Comparison of PRL1 mRNA and protein levels in plant organs
(A) Microarray data from the Genevestigator database showing PRL1 mRNA levels in various plant organs. (B) Immunodetection of PRL1-HA protein expressed by the 35S::PRL1cDNA-HiA and PRL1::PRL1genomic-HA constructs in *prl1* plants. 25 μg of total protein samples were separated on 12% SDS-PAGE gels and subjected to western blotting with an anti-HA antibody.

3.4.2.   Analysis of PRL1 protein stability

In order to examine the stability of PRL1 protein, *prl1* seedlings carrying the estradiol-inducible pER8(Km)-PRL1-cDNA-HA construct tested previously in genetic complementation assay (3.1.4) were used. Two weeks old T2 seeds grown on selective plates were transferred into liquid MS medium supplemented with 2 μM estradiol to induce PRL1 expression for 24 h. Subsequently, the seedlings were washed several times to remove estradiol and then cultured in liquid MS medium. Samples were collected 0, 4, 8, 24, 48, 72 and 96 h after removal of estradiol for preparation of protein extracts. Samples containing 15 μg of protein were resolved by 12% SDS-PAGE and subjected to western blotting followed by immunodetection with anti-HA antibody. Equal loading was checked by staining the membranes with Ponceau-S and, after stripping, with immunodetection using an anti-tubulin antibody. The results showed that after removal of estradiol, which was used to achieve a high level induction of *PRL1* gene expression, the PRL1-HA protein level decreased gradually. After 72 h,

hardly any PRL1 protein could be detected (Figure 32). This result indicated that the PRL1 protein is subjected to degradation with a relatively slow rate. The apparently slow degradation of PRL1 protein could be explained by the fact that after estradiol removal the translation of the available mRNA pool continued and hence the synthesis of PRL1-HA protein did not stop at 0 time point.
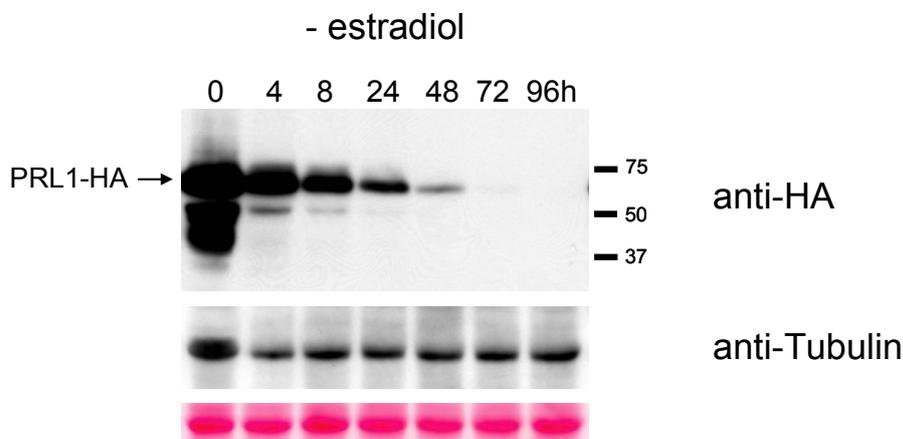
Figure 32.   Analysis of PRL1 protein stability
Seedlings carrying the estradiol-inducible pER8(Km)-PRL1-cDNA-HA construct in *prl1* mutant background were induced with estradiol for 24 h. After removal of estradiol, seedlings were cultured in liquid MS medium and samples were collected at 0, 4, 8, 24, 48, 72 and 96 h. PRL1-HA was detected with anti-HA antibody. Equal loading was confirmed by western blotting with anti-tubulin antibody and Ponceau-S staining.

3.4.3.   Degradation of PRL1 is inhibited by the proteasome inhibitor MG132

To assay whether the degradation of PRL1 is proteasome dependent, we examined the effect of reversible proteasome inhibitor MG132 on PRL1 protein stability. Seedlings carrying the estradiol-inducible pER8(Km)-PRL1-cDNA-HA construct in *prl1* mutant background were grown for two weeks on selective MSAR plates. Subsequently the plants were transferred to liquid MS medium containing DMSO, 2 μM estradiol or seedlings treated with estradiol in the presence of 100 μM MG132. Samples were collected at 4, 8 and 24 h for preparation of protein extracts, which were separated by 12% SDS-PAGE and subjected to immunoblotting with anti-HA antibody (Figure 33).
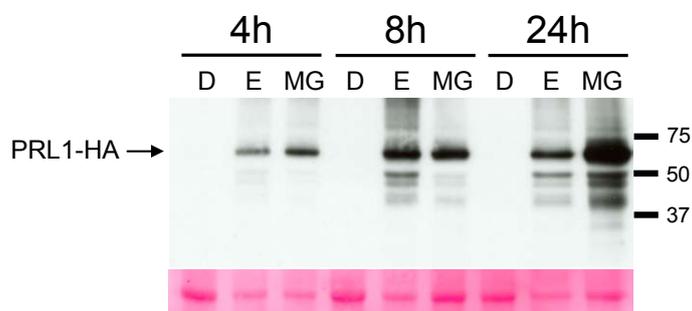
Figure 33.   Estradiol induced accumulation of PRL1 protein is enhanced by MG132 proteasome inhibitor treatment
Two-weeks old *prl1* seedlings carrying the estradiol-inducible pER8(Km)-PRL1-cDNA-HA construct were incubated with DMSO (D), 2 μM estradiol (E) or 2 μM estradiol and 100 μM MG132 (MG) in liquid MS medium for 4, 8 and 24 h. After preparation of protein extracts, samples were by 12% SDS-PAGE and the PRL1-HA was detected with anti-HA antibody. Equal loading of gel was verified by Ponceau-S staining.

Comparison of PRL1-HA levels in samples induced by estradiol in the presence or absence of MG132 showed that accumulation of PRL1 protein was significantly enhanced by the proteasome inhibitor suggesting that PRL1 is a potential substrate for proteasome-dependent degradation *in vivo*.

In order to exclude the possibility that the observed degradation of PRL1 protein was caused by its ectopic overexpression by the CaMV35S promoter driven pER8(Km)-PRL1-cDNA-HA construct, we have assayed the PRL1 protein stability in cells that expressed a wild type *PRL1* gene marked with a HA epitope coding sequence in pPCV002-PRL1-HA. At the same time, translation of the *PRL1* mRNA pool was inhibited in the cells by cycloheximide to block *de novo* PRL1 protein synthesis and thereby only examine the process of PRL1 protein degradation. A light-grown cell suspension stably transformed with the pPCV002-PRL1-HA construct was treated three days after subculturing with either 50 μM cycloheximide (CHX) or 50 μM cycloheximide and 50 μM MG132 proteasome inhibitor. From samples collected at 0, 4, 8, 24 and 48 h time points, protein extracts were prepared, separated by 8% SDS-PAGE gel and analyzed by western blotting using anti-HA antibody (Figure 34). The results showed that slow degradation of the PRL1-HA protein was not accelerated by the protein synthesis inhibitor cycloheximide indicating that the slow kinetics of PRL1 degradation did not appear result from compensation through de novo translation from a stable mRNA pool but rather indicated that PRL1 is a relatively stable protein. As in the previous experiments, MG132 prevented degradation of PRL1 also in the presence of cycloheximide confirming that PRL1 is likely degraded by the 26S proteasome.
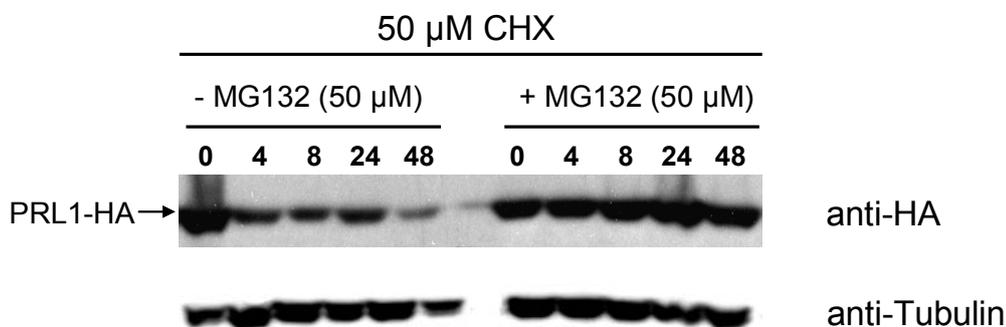
Figure 34.   **Inhibition of translation by cycloheximide does not affect the kinetics of PRL1 degradation**
Light-grown cell suspension stably transformed with pPCV002-PRL1-HA was treated with either 50 μM cycloheximide (CHX) or 50 μM cycloheximide and 50 μM MG132 26S proteasome inhibitor. 25 μg of extracted protein samples were resolved by 8% SDS-PAGE and the PRL1-HA protein was detected by immunoblotting with anti-HA antibody. Equal loading was monitored on the same membrane using an anti-tubulin antibody.

3.4.4.   Identification and site-specific mutagenesis of a putative destruction-box motif in PRL1

Sequence analysis revealed that the PRL1 protein contains degradation motives recognized potentially by E3 ubiquitin ligase Anaphase Promoting Complex (APC) activating factors. One of the canonical APC degron motives is the destruction box (D box), which was first identified in mitotic cyclins. The D box is defined by a motif of nine amino acids $\mathbf{R}xx_aLx_bxx_cxN$, where x_a is often A or V, x_b can be G, and x_c is frequently I or L). In this motif, amino acids at positions 1 and 4 are conserved in all APC

substrates. In addition to the D box, APC substrates may carry KEN-, A- or GxEN boxes. Our analysis of the PRL1 protein sequence has identified a perfect D box element in the N-terminal region between positions 113-121 (Figure 35).
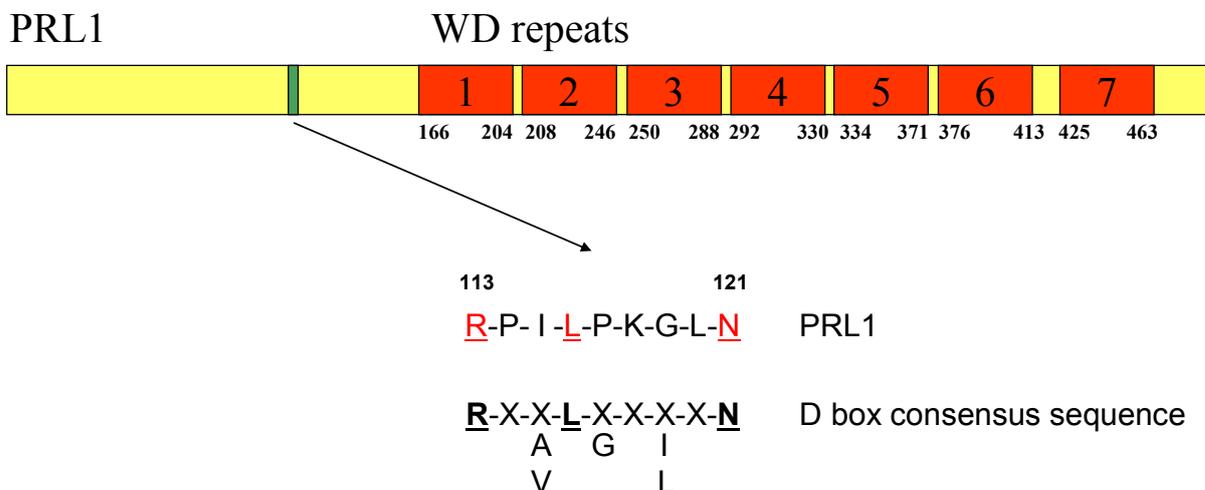
Figure 35. **Identification of putative D-box motif in the PRL1 protein sequence**
A D box element was identified in the PRL1 protein sequence between at amino acid positions 113-121 (marked with green colour). WD repeats are represented with red boxes and amino acid positions are labelled with numbers.

3.4.4.1. *Site-directed mutagenesis of the putative PRL1 D box*

As site-specific mutagenesis of the D box has been observed to stabilize APC substrates (for review see Peters, 2002), we designed a site-specific mutagenesis experiment for introduction of point mutations R113G and L116V at the two highly conserved amino acid positions in the putative D box of PRL1. Plasmid pBS-PRL1-2introns-cDNA-GFP was mutated using Transformer™ site-directed mutagenesis kit using the STABmut and Sca primers (2.1.6.3). The mutagenesis was verified by DNA sequencing and then the PRL1-GFP cassette was isolated as an *Xho*I-*Sac*II fragment from pBS-PRL1-2introns-cDNA-GFP, the ends were filled in with T4 DNA polymerase and the fragment was ligated into *Sma*I digested pPCV002-PRL1-PROM-UTR. The obtained pPCV002-STAB-PRL1-GFP construct was introduced into green cell suspension, wild type and *prl1* mutant plants.

3.4.4.2. *Assay of stability of D-box mutant PRL1-GFP protein in cell suspension*

In order to test whether mutation of the D box would affect the stability (i.e., reflected by the expression level) of PRL1-GFP protein, light-grown cell suspensions were stably transformed wild type and D-box mutant PRL1::PRL1-GFP constructs. From both cell suspensions, protein samples were prepared at 1, 3, 7 and 14 days after subculturing, separated by an 8% SDS-PAGE gel and immunoblotted with anti-PRL1 antibody (Figure 36). As compared to wild type PRL1-GFP, the levels of D-box mutant PRL1-GFP were higher in the cell suspesions at all the time points of the logarithmic

growth phase. This result suggested that PRL1 protein may represent a potential APC ubiquitin ligase substrate since the only difference between the two constructs was the mutation in the D box element.
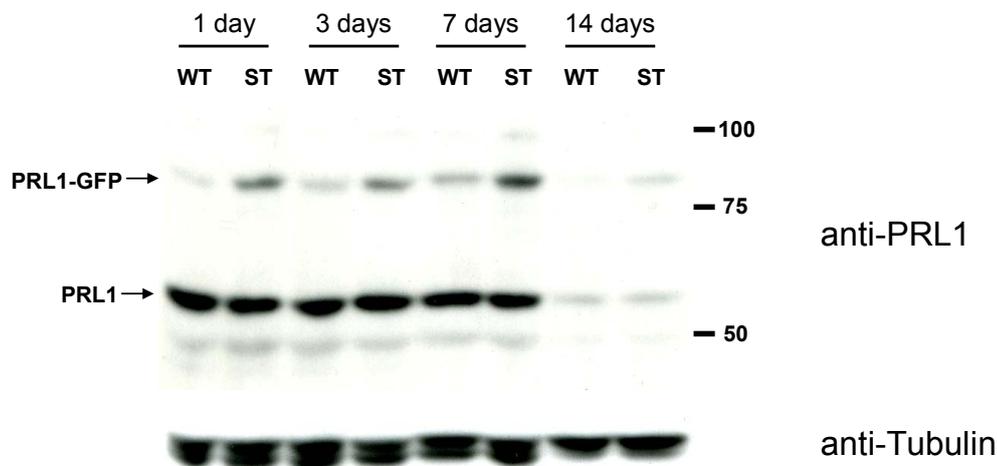
Figure 36. **Assay of levels of wild type and D-box mutant PRL1-GFP proteins in cell suspension**
Samples from light-grown cell suspensions expressing the wild type (WT) and D-box mutant "stabilized" (ST) PRL1-GFP proteins from PRL1 promoter driven constructs were collected at 1, 3, 7 and 14 days after subculturing. 25 μg of protein samples were size separated on 8% SDS-PAGE gel and immunoblotted with anti-PRL1 and anti-tubulin antibodies.

As internal control, the anti-PRL1 antibody also detected the levels of intrinsic PRL1 protein, which were equal in collected samples. In stationary phase cultures (i.e., 14 days old), the levels of PRL1-GFP and intrinsic PRL1 proteins showed a notable decrease, which was probably due to partial loss of the cells' viability.

3.4.4.3. *Immunodetection of stabilized PRL1-GFP in wild type plants*

The *PRL1* promoter driven wild type and D-box mutant PRL1-GFP constructs were also transformed into Col-0 wild type *Arabidopsis thaliana*. For both constructs, seedlings from five independent T2 families were grown on selective kanamycin plates for 3 weeks and analyzed by immunoblotting with anti-PRL1 antibody after separation of protein extracts on 8% SDS-PAGE gel. Despite considerable variation of PRL1-GFP levels between the transformants, the assay provided no evidence for higher stability of D-box mutant PRL1-GFP protein in seedlings (Figure 37). This observation may correlate with the fact that the APC complex is primarily active during the cell cycle from metaphase until S phase (i.e., especially, during metaphase anaphase transition and mitotic exit; Harper et al., 2002). Since the proportion of the meristematic cells as compared to the number of vegetative cells is small in plants, stabilization of D-box mutant PRL1-GFP may not simply detected by assaying for higher protein levels. Further analysis of the initiated cell suspensions from these transgenic lines could however provide a means for proper analysis of stability of D-box mutant PRL1-GFP protein during cell cycle progression using synchronization.
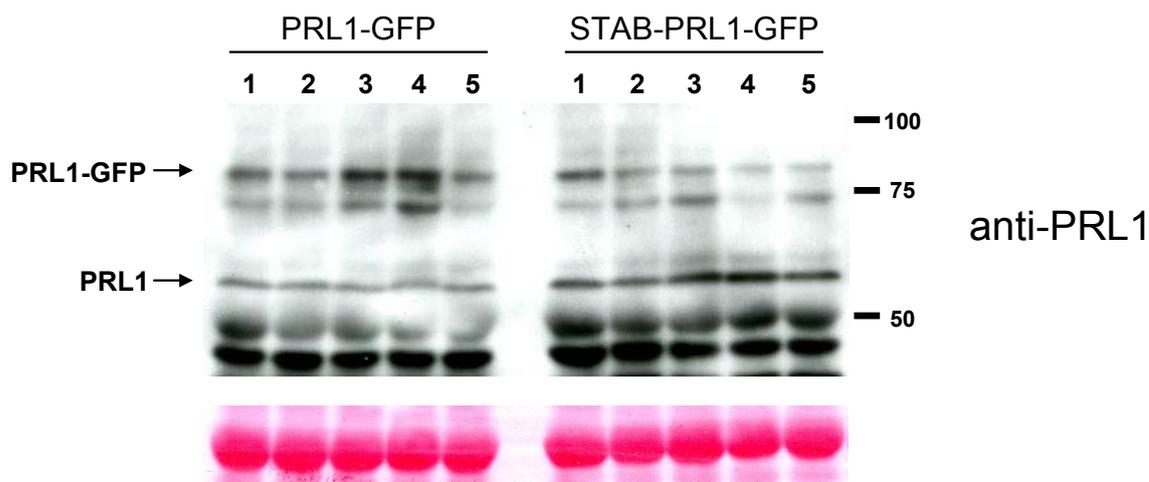
Figure 37. **Immunodetection of wild type and D-box mutant PRL1-GFP proteins *in planta***
From seedlings grown for 3 weeks on selective plates protein extracts were prepared. 25 μg of proteins samples was separated on an 8% SDS-PAGE gel and analyzed by western blotting with anti-PRL1 antibody. Equal loading was verified by staining the corresponding membrane with Ponceau-S solution.

To test whether overexpression of D-box mutant form of PRL1-GFP protein would cause any alteration in the development of wild type plants, the PRL1-GFP coding region was also fused to CaMV35S promoter. This was achieved by exchanging the 5' *Xho*I-*Bmg*BI fragment of pBS-STAB-PRL1-2introns-GFP for an *Xho*I-*Bmg*BI fragment from the pBS-PRL1-cDNA-HA construct. The STAB-PRL1-cDNA-GFP cassette was isolated after *Sac*II digestion, T4 DNA polymerase fill-in and *Xho*I digestion and cloned into *Xho*I-*Sma*I sites of the binary vector pPAMnptII. A pPAMnptII carrying the wild type PRL1-GFP expression cassette was constructed similarly. Both wild type and D-box mutant PRL1-GFP expression constructs were transformed into wild type plants and T1 lines were selected in the presence of kanamycin. However, in the T2 generation of these plants no phenotypic changes were detected (data not shown).

3.5. Characterization of PRL1 protein interactions

3.5.1. Yeast two hybrid assay with AtCDC5

PRL1 homologs were identified to interact with CDC5 orthologs in spliceosome activating complexes in yeast and mammalian cells (see section 1.5). To determine whether this protein interaction is also conserved in *Arabidopsis*, yeast two-hybrid assays were performed with PRL1 and AtCDC5 (At1g09770). Full-length *AtCDC5* cDNA was PCR amplified from a cell suspension cDNA library with CDC5-F and CDC5-R primers (2.1.5 and 2.1.6.2). The amplified DNA fragment was digested with *Eco*RI and *Xho*I and inserted into the pACT2 prey vector in frame with the Gal4 activating domain (AD). Y187 and Y190 yeast strains were co-transformed with pACT2-CDC5 in combination with pAS2-PRL1, pAS2-PRL2, pAS2-PRL1-N-term (PRL1 sequences between cDNA positions 40 and 570 bp), pAS2-PRL1-C-term (PRL1 sequences between cDNA positions 1000 and 1500) or the

empty pAS2 vector. From the Matchmaker kit (Clontech), we used pVA3-1 (DNA-BD/ murine p53 protein) and pTD1-1 (AD/ SV40 large T antigen protein) as positive and pLAM5'-1 (DNA BD/ human lamin C protein) and pTD1-1 as negative controls. Selected and purified yeast colonies were tested by colony lift assay. Full-length PRL1 and PRL2 (i.e., PRL1 homolog) and the N-terminal domain of the PRL1 failed to interact with CDC5. However, interaction of AtCDC5 was observed in combination with the PRL1 C-terminal domain, which carried the WD-40 repeat region. CDC5 was found to interact only with WD-repeats of PRL1 orthologs in yeast and mammals (Ajuh et al., 2002). Despite the negative result obtained with full-length PRL1 and PRL2, which carry homologous WD-40 repeats, we decided therefore to examine interaction of PRL1 with AtCDC5 *in vivo*.
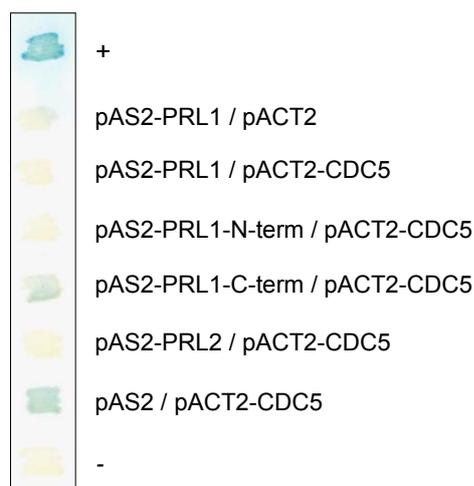
Figure 38.   Yeast two hybrid assays using AtCDC5 as prey
AtCDC5 was fused to Gal4 activation domain and tested with full-length PRL1 and PRL2 baits, along with pAS2 bait vectors coding for N- and C-terminal segments of PRL1. As positive control (+) yeast was co-transformed with pVA3-1 (DNA-BD/ murine p53 protein) and pTD1-1 (AD/ SV40 large T antigen protein), whereas as negative control (-) cells carrying pLAM5'-1 (DNA BD/ human lamin C protein) and pTD1-1 were used. As further control, the pAS2-PRL1 bait was transformed with the empty prey vector pACT2. The empty bait vector pAS2 alone or in combination with pACT2 showed artificial activation of the *LacZ* reporter gene as described by Durfee et al. (1993), but none of the recombinant pAS2 bait vectors displayed any LacZ activity.

3.5.2.   Detection of PRL1-AtCDC5 interaction *in vivo*

To detect AtCDC5 *in vivo*, the 3'-end of full length cDNA was tagged with a HA-epitope coding sequence and inserted into an expression vector downstream of a CaMV35S promoter carrying a duplicated enhancer domain. The *AtCDC5* cDNA was PCR amplified using CDC5-F and CDC5-HA primers (2.1.6.2) and upon *Eco*RI-*Xba*I digestion the amplified DNA fragment was inserted into *Eco*RI-*Xba*I sites of the pPAMpat binary vector. After sequencing pPAMpat-CDC5-HA was introduced into the *Agrobacterium* strain GV3101 (pMP90RK) and used for transformation of green cell suspension, and wild type (Col-0) and *prl1* mutant plants.

First, the expression of the CDC5-HA protein in cell suspension was verified by western blotting with anti-HA antibody (data not shown). Subsequently, in a scaled up experiment the AtCDC5-HA protein was immunoprecipitated from protein extract prepared from light-grown cell suspension 7 days after subculturing. The protein extract was incubated with anti-HA IgG, the antibody-protein complex was immobilized on protein A/G agarose and then non-specific proteins

were removed by stringent washes. The CDC5-HA complex was eluted by HA peptide from the beads and then total input and immunoprecipitated protein fractions were analyzed by western blotting using anti-HA and anti-PRL1 antibodies (Figure 39). The immunoprecipitated and stringently eluted AtCDC5-HA protein pulled down PRL1 from the extract indicating that, despite the detected weak interaction in yeast, AtCDC5 and PRL1 interact and occur in a common protein complex in cultured *Arabidopsis* cells.
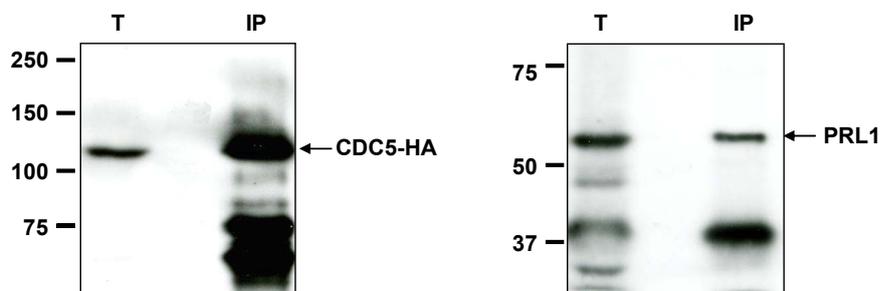
Figure 39.   **AtCDC5-HA immunoprecipitates PRL1 from protein extracts prepared from *Arabidopsis* cell suspension.**
Protein extract was prepared from a light-grown cell suspension expressing the AtCDC5-HA protein from a CaMV35S promoter-driven expression construct. AtCDC5-HA was immunoprecipitated with anti-HA IgG, bound to protein A/G Sepharose matrix, and eluted with HA peptide. Samples from the total input (T) and immunoprecipitate (IP) protein fractions were size separated on an 8% SDS-PAGE gel and immunoblotted with an anti-HA antibody. After stripping, the same membrane was probed with anti-PRL1 antibody.

3.5.3.   AtCDC5-HA is associated with the components of the protein degradation system

PRL1 was reported to interact with the catalytic α-subunits of SnRK1 class of plant AMP-activated protein kinases by Bhalerao et al. (1999). Subsequently, Farras et al. (2001) found a SnRK1α kinase subunit in stable association with the proteasome and with common CULLIN 1 and SPK1/ASK1 subunits of SCF E3 ubiquitin ligase complexes by performing a series of western blotting experiments; therefore, we have addressed the question whether AtCDC5 would immunoprecipitate core components of the proteasome. In this experiment, the total input and AtCDC5-HA immunoprecipitated protein fractions were tested with an anti-20S antibody raised against the α1, α2, α3, α5, α6 and α7 subunits of the proteasome 20S core particle and with an antibody detecting the Rpn6 regulator non-ATPase subunit of 19S lid of the proteasome. In the AtCDC5-HA immunoprecipitated protein fraction the anti-20S antibody detected a protein band displaying the site of proteasome α-subunits, whereas similarly the anti-19S antibody cross-reacted with a protein corresponding to the site of Rpn6 19S subunit. This data suggested that at least part of AtCDC5-HA protein pool is found in proteasomal association (Figure 40).

Subsequently, we tested whether some specific components of SCF E3 enzymes or SCF regulator COP9 signalosome (CSN) were present in the immunoprecipitated AtCDC5-HA protein fraction. Results of the immonoblotting experiments in Figure 40 show that AtCDC5-HA co-immunoprecipitated with the CSN5 subunit of COP9 signalosome and CULLIN 1 subunit of SCF E3 ubiquitin ligases. However, remarkably the immunoprecipitated complex did not cross-react with a highly specific anti-SKP1/ASK1 antibody suggesting that AtCDC5-HA occurs in a complex with

CULLIN 1 that does not contain the SKP1/ASK1 SCF subunit. Finally, western blotting with anti-ubiquitin antibody detected several unknown ubiquitinated proteins, one of which was present in notably high quantity in the AtCDC5-HA immunoprecipitate. In conclusion, these data indicated that AtCDC5-HA, alone or in complex with PRL1, interacts with several known components of ubiquitination and proteasome-dependent proteolysis pathways.
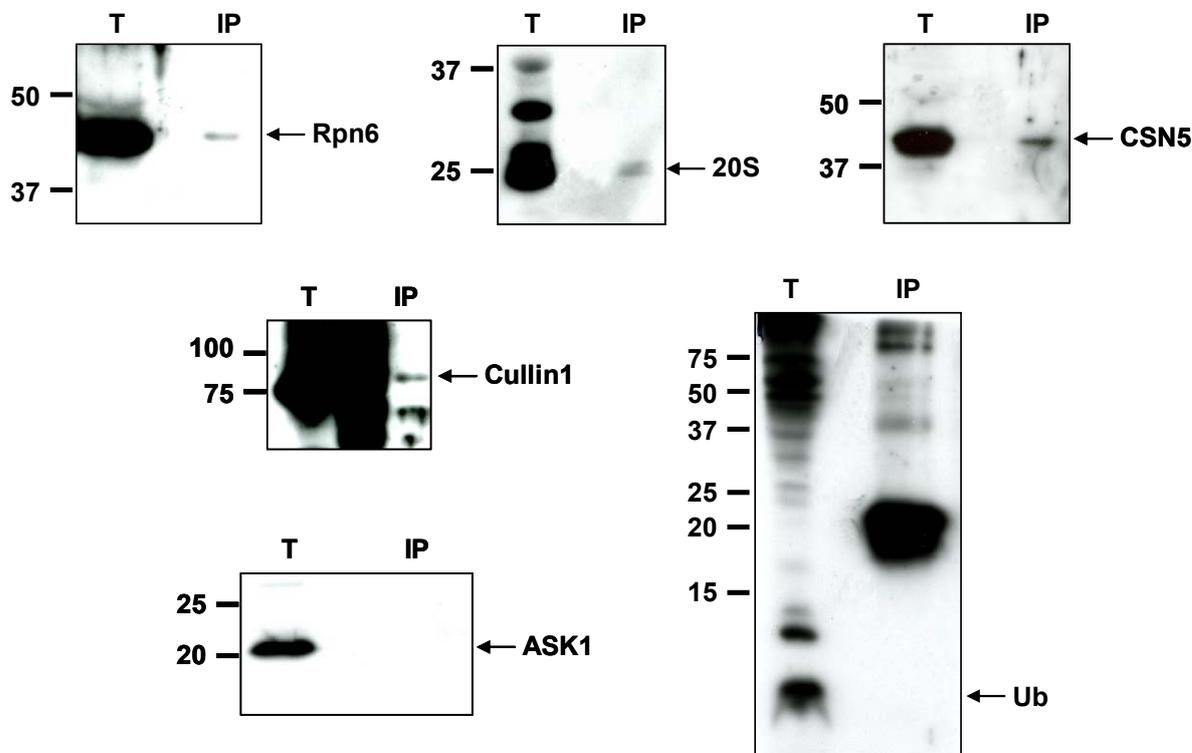
Figure 40.   Detection of subunits proteasome, SCF and COP9 complexes in the AtCDC5-HA immunoprecipitated protein fraction.
The total input and immunoprecipitated protein fractions were immunoblotted with anti-Rpn6 (specific to the non-ATPase regulator subunit of the 19S lid of the 20S proteasome), anti-20S (raised against α subunits of the core particle of the 26S proteasome), anti-CSN5 (COP9 signalosome subunit), anti-CULLIN 1, anti-SKP1 (ASK1) (detects members of the SCF type E3 ubiquitin ligase complex) and anti-ubiquitin (Ub) antibodies. T: total input, IP: immunoprecipitate, Ub: ubiquitin.

3.5.4.   Size fractionation of AtCDC5 complex on glycerol gradient

To estimate the approximate size of AtCDC5 complex, whole cell extract prepared from light-grown cell suspension expressing the AtCDC5-HA protein was isolated and size fractionated on 10-40% glycerol density gradient (100,000 g, 16h at 4°C). Gradient fractions were separated on SDS-PAGE and immunoblotted with anti-HA antibody to follow distribution of CDC5-HA. Subsequently, the same membrane was tested with anti-PRL1 antibody. AtCDC5-HA was detected in three separated peaks (Figure 41). The monomeric form of AtCDC5-HA was present in fractions 3-13, in a complex corresponding to a size of approximately 400 kDa in fractions 18-22, and was also present in a very large complex (fraction 36) and insoluble pellet migrating to the bottom of the gradient. Immunoblotting of fractions with the anti-PRL1 antibody revealed a similar size distribution of PRL1 containing protein complexes. Together with the data showing co-immunoprecipitation of AtCDC5-

HA with PRL1, the analysis of glycerol gradient fractions indicated that PRL1 may co-purify and occur in common protein complex(es) with AtCDC5.

CDC5-HA (anti-HA)
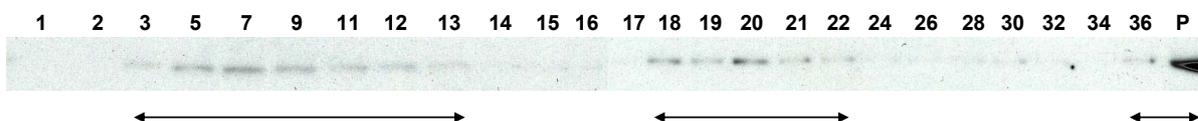
PRL1 (anti-PRL1)
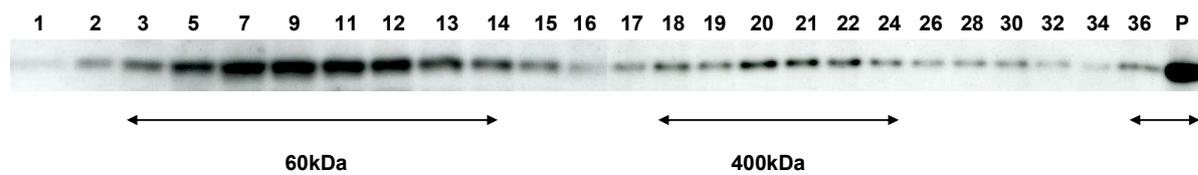
Figure 41.   Size fractionation of AtCDC5 complex on glycerol density gradient
Whole cell protein extract was isolated from a light-grown green cell suspension carrying the 2XCaMV35S::CDC5-HA construct and separated on 10-40% glycerol gradient. 300 μl fractions were collected and separated by 8% SDS-PAGE, and analyzed by western blotting with anti-HA antibody. Subsequently, the same membrane was probed with anti-PRL1 antibody. A parallel glycerol gradient was run to calibrate the resolution of the 10-40% glycerol gradient. The glycerol gradient was calibrated using a high molecular weight Gel Filtration Calibration Kit (Amersham) containing albumin (66 kDa), lactate dehydrogenase (140 kDa), catalase (232 kDa) and ferritin (440 kDa).

3.5.5.   Distribution of AtCDC5 in nuclear and cytoplasmic fractions

To determine the cellular localization of AtCDC5 protein, nuclear and cytoplasmic protein fractions were extracted from the cell suspension carrying the 2XCaMV35S::CDC5-HA construct, size separated on SDS-PAGE gels and immunoblotted with anti-HA antibody. Two identical membranes were probed with anti-histone H2A and anti-PRL1 antibodies to quality test the preparation and to confirm subcellular co-localization of the PRL1 protein. The cell fractionation experiment revealed that AtCDC5-HA was present exclusively in the nucleus (Figure 42).
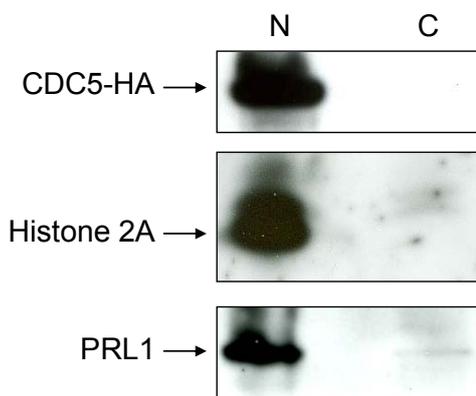
Figure 42.   Biochemical assay of subcellular localization of AtCDC5-HA protein.
Nuclear and cytoplasmic protein fractions were isolated from AtCDC5-HA expressing green cell suspension 7 days after subculturing. The protein samples were size separated on either 8% or 16% (for H2A) SDS-PAGE and immunoblotted subsequently with anti-HA, anti-histone H2A and anti-PRL antibodies.

Analogously, the bulk of PRL1 protein was present in the nuclear extract, but traces of the protein were also detected in the cytoplasmic fraction. The data of this subcellular localization experiments thus also supported our hypothesis that AtCDC5 and PRL1 are associated in nuclear protein complex(es).

3.5.6. Search for protein interactions with the N-terminal domain of PRL1

In our laboratory, K. Salchert (1997) identified previously 13 putative PRL1-interacting partners (PIPs) by performing yeast two-hybrid screens with a pACT2 cDNA library prepared from mRNA derived from a dark-grown root-derived cell suspension. In addition, Bhalerao et al. (1998) found that the N-terminus of PRL1 interacts specifically with the SnRK1 kinase α-subunits AKIN10 and AKIN11. To test whether some of the known PRL1-interacting partners are also found in association with PRL1 *in vivo*, we performed a series of immunoprecipitation experiments. In these studies we used analytical tools generated by other members of the group during the characterization of histone protein arginine methylase PAM1 (PIP-H, At4g29510), ATAM1 amidase of unknown function (PIP-I, At5g07360), AKIN11, and Ufd1 (ubiquitin fusion degradation 1, PIP-K, At4g15420), a CDC48 and polyubiquitin binding component of a putative membrane-bound ubiquitin ligase. Immunoprecipitation experiments were performed with protein extracts prepared from three weeks old seedlings. Seedlings carrying T-DNAs of either pER8-PAM1-cMyc or pER8-AKIN11-HA constructs for inducible expression of epitope labelled PAM1-cMyc and AKIN11-HA proteins, respectively, were treated for 24h with 2 μM estradiol prior protein extraction. Extract containing the HA-epitope labelled
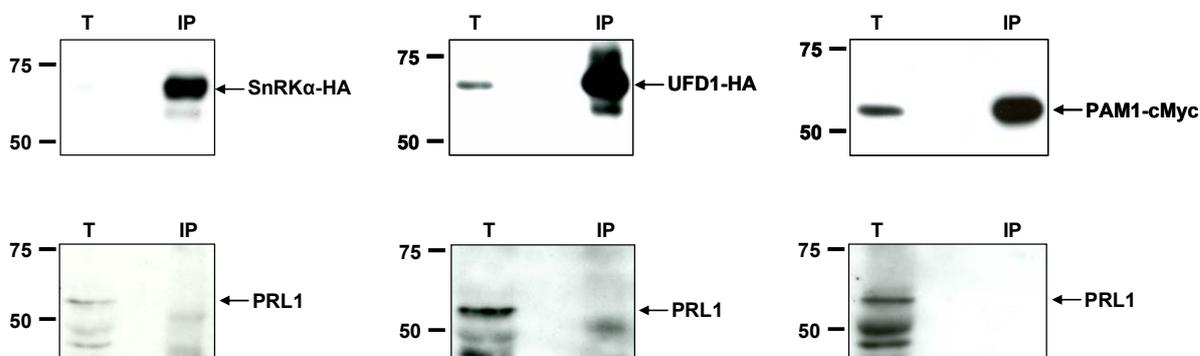
Figure 43.   Assay of PRL1 co-immunoprecipitation with AKIN11-HA, UFD1-HA and PAM1-cMyc baits
Immunoprecipitations were performed with anti-HA or anti-cMyc IgGs using whole cell protein extracts from 3 weeks old seedlings. The total input (T) and immunoprecipitated (IP) protein fractions were resolved on 8% SDS-PAGE and analyzed by western blotting with anti-HA and anti-cMyc antibodies. The same membranes were treated tested subsequently with the anti-PRL1 antibody.

UFD1-HA protein was prepared from plants carrying a CaMV35 promoter driven UFD1-HiA construct. Whole cell extracts were immunoprecipitated with either anti-HA or anti-cMyc antibodies followed by elution with the appropriate peptide. Aliquots from the total input and immunoprecipitated fractions were analyzed by western blotting using anti-HA or anti-cMyc antibodies to confirm the presence of bait proteins. Subsequently, the membranes were stripped to

perform immunodetection with anti-PRL1 antibody. As shown in Figure 43, PRL1 could not be detected in the immunoprecipitates of AKIN11-HA, UFD1-HA and PAM1-cMyc proteins.

A similar immunoprecipitation assay was performed with protein extracts prepared also from 3 weeks old seedlings that carried the pPCV002PRL1-HA construct for expression of an HA-tagged form of PRL1 by the full-length native *PRL1* promoter in the *prl1* mutant background. PRL1-HA was immunoprecipitated with anti-HA IgG, the immunocomplex was bound to protein A/G agarose, washed several times to remove unspecific proteins and then eluted by HA peptide. The immunoprecipitated proteins were subjected to western blotting with anti-HA antibody to detect PRL1-HA, as well as with an antibody was raised against the tobacco NPK5 protein that can recognize all SnRK1α subunits expressed in *Arabidopsis* and with an anti-AtATAM1 amidase antibody. However, we could reveal no PRL1 association with SnRK1α and ATAM1 amidase proteins (Figure 44). The immunoprecipitated protein fractions were further tested by immunodetection with anti-19S proteasome, anti-20S proteasome, anti-CULLIN 1 and anti-SKP1/ASK1 antibodies, however, these also failed to detect co-immunoprecipitation of the corresponding proteins (data not shown).
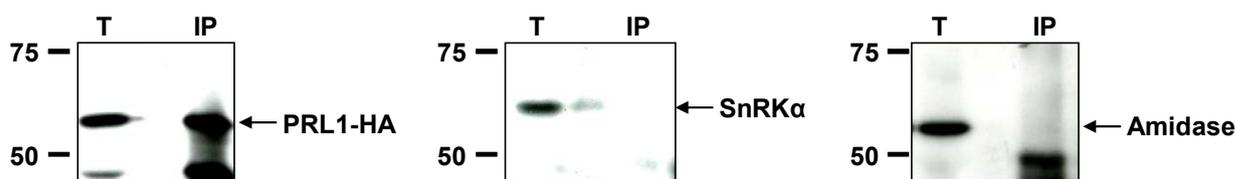
Figure 44. **Assay of co-immunoprecipitation of PRL1-HA with SnRK1α and ATAM1 amidase proteins.**
Whole cell protein extracts were prepared from 3 weeks PRL1-HA expressing seedlings and immunoprecipitated with anti-HA antibody. After HA peptide elution, the immunoprecipitated protein fraction was analyzed by western blotting using anti-HA, anti-SnRKα and anti-amidase antibodies.

These negative data were puzzling as our experiment previous experiments clearly demonstrated *in vivo* association of PRL1 with the AtCDC5 protein, which was also found to co-immunoprecipitate components of the proteasome, signalosome and CULLIN 1. However, these protein interactions were observed in actively dividing cultured cells, whereas the above described co-immunoprecipitation assays were performed with plant materials representing mostly leaves. As shown by Figure 44, PRL1-HA is significantly degraded in these samples. It is thus possible that in leaves where PRL1 levels are low, probably due to enhanced degradation, the tested proteins do not interact with PRL1. The fact that cDNAs of all PIPs identified in previous yeast two-hybrid interactions were isolated from a dark grown cell suspension also suggest that interaction of PRL1 with the tested PIP proteins may not occur in leaves, but in other cell types, such as actively dividing cells of shoot or root meristems.

One of the most problematic technical aspects of biochemical work with PRL1 (and AtCDC5) is the establishment of proper conditions for isolation of intact nuclear protein complexes. As shown in Figure 45, size fractionation of protein complexes prepared from purified nuclei of PRL1-HA expressing plants yields primarily a peak of non-complexed free PRL1-HA protein, whereas the bulk

of PRL1-HA protein migrates to the pellet, indicating a severe solubilization problem. On the other hand, glycerol gradient size fractionation of whole cell extract indicates that protein complexes

Nuclear fraction

Total protein
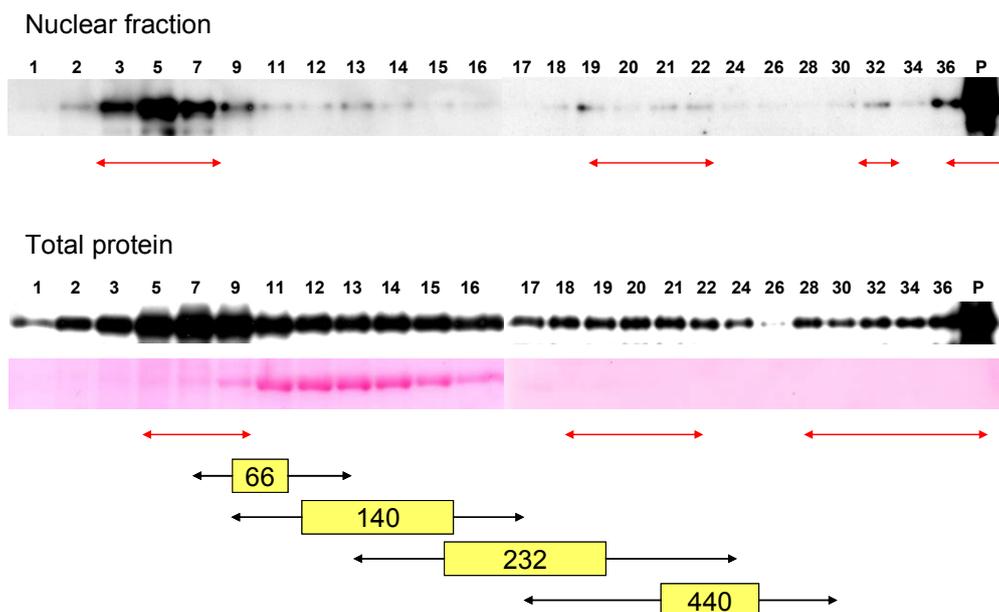
Figure 45.   Size fractionation of PRL1-HA complexes from nuclear and whole cell protein extracts
Nuclear and whole cell protein extracts were prepared from three weeks old plants expressing the PRL1-HA protein under the control of the native *PRL1* promoter of the pPCV002-PRL1-HA construct. The samples were size fractionated on 10-40% glycerol gradients. 300 µl fractions were collected and analyzed by immunodetection with anti-HA antibody after SDS-PAGE separation and western blotting. In case of whole cell extract (total protein); the western blot was stained with Ponceau-S solution. Calibration of the glycerol gradient was performed with a HMW Gel Filtration Calibration Kit represented by yellow boxes. P: pellet indicates a small aliquot from the poorly solubilised protein fractions that contain high molecular weight protein complexes.

pER8-PAM1-c-Myc (PIP-H)

Anti-Amidase (PIP-I)
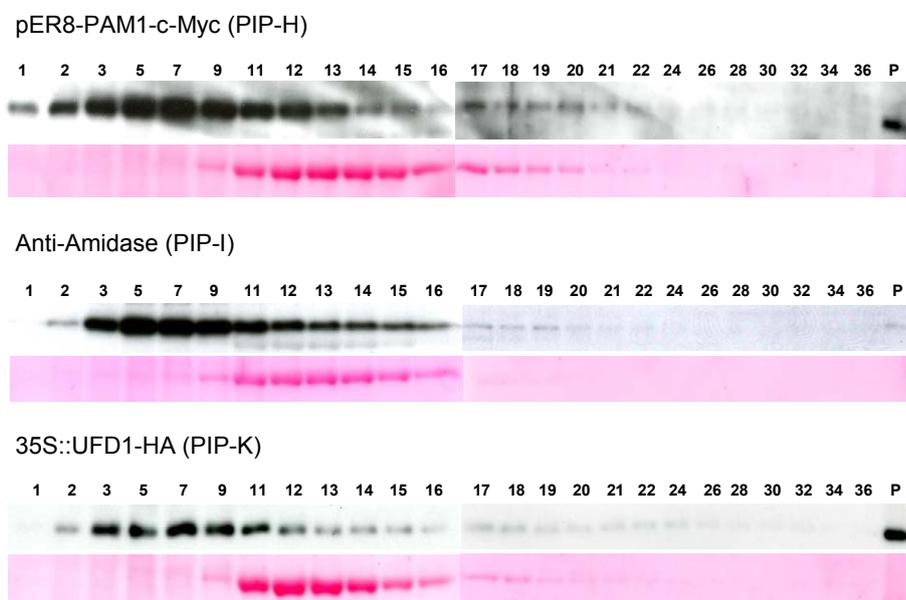
35S::UFD1-HA (PIP-K)

Figure 46.   Size separation of protein complexes containing putative PRL1 interacting partner proteins
Whole cell extracts from three weeks old plants carrying T-DNA of either pER8-PAM1-c-Myc, PRL1::PRL1genomic-HA or 35S::UFD1-HA expression vectors were prepared and size fractionated on 10-40% glycerol gradients. 300 µl fractions were collected and analyzed by western blotting using anti-cMyc, anti-ATAM1 amidase and anti-HA antibodies. Corresponding membranes were stained with Ponceau solution. P: pellet. As in Figure 45, in addition to fractions containing monomeric free forms of epitope labelled proteins, significant amounts of PAM1 methylase, ATAM1 amidase and UFD1 occur only in the pellet fractions of gradients.

containing PRL1-HA are distributed through the whole size range of the gradient, which is a clear sign for artificial dissociation of large protein complexes. As shown in Figure 46, very similar problems were uncovered by size fractionation experiments performed with whole cell extracts containing the PAM1-cMyc, ATAM1 amidase and Ufd1-HA proteins, a significant proportion of which is also found in insoluble pellets at the bottom of glycerol gradient. These observations indicate that further biochemical analysis of PRL1 and AtCDC5 complexes requires the application of better solubilization and high-affinity binding technologies for isolation of large protein complexes.

3.6. Genetic approaches to functional characterization of PRL1 and its putative interacting partners

3.6.1. Isolation of new *prl1* insertion mutant alleles

In our experiments described above, we showed that AtCDC5 interacts with the C-terminal WD-40 repeat region of the PRL1 protein. In the first identified *prl1-1* mutant allele (Nemeth et al., 1998), the T-DNA insertion was localized close to the 3'-end of the PRL1 coding region. Although nearly the full-length upstream PRL1 coding sequence is transcribed in the *prl1-1* mutant, as Nemeth et al. (1998) we also failed to detect the synthesis of a C-terminally truncated protein product in this mutant. This observation suggests that C-terminal sequences of *PRL1* play a role in either proper folding or regulation of stability of the protein, or both. As all public *Arabidopsis* T-DNA insertion mutant collections were generated with T-DNA tags that carry in close vicinity of their left borders various strong promoters (i.e., that initiate transcription through the border), we have examined whether any currently available T-DNA insertion would promote the expression of a partially functional PRL1 protein resulting in a phenotype different from that of the *prl1-1* mutant.

Three *prl1* mutant lines were obtained from the SALK T-DNA insertion population. The genotypes of individuals in the obtained segregating populations were determined by PCR amplification using combinations of gene and T-DNA end specific primers. Seeds were germinated on MSAR plates and after 15 days planted in soil for harvesting leaf material for individual plants for preparation of template DNAs. Results of PCR genotyping performed in this thesis work are summarized briefly below.

3.6.1.1. *PCR genotyping of the prl1-2 SALK_008466 line*

PCR analysis of the SALK_008466 line was performed with three sets of primers. The gene specific primers (PRL1 5' and PRL1 3') located upstream and downstream of *PRL1* gene amplified a 3.5 kb fragment only when the wild type copy of *PRL1* was present. The PRL1 5' and SALK LB primers were specific for the left border and FISH2 and PRL1 3' for the right border junction of the T-DNA. PCR analysis with the gene specific primers indicated that lines 17, 18, 19 and 20 in Figure 47 were homozygous, whereas lines 6, 9, 10, 11, 14 and 15 did not carry T-DNA insertion. The T-DNA specific primer sets were able to amplify DNA fragments from these samples that verified the

presence of the insertion. In case of the FISH2 and PRL1 3' primers instead of an expected 3 kb fragment the PCR reaction resulted in a product of 1.9 kb. The amplified PCR fragments were sequenced in order to reveal the exact position of the T-DNA. This showed precisely that the SALK_008466 T-DNA insertion occurred in the fifth exon of the *PRL1* gene and caused a large internal deletion of 1290 bp between exons 5 and 11 (Figure 47).

SALK_008466

PRL1 5' and PRL1 3' primers

PRL1 5' and SALK LB primers

FISH2 and PRL1 3'primers

tacaggttcc**ACAACAAATTAATGTACAC**<u>ATTGACGC</u>   <u>GAACAGATTGTCGTTT</u>**CACGTCAAGNT**tgtgggatat
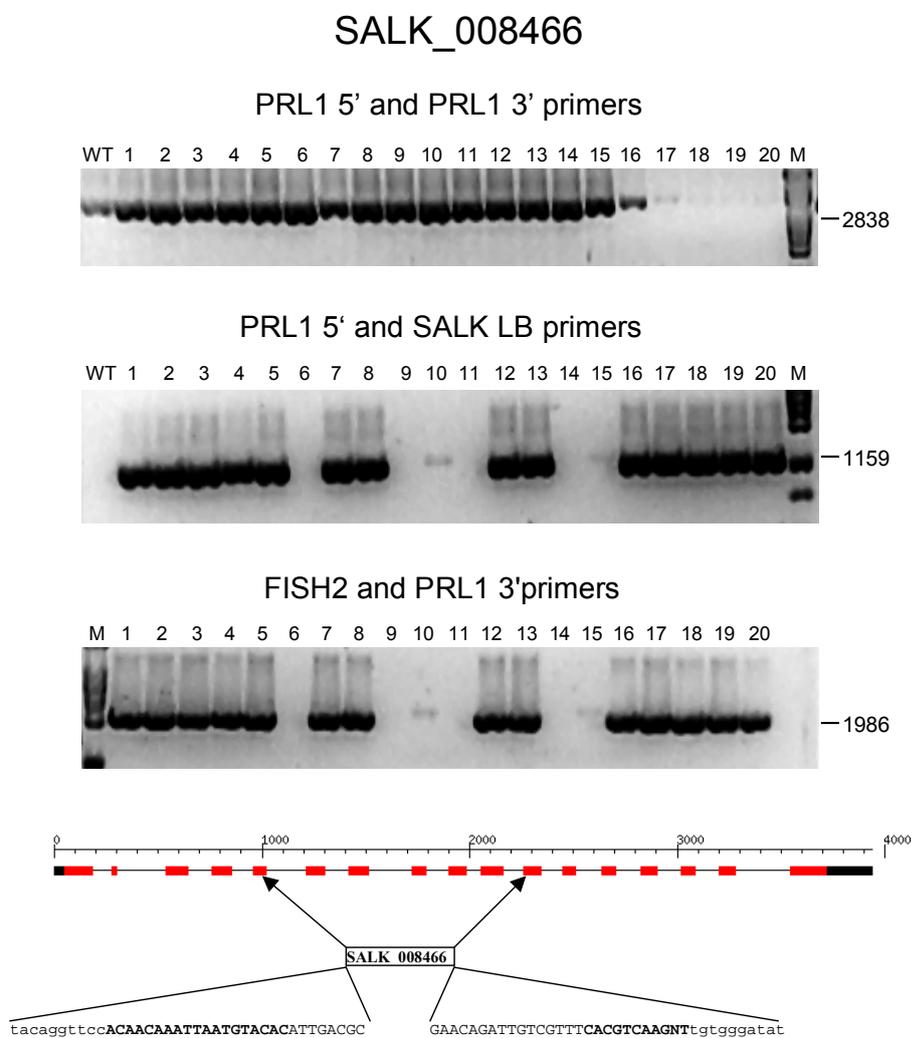
Figure 47.   PCR analysis of *prl1-2* SALK_008466 allele
M3 individuals carrying the *prl1-2* SALK-008466 allele were analyzed using gene and T-DNA specific primer combinations. Sequencing of amplified PCR fragments indicated that the insertion occurred in exon 5 causing a large internal deletion between exons 5 and 11. The sequence of the T-DNA below schematic presentation of the *PRL1* gene is marked with underlined capital letters, bold letters indicate filler DNA sequences, and letters in lower case correspond to *PRL1* sequences. WT, wild type control DNA; M: DNA size marker (λ-*Hind*III).

3.6.1.2.   PCR genotyping of prl1-3 SALK_096289 and prl1-4 SALK_039427 lines

In the analysis of the SALK-039427 *prl1* and SALK_096289 mutant alleles the same principle and primer combinations were used as described above for SALK_008466. PCR amplification of SALK-039427 lines with the gene specific primers failed to yield a product for lines 21, 22, 23, 24, 25, 26, 28, 29, 30, 31 and 32 (Figure 48). Amplification of the T-DNA left and right insert junctions confirmed that these lines were indeed homozygous mutants and indicated that lines 1, 2, 5, 6, 7, 10, 13, 15, 17, 18 and 19 did not carry T-DNA. Sequencing the T-DNA junction fragments showed that

prl1-3 SALK-039427 allele carried a T-DNA insertion in intron 4 and caused a target site deletion of 39 bp.
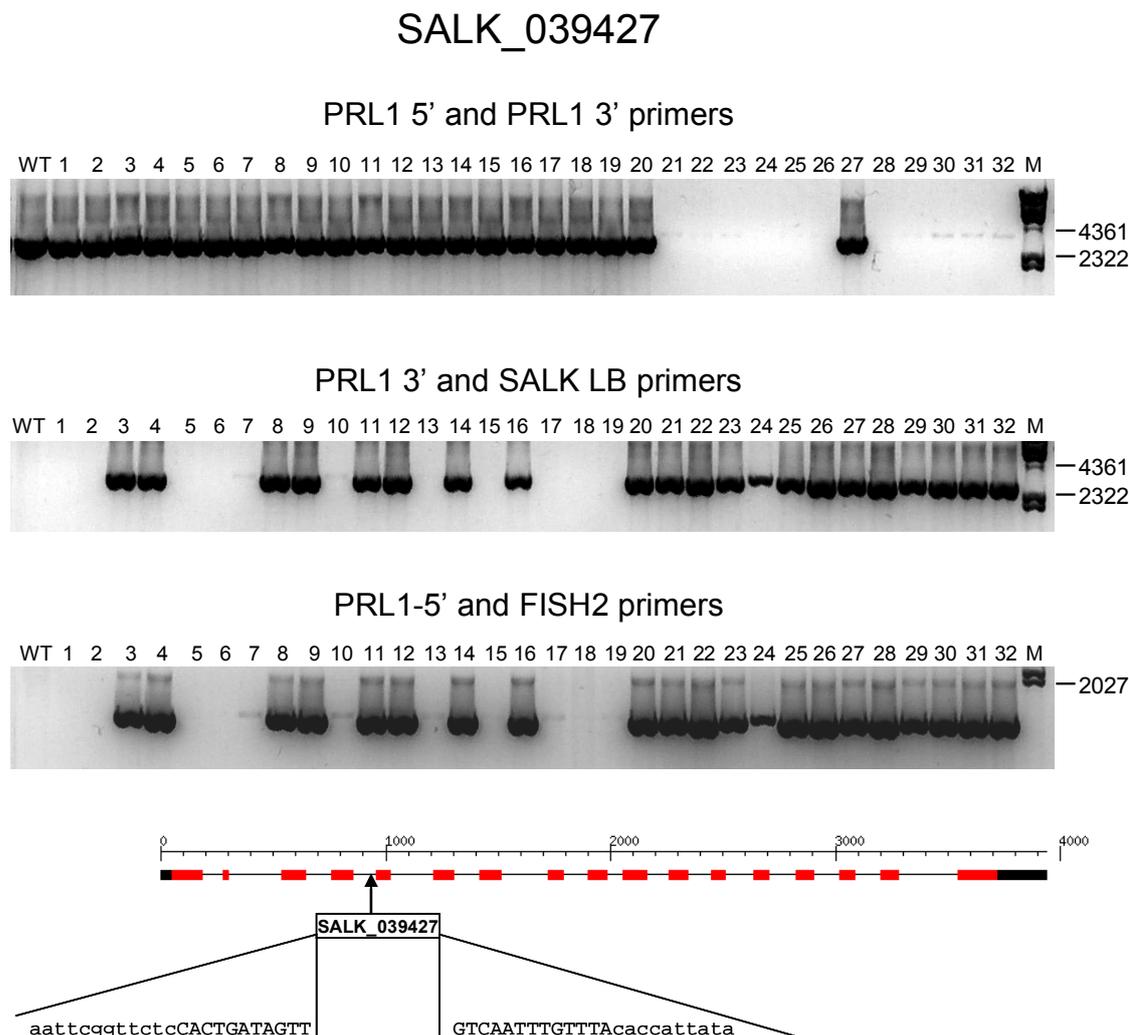
Figure 48.   PCR genotyping of *prl1-3* SALK_039427 lines
32 M3 lines were analyzed by PCR amplification using different combinations of gene specific and T-DNA specific primers. Homozygous candidates lines were identified using the PRL1 5' and PRL1 3' primers Amplification with the T-DNA specific and the gene specific primers confirmed indicated the presence of T-DNA insertion in the *PRL1* gene. Sequencing of the amplified border junctions revealed that the T-DNA insertion occurred in intron 4. Below the schematic map of the *PRL1* gene, T-DNA sequences are marked with capital letters, whereas letters in lower case correspond to *PRL1* sequences. WT, wild type control, M: DNA size marker (λ-HindIII).

In case of *prl1-4* SALK_096289 allele, gene specific PRL1 ups and PRL1 3' primers failed to amplify a DNA fragment in line 21 indicating that this line was likely homozygous for the mutation (Figure 49). PCRs reactions performed with the PRL 3' and SALK LB primers verified the presence of the T-DNA insertion confirming that this line was homozygous, and showed that lines 9, 11 and 21 were heterozygous for the mutation. No PCR fragment was obtained with the right border specific PRL1 ups and FISH2 primers, which suggested that the right T-DNA border suffered a larger deletion. The

location of the T-DNA insertion was identified by sequencing of the border junctions and showed that the T-DNA was situated in the second intron of the *PRL1* gene.
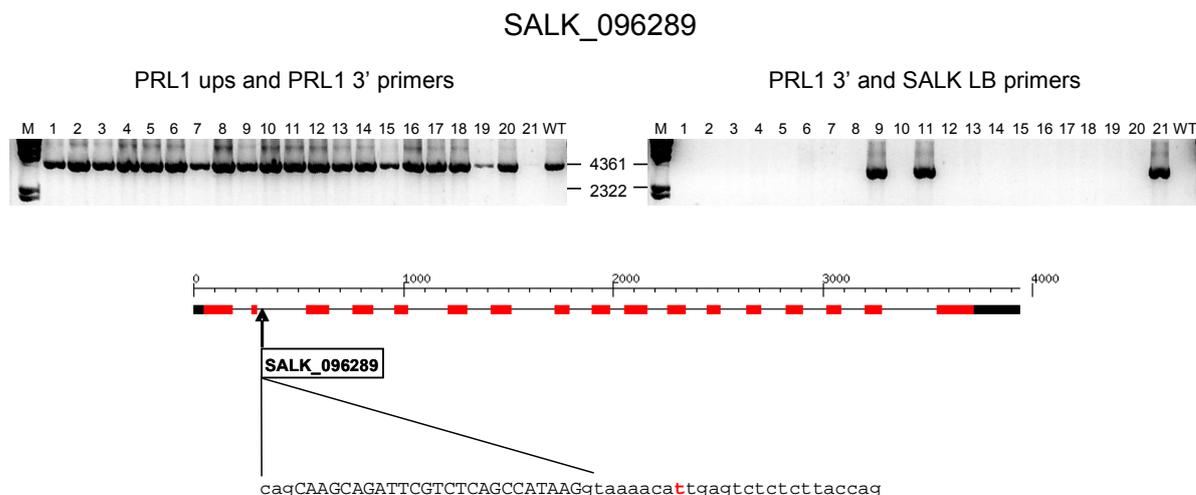
Figure 49.   PCR genotyping of the *prl1-4* SALK_096289 allele
From the SALK_096289 allele 21 M3 lines were analyzed by PCR reactions with the PRL1 ups and PRL1 3' gene specific primers, and the PRL1 3' and SALK LB primer combination. Line 21 was identified to be homozygous for the mutation. Sequencing of the amplified T-DNA junction indicated that the T-DNA was located in the second intron. Below: the schematic figure of the *PRL1* gene, T-DNA sequences are marked with capital letters, whereas letters in lower case letters indicate *PRL1* sequences. WT, wild type control, M: DNA size marker (λ-*Hind*III).

Phenotypic characterization of seedlings carrying the new *prl1* alleles

The phenotype caused by the new *prl1-2* to *prl1-4* mutant alleles was compared to that of originally isolated *prl1-1* mutant (Nemeth et al., 1998) by germination of homozygous M3 seeds in the presence of 0.1 and 0.2 μM ABA, 3 and 5% glucose, 5% sucrose and ethylene. In addition, root elongation of these mutants was analyzed by growing seedlings on vertically oriented MSAR agar plates containing 0.5% sucrose and measuring root length of 50 two weeks old seedlings in each case (Figure 50). The phenotype of all four newly isolated *prl1* alleles was indistinguishable from that of *prl1* under all conditions examined. Allelism tests performed by C. Koncz with all combinations of *prl1* mutant alleles also showed no change in the assayed *prl1* phenotypic traits.
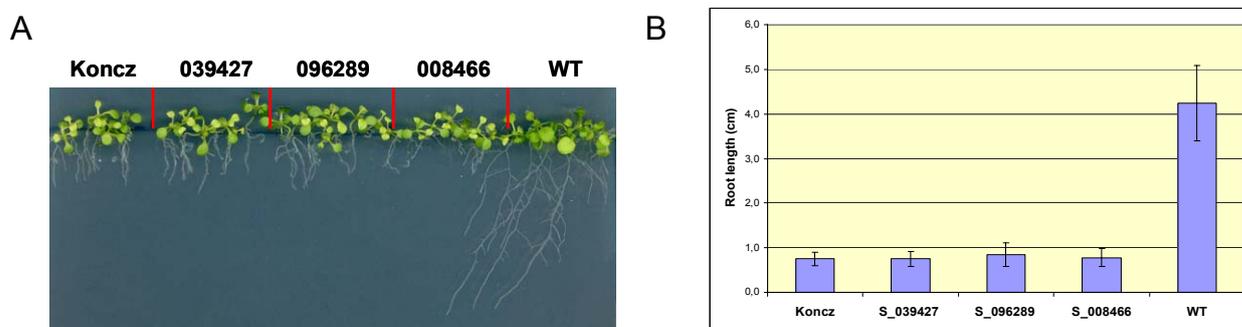
Figure 50.   Root elongation phenotype of seedlings carrying the *prl1-2* to *prl1-4* mutant alleles
(A) Seeds were germinated on vertically positioned MSAR agar plates containing 0.5% MSAR. (B) Root length of 50 individuals was measured two weeks after germination.

3.6.2. Isolation of *prl2* T-DNA insertion mutations

The *Arabidopsis* genome encodes a PRL1 homolog, PRL2. Similarly, other plant species examined carry two genes coding for potential PRL1 orthologs, which distinguishes them from all other eukaryotes (i.e., including budding and fission yeast, *Caenorhabditis elegans*, *Drosophila melanogaster*, mouse, rat and humans; Nemeth et al., 1998) that carry only a single gene for PRL1 ortholog. Although PRL1 and PRL2 carry divergent N-terminal sequences, their WD40 domains show very high level of sequence similarity. Inspection of transcript profiling data deposited in the Genevestigator database indicated that both *PRL1* and *PRL2* are expressed in most of the tissues (Figure 51). The highest *PRL2* mRNA levels were detected in pollen and cell suspensions, whereas *PRL2* transcript levels are lower in radicles, petals, sepals, and roots. In comparison, *PRL1* transcript levels were found to be the highest in callus and the shoot apex, and the lowest in the pollen.

Figure 51. **Comparison of *PRL1* and *PRL2* gene expression patterns based on microarray data in the Genevestigator database.**
Microarray expression data was obtained from the Genevestigator database to compare *PRL1* and *PRL2* mRNA levels in different plant organs. Dark blue colour indicates high expression level.

Albeit we did not detect any interaction between PRL2 and AtCDC5 in the yeast two-hybrid system, the fact that also only a weak interaction was detected between PRL1 and AtCDC5 suggested that this assay did not provide completely reliable data. Indeed, subsequently we found that the WD40-repeat domain of PRL1 interacts *in vivo* with AtCDC5. It is therefore plausible that PRL2, as PRL1, may interact through its WD40 domain with AtCDC5. If this is the case, PRL1 and PRL2 could perform at least partially overlapping functions in the CDC5-related pathways, whereas their N-terminal sequences may interact with different signalling factors. To generate genetic tools for further analysis of the PRL2 function, we have identified *prl2* T-DNA insertion mutants.

3.6.2.1. *PCR genotyping of the prl2-1 KONCZ16136 line*

Our mutant collection represented by super-pools with DNA templates from 4000 and 5000 plants was screened by PCR with *PRL2* gene specific primers to identify a P100 pool carrying T-DNA insertion in the *PRL2* gene (Rios et al., 2002, data not shown). From this P100 pool DNA was extracted from all individual lines to identify a line (Koncz16136-#4) hemizygous for the *prl2* mutation. 20 seedlings from the M2 progeny of this line were grown on selective medium and PCR genotyped with combinations of gene and T-DNA end specific primers (Figure 52). All lines examined were heterozygous for the *prl2* mutation suggesting that inactivation of the *PRL2* gene affects either male or

female transmission. Sequencing the insert junctions showed that the T-DNA tag was located in exon 9 of the *PRL2* gene and that the integration event caused a target site deletion of 51 bp.

Koncz #4

PRL2 5' and PRL2 3' primers

PRL2 5' and FISH1 primers

PRL2 3' and FISH1 primers

PRL2 Koncz #4

aatgctgggaAATCTACATGGATCAG   ACATGAAGCCATattaattactcttct
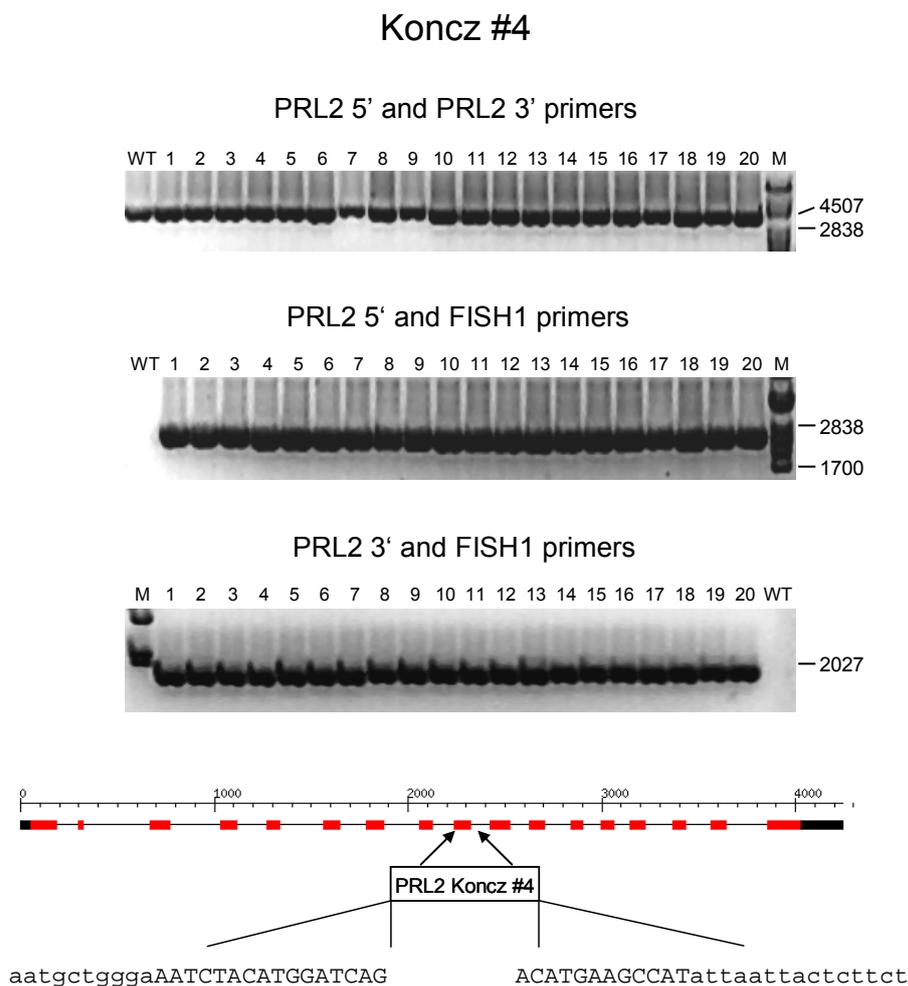
Figure 52.   PCR analysis of the *prl2-1* Koncz16136 (#4) mutant
20 M2 lines were analyzed by PCR amplification. All primer combinations resulted in PCR products, which suggested that there was no homozygous *prl2* mutant among these lines. Sequencing the amplified insert junctions revealed that the insertion was located in exon 9. Below: the schematic figure of the *PRL2* gene, T-DNA sequences are marked with capital letters, whereas letters in lower case indicate *PRL2* sequences. Sequences duplicated in the insert junction are underlined. WT, wild type control; M: DNA size marker (λ-*Pst*I and λ-*Hind*III).

3.6.2.2.   *PCR genotyping of the prl-2-2 GABI 228D02 mutant line*

A second mutant was isolated from the GABI-KAT collection and analyzed by PCR amplification (Figure 53). Using the gene specific primer combination PRL2 5' and PRL2 3' a PCR product was always detected. When PCR was performed with the T-DNA specific primer combinations, the right border primer failed to yield any PCR product, but with the PRL2 3' and left border specific FISH1 primers the insertion event was verified in the *PRL2* gene. Line 7 escaped selection and did not carry any T-DNA insertion. As in case of the *prl2-1* allele, this PCR screen did not yield either homozygous *prl2* mutant. Sequencing the left border junction of the insertion site showed that the T-DNA was located in the second intron of the gene.

GABI 228D02

PRL2 5' and PRL2 3' primers   PRL2 3' and FISH1 primers

GCTGATCCATgcttatcacttt
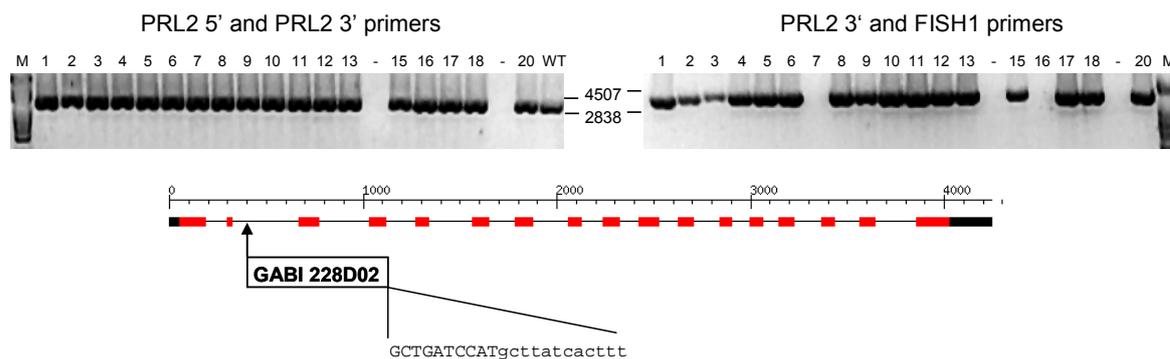
Figure 53.   **PCR analysis of *prl2-2* GABI 228D02 insertion line**
18 M2 plants were analyzed by PCR amplification. Gene specific primers PRL2 5' and PRL2 3' amplified a DNA fragment of expected size in each line indicating that these lines were not homozygous. The presence of the T-DNA insertion was confirmed by PCR amplification with the primer combination PRL2 3' and FISH1. Lines 7 and 16 did not carry any T-DNA. Below: the schematic figure of the *PRL2* gene, T-DNA sequences are marked with capital letters, whereas letters in lower case indicate *PRL2* sequences. WT, wild type control; M: DNA size marker (λ-*Pst*I).

prl2-1	HygR	HygS	PCR
#1	156	88	+/-
#2	73	32	+/-
#3	204	90	+/-
#4	108	43	+/-
#5	166	88	+/-
#6	81	40	+/-
#7	96	41	+/-
#8	145	79	+/-
#9	74	44	+/-
#10	110	51	+/-
#11	66	34	+/-
#12	84	45	+/-
#13	175	97	+/-
#14	157	77	+/-
#15	-	-	+/-
#16	178	81	+/-
#17	195	111	+/-
#18	166	83	+/-
#19	207	100	+/-
#20	169	99	+/-
Total	1397	727	

prl2-2	SuR	SuS	PCR
#1	172	79	+/-
#2	218	98	+/-
#3	131	59	+/-
#4	109	56	+/-
#5	78	37	+/-
#6	189	82	+/-
#7	76	45	-
#8	148	61	+/-
#9	121	66	+/-
#10	68	37	+/-
#11	169	68	+/-
#12	93	49	+/-
#13	175	80	+/-
#14	x	x	x
#15	135	61	+/-
#16	92	45	-
#17	111	41	+/-
#18	214	81	+/-
#19	x	x	x
#20	116	45	+/-
Total	2414	1090	

	χ^2	DF
Total	10,373	19
All	0,165	1
Homogeneity	10,208	18
P=	93%	for 2:1

	χ^2	DF
Total	18,779	18
All	7,812	1
Homogeneity	10,96	17
P=	89%	for 2:1

Table 2. Segregation analysis of *prl2* mutant lines
Seed from each PRC analyzed *prl2-1* and *prl2-2* M2 family was germinated on selective MSAR plates and the ratio of resistant versus sensitive seedlings was determined. Hyg: Hygromycin, Su: Sulfadiazine, R: resistant, S: sensitive.

3.6.2.3. Segregation analysis of prl2-1 and prl2-2 mutants

To determine the segregation of T-DNA encoded selectable marker genes, seeds of PCR genotyped M2 lines were germinated on hygromycin (*prl2-1*) or sulfadiazine (*prl2-2*) containing MSAR agar plates (Table 2). Both *prl2-1/+* and *prl2-2/+* mutant lines showed 2:1 segregation ratio indicating that plants homozygous for *prl2* mutations were non-viable. Examination of siliques of hygromycin and sulfadiazine resistant plants transferred into soil from each M2 families revealed segregation of albino and aborted embryos suggesting a possible embryo-lethal phenotype for both *prl2* mutations. Further characterization of this phenotype may help to better understand the function of *PRL2* gene.

3.6.3. Generation of *prl1* double mutants with mutations in genes coding for putative PRL1 interacting partners

As described in section 3.5.6, K. Salchert (1997) in our laboratory has previously identified 13 putative PRL1-interacting partners (PIPs), most of which showed interaction with the N-terminus of the PRL1 protein in yeast two-hybrid screens. All putative PRL1 interacting partners (PIPs) showed also specific interaction with PRL1 in protein-binding assays *in vitro*. Nonetheless, due to reasons discussed in section 3.5.6, we failed to confirm interaction *in vivo* between PRL1 and some of the PIPs tested. To develop resources for exploring possible genetic interactions (i.e., synthetic lethality or suppression) between the *prl1* mutation and mutations affecting the PIP coding genes, C. Koncz and S. Schaefer have identified multiple T-DNA insertion mutant alleles of all *PIP* genes. In this thesis work, we initiated the construction of *prl1* double mutants with mutations affecting the PIPs listed in Table 3. The location of these *PIP* genes in *Arabidopsis* chromosomes is shown in Figure 54. In crosses with the *pip* mutants, we used either the *prl1-1* or *prl1-2* mutants (Table 4) in order to take advantage of the T-DNA encoded selectable markers in selection for the presence of at least one of the combined mutations.

PRL2	At3g16650	PRL1 homolog
PIP-A	At5g19900	Unknown protein
PIP-C	At5g58720	Unknown protein
PIP-D	At3g50530	Putative calcium dependent protein kinase
PIP-E	At1g69830	Alpha-amylase-like protein
PIP-F	At4g01480	Putative inorganic pyrophosphatase
PIP-H	At4g29510	Protein arginine N-methyltransferase
PIP-I	At5g07360	Amidase family protein
PIP-K	At4g15420	Ubiquitin fusion degradation protein UFD1
PIP-L	At1g15730	Cobalamin synthesis protein-like
CBP20	At5g44200	Cap binding protein 20 (mRNA binding factor)

Table 3. List of PIP genes, in which insertion mutations were isolated and used in crosses with the *prl1* mutant.
A mutation in the *CBP20* gene, encoding the 20 kDa subunit of the mRNA CAP-binding complex, causes ABA hypersensitivity similarly to the *prl1* mutation (Papp et al., 2004). Therefore, crosses were also performed to test potential genetic interaction between *cbp20* and *prl1*.
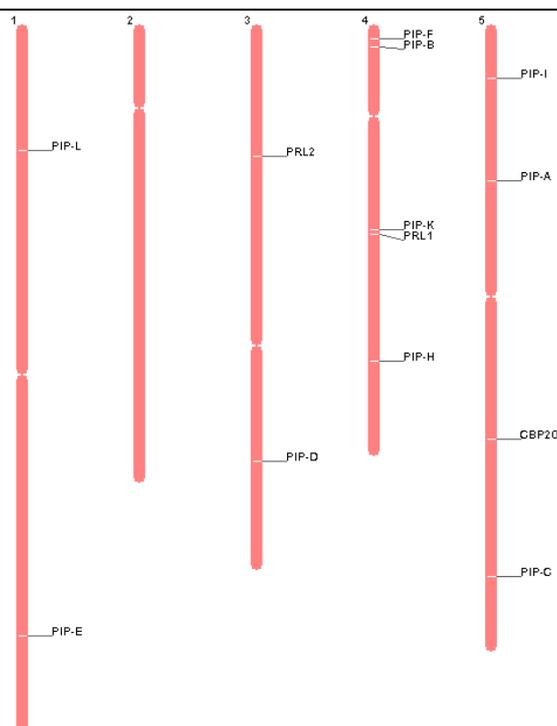
Figure 54.   Map positions of *PIP* genes in the *Arabidopsis* chromosomes
The figure was generated using the Chromosome Map Tool of Tair (http://www.arabidopsis.org).

♀	♂	Status
1. *prl1-1*	x *prl2-2*	Discarded, no *prl2* insertion
2. *prl1-2*	x *prl2-1*	*prl1/prl1 PRL2/prl2*
3. *prl1-1*	x *pip-a* GABI 197C07	Homozygous double mutants
4. *pip-c* SALK_010773	*x prl1-1*	Homozygous double mutants
5. *pip-c* SALK_039094	*x prl1-1*	Homozygous double mutants
6. *prl1-1*	x *pip-d* SAIL 586 H06	M2 did not germinate
7. *prl1-2*	x *pip-d* Koncz38225	Homozygous double mutants
8. *prl1-1*	x *pip-e* SAIL 613 D12	Homozygous double mutants
9. *pip-f* SALK_014647	*x prl1-1*	Pooled sample-further analysis
10. *prl1-1*	x *pip-f* SALK_014647	Not analyzed.
11. *prl1-2*	x *pip-h* KONCZ65425	Pooled sample-further analysis
12. *pip-i* SALK_000718	*x prl1-1*	Homozygous double mutants
13. *pip-i* SALK_011213	*x prl1-1*	Homozygous double mutants
14. *prl1-1*	x *pip-i* GABI 160C01	Homozygous double mutants
15. *prl1-1*	x *pip-i* Wisc446.659-3	Homozygous double mutants
16. *prl1-1*	x *pip-k* SAIL 1284 G09	Pooled sample-further analysis
17. *prl1-2*	x *pip-k* Koncz77621	Homozygous double mutants
18. *prl1-1*	x *pip-k* SAIL 1053 H01	Heterozygous *prl1/prl1 PIP-K/pip-k*
19. *pip-l* SALK_037227	*x prl1-1*	Homozygous double mutants
20. *prl1* SALK_008466	x *pip-l* Koncz 22893	Homozygous double mutants
21. *prl1-2* 0	x *cpb20* Koncz 372	Homozygous double mutants

Table 4. List of crosses performed between *prl1* and *pip* mutants
Current status of double mutant analyses is indicated in the third column.

In all insertion mutants derived from the SALK collection, we observed silencing of the selectable kanamycin resistance marker gene. From each cross, 10 F1 families were grown to produce F2 seeds. From 5 independent F2 families, 20 individuals selected in antibiotics containing media (if it was possible) were grown in soil for collecting DNA samples. When it was possible, only F2 plants selected for the short root phenotype of *prl1* were genotyped for the combined second mutation. The *PIP-F*, *PIP-H* and *PIP-K* genes are located in the same chromosome as *PRL1,* which made the isolation of homozygous double mutants more difficult. From these crosses 100 M3 lines were analyzed. The collected plant material was pooled (10 independent lines in each pool) and analyzed by PCR. The *pip-f, pip-h* and *pip-k* T-DNA insertions were detected in the pooled DNA samples and these pools are now being further analyzed to identify individual lines containing the combined mutations. All thus far identified homozygous double mutants showed the characteristic *prl1* root elongation defect indicating that PIPs do not affect pathways controlling root elongation. Further ongoing assays aim to reveal whether any of the *pip* mutations affect glucose and hormone hypersensitivity responses caused by the *prl1* mutation.

3.6.4. Isolation of point mutations in the *PRL1* coding region

The yeast two hybrid and *in vitro* protein interaction assays performed by K. Salchert (1997) indicated that PIP-C, PIP-F, PIP-H, PIP-K, PIP-M and the two SnRK1 α subunits AKIN10 and AKIN11 bound to N-terminal sequences of PRL1. By contrast, PIP-A, PIP-B, PIP-D, PIP-E, PIP-G, PIP-I and PIP-L were found to interact with C-terminal PRL1 sequences downstream of the sixth WD40-repeat. Computer-based structure predictions suggested that the N- and C-terminal ends form a rod-like structure sticking out from the cone-like WD40 repeat domain. To search for point mutations causing amino acid exchanges in the N-terminus of PRL1 and thereby possible alteration of interactions with PIPs, we have screened by TILLING for EMS-induced mutations and developed a site-specific mutagenesis approach.

3.6.4.1. Screening for EMS-induced point mutations by TILLING

A large population of ethylmethanesulfonate (EMS) mutagenised *Arabidopsis* plants was screened to identify point mutations in the *PRL1* gene using TILLING (Targeting Induced Local Lesions in Genomes) technology and facilities provided by *Arabidopsis* TILLING project (ATP, http://tilling.fhcrc.org:9366; Till *et al.* 2003). K. Berendzen from our laboratory designed screening primers for point mutations in *PRL1* sequences encoding the N-terminal domain. 23 point mutations were found in this screen. From these EMS mutations, 12 was located in non-coding intron regions, 3 substitutions did not result in amino acid changes, but in 8 lines the sequenced nucleotide mutations induced amino acid exchanges (Table 5). M2 seeds of TILLING lines were germinated on MSAR plates to search for *prl1*-like phenotypic traits, including short root and serrated leaf. The CS87948 TILLING line, which carried a P22S mutation, segregated 104 wild type and 24 albino plants. Line CS93156 carrying a S33L substitutions showed wild type phenotype. Line CS93711 line, containing a

P58S substitution, showed a segregation of 21 wild type plants, 3 plants with shorter roots and 8 albinos.

	Line	Nucleotide	Effect	Genotype
1.	CS87948	C115T	P22S	hetero
2.	CS93156	C149T	S33L	hetero
3.	CS90002	C168T	L39=	homo
4.	CS93711	C223T	P58S	homo
5.	CS89680	C231T	D60=	hetero
6.	CS93970	G244A	Intron	hetero
7.	CS94048	C258T	Intron	homo
8.	CS89522	G302A	Intron	hetero
9.	CS87940	C454T	Intron	hetero
10.	CS89552	C487T	Intron	hetero
11.	CS87753	C508T	Intron	hetero
12.	CS89433	C509T	Intron	hetero
13.	CS88580	G522A	Intron	hetero
14.	CS92210	G525A	Intron	homo
15.	CS91910	G613A	G77E	homo
16.	CS92359	G613A	G77E	hetero
17.	CS86130	C625T	P81L	hetero
18.	CS93235	G727A	Intron	hetero
19.	CS88592	G780A	Intron	homo
20.	CS85391	G825A	G110R	homo
21.	CS93290	G833A	K112=	hetero
22.	CS86061	C900T	P135S	hetero
23.	CS88018	G933A	Intron	hetero

Table 5. Identification of EMS-induced mutations in the 5' coding region of the *PRL1* gene by TILLING.
EMS mutagenized lines were screened for point mutations affecting the N-terminal sequences of PRL1. The nucleotide substitutions were confirmed by DNA sequencing and the genotype of identified point mutants is indicated.

Line CS92359 harbouring G77E substitution showed a segregation of 48 wild type plants and 8 plants with short roots, but showing normal leaf morphology. In the M2 progeny of line CS86130, which carried a P81L substitution, 56 wild type seedlings and 11 plants with shorter roots were observed. Finally, line CS86061 (P135S substitution) segregated 43 wild type, 11 albino, 2 pale seedlings and 5 plants with shorter roots. As the root elongation defect appeared to be frequently observed in the TILLING lines, further analysis of these mutations in allelism assays with *prl1* is necessary. In case of line CS92359 (which proved to be identical to line CS91910, which carried a mutation causing G77E exchange in homozygous form), we performed a direct assay to test whether the identified mutation caused indeed the observed short root phenotype. This mutation was introduced into pPCV002-PRL1-HA by site-specific mutagenesis and tested in genetic complementation experiment performed with the *prl1-1* mutant. Briefly, site-directed mutagenesis was performed on pBS-PRL1-HA template DNA using the G77E and NotI primers (2.1.6.3). The presence of mutation was confirmed by DNA sequencing and then the *Xba*I-*Xma*I *PRL1* genomic fragment was subcloned into the pPCV002 vector. This construct was transferred to *Agrobacterium* GV3101(pMP90RK) and transformed into the *prl1*

mutant. The phenotype of six transformed T1 plants was analyzed after germination on selective plates containing kanamycin and all of them showed wild type phenotype (Figure 55). The expression of the PRL1-HA protein in the first three transgenic lines was confirmed by immunodetection using anti-HA antibody (data not shown). This result clearly indicated that the G77E point mutation does not affect the PRL1 function and thus provided a warning example for avoiding direct phenotypic analysis of TILLING lines, instead of performing allelism tests. As confirmation, germination of line CS91910 that was received later and carried the G77E mutation in homozygous form yielded only wild type plants.
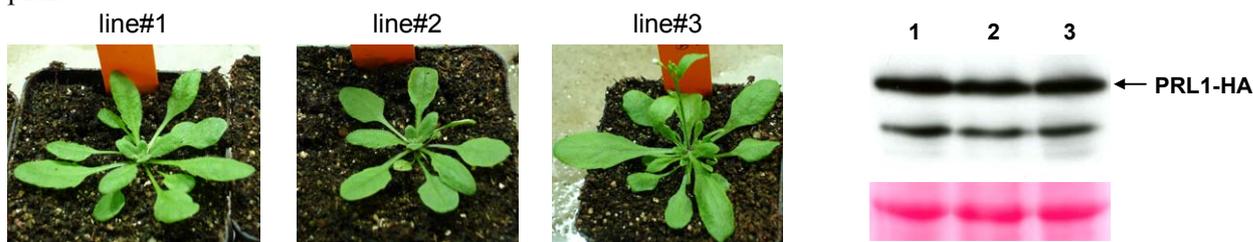
Figure 55.   Genetic complementation assays with G77E mutation
Point mutation causing G77E substitution in PRL1 was introduced into the PRL1::PRL1genomic-HA construct by site-specific mutagenesis and assayed in genetic complementation test with the *prl1-1* mutant. The phenotypes of the soil-grown transgenic plants are shown. Expression of the modified PRL1-HA(G77E) protein was detected by Western blotting using anti-HA antibody.

3.6.4.2.   *Site-directed mutagenesis of the PRL1 gene*

As an alternative approach to genetic mapping functionally important domains in the N- and C-terminal extensions flanking the WD40-repeats of PRL1 protein, we performed a site-directed alanine scanning mutagenesis experiment. Design of the mutagenesis experiment was based on previous two dimensional modelling of the PRL1 protein structure. Residues that were predicted to play a potential role (such as prolines) in determination of protein structure were not targeted by the mutagenesis. The list of point mutations generated is shown in Table 6. Mutagenesis was performed using the Transformer™ site-directed mutagenesis kit with different Mut primers in combination with the NotI primer on pBS-PRL1-HA (2.1.6.4). The mutations were verified by sequencing, and then an *Xba*I-*Xma*I fragment of pBS-PRL1-HA carrying the modified *PRL1-HA* gene was inserted into *Xba*I-*Xma*I sites of pPCV002 vector. Subsequently, *prl1* mutant plants were transformed with these constructs and the phenotype of T1 transgenic plants was analyzed for complementation of the *prl1* root elongation defect. Site-directed mutagenesis failed so far with the Mut26 and Mut29 primers. The Mut2 primer contained originally three mutations but the only mutation causing a single amino acid exchange was recovered. In summary, this experiment generated 28 modified PRL1 sequences, which carried 53 point mutations, and for each modified *PRL1* construct 20 independent T1 plants were analyzed. Although the success of the genetic complementation experiment was clearly dependent on the expression level and stability of mutagenized versions of the PRL1 protein, the majority of T1 plants obtained by transformation of the *prl1* mutant with all 28 modified *PRL1* genes showed wild type root elongation. This suggested that the N- and C-terminal extensions of the PRL1 protein do not play a

role in the control of this phenotypic trait of the *prl1* mutant. Whether these site specific mutations affect other phenotypic traits, such as hypersensitivity to ABA, is being clarified by ongoing experiments.

Line	Mutation	Line	Mutation	Line	Mutation
Mut1	E7A, E9A, E12A	Mut11	R49A, S51A	Mut21	Q97A, K98A
Mut2	P10A	Mut12	H52A, K53A	Mut22	E102A, S103A
Mut3	K17A, K18A	Mut13	K55A, F58A	Mut23	S125A, S126A
Mut4	K22A, K25A	Mut14	E62A, S66A	Mut24	K128A, S129A
Mut5	S20A, S23A	Mut15	R70A, Q71A	Mut25	S138A, S139A
Mut6	R26A, S27A	Mut16	D73A. R74A	Mut26	E465A, D466A, E467A
Mut7	E29A, S32A	Mut17	E77A, Q78A	Mut27	E472A, H474A
Mut8	P33A	Mut18	S82A, S86A	Mut28	K478A
Mut9	H35A, Q35A	Mut19	E91A, S93A	Mut29	K481A, E482A
Mut10	D42A, E44A	Mut20	K94A, S95A	Mut30	R484A, R485A

Table 6. Site-directed mutagenesis of the *PRL1* gene
List of mutagenesis primers used and amino acid exchanges generated in site-directed alanine-scanning mutagenesis of the *PRL1* gene.

The results of site-specific mutagenesis experiment also suggested that the cell elongation and polarity-related defects observed in *prl1* roots (Figure 56) may be primarily related to the function and interacting partners of PRL1 WD40-repeats.
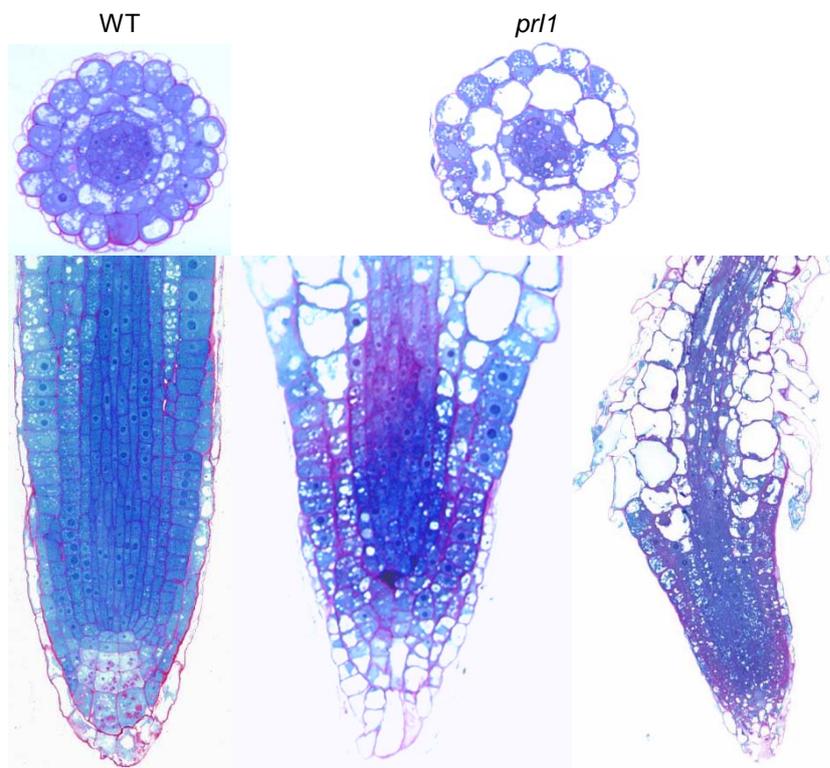
Figure 56.   Cytological analysis of prl1 root structure
The root structure of the *prl1* mutant was investigated collaboration with J. Jásik. Longitudinal cross sections of roots were prepared from five days old wild type and *prl1* plants after embedding in PEG. Although all basic layers of the root structure are present in *prl1*, the well conserved organization of linear cell files is largely disturbed. Serious polarity and elongation defects are observed in cells of the elongation zone, the cortex and the endodermis cells are swollen and highly vacuolized. The diameter of central cylinder is reduced in *prl1*. Furthermore, *prl1* displays ectopic root hair development due to mispositioning of trichoblast mother cells.

Interaction of the PRL1 WD-40 repeat region with AtCDC5 and functional conservation of CDC5 in eukaryotes suggested that the loss of PRL1 from the AtCDC5 complex in the *prl1* mutant could cause cell cycle-related defects in addition to influencing potentially spliceosome-assembly or splicing related functions. In fact, recent microarray profiling experiments performed by G. Molnar and others in our laboratory indicated that a gene encoding cyclin B1;1, which is involved in the control of G2/M transition, is upregulated in the *prl1* mutant. In order to confirm this observation, we have introduced a CycB1;1::GUS reporter gene (Ferreira et al., 1994) into the *prl1-1* mutant and monitored its activity by histochemical GUS assay (Figure 57).
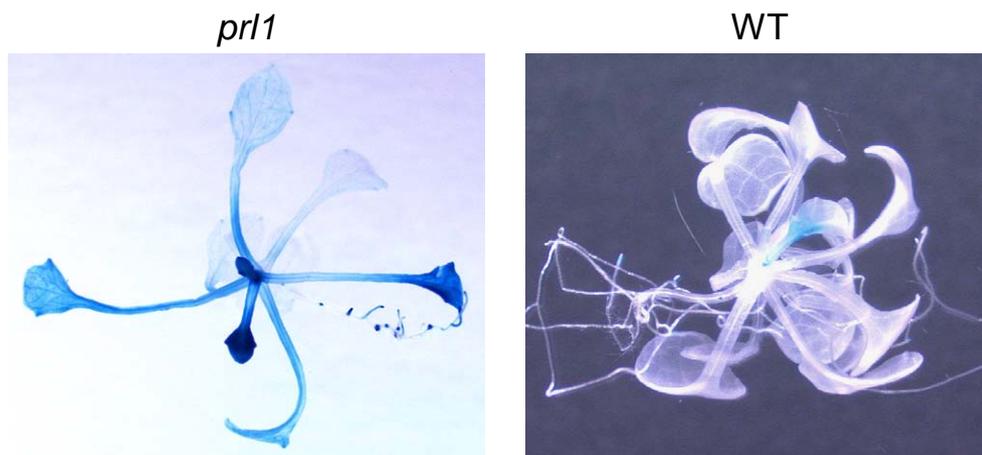
Figure 57.   **Histochemical staining of *prl1* and wild type plants carrying the CycB1;1::GUS reporter gene.**
Wild type and *prl1* seedlings grown in MSAR medium for 2 weeks were stained with X-Gluc to monitor the expression of GUS reporter enzyme encoded by the *CycB1;1::GUS* gene.

As compared to wild type plants, in which CycB1;1::GUS expression was only observed in root tips, the *prl1* mutant displayed overall activation of cyclin B1;1 gene in rosette leaves and other organs of 2 weeks old seedlings tested in this experiment. Together with the PRL1-AtCDC5 protein interaction data, this experiment directs attention to future analysis of potential functions of PRL1 and AtCDC5 in the regulation of cell cycle and polarity.

4. DISCUSSION

4.1. <u>Characterization of PRL1 gene expression</u>

Our studies, focusing on functional characterization of the *Arabidopsis PRL1* gene and its nuclear WD40 protein product, were initiated by the analysis of temporal and spatial expression pattern of *PRL1* using reporter constructs. A *PRL1* promoter fragment containing a 3.5 kb upstream regulatory region, the 5' UTR, and the first two exons and introns was fused to the *GUS* reporter gene in frame with the third *PRL1* exon. Histochemical analysis of the *GUS* expression pattern revealed that the *PRL1* promoter is active in most tissues. The *PRL1::GUS* reporter showed the highest activities in shoot and root apical meristems and emerging lateral meristems. However, young hypocotyls and leaf primordia were also stained robustly, although during further development *PRL1::GUS* expression became more restricted to the vascular tissues. The strong meristematic activity of the *PRL1::GUS* reporter underlies a potential *PRL1* function in cell division or in cell elongation. Such a function is also suggested by the *prl1* mutant phenotype, as mutant plants have characteristic short roots and the elongation of hypocotyl cells are also inhibited.

Further characterization of subcellular localization and expression pattern of the PRL1 protein was performed using indirect immunofluorescence microscopy in collaboration with Dr. J. Jásik. In these experiments, a genomic construct driven by the native *PRL1* promoter was labelled with HA epitope coding sequences, and its expression was studied in *prl1* mutant plants. PRL1-HA signal is predominantly detected in the nucleus; specifically in the nucleoplasm, but not in the nucleolus. Chromosomes were identified by specific DAPI staining and their localization was compared to the PRL1-HA subcellular pattern showing that PRL1 is not a chromatin-associated protein during mitosis.

A third approach focused on the analysis of localization of *PRL1::PRL1-GFP* expression in transgenic plants *in vivo* using confocal laser scanning microscopy in collaboration with Dr. E. Schmelzer. The observed localization pattern of the PRL1-GFP reporter further validates that PRL1 is a nuclear protein, although significantly lower levels of GFP signal was also detected in the cytoplasm. This data was verified later by biochemical studies, in which nuclear and cytoplasmic protein fractions were prepared from plants and cell suspension, and low amount of PRL1 was also shown to be present in the cytoplasmic fractions by immunodetection experiments. The cellular localization experiments showed that PRL1-GFP is expressed in all cell types analyzed. This data explains why the native PRL1 (Nemeth et al. 1998) and PRL::PRL1-HA proteins were detected in all plant organs by western blotting and postulates a general role for PRL1 that is necessary in most *Arabidopsis* cell types. In particular, high level expression of PRL1-GFP in meristematic tissues and leaf primordia strongly suggests a possible role for PRL1 in the regulation of cell cycle and/or cell elongation.

4.2.   *PRL1* gene expression is regulated by intragenic regions

Previous experiments performed by J. Jásik indicated that *PRL1* promoter sequences located 5'-upstream of the ATG codon are not sufficient to drive transcription of reporter constructs in plants. Nemeth et al. (1998) showed that a 7.9 kb genomic fragment containing 3.5 kb upstream sequence and the coding region contained all sequences necessary for genetic complementation of the *prl1* mutation. We have observed that a *PRL1* gene segment carrying only 62 bp upstream of the ATG codon of a full-length coding region cloned in the estradiol-inducible expression vector pER8 was also sufficient to complement the *prl1* mutant phenotype and conferred high levels of protein expression even in the absence of estradiol induction. In order to examine the stringency of estradiol inducibility of the pER8 vector, we tested the regulation of a control pER8-*GUS* reporter gene construct. Histochemical analyses detected GUS activities only estradiol-treated plants indicating that the observed activity of 5'-truncated *PRL1* gene was not due to leaky regulation of transcription by the estradiol-inducible promoter of pER8. Another control experiment showed that expression of *PRL1* cDNA controlled by the estradiol inducible pER8 vector was insufficient for complementation of the *prl1* mutation and synthesis of the PRL1 protein in the absence of estradiol induction. These results clearly indicated that an extremely short upstream promoter region containing a TATA-box consensus and transcription initiation sequences are required for proper transcriptional regulation of *PRL1* gene. This conclusion was also supported by the observation that a T-DNA insertion identified in the *prl1-5* SAIL-1276G04 allele at position -85 bp from the *PRL1* ATG codon did not result in *prl1* mutant phenotype.

A series of promoter deletion constructs was generated in order to identify the essential transcription regulatory region in the 5'-coding region of the *PRL1* gene by monitoring the expression of *GUS* reporter in cultured cells and plants. GUS activity was detected when the 3.5 kb full length promoter was linked to the first two exons and introns, as well as when a short promoter sequence between position -62 and the ATG codon was linked to the first two exons and introns of the coding region. *GUS* expression diminished when the reporter gene was linked to the 3.5 kb *PRL1* promoter terminating at the ATG, and also when sequences of the second intron were removed from the short promoter (i.e. extending from position -62 to the second exon). These experiments proved that promoter sequences located upstream of the ATG codon are not sufficient for the *PRL1* gene expression and that essential transcription regulatory elements are located in a 300 bp intragenic region carrying the second intron and short sequences from the second and third exons. The presence of essential transcription regulatory sequences in the coding region is not a unique property of the *PRL1* gene, but appears to be rather common in other genes of *Arabidopsis* and different plant species. For example, expression the *AGAMOUS* (*AG*) floral homeotic gene is restricted to the inner two whorls of the flower and regulated by positive and negative transcription factors that bind to the 3 kb second intron of *AG* (Sieburth and Meyerowitz, 1997, Busch et al., 1999, Deyholos and Sieburth, 2000). Comparative analysis of expression patterns of *GUS* reporters driven by *PRL1* promoters carrying or lacking sequences 5'-upstream of position -62 show that the intragenic regulatory sequences are also fully sufficient for proper tissue specific expression of *PRL1*. Short promoter

driven *GUS* gene construct displays thus the same expression pattern as reporter constructs driven by the long promoter, both showing especially high activities in the apical and lateral meristems. Nonetheless, somewhat lower activity of the short promoter suggests that sequences located 5'-upstream of position -62 contain enhancer elements that quantitatively regulate *PRL1* transcription.

Sequence analysis of the intragenic promoter region suggested that TC-repeats present in the 5' UTR and the second intron might be important in the control of transcription. In the CaMV35S promoter sequence downstream of the transcription initiation site a CT-rich region was reported to act as an enhancer (Pauli et al., 2004). Specific binding factors for the TC/GA repeat were initially identified in *Drosophila* (Farkas et al., 1994), but found later also in *Arabidopsis*. These factors are represented by the *BASIC PENTACYSTEINE* (*BPC*) protein in *Arabidopsis* (Meister et al., 2004; Kooiker et al., 2005) and the barley b recombinant (BBR) protein in barley (Santi et al., 2003). However, removal of these sequences did not result in dramatic changes in the activity of *PRL1* promoter.

Regulatory importance of the second intron was also confirmed by genetic complementation assays performed with the *prl1* mutant. Constructs carrying the full-length coding region of 3.7 kb in fusion with either the 5'-upstream promoter region of 3.5 kb or only the short promoter extending from position -62 complemented the *prl1* mutant equally well. Similarly, the full-length (i.e., 3.5 kb) promoter and the genomic sequence carrying the first two exons and introns fused in frame with exon 3 sequences of the *PRL1* cDNA was sufficient to complement the *prl1* mutation. However, the *prl1* phenotype was not complemented by a *PRL1* cDNA construct that carried only 5'-upstream promoter sequences terminating at the ATG codon. These data verified that in the absence of intragenic regulatory sequences the *PRL1* promoter region located 5'-upstream of the ATG codon can drive only low level of transcription. The results based on monitoring GUS reporter enzyme activities conferred by the different promoter constructs were faithfully confirmed by the analysis of expression levels of PRL1-HA protein in the complemented *prl1* mutant lines. Whereas all complemented *prl1* lines expressed comparable amounts of the PRL1-HA protein, lines showing no complementation contained significantly lower amounts of PRL1-HA protein. Genetic complementation of the *prl1* mutation appeared to require a critical threshold of PRL1-HA expression, as it was observed in overexpression experiments of PRL1-cDNA-HA controlled by the estradiol-inducible pER8 vector.

Studies of *PRL1* promoter deletion constructs clearly indicated that important transcription regulatory sequences are located in the area of the second intron, including short sequence elements from the second and third exons. These sequences were analyzed by the PlantCARE program (Lescot et al., 2002) in order to identify putative plant transcription factor binding sites. However, transcription factors suggested by the PlantCare program showed completely different expression patterns, as indicated by subsequent analysis of microarray databases, than the *PRL1* gene. Therefore, we decided to perform a yeast one-hybrid experiment to search for transcription factors that bind to intragenic regulatory sequences of *PRL1* intron 2 region. In this screen, a plant specific regulator *AtNAM* (*NO APICAL MERISTEM*, At1g52880) was identified. *AtNAM* belongs to the NAC (N̲AM, A̲TAF1/2,

CUC2) family of transcription factors. The protein carries a highly conserved DNA-binding domain at the N-terminus and a trans-activation domain at the C-terminus. The target sequence of AtNAM was identified in the CaMV35S promoter (Duval et al., 2002), and we found that two potential AtNAM binding sites are present in the third exon of the *PRL1* coding region. We have analyzed the regulation of *AtNAM* transcription in the Genevestigator database and compared these data with the Northern blot data of Duval et al. (2002). A negative correlation was detected between *AtNAM* and *PRL1* expression suggesting that *AtNAM* could be a possible repressor of *PRL1* promoter activity. However, we argued that the predicted AtNAM-binding site in exon 3, if indeed targeted by AtNAM, is also present in the cDNA, which did not confer genetic complementation of the *prl1* mutation in the absence of other transcription regulatory sequences located in the first and second exons and introns. Alternatively, potential negative exonic regulation could also be proposed, however this would not explain the behaviour of the studied promoter deletion constructs. Clearly, further analysis of this question is required. Preferably, a new yeast one-hybrid screen should be performed using a Gal4-activation domain library representing transcripts from different organs. In addition, the 300 bp intron 2-centered intragenic regulatory region must be further resolved to precisely map the binding site of AtNAM and confirm its possible role in regulation of *PRL1* transcription.

In order to identify the cell layers where *PRL1* is active in the apical meristem, a misexpression approach was carried out using the genetic complementation test with the *prl1* mutant. *PRL1* expression was targeted either to the entire shoot apical meristem (SAM) by the *AtKNAT1* and *AtSTM* promoters or to a specific region of SAM by the *AtUFO* promoter. Using the promoter of *ASYMMETRIC LEAF 1* (*AtAS1*) *PRL1* was expressed in leaf primordia. As controls, the phloem companion cell specific *AtSUC2*, the xylem specific *At4CL1*, and the root central cylinder specific *TobRB7* promoters were used and both *PRL1* genomic and cDNA constructs were introduced under the control of these promoters into *prl1* mutant plants. As the *PRL1* genomic fragment carries the short promoter region with all essential intragenic regulatory elements, all promoter constructs tested complemented the *prl1* mutant probably due to *PRL1*-specific regulation of gene expression. However, in case of the cDNA constructs only the *AtSUC2* and *AtAS1* driven PRL1 expression resulted in complementation of the leaf phenotype of the *prl1* mutant. On the other hand, none of the heterologous promoter driven cDNA constructs restored the root elongation defect of the *prl1* mutant. These data suggest that during leaf development *PRL1* probably does not function in the shoot apical meristem, but rather in the leaf primordia and vascular meristem or differentiating phloem. The *AtSUC2* gene encodes a sucrose-H^+ symporter. The *AtSUC2* promoter activity pattern was characterized using *GUS* reporter gene fusions (Truernit and Sauer 1995) and localized to the phloem vessels throughout the entire plant from the roots to developing fruits. Restoration of *prl1* serrated leaf phenotype to wild type by the *AtSUC2-PRL1* cDNA construct suggests that *PRL1* may have a function in the phloem in leaves, but not in the roots. The *prl1* leaf phenotype was also converted to wild type by the *AS1* promoter driven cDNA construct. *AS1* encodes a Myb family transcription factor and acts as a negative regulator of homeotic genes, such as *KNAT1* and *STM* in leaf primordia (for review see

Bowman and Eshed, 2000; Baurle and Laux, 2003). *In situ* hybridization of *AS1* during embryo development showed that AS1 is predominantly expressed in leaf primordia (Byrne et al 2000). RNA hybridization data indicate that *AS1* is preferentially transcribed in young and immature plant tissues, including roots, stems, leaves, flowers and siliques; whereas fully developed rosette and cauline leaves shows low *AS1* expression (Sun et al., 2001). Complementation of the *prl1* leaf phenotype by the AtAS1-PRL1 cDNA construct suggests a potential role for *PRL1* during early leaf development. In general, data of the *PRL1* misexpression experiment also indicate that the PRL1 protein signal is not transmittable between plant organs and cells. The failure of complementation in case of *AtSTM* and *AtUFO* promoter driven constructs may be due to the very low expression levels of *PRL1*, which is probably below the threshold seen in analysis of *PRL1* promoter deletion constructs. However, plants expressing PRL1 from the *AtKNAT1* promoter construct displayed *prl1* mutant phenotype despite high levels of PRL1 expression.

4.3. PRL1 protein is a potential proteasome substrate

Comparison of regulation of PRL1 mRNA and protein levels in different plant organs indicated that while the amount of *PRL1* mRNA is relatively constant in the plant organs, the PRL1 protein levels show a remarkable variation. We noted that the PRL1 protein is present at high levels in dividing and developing organs, such as roots and flowers, whereas mature rosette and cauline leaves contained very low levels of PRL1 protein. These data suggested that the PRL1 protein levels may be differentially regulated in diverse plant organs by a posttranscriptional or posttranslational mechanism.

The stability of PRL1 protein was tested using an estradiol-inducible pER8-*PRL1-HA* cDNA construct. After inducing the transcription of *PRL1-HA* cDNA by estradiol, the inducer was removed and the stability of PRL1-HA protein was monitored in various time points during 96 h. In this experiment a linear decrease was detected in the PRL1-HA protein level, and the half life of PRL1-HA protein was estimated approximately 8 h. This indicated that the PRL1 protein is probably not extremely unstable, although continued translation of the *PRL1-HA* mRNA after blocking transcription by the removal of estradiol was not prevented in this experiment. Also, this experiment was performed by expressing the PRL1-HA protein in the *prl1* mutant hence there was a possible selection for synthesis of functional PRL1 protein.

To examine whether the stability of the PRL1 protein is regulated through proteasomal degradation, we examined the effect of the reversible proteasome inhibitor MG132 in two independent experiments. First, we induced the transcription of an estradiol-inducible *PRL1-HA* expression construct in the *prl1* mutant background in the presence and absence of MG132 and found that MG132 enhances the accumulation of the PRL1 protein. However, this result could well be criticized, if the degradation of PRL1 protein was induced by its overproduction. Therefore, in a second experiment, we expressed the PRL1-HA protein from a construct, which was transcribed by the native *PRL1* promoter in cultured cells, and we blocked translation of the *PRL1-HA* mRNA using cycloheximide treatment in the presence or absence of proteasome inhibitor MG132. In the

cycloheximide treated samples, the PRL1-HA protein showed the previously observed slow degradation, whereas in the MG132 treated samples the protein remained stable throughout 48 to 72 h.

MG132 is a known blocking agent of the cell cycle (Planchais et al., 2000). Based on preferential expression of *PRL1* in meristematic tissues, we have hypothesized that degradation of PRL1 could be controlled in a cell cycle dependent fashion. Therefore, we examined the PRL1 protein sequence for potential motives, which could direct cell cycle dependent regulation of PRL1 degradation. We have found that the PRL1 carries in its N-terminal region upstream of the WD-40 repeats a perfect destruction box (D-box), which is known to be recognized by the anaphase promoting/cyclosome APC complex and its activators that are involved in the control of cell cycle progression from G2 to M phase (for reviews see: Vodermaier, 2004; Peters, 2002; Castro et al., 2005). In order to test a possible role of D-box in regulation of PRL1 protein stability, we have performed a site-specific mutagenesis experiment by exchanging two conserved amino acids of the D box motive in a GFP-tagged PRL1 construct and then examined the stability of this protein in cultured cells (i.e. in comparison to a wild type PRL1-GFP protein). In logarithmically growing cell culture, where the intrinsic PRL1 protein levels were constant, the levels of D-box mutant PRL1-GFP protein were significantly higher than those of the wild type PRL1-GFP protein suggesting that mutation of the D-box could stabilize PRL1 and hence PRL1 may be targeted to proteasomal degradation by the APC E3 ubiquitin ligase. The levels of both wild type and D-box mutant GFP-PRL1 proteins decreased significantly in cell suspension after two weeks. Cultured *Arabidopsis* cells reach a stationary phase after approximately seven days, thus upon two weeks without subculturing the cells stop dividing and enter a senescent phase accompanied by induction of cell death. As probably many other proteins, PRL1 is also quickly degraded in non-dividing senescent cell cultures. In contrast to actively dividing cultured cells, we observed no significant difference between the stabilities of wild type and D-box mutant PRL1-GFP proteins in seedlings. As in seedlings the proportion of actively dividing cells is rather low as compared to the proportion of differentiated cells, the changes in the stability of wild type and D-box mutant GFP-PRL1 proteins were probably too small to be detected in these experiments. In addition, we noted that expression of the D-box mutated PRL1-GFP under the control of either native *PRL1* or CaMV35S promoters caused no phenotypic changes in wild type plants, indicating that PRL1 is not limiting in dividing cells or at least not efficiently competed by the D-box mutant form of GFP-PRL1 fusion protein. Experiments designed for testing the effects of plant hormones on the stability of PRL1 protein revealed that during induction of cell death by treatment of plants with 50 mM salicylic acid PRL1 undergoes enhanced degradation. Since several distinct PRL1 proteolysis products were detected by the anti-PRL1 antibody (which was raised against a specific N-terminal PRL1 peptide), we hypothesized that under cell death inducing condition PRL1 may also be degraded by proteases (i.e., instead of the proteasomal pathway).

4.4. PRL1 is present in an AtCDC5-associated protein complex

PRL1 orthologs in budding and fission yeast (McDonald et al., 1999; Ohi and Gould, 2002; Ohi et al., 2002; Tsai et al., 1999; Hazbun et al. 2003), as well as in human cells (Ajuh et al., 2000), have been identified in association with CDC5 in spliceosome activating Prp19/CDC5 protein complexes. As both PRL1 and CDC5 orthologs are highly conserved in eukaryotes, we have tested whether AtCDC5 would bind PRL1 in yeast two-hybrid protein interaction assays. Although we found no interaction of full-length PRL1 with AtCDC5, an N-terminally truncated version of PRL1 carrying the WD-40 repeat region, showed interaction with AtCDC5. As the CDC5-binding region was mapped to the WD-40 domains of yeast PRL1 orthologs ScCef1p and ScPrp46p (Ohi and Gould, 2002), we decided to test interaction of PRL1 with AtCDC5 also *in vivo*. Using a CaMV35S promoter driven construct, we overexpressed an HA-epitope labelled version of AtCDC5-HA protein in a light-grown *Arabidopsis* cell suspension. CDC5-HA was detected in nuclear protein extracts, and observed that the size distribution of AtCDC5-HA containing protein complexes on glycerol gradients is similar to those of PRL1-containing protein complexes. These data suggested potential co-localization and co-fractionation of AtCDC5 and PRL1. Therefore, we have tested co-immunoprecipitation of AtCDC5-HA protein and PRL1, and found that AtCDC5-HA pulled down PRL1 from whole cell protein extract. This data suggested that PRL1 is found in association with AtCDC5 in a nuclear protein complex that – based on evolutionary conservation of CDC5 interacting factors – may represent a Prp19/CDC5-like spliceosome-associated complex also in *Arabidopsis*.

As our group has previously demonstrated that PRL1 is a binding partner of SnRK1α AMP-activated protein kinases, which were found in proteasomal associated SCF E3 ubiquitin ligase complexes (Farras et al., 2001), we have tested whether AtCDC5 would also interact with components of the proteasomal protein degradation system. In these immunoprecipitation experiments, AtCDC5 pulled down subunits of 20S core particle and 19S lid of the 26S proteasome, the CSN5 subunit of COP9 signalosome, and the CULLIN 1 subunit of SCF E3 ubiquitin ligases. Furthermore, an anti-ubiquitin antibody detected several distinct protein bands in the protein sample immunoprecipitated by AtCDC5-HA suggesting that these ubiquitinated factors may correspond to substrates of the AtCDC5-HA associated proteasome complex. Our results would excellently support a predicted role for the Prp19/Ntc spliceosome activating complex in the proteasome pathway, if further experiments could prove that the proteasome-associated AtCDC5-HA complex also contains conserved subunits of the Prp19/Cdc5 spliceosomal complex. Namely, Prp19 carries a U-box domain, which has been proved to possess ubiquitin ligase activity (Hatakeyama and Nakayama, 2003; Ohi et al., 2003). Moreover, in fission yeast Prp19 interacts with the β7 subunit of 20S proteasome core particle both *in vitro* and *in vivo* (Loscher et al. 2005). However, no specific substrates for the proteasome-associated Prp19 ubiquitin ligase have been identified thus far. In our experiments, CULLIN 1, a conserved subunit of SCF E3 ubiquitin ligases was found to interact with AtCDC5-HA. The apparent contradiction that two ubiquitin ligases are present in the same complex may be resolved by accounting that Prp19 was proposed to act as an E4 rather than E3 ligase. E4 enzymes represent a recently identified group of

ubiquitin ligases, which bind proteins marked with one to three ubiquitin molecules and catalyze further conjugation of ubiquitins together with the canonical E1, E2 and E3 complex (for review see Hoppe, 2005). In yeast, several transcription factors are known to become activated by covalent attachment of ubiquitin molecules and degraded later upon further addition of ubiquitins (Muratani and Tansey, 2003). UFD2, a U-box family member is one of the best characterised examples of E4 ligases. So far, SKP1 as another core component of SCF type E3 ligases was not detected in our AtCDC5-HA immunoprecipitation experiments. If SKP1 is indeed not associated to the AtCDC5-CULLIN 1 complex than probably this complex contains another members of the *Arabidopsis* SKP1/ASK1 protein family, which contains 19 proteins. However, ongoing experiments performed with a cell line carrying the *PRL1::PRL1-HA* expression construct indicate that PRL1-HA immunoprecipitated protein samples cross-react with anti-19S proteasome, anti-CULLIN 1, anti-SKP1 and anti-ubiquitin antibodies. However, when performing similar immunoprecipitation experiments with protein extracts prepared from three weeks old seedlings we could not detect association of PRL1 with SCF and proteasome subunits. These results, together with data showing degradation of PRL1 in leaves, suggest that PRL1 is only found in complex with AtCDC5, proteasome and other components of ubiquitination-dependent proteasome pathway in actively dividing cells, such as cell suspensions and meristems. This assumption is also supported by our failure to detect any *in vivo* interaction of the PRL1 protein with several previously identified PRL1-interacting partners (PIPs), including the SnRK1α protein kinases, in seedlings and mature plants.

Of course, the above discussed data also raise the question how a splicing related complex can influence the regulation of sugar signalling. A week indication was found for that ScCdc5p/Cef1p interacts in yeast two-hybrid assays with the Met30p F-box protein (Hazbun et al., 2003; http://www.yeastrc.org/unknown_orfs). Major target of the SCF^{Met30} E3 enzyme is a bZIP transcription factor, Met4p, which is responsible for the expression of genes involved in methionine biosynthesis and activated by low intracellular S-adenosylmethionine levels and oxidative stress (Kuras et al., 2002). It was reported that in yeast Met4p is activated by the attachment of a single ubiquitin molecule, however, this modification does not lead to immediate degradation of Met4p (Flick et al., 2004). Destabilization of Met4p could for example be accelerated by an E4 ligase, such as Prp19. Unfortunately, as compared to the 21 predicted F-box proteins in yeast, the *Arabidopsis* genome codes for approximately 700 putative F-box factors. Moreover, a clear homologue of Met4p was not yet identified from plants.

4.5.   <u>Genetic approaches to functional characterization of PRL1 interactions</u>

To enhance functional dissection of the regulatory domain of the PRL1 protein, we have isolated three additional T-DNA insertion mutations in the *PRL1* gene. As all T-DNA tags in the currently available T-DNA insertion mutant collections carry plant promoters close to their left borders, we wished to test whether any of the newly identified T-DNA insertion mutant alleles would allow expression of an N-terminally truncated PRL1 protein, which could have helped to study more

specifically the function of the WD40-repeat region. The three new T-DNA insertion mutants carrying the *prl1-2* SALK_008466, *prl1-3* SALK_039427 and *prl1-4* SALK_096289 however did not show any phenotypic difference as compared to the originally characterized *prl1-1* mutant, including block of root elongation and hypersensitivity to glucose, sucrose, and plant hormones ABA and ethylene. Pair-wise interallelic complementation test also revealed *prl1* phenotype, which correlated with our observation that none of the available *prl1* mutants contained detectable amounts of PRL1 protein.

Although we failed to detect interaction between AtCDC5 and the PRL2 homolog of PRL1 in our yeast two-hybrid assays, the fact that these two proteins carry nearly identical WD40-repeats suggests that PRL2 may turn out to interact also with AtCDC5 *in vivo*. To facilitate later analysis of the PRL2 function, we have also searched for T-DNA insertion mutations inactivating the *PRL2* gene. Two alleles, *prl2-1* Koncz16136 and *prl2-2*GABI_228D02 were identified. As we failed to identify homozygous *prl2* mutant lines, we performed a detailed segregation analysis for both mutant alleles. This analysis revealed a 2:1 segregation of T-DNA tagged *prl2* alleles and observation of embryo lethality in the siliques suggested that the PRL2 is probably required for proper female gametogenesis. Nonetheless, high level of *PRL2* transcription in the pollen indicated by transcript profiling data also suggests that the *prl2* mutation could also affect male instead of female transmission. This should be clarified by the ongoing reciprocal crosses between wild type and *prl2* mutants.

To facilitate further analysis of potential genetic interactions between the *prl1* mutation and mutations isolated in genes coding for some previously identified PRL1 interacting partners (PIPs), we have initiated the construction of double mutant lines. This collection of double mutants will be particularly useful, if further biochemical experiments would confirm *in vivo* association of PIPs with PRL1 in actively dividing cells. As all PIPs identified earlier by yeast two-hybrid screens performed with a cDNA library prepared from dark-grown cell suspension interact with N- and C-terminal extensions flanking the WD-40 repeat region in the PRL1 protein, there is a need for identification of specific point mutations that destroy binding of PIPs to these protein domains. In order to identify such mutations, we have exploited the public TILLING service and identified several point mutations causing amino acid exchanges in the N-terminus of the PRL1 protein. However, direct phenotypic analysis of TILLING EMS mutants is greatly disturbed by high number of background mutations, which frequently cause altered root elongation and serrated leaf phenotypes that are also characteristic for the *prl1* mutant. At least in case of one point mutation causing a G77E amino acid exchange in the N-terminus of PRL1, we have demonstrated that the mutation was not linked to the short root and serrated leaf phenotypes. To develop an alternative approach, we performed site-directed alanine mutagenesis of N- and C-terminal extensions of the PRL1 protein. Altogether 28 modified PRL1 protein carrying 53 amino acid exchanges were tested for complementation of the *prl1* phenotype. The fact that all these mutations complemented the root elongation defect of the *prl1* mutant strongly suggests that the N- and C-terminal domains of PRL1 do not play a role in regulation of cell division and/or cell elongation in roots. Based on the observation of the AtCDC5-PRL1 interaction, we hypothesize that this effect is associated to the function of PRL1 WD40-repeats. Nonetheless, the

availability of point mutations causing amino acid exchanges in the N- and C-terminal domains of PRL1 offer now useful tools for mapping the potential binding domains of several known PRL1 interacting proteins. In addition, these mutations may also be useful to test whether individual regulatory domains of PRL1 would control different phenotypic traits caused by the *prl1* null mutations, including hypersensitivity to sugar and plant hormones.

5. REFERENCES

Albers M, Diment A, Muraru M, Russell CS, Beggs JD. (2003) Identification and characterization of Prp45p and Prp46p, essential pre-mRNA splicing factors. RNA 9: 138-150.

Ajuh P, Kuster B, Panov K, Zomerdijk JC, Mann M, Lamond AI. (2000) Functional analysis of the human CDC5L complex and identification of its components by mass spectrometry. EMBO J. 19: 6569-6581.

Ajuh P, Sleeman J, Chusainow J, Lamond AI. (2001) A direct interaction between the carboxyl-terminal region of CDC5L and the WD40 domain of PLRG1 is essential for pre-mRNA splicing. J. Biol. Chem. 276: 42370-42381.

An H, Roussot C, Suarez-Lopez P, Corbesier L, Vincent C, Pineiro M, Hepworth S, Mouradov A, Justin S, Turnbull C, Coupland G. (2004) CONSTANS acts in the phloem to regulate a systemic signal that induces photoperiodic flowering of *Arabidopsis*. Development 131: 3615-3626.

Aravind L, Koonin EV. (2000) The U box is a modified RING finger - a common domain in ubiquitination. Curr Biol. 10: R132-134.

Ausubel, F. M., Brent, R., Kingston, R. E., Moore, D. D., Deidman, J. G., Smith, J. A. and Struhl, K. (1999) Current protocols in molecular biology, John Wiley & Sons, Inc.

Avonce N, Leyman B, Mascorro-Gallardo JO, Van Dijck P, Thevelein JM, Iturriaga G. (2004) The *Arabidopsis* trehalose-6-P synthase *AtTPS1* gene is a regulator of glucose, abscisic acid, and stress signaling. Plant Physiol. 136: 3649-3659.

Azevedo C, Santos-Rosa MJ, Shirasu K. (2001) The U-box protein family in plants. Trends Plant Sci. 6: 354-358.

Baurle I, Laux T. (2003) Apical meristems: the plant's fountain of youth. Bioessays 25: 961-970.
Berendzen K. (2005) Functional analysis of AMP-activated protein kinases in *Arabidopsis thaliana*. Dissertation zur Erlangung der Doktorgrades der Naturwissenschaften, Fachbereich Biologie der Phlipps-Universität Marburg.

Bernstein HS, Coughlin SR. (1997) Pombe Cdc5-related protein. A putative human transcription factor implicated in mitogen-activated signaling. J. Biol. Chem. 272: 5833-5837.

Bhalerao RP, Salchert K, Bako L, Okresz L, Szabados L, Muranaka T, Machida Y, Schell J, Koncz C. (1999) Regulatory interaction of PRL1 WD protein with *Arabidopsis* SNF1-like protein kinases. Proc. Natl. Acad. Sci. U. S. A. 96: 5322-5327.

Birnboim HC, Doly J. (1979) A rapid alkaline extraction procedure for screening recombinant plasmid DNA. Nucleic Acids Res. 7: 1513-1523.

Blatch GL, Lassle M. (1999) The tetratricopeptide repeat: a structural motif mediating protein-protein interactions. Bioessays 21: 932-939.

Bowman JL, Eshed Y. (2000) Formation and maintenance of the shoot apical meristem. Trends Plant Sci. 5: 110-115.
Bradford MM. (1976) A rapid and sensitive method for the quantitation of microgram quantities of protein utilizing the principle of protein dye binding. Anal. Biochem. 72: 248-254.

Brendel M, Bonatto D, Strauss M, Revers LF, Pungartnik C, Saffi J, Henriques JA. (2003) Role of PSO genes in repair of DNA damage of *Saccharomyces cerevisiae*. Mutat. Res. 544: 179-193.

Breuer F. (2000) Untersuchungen zur Funktion zweier PRL-WD-Proteine und deren Proteininteraktions-partnern in pflanchlichen Glukose- und Streßsignaltransduktionswegen. Inaugural-Disertation, Matematisch-Naturwissenschaftlichen Fakultät der Universität zu Köln.

Boudrez A, Beullens M, Groenen P, Van Eynde A, Vulsteke V, Jagiello I, Murray M, Krainer AR, Stalmans W, Bollen M. (2000) NIPP1-mediated interaction of protein phosphatase-1 with CDC5L, a regulator of pre-mRNA splicing and mitotic entry. J. Biol. Chem. 275: 25411-25417.

Busch MA, Bomblies K, Weigel D. (1999) Activation of a floral homeotic gene in *Arabidopsis*. Science 285: 585-587.

Byrne ME, Barley R, Curtis M, Arroyo JM, Dunham M, Hudson A, Martienssen RA. (2000) *ASYMMETRIC LEAVES* 1 mediates leaf patterning and stem cell function in *Arabidopsis*. Nature 408: 967-971.

Carr MD, Wollborn U, McIntosh PB, Frenkiel TA, McCormick JE, Bauer CJ, Klempnauer KH, Feeney J. (1996) Structure of the B-Myb DNA-binding domain in solution and evidence for multiple conformations in the region of repeat-2 involved in DNA binding: implications for sequence-specific DNA binding by Myb proteins. Eur. J. Biochem. 235: 721-735.

Castro A, Bernis C, Vigneron S, Labbe JC, Lorca T. (2005) The anaphase-promoting complex: a key factor in the regulation of cell cycle. Oncogene 24: 314-325.

Chaconas, G. and van de Sande, J. H. (1980) 5'-32P labeling of RNA and DNA restriction fragments. Methods Enzymol. 65: 75-85.

Chan SP, Cheng SC. (2005) The Prp19-associated complex is required for specifying interactions of U5 and U6 with pre-mRNA during spliceosome activation. J. Biol. Chem. 280: 31190-31199.

Chan SP, Kao DI, Tsai WY, Cheng SC. (2003) The Prp19p-associated complex in spliceosome activation. Science 302: 279-282.

Chen HR, Jan SP, Tsao TY, Sheu YJ, Banroques J, Cheng SC. (1998) Snt309p, a component of the Prp19p-associated complex that interacts with Prp19p and associates with the spliceosome simultaneously with or immediately after dissociation of U4 in the same manner as Prp19p. Mol Cell Biol. 18: 2196-2204.

Chen HR, Tsao TY, Chen CH, Tsai WY, Her LS, Hsu MM, Cheng SC. (1999) Snt309p modulates interactions of Prp19p with its associated components to stabilize the Prp19p-associated complex essential for pre-mRNA splicing. Proc. Natl. Acad. Sci. U. S. A. 96: 5406-5411.

Chen CH, Tsai WY, Chen HR, Wang CH, Cheng SC. (2001) Identification and characterization of two novel components of the Prp19p-associated complex, Ntc30p and Ntc20p. J. Biol. Chem. 276: 488-494.

Chen CH, Yu WC, Tsao TY, Wang LY, Chen HR, Lin JY, Tsai WY, Cheng SC. (2002) Functional and physical interactions between components of the Prp19p-associated complex. Nucleic Acids Res.30: 1029-1037.
Chung S, McLean MR, Rymond BC. (1999) Yeast ortholog of the *Drosophila* crooked neck protein promotes spliceosome assembly through stable U4/U6.U5 snRNP addition. RNA 5: 1042-1054.

Chung S, Zhou Z, Huddleston KA, Harrison DA, Reed R, Coleman TA, Rymond BC. (2002) Crooked neck is a component of the human spliceosome and implicated in the splicing process. Biochim. Biophys. Acta 1576: 287-297.

Carlson M. (1999) Glucose repression in yeast. Curr. Opin. Microbiol. 2: 202-207.

Clough SJ, Bent AF. (1998) Floral dip: a simplified method for *Agrobacterium*-mediated transformation of *Arabidopsis thaliana*. Plant J. 16: 735-743.

Corbesier L, Lejeune P, Bernier G. (1998) The role of carbohydrates in the induction of flowering in *Arabidopsis thaliana*: comparison between the wild type and a starchless mutant. Planta 206:131-137.

Dekkers BJ, Schuurmans JA, Smeekens SC. (2004) Glucose delays seed germination in *Arabidopsis thaliana*. Planta 218: 579-588.

Deng XW, Caspar T, Quail PH. (1991) COP1: a regulatory locus involved in light-controlled development and gene expression in *Arabidopsis*. Genes Dev. 5: 1172-1182.

Deyholos MK, Sieburth LE. (2000) Separable whorl-specific expression and negative regulation by enhancer elements within the AGAMOUS second intron. Plant Cell 12: 1799-1810.

Dower WJ, Miller JF, Ragsdale CW. (1988) High efficiency transformation of *E. coli* by high voltage electroporation. Nucleic Acids Res. 16: 6127-6145.

Durfee TK, Becherer PL, Chen SH, Yeh Y, Yang A, Kilburn W, Lee H, Elledge SJ. (1993) The retinoblastoma protein associates with the protein phosphatase type 1 catalytic subunit. Genes Devel. 7: 555-569.

Duval M, Hsieh TF, Kim SY, Thomas TL. (2002) Molecular characterization of AtNAM: a member of the Arabidopsis NAC domain superfamily. Plant Mol. Biol. 50: 237-248.

Eastmond PJ, Li Y, Graham IA. (2003) Is trehalose-6-phosphate a regulator of sugar metabolism in plants? J. Exp. Bot. 54: 533-537.

Engemann H, Heinzel V, Page G, Preuss U, Scheidtmann KH. (2002) DAP-like kinase interacts with the rat homolog of *Schizosaccharomyces pombe* CDC5 protein, a factor involved in pre-mRNA splicing and required for G2/M phase transition. Nucleic Acids Res. 30: 1408-1417.

Farkas G, Gausz J, Galloni M, Reuter G, Gyurkovics H, Karch F. (1994) The Trithorax-like gene encodes the Drosophila GAGA factor. Nature 371: 806-808.

Farras R, Ferrando A, Jasik J, Kleinow T, Okresz L, Tiburcio A, Salchert K, del Pozo C, Schell J, Koncz C. (2001) SKP1-SnRK protein kinase interactions mediate proteasomal binding of a plant SCF ubiquitin ligase. EMBO J. 20: 2742-2756.

Ferrando A, Farras R, Jasik J, Schell J, Koncz C. (2000) Intron-tagged epitope: a tool for facile detection and purification of proteins expressed in *Agrobacterium*-transformed plant cells. Plant J. 22: 553-560.

Ferreira PC, Hemerly AS, Engler JD, van Montagu M, Engler G, Inze D. (1994) Developmental expression of the arabidopsis cyclin gene cyc1At. Plant Cell 6: 1763-1774.

Finkelstein RR, Lynch TJ. (2000) Abscisic acid inhibition of radicle emergence but not seedling growth is suppressed by sugars. Plant Physiol. 122: 1179-1186.

Flick JS, Johnston M. (1990) Two systems of glucose repression of the GAL1 promoter in *Saccharomyces cerevisiae*. Mol. Cell Biol. 10: 4757-4769.

Flick K, Ouni I, Wohlschlegel JA, Capati C, McDonald WH, Yates JR, Kaiser P. (2004) Proteolysis-independent regulation of the transcription factor Met4 by a single Lys 48-linked ubiquitin chain. Nat. Cell Biol. 6: 634-641.

Gazzarrini S, McCourt P. (2001) Genetic interactions between ABA, ethylene and sugar signaling pathways. Curr. Opin. Plant Biol. 4: 387-391.

Gibson SI. (2005) Control of plant development and gene expression by sugar signaling. Curr. Opin. Plant Biol. 8: 93-102.

Gotzmann J, Gerner C, Meissner M, Holzmann K, Grimm R, Mikulits W, Sauermann G. (2000) hNMP 200: a novel human common nuclear matrix protein combining structural and regulatory functions. Exp Cell Res. 261: 166-179.

Gray WM, del Pozo JC, Walker L, Hobbie L, Risseeuw E, Banks T, Crosby WL, Yang M, Ma H, Estelle M. (1999) Identification of an SCF ubiquitin-ligase complex required for auxin response in Arabidopsis thaliana. Genes Dev. 13: 1678-1691.

Grey M, Dusterhoft A, Henriques JA, Brendel M. (1996) Allelism of PSO4 and PRP19 links pre-mRNA processing with recombination and error-prone DNA repair in *Saccharomyces cerevisiae*. Nucleic Acids Res. 24: 4009-4014.

Grillari J, Hohenwarter O, Grabherr RM, Katinger H. (2000) Subtractive hybridization of mRNA from early passage and senescent endothelial cells. Exp. Gerontol. 35: 187-197.

Grillari J, Ajuh P, Stadler G, Loscher M, Voglauer R, Ernst W, Chusainow J, Eisenhaber F, Pokar M, Fortschegger K, Grey M, Lamond AI, Katinger H. (2005) SNEV is an evolutionarily conserved splicing factor whose oligomerization is necessary for spliceosome assembly. Nucleic Acids Res. 33: 6868-6883.

Hardie DG. (2004) The AMP-activated protein kinase pathway--new players upstream and downstream. J. Cell Sci. 117: 5479-5487.

Hardie DG, Carling D, Carlson M. (1998a) The AMP-activated/SNF1 protein kinase subfamily: metabolic sensors of the eukaryotic cell? Annu. Rev. Biochem. 67: 821-855.

HarperJW, Adami GR, Wei N, Keyomarsi K, Elledge SJ. (1993) The p21 Cdk-interacting protein Cip1 is a potent inhibitor of G1 cyclin-dependent kinases. Cell 75: 805-816.

Harper JW, Burton JL, Solomon MJ. (2002) The anaphase-promoting complex: it's not just for mitosis any more. Genes Dev. 16: 2179-2206.

Hatakeyama S, Nakayama KI. (2003) U-box proteins as a new family of ubiquitin ligases. Biochem. Biophys. Res. Commun. 302: 635-645.

Hauffe KD, Lee SP, Subramaniam R, Douglas CJ. (1993) Combinatorial interactions between positive and negative *cis*-acting elements control spatial patterns of 4CL-1 expression in transgenic tobacco. Plant J. 4: 235-253.

Hazbun TR, Malmstrom L, Anderson S, Graczyk BJ, Fox B, Riffle M, Sundin BA, Aranda JD, McDonald WH, Chiu CH, Snydsman BE, Bradley P, Muller EG, Fields S, Baker D, Yates JR 3rd, Davis TN.(2003) Assigning function to yeast proteins by integration of technologies. Mol. Cell. 12: 1353-1365.

Higo, K., Y. Ugawa, M. Iwamoto and T. Korenaga (1999) Plant *cis*-acting regulatory DNA elements (PLACE) database. Nucleic Acids Res. 27: 297-300.

Himanen K, Boucheron E, Vanneste S, de Almeida Engler J, Inze D, Beeckman T. (2002) Auxin-mediated cell cycle activation during early lateral root initiation. Plant Cell 14: 2339-2351.

Hirayama T, Shinozaki K. (1996) A cdc5[+] homolog of a higher plant, *Arabidopsis thaliana*. Proc. Natl. Acad. Sci. U. S. A. 93: 13371-13376.

Hoppe T. (2005) Multiubiquitylation by E4 enzymes: 'one size' doesn't fit all. Trends Biochem. Sci. 30: 183-187.

Hughes JH, Mack K, Hamparian VV. (1988) India ink staining of proteins on nylon and hydrophobic membranes. Anal Biochem. 173: 18-25.

Ingram GC, Goodrich J, Wilkinson MD, Simon R, Haughn GW, Coen ES. (1995) Parallels between *UNUSUAL FLORAL ORGANS* and *FIMBRIATA*, genes controlling flower development in *Arabidopsis* and *Antirrhinum*. Plant Cell 7: 1501-1510.

Jang JC, Sheen J. (1994) Sugar sensing in higher plants. Plant Cell 6: 1665-1679.

Jang JC, Leon P, Zhou L, Sheen J. (1997) Hexokinase as a sugar sensor in higher plants. Plant Cell 9: 5-19.

Jang IC, Yang JY, Seo HS, Chua NH. (2005) HFR1 is targeted by COP1 E3 ligase for post-translational proteolysis during phytochrome A signaling. Genes Dev. 19: 593-602.

Jawad Z, Paoli M. (2002) Novel sequences propel familiar folds. Structure 10: 447-454.

Jeffery CJ. (2003) Moonlighting proteins: old proteins learning new tricks. Trends Genet. 19: 415-417.
Jin H, Martin C. (1999) Multifunctionality and diversity within the plant MYB-gene family. Plant Mol. Biol. 41: 577-585.

Koch K. (2004) Sucrose metabolism: regulatory mechanisms and pivotal roles in sugar sensing and plant development. Curr Opin. Plant Biol. 7: 235-246.

Kooiker M, Airoldi CA, Losa A, Manzotti PS, Finzi L, Kater MM, Colombo L. (2005) BASIC PENTACYSTEINE1, a GA-binding protein that induces conformational changes in the regulatory region of the homeotic *Arabidopsis* gene SEEDSTICK. Plant Cell 17: 722-729.

Koncz C, Schell J. (1986) The promoter of TL-DNA gene 5 controls the tissue specific expression of chimaeric genes carried by a novel type of *Agrobacterium* binary vector. Mol. Gen. Genet. 204: 383-396.
Koncz C, Martini N, Szabados L, Hrouda M, Bachmair A, Schell J. (1994) Specialized vectors for gene tagging and expression studies. In: Plant Molecular Biology Manual (eds. Gelvin S, Schilperoort B) Kluwer Academic, Dordrect, B2: 1-22.

Kreivi JP, Lamond AI. (1996) RNA splicing: unexpected spliceosome diversity. Curr. Biol. 6: 802-805.

Kuras L, Rouillon A, Lee T, Barbey R, Tyers M, Thomas D. (2002) Dual regulation of the met4 transcription factor by ubiquitin-dependent degradation and inhibition of promoter recruitment. Mol. Cell 10: 69-80.

Laemmli U.K. (1970) Cleavage of structural proteins during assembly of the head of bacterophage T4. Nature 227: 680-685.

Lafos M. (2006) Komplementationstudien der *cpd*-Mutante und Analyse der CPD-interaktionspartner mittels reverser Genetik. Inaugural-Dissertation, Mathematisch-Naturwissenschaftlichen Fakultät der Universität zu Köln.

Lambright DG, Sondek J, Bohm A, Skiba NP, Hamm HE, Sigler PB. (1996) The 2.0 A crystal structure of a heterotrimeric G protein. Nature 379: 311-319.

Larsen NA, Harrison SC. (2004) Crystal structure of the spindle assembly checkpoint protein Bub3. J. Mol. Biol. 344: 885-892.

Lei XH, Shen X, Xu XQ, Bernstein HS. (2000) Human Cdc5, a regulator of mitotic entry, can act as a site-specific DNA binding protein. J. Cell Sci. 113: 4523-4531.

Leon P, Sheen J. (2003) Sugar and hormone connections. Trends Plant Sci. 8: 110-116.

Lescot M, Dehais P, Thijs G, Marchal K, Moreau Y, Van de Peer Y, Rouze P, Rombauts S. (2002) PlantCARE, a database of plant *cis*-acting regulatory elements and a portal to tools for *in silico* analysis of promoter sequences. Nucleic Acids Res. 30: 325-327.

Lincoln C, Long J, Yamaguchi J, Serikawa K, Hake S. (1994) A *knotted1-like* homeobox gene in *Arabidopsis* is expressed in the vegetative meristem and dramatically alters leaf morphology when overexpressed in transgenic plants. Plant Cell 6: 1859-1876.

Liu J, Wilson TE, Milbrandt J, Johnston M. (1993) Identifying DNA-binding sites and analyzing DNA-binding domains using a yeast selection system. In: Methods: A Companion to Methods in Enzymology 5:125–137.

Long JA, Moan EI, Medford JI, Barton MK. (1996) A member of the KNOTTED class of homeodomain proteins encoded by the *STM* gene of *Arabidopsis*. Nature 379: 66-69.

Lorkovic ZJ, Wieczorek Kirk DA, Lambermon MH, Filipowicz W. (2000) Pre-mRNA splicing in higher plants. Trends Plant Sci. 5: 160-167.

Löscher M, Fortschegger K, Ritter G, Wostry M, Voglauer R, Schmid JA, Watters S, Rivett AJ, Ajuh P, Lamond AI, Katinger H, Grillari J. (2005) Interaction of U-box E3 ligase SNEV with PSMB4, the beta7 subunit of the 20 S proteasome. Biochem J. 388: 593-603.

Mahajan KN, Mitchell BS. (2003) Role of human Pso4 in mammalian DNA repair and association with terminal deoxynucleotidyl transferase. Proc. Natl. Acad. Sci. U. S. A. 100: 10746-10751.

Madrona AY, Wilson DK. (2004) The structure of Ski8p, a protein regulating mRNA degradation: Implications for WD protein structure. Protein Sci. 13: 1557-1565.

Meister RJ, Williams LA, Monfared MM, Gallagher TL, Kraft EA, Nelson CG, Gasser CS. (2004) Definition and interactions of a positive regulatory element of the Arabidopsis INNER NO OUTER promoter. Plant J. 37: 426-438.

Mathur J, Koncz C. (1998) Establishment and maintenance of cell suspension cultures of *Arabidopsis thaliana*. In: *Arabidopsis* Protocols., (eds. Martinez-Zapater JM, Salinas J), Humana Press, pp. 27-30.

Miyazaki Y, Jojima T, Ono T, Yamazaki T, Shishido K. (2004) A cDNA homologue of *Schizosaccharomyces pombe* cdc5(+) from the mushroom *Lentinula edodes*: characterization of the cDNA and its expressed product. Biochim. Biophys. Acta. 1680: 93-102.

Muranaka T, Banno H, Machida Y. (1994) Characterization of tobacco protein kinase NPK5, a homolog of Saccharomyces cerevisiae SNF1 that constitutively activates expression of the glucose-repressible SUC2 gene for a secreted invertase of S. cerevisiae. Mol. Cell. Biol. 14: 2958-2965.

Muratani M, Tansey WP. (2003) How the ubiquitin-proteasome system controls transcription. Nat. Rev. Mol. Cell. Biol. 4: 192-201.

Ogata K, Kanei-Ishii C, Sasaki M, Hatanaka H, Nagadoi A, Enari M, Nakamura H, Nishimura Y, Ishii S, Sarai A. (1996) The cavity in the hydrophobic core of Myb DNA-binding domain is reserved for DNA recognition and trans-activation. Nat. Struct. Biol. 3: 178-187.

Ohi R, McCollum D, Hirani B, Den Haese GJ, Zhang X, Burke JD, Turner K, Gould KL. (1994) The *Schizosaccharomyces pombe* cdc5$^+$ gene encodes an essential protein with homology to c-Myb. EMBO J. 13: 471-483.

Ohi R, Feoktistova A, McCann S, Valentine V, Look AT, Lipsick JS, Gould KL. (1998) Myb-related *Schizosaccharomyces pombe* cdc5p is structurally and functionally conserved in eukaryotes. Mol. Cell Biol. 18: 4097-4108.

Ohi MD, Gould KL. (2002) Characterization of interactions among the Cef1p-Prp19p-associated splicing complex. RNA. 8: 798-815.

Ohi MD, Link AJ, Ren L, Jennings JL, McDonald WH, Gould KL. (2002) Proteomics analysis reveals stable multiprotein complexes in both fission and budding yeasts containing Myb-related Cdc5p/Cef1p, novel pre-mRNA splicing factors, and snRNAs. Mol. Cell Biol. 22: 2011-2024.

Ohi MD, Vander Kooi CW, Rosenberg JA, Chazin WJ, Gould KL. (2003) Structural insights into the U-box, a domain associated with multi-ubiquitination. Nat. Struct. Biol. 10: 250-255.

Ohi MD, Vander Kooi CW, Rosenberg JA, Ren L, Hirsch JP, Chazin WJ, Walz T, Gould KL. (2005) Structural and functional analysis of essential pre-mRNA splicing factor Prp19p. Mol. Cell. Biol. 25: 451-460.

Ohto M, Onai K, Furukawa Y, Aoki E, Araki T, Nakamura K. (2001) Effects of sugar on vegetative development and floral transition in *Arabidopsis*. Plant Physiol. 127: 252-261.

Mahajan KN, Mitchell BS. (2003) Role of human Pso4 in mammalian DNA repair and association with terminal deoxynucleotidyl transferase. Proc. Natl. Acad. Sci. U. S. A. 100: 10746-10751.

McDonald WH, Ohi R, Smelkova N, Frendewey D, Gould KL. (1999) Myb-related fission yeast cdc5p is a component of a 40S snRNP-containing complex and is essential for pre-mRNA splicing. Mol Cell Biol. 19: 5352-5362.

Moon J, Parry G, Estelle M. (2004) The ubiquitin-proteasome pathway and plant development. Plant Cell 16: 3181-3195.

Murray HL, Jarrell KA. (1999) Flipping the switch to an active spliceosome. Cell 96: 599-602.

Nemeth K. (2004) T-DNA insertion mutagenesis in *Arabidopsis*: Isolation and characterization of a gene encoding a member of WD-40 protein family. Candidate Thesis, Hungarian Academy of Sciences, Budapest

Nemeth K, Salchert K, Putnoky P, Bhalerao R, Koncz-Kalman Z, Stankovic-Stangeland B, Bako L, Mathur J, Okresz L, Stabel S, Geigenberger P, Stitt M, Redei GP, Schell J, Koncz C. (1998) Pleiotropic control of glucose and hormone responses by PRL1, a nuclear WD protein, in *Arabidopsis*. Genes Dev. 12: 3059-3073.

Papp I, Mur LA, Dalmadi A, Dulai S, and Koncz C. (2004) A mutation in the Cap Binding Protein 20 gene confers drought tolerance to *Arabidopsis*. Plant Mol. Biol. 55: 679-686.

Paul MJ, Pellny TK. (2003) Carbon metabolite feedback regulation of leaf photosynthesis and development. J. Exp. Bot. 54: 539-547.

Pauli S, Rothnie HM, Chen G, He X, Hohn T. (2004) The cauliflower mosaic virus 35S promoter extends into the transcribed region. J. Virol. 78: 12120-12128.

Perrimon N, Engstrom L, Mahowald AP. (1984) Developmental genetics of the 2E-F region of the *Drosophila* X chromosome: a region rich in "developmentally important" genes. Genetics 108: 559-572.

Peters JM, (2002) The anaphase-promoting complex: proteolysis in mitosis and beyond, Mol. Cell 9: 931-943.

Planchais S, Glab N, Inze D, Bergounioux C. (2000) Chemical inhibitors: a tool for plant cell cycle studies. FEBS Lett. 476: 78-83.

Potashkin J, Kim D, Fons M, Humphrey T, Frendewey D. (1998) Cell-division-cycle defects associated with fission yeast pre-mRNA splicing mutants. Curr. Genet. 34: 153-163.

Quirino BF, Noh YS, Himelblau E, Amasino RM. (2000) Molecular aspects of leaf senescence. Trends Plant Sci. 5: 278-282.

Raisin-Tani S, Leopold P. (2002) *Drosophila* crooked-neck protein co-fractionates in a multiprotein complex with splicing factors. Biochem. Biophys. Res. Commun. 296: 288-292.

Rédei GP. (1992) A heuristic glance at the past of *Arabidopsis* genetics. In: Methods in *Arabidopsis* Research, (eds. Koncz C, Chua NH, Schell J.), World Scientific, Singapore, pp.1-15.

Ríos G, Lossow A, Hertel B, Breuer F, Schaefer S, Broich M, Kleinow T, Jásik J, Winter J, Ferrando A, Farrás R, Panicot M, Henriques R, Mariaux J-B, Oberschall A, Molnár G, Berendzen K, Shukla V, Lafos M, Koncz Z, Rédei GP, Schell J, Koncz C (2002) Rapid identification of *Arabidopsis* insertion mutants by nonradioactive detection of T-DNA tagged genes. Plant J. 32: 243-253.

Rogers SO, Bendich AJ. (1985) Extraction of DNA from milligram amounts of fresh, herbarium and mummified plant tissues. Plant Mol. Biol. 5: 69-76.

Roitsch T, Gonzalez MC. (2004) Function and regulation of plant invertases: sweet sensations. Trends Plant Sci. 9: 606-613.

Roldan M, Gomez-Mena C, Ruiz-Garcia L, Salinas J, Martinez-Zapater JM. (1999) Sucrose availability on the aerial part of the plant promotes morphogenesis and flowering of *Arabidopsis* in the dark. Plant J. 20: 581-590.
Rolland F, Moore B, Sheen J. (2002) Sugar sensing and signaling in plants. Plant Cell. 14 Suppl: S185-205.
Russell CS, Ben-Yehuda S, Dix I, Kupiec M, Beggs JD. (2000) Functional analyses of interacting factors involved in both pre-mRNA splicing and cell cycle progression in *Saccharomyces cerevisiae*. RNA. 6: 1565-1572.

Salchert K. (1997) Untersuchungen zur Funktion von PRL1 durch Identifizierung und Charakterisierung von PRL1-interagierenden- Proteinen. Inaugural-Dissertation, Mathematisch-Naturwissenschaftlichen Fakultät der Universität zu Köln.
Saijo Y, Sullivan JA, Wang H, Yang J, Shen Y, Rubio V, Ma L, Hoecker U, Deng XW. (2003) The COP1-SPA1 interaction defines a critical step in phytochrome A-mediated regulation of HY5 activity. Genes Dev. 17: 2642-2647.

Sambrook, J., E.F. Fritsch, and T. Maniatis. (1989) Molecular cloning. A laboratory manual. Cold Spring Harbor Laboratory, Cold Spring Harbor, N.Y.

Santi L, Wang Y, Stile MR, Berendzen K, Wanke D, Roig C, Pozzi C, Muller K, Muller J, Rohde W, Salamini F. (2003) The GA octodinucleotide repeat binding factor BBR participates in the transcriptional regulation of the homeobox gene Bkn3. Plant J. 34: 813-826.

Sieburth LE, Meyerowitz EM. (1997) Molecular dissection of the AGAMOUS control region shows that cis-elements for spatial regulation are located intragenically. Plant Cell 9: 355-365.

Simpson CG, Jennings SN, Clark GP, Thow G, Brown JW. (2004) Dual functionality of a plant U-rich intronic sequence element. Plant J. 37: 82-91.

Smalle J, Vierstra RD. (2004) The ubiquitin 26S proteasome proteolytic pathway. Annu. Rev. Plant Biol. 55: 555-590.

Smeekens S. (2000) Sugar-induced signal transduction in plants. Annu. Rev. Plant Physiol. Plant Mol. Biol. 51: 49-81.

Staley JP, Guthrie C. (1998) Mechanical devices of the spliceosome: motors, clocks, springs, and things. Cell 92: 315-326.

Stracke R, Werber M, Weisshaar B. (2001) The R2R3-MYB gene family in *Arabidopsis thaliana*. Curr. Opin. Plant Biol. 4: 447-456.

Stukenberg PT, Lustig KD, McGarry TJ, King RW, Kuang J, Kirschner MW. (1997) Systematic identification of mitotic phosphoproteins. Curr Biol. 7: 338-348.

Sun Y, Zhou Q, Zhang W, Fu Y, Huang H. (2002) ASYMMETRIC LEAVES1, an Arabidopsis gene that is involved in the control of cell differentiation in leaves. Planta 214: 694-702.

Tarn WY, Steitz JA. (1997) Pre-mRNA splicing: the discovery of a new spliceosome doubles the challenge. Trends Biochem. Sci. 22: 132-137.

Tarn WY, Hsu CH, Huang KT, Chen HR, Kao HY, Lee KR, Cheng SC. (1994) Functional association of essential splicing factor(s) with PRP19 in a protein complex. EMBO J. 13: 2421-2431.

Till BJ, Colbert T, Tompa R, Enns LC, Codomo CA, Johnson JE, Reynolds SH, Henikoff JG, Greene EA, Steine MN, Comai L, Henikoff S. (2003) High-throughput TILLING for functional genomics. Methods Mol Biol. 236: 205-220.

Towbin H, Staehelin T, Gordon, J. (1979) Electrophoretic transfer of proteins from polyacrylamide gels to nitrocellulose sheets: procedure and some applications. Proc. Natl. Acad. Sci. U. S. A. 76: 4350-4354.

Tsai WY, Chow YT, Chen HR, Huang KT, Hong RI, Jan SP, Kuo NY, Tsao TY, Chen CH, Cheng SC. (1999) Cef1p is a component of the Prp19p-associated complex and essential for pre-mRNA splicing. J. Biol. Chem. 274: 9455-9462.

Truernit E, Sauer N. (1995) The promoter of the Arabidopsis thaliana SUC2 sucrose-H$^+$ symporter gene directs expression of beta-glucuronidase to the phloem: evidence for phloem loading and unloading by SUC2. Planta 196: 564-570.

Vander Kooi CW, Ohi MD, Rosenberg JA, Oldham ML, Newcomer ME, Gould KL, Chazin WJ. (2006) The Prp19 U-box crystal structure suggests a common dimeric architecture for a class of oligomeric E3 ubiquitin ligases. Biochemistry 45: 121-130.

van der Voorn L, Ploegh HL. (1992) The WD-40 repeat. FEBS Lett. 307: 131-134.

van Nocker S, Ludwig P. (2003) The WD-repeat protein superfamily in Arabidopsis: conservation and divergence in structure and function. BMC Genomics 4: 50.

Vijayraghavan U, Company M, Abelson J. (1989) Isolation and characterization of pre-mRNA splicing mutants of *Saccharomyces cerevisiae*. Genes Dev. 3: 1206-1216.

Vincent K, Wang Q, Jay S, Hobbs K, Rymond BC. (2003) Genetic interactions with CLF1 identify additional pre-mRNA splicing factors and a link between activators of yeast vesicular transport and splicing. Genetics 164: 895-907.

Vodermaier HC. (2004) APC/C and SCF: controlling each other and the cell cycle. Curr Biol. 14: R787-796.

Voglauer R, Chang MW, Dampier B, Wieser M, Baumann K, Sterovsky T, Schreiber M, Katinger H, Grillari J. (2006) SNEV overexpression extends the life span of human endothelial cells. Exp. Cell Res. 312: 746-759.

Wilson TE, Fahrner TJ, Johnston M, Milbrandt J. (1991) Identification of the DNA binding site for NGFI-B by genetic selection in yeast. Science 252: 1296–1300.

Yamamoto YT, Cheng CL, Conkling MA. (1990) Root-specific genes from tobacco and *Arabidopsis* homologous to an evolutionarily conserved gene family of membrane channel proteins. Nucleic Acids Res. 18: 7449.

Yi C, Deng XW. (2005) COP1 - from plant photomorphogenesis to mammalian tumorigenesis. Trends Cell Biol. 15: 618-625.

Zimmermann P, Hirsch-Hoffmann M, Hennig L, Gruissem W. (2004) GENEVESTIGATOR. *Arabidopsis* microarray database and analysis toolbox. Plant Physiol. 136: 2621-2632.

Zhang N, Kaur R, Lu X, Shen X, Li L, Legerski RJ. (2005) The Pso4 mRNA splicing and DNA repair complex interacts with WRN for processing of DNA interstrand cross-links. J. Biol. Chem. 280: 40559-40567.

Zhu W, Rainville IR, Ding M, Bolus M, Heintz NH, Pederson DS. (2002) Evidence that the pre-mRNA splicing factor Clf1p plays a role in DNA replication in *Saccharomyces cerevisiae*. Genetics 160: 1319-1333.

Zuo J, Niu QW, Chua NH. (2000) An estrogen receptor-based transactivator XVE mediates highly inducible gene expression in transgenic plants. Plant J. 24: 265-273.

Acknowledgements

Erklärung

Ich versichere, daß ich die von mir vorgelegte Dissertation selbständig angefertigt, die benutzten Quellen und Hilfsmittel vollständig angegeben und die Stellen der Arbeit - einschließlich Tabellen, Karten und Abbildungen -, die anderen Werken im Wortlaut oder dem Sinn nach entnommen sind, in jedem Einzelfall als Entlehnung kenntlich gemacht habe; daß diese Dissertation noch keiner anderen Fakultät oder Universität zur Prüfung vorgelegen hat; daß sie - abgesehen von unten angegebenen Teilpublikationen - noch nicht veröffentlicht worden ist sowie, daß ich eine solche Veröffentlichung vor Abschluß des Promotionsverfahrens nicht vornehmen werde.

Die Bestimmungen der Promotionsordnung sind mir bekannt. Die von mir vorgelegte Dissertation ist von Prof. Dr. George Coupland betreut worden.

Köln den 04 Mai 2006

Dóra Szakonyi

Lebenslauf

Name, Vorname:	Szakonyi, Dóra
Geburtsdatum:	25. November 1978
Geburtsort:	Kecskemét, Ungarn
Staatsangehörigkeit:	Ungarisch
Familienstand:	ledig

Schulbildung

1985-1993	Vörösmarty Mihály Általános Iskola, Kecskemét, Ungarn
1993-1997	Katona József Gimnázium, Kecskemét, Ungarn
1997	Abitur: Biologie, Chemie, Ungarische Grammatik und Literatur, Mathematik, Geschichte

Ausbildung

1997-2002	Studium der Biologie an der Universität zu Szeged, Ungarn
1999-2000	Erasmus stipendium an der Freie Universitát Brüssel (Vrije Universiteit Brussel), Belgien
2000-2002	Diplomarbeit bei Dr. Attila Fehér, BRC Szeged, Ungarn Functional analysis of an alfalfa Rho GTPase in yeast
2002	Diplomprüfung in den Fächern Molekulare Biologie der Pflanzen, Genetik
2003-2006	Promotion an der Universität zu Köln, in der Abteilung für Entwicklungsbiologie von Prof. Dr. George Coupland am Max-Planck-Institut für Züchtungsforschung in Köln. Das Thema der Dissertation lautet „Genetic dissection of regulatory domains and signalling interactions of PRL1 WD-protein in *Arabidopsis*".

Publikation

Dorjgotov D, Szucs A, Otvos K, Szakonyi D, Kelemen Z, Lendvai A, Ponya Z, Barnabas B, Brown S, Dudits D, Feher A. (2003) Specific features of RHO GTPase-dependent signaling in plants. Cell Biol Int. 27(3):191-2.